USGS
science for a changing world

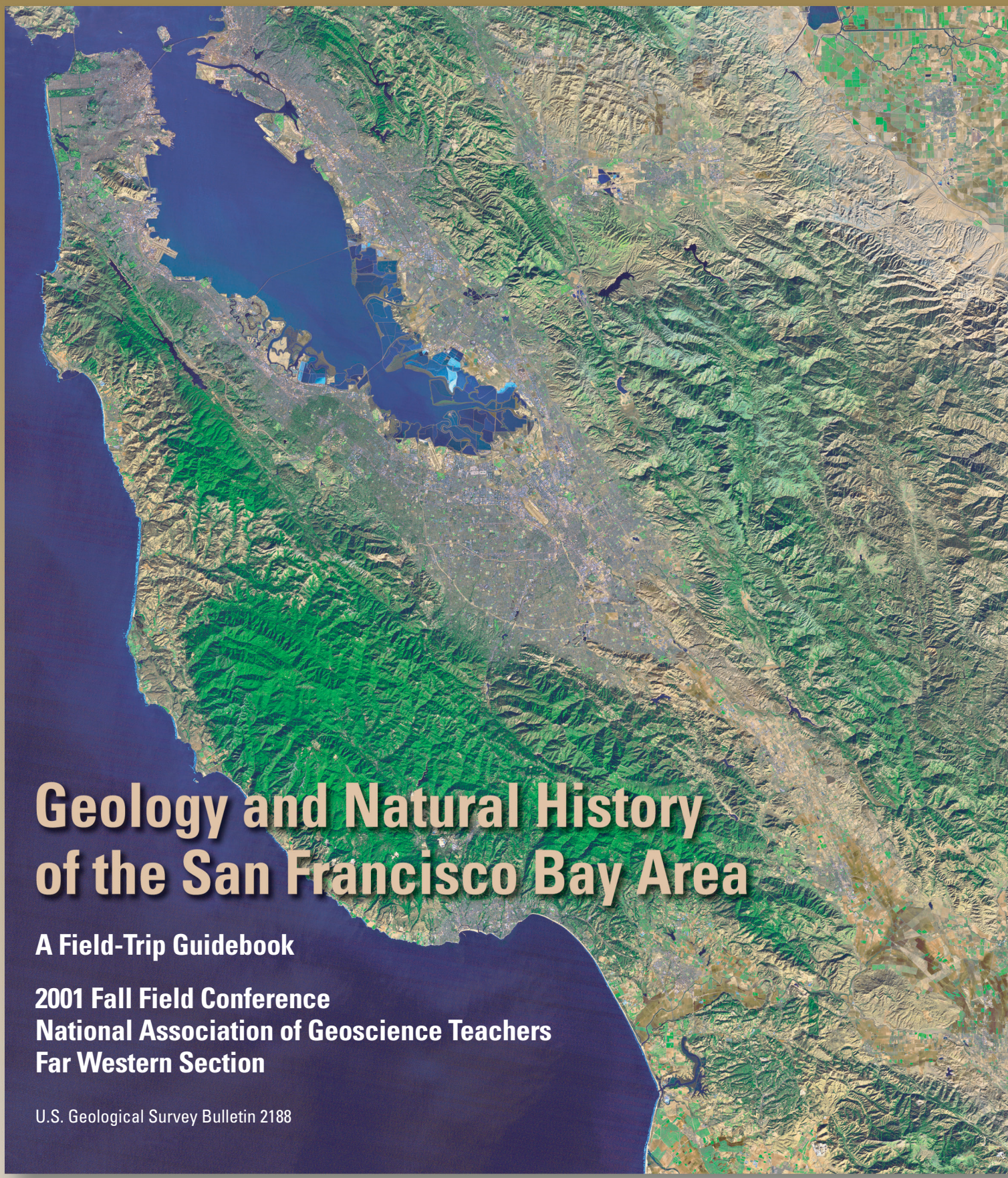

Geology and Natural History of the San Francisco Bay Area

A Field-Trip Guidebook

2001 Fall Field Conference
National Association of Geoscience Teachers
Far Western Section

U.S. Geological Survey Bulletin 2188

U.S. Department of the Interior
U.S. Geological Survey

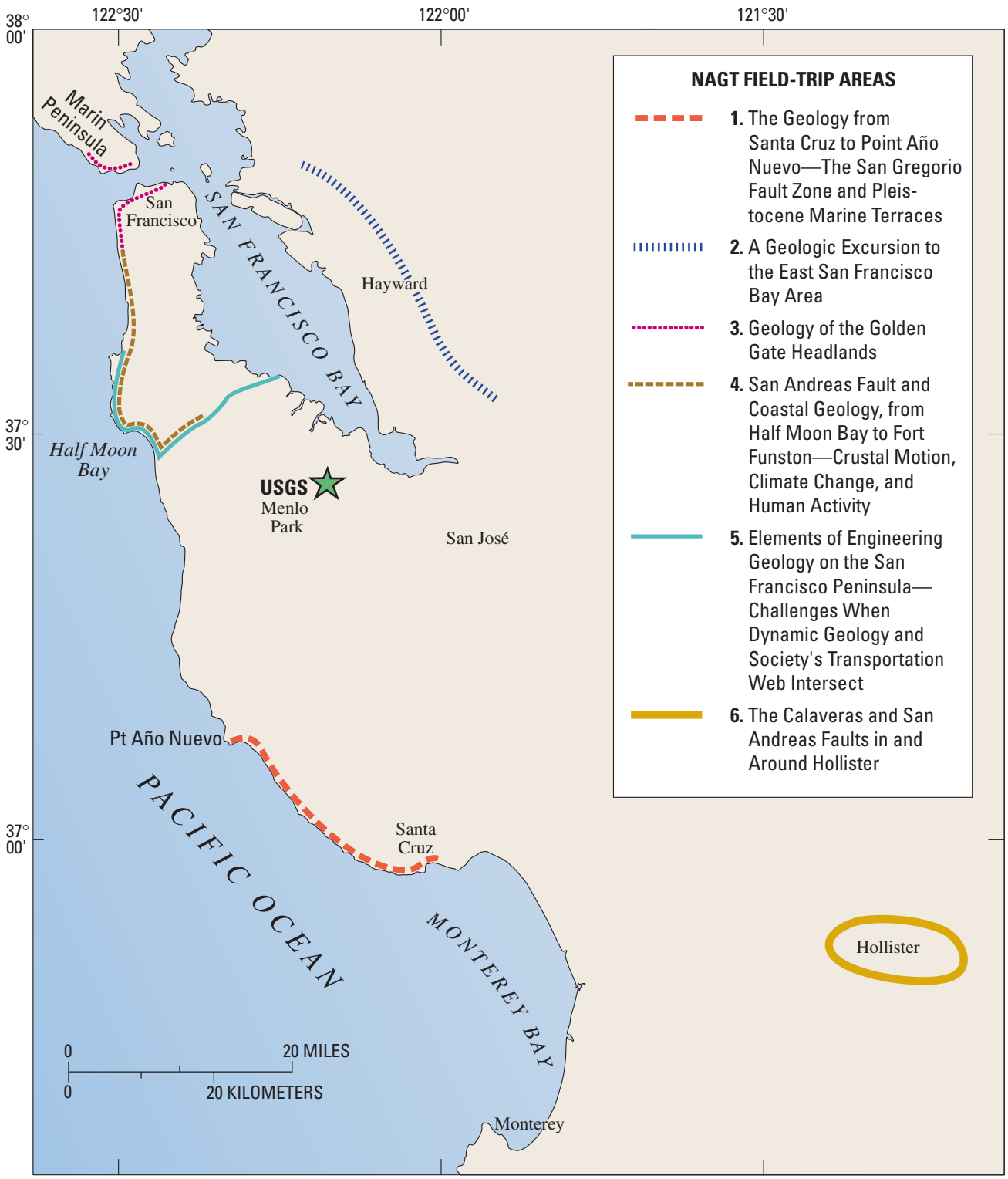

Map showing field-trip areas for the National Association of Geoscience Teachers, Far Western Section, 2001 Fall Field Conference.

Cover: Satellite image of San Francisco Bay area processed by Michael J. Rymer, USGS. Data from Landsat 5, path 44, row 34, bands 7, 4, and 2 in a respective red, green, and blue (RGB) assemblage. Date of imagery November 30, 1991.

U.S. Department of the Interior
U.S. Geological Survey

Geology and Natural History of the San Francisco Bay Area

A Field-Trip Guidebook

2001 Fall Field Conference
National Association of Geoscience Teachers
Far Western Section

September 14–16, 2001
Menlo Park, California

U.S. Geological Survey Bulletin 2188

Philip W. Stoffer and Leslie C. Gordon, Editors

U.S. Department of the Interior
Gale A. Norton, Secretary

U.S. Geological Survey
Charles G. Groat, Director

U.S. Geological Survey, Reston, Virginia: 2001

Electronic copies of the guidebook are available online at:
http://pubs.usgs.gov/bul/b2188/

Additional USGS publications can be found online at
http://www.usgs.gov/pubprod/

For more information about the USGS and its products:
Telephone: 1–888–ASK–USGS
World Wide Web: http://www.usgs.gov/

Published in the Western Region, Menlo Park, California
Manuscript approved for publication, August 20, 2001
Text and illustrations edited by James W. Hendley II and Peter H. Stauffer
Production by Sara Boore and Susan Mayfield

Table of Contents

Preface

A National Association of Geoscience Teachers Far Western Section (NAGT-FWS) field conference is an ideal forum for learning about the geology and natural history of the San Francisco Bay area. We visit classic field sites, renew old friendships, and make new ones. This collection of papers includes field guides and road logs for all of the Bay-area trips held during the NAGT-FWS 2001 Fall Field Conference and supplemental chapters on other aspects of the area's natural and human history. The trips touch on many aspects of the geology and natural hazards of the Bay area, especially urban problems associated with living on an active tectonic plate margin: earthquake faults, coastal erosion, landslides, and the utilization of land and natural resources. We hope this conference not only provides a two-day learning opportunity for conference participants but that students and educators will use this field guidebook for future teaching and research.

Many thanks are due to the U.S. Geological Survey (USGS) and San José State University (SJSU) for cohosting the conference. We are grateful to each of the field trip leaders for preparing the trips and writing the accompanying guides. We especially appreciate the many hours put in by the guidebook reviewers, Robert I. Tilling (USGS) and Paula Messina (SJSU), and to the USGS Western Publications Group for editing, layout, and web posting. Additional guidebook contributions include articles by John Galloway, Scott Starratt, Page Mosier, and Susan Toussaint. During the conference guest speakers include Robert I. Tilling (USGS Volcano Hazards Team) and Ross Stein (USGS Earthquake Hazards Team). Workshops prepared for the conference include GIS in the classroom, using USGS data by John Vogel (USGS) and Paula Messina (SJSU), and The Best of BAESI (Bay Area Earth Science Institute), a teacher training organization under the direction of Ellen Metzger (SJSU) and Richard Sedlock (SJSU). The conference provides an opportunity to showcase USGS scientific and education resources with self-guided tours of the USGS Library, the Earth Science Information Center (ESIC), the Visitor Center, and various laboratories on the USGS campus and includes a half-day participatory tour of the USGS research vessel the R/V *Polaris* and the USGS Marine Facility at the Port of Redwood City under the direction of Cynthia L. Brown, Francis Parchaso, and Tara Schraga. Beyond the names mentioned above, a host of USGS and SJSU staff, SJSU students, and NAGT-FWS members contributed to the preparation and orchestration of the conference. We couldn't have done it alone.

Leslie C. Gordon (USGS), Philip W. Stoffer (USGS), and Deborah Harden (SJSU)
NAGT-FWS 2001 Fall Field Conference Organizers

The Geology from Santa Cruz to Point Año Nuevo— The San Gregorio Fault Zone and Pleistocene Marine Terraces

Gerald E. Weber
University of California, Santa Cruz, Calif.

Alan O. Allwardt
Geologic Consultant, Santa Cruz, Calif.

Introduction

On this field trip, we will illustrate two aspects of the tectonic unrest along the coastline between Santa Cruz and Point Año Nuevo: (1) late Quaternary activity in the San Gregorio Fault Zone at Año Nuevo State Reserve and (2) Pleistocene marine terraces in the vicinity of Wilder Ranch State Park, formed in response to regional uplift and fluctuating sea level. Among the topics of discussion will be rates of soil development on the terrace surfaces, techniques for dating terrace sequences and determining rates of uplift, and problems in using offset Pleistocene strandlines to estimate slip rates across the fault zone.

Our goal in scheduling only two field trip stops is to maximize the time spent outside the bus. For much of the day we will be walking and examining outcrops on State Parks land, where sample collecting is prohibited. However, the quality of the exposures will more than compensate for this handicap. Time permitting, we may also visit some of the optional field-trip stops described in the road log, which will provide additional background on the geology and cultural history of this stretch of coastline.

The San Gregorio Fault Zone (SGFZ) is the principal fault west of the San Andreas Fault Zone (SAFZ) in central California and is part of the larger San Andreas Fault system, representing the active tectonic boundary between the Pacific and North American lithospheric plates (fig. 1.1). At its type locality at Point Año Nuevo, the SGFZ is 2 to 3 km wide and includes seven fault strands with late Quaternary activity. From here, the SGFZ has been traced northward to its juncture with the SAFZ near Bolinas Lagoon in Marin County and southward across Monterey Bay, a cumulative length approaching 200 km (125 miles). Based on its dimensions and late Quaternary activity, this fault zone appears to be a potential source of significant earthquakes and has been assigned a 7.3 M_{max} (Petersen and others, 1996).

Based on cross-fault matches, Clark (1998) infers 150 to 160 km of cumulative dextral (right-lateral) slip on the SGFZ, whereas Burnham (1998) postulates between 150 to 185 km of dextral slip. Sedlock and Hamilton (1991) suggest 150 km of dextral slip between the early Paleocene and Miocene, but only 5 km of dextral slip during the late Cenozoic (Neogene). Clark (1997), on the other hand, suggests that slip on the SGFZ was initiated about 10 Ma (late Miocene) with the following rates:

Time Interval	Displacement	Slip Rate
10 to 8 Ma (late Miocene)	50 to 60 km	25 to 30 mm/yr
8 to 3 Ma (late Miocene-late Pliocene)	81 km	16 mm/yr
3 to 0 Ma (late Pliocene-Holocene)	19 km	6 mm/yr

The post-late Pliocene slip rate of 6 mm per year falls within the slip-rate estimates for late Quaternary of Weber and others (1995): 5 to 9 mm per year, based on offset marine terraces and offset streams on alluvial fans at Point Año Nuevo. Exploratory trenching of the eastern, onland trace of the SGFZ at Seal Cove indicates a post-late Pleistocene slip rate of 3.5 to 4.5 mm per year for the SGFZ (Simpson and others, 1997). This is a minimum rate because it does not include the western, offshore strand of the SGFZ. The addition of dextral slip from the SGFZ to the SAFZ may also explain why the present-day slip rate along the SAFZ northwest of their juncture in Marin County appears to be greater than that on the San Francisco Peninsula segment of the SAFZ.

A major unresolved question for seismic hazard analysis is the location of the southern terminus of the SGFZ in central coastal California and its postulated continuity with the Hosgri Fault Zone (HFZ). Most workers have followed Silver (1978) and Graham and Dickinson (1978), who postulated that the SGFZ is linked, via a segment of the Sur Fault Zone, with the HFZ (fig. 1.1). Greene and others (1973), alternatively, have suggested that the

SGFZ curves inland south of Monterey Bay to join the Palo Colorado Fault in the northern Santa Lucia Range.

A related problem is the apparent discrepancy between recent estimates of cumulative offsets on the SGFZ and the HFZ. For example, Dickinson's (1996) reconstruction infers 156±8 km of dextral slip on the SGFZ and 110±5 km of slip on the HFZ. One hypothesis explaining this discrepancy is that the shear to the south is distributed along en echelon faults within the Santa Lucia Range, rather than being restricted to a continuous, offshore HFZ.

This trip will examine some of the field evidence for recent faulting along the SGFZ at its type locality near Point Año Nuevo, in western San Mateo County. The bus will pass through Santa Cruz and, after stopping near the western boundary of Wilder Ranch State Park, follow the coastline northward to Año Nuevo State Reserve (fig. 1.2). We will discuss recent (and not so recent) onshore work relating to problems of the SGFZ, including (1) marine terrace stratigraphy, ages, and cross-fault correlation, (2) Neogene stratigraphic contrasts across the SGFZ in the central Santa Cruz Mountains, including the postulated offset of a thick upper Miocene unit (Santa Cruz Mudstone), and (3) late Pleistocene and Holocene deformation along the SGFZ at Point Año Nuevo.

Approaching Santa Cruz by Highway 17

As we approach Santa Cruz on Highway 17, the bus will take the Highway 1 off-ramp and head through town. About a quarter-mile to the west, we will cross the San Lorenzo River bridge.

San Lorenzo River. To the left (south) is downtown Santa Cruz. The downtown area is built on the floodplain of the San Lorenzo River, underlain by soft, unconsolidated Holocene sediments that back-filled the ancestral San Lorenzo Valley during the rise in sea level associated with the end of the Wisconsin glaciation. During the Wisconsin glaciation, the San Lorenzo River channel had become incised about 20 to 30 meters (or more) below its current elevation in this area, in response to a sea level that was about 100 meters lower than present.

During both the April 18, 1906, and October 17, 1989, earthquakes downtown Santa Cruz suffered partial to nearly complete collapse of many older, unreinforced brick and masonry buildings. The higher intensity shaking in the downtown area resulted from the unconsolidated substrate. Ground cracking related to lateral spreading, along with other liquefaction phenomena, occurred in this area during both earthquakes.

At the intersection of Highway 1 and Highway 9/River Street (first traffic light), the bus will continue straight ahead.

Mission Street intersection with Highway 1 (second traffic light). The bus will turn right and continue west on Mission Street/Highway 1. We have now climbed above the floodplain of the San Lorenzo River to the Santa Cruz terrace. Most of the city of Santa Cruz is built on this terrace, both east and west of the San Lorenzo River floodplain. The geologic setting of the terrace—a thin layer of well-drained sands and silts overlying firm to hard bedrock—resulted in a reduced level of seismic shaking in 1989, when compared to the floodplain of the San Lorenzo. Although numerous chimneys were knocked down, most buildings on the terrace sustained only minor damage during the Loma Prieta earthquake.

From this point north to Waddell Creek, Highway 1 lies near the back edge of the Santa Cruz terrace of Bradley and Griggs (1976), the first (lowest) of five prominent marine terraces cut into the southwestern flank of Ben Lomond Mountain (fig. 1.3). The modern seacliff, the first emergent terrace, and also most of the older, higher terraces from here north to Point Año Nuevo are cut into a single rock type—the Santa Cruz Mudstone, a hard, blocky fracturing, siliceous mudstone of Delmontian age (late Miocene). The marine terraces are essentially undeformed from Santa Cruz to Point Año Nuevo, except for some minor warping, tilting and fault offset near Greyhound Rock. Two terraces (the Wilder and Cement terraces) are discontinuous and are not present along the entire coastline (fig. 1.3).

Bay Street. The University of California Santa Cruz campus lies about 1 mile to the north (right), on one of the few well-developed karst landscapes in California. Between here and Almar Street we will cross the surface trace of the Ben Lomond Fault, the structural element that bounds Ben Lomond Mountain on the north and east. The late Tertiary through middle Pleistocene vertical slip on this fault (west side up, east side down) is between 300 and 600 meters; however, there is no evidence of offset in the marine terrace deposits or the wave-cut platform (wcp) of the Santa Cruz terrace, as exposed in the seacliff near Almar Street. Stanley and McCaffrey (1983) argue that the wcp is offset about 2 to 3 cm, but they agree that the terrace deposits are not offset. Consequently, the Ben Lomond Fault may display movement since the formation of the abrasional platform but no movement since the deposition of the shallow marine sands; these observations suggest the possibility of a brief episode of minor movement approximately 80,000 years ago (see discussion of terrace ages, below).

Road Log: Santa Cruz to Point Año Nuevo

For this field trip our mileage log will begin at the intersection of Highway 1 and Almar Street in westside Santa Cruz.

Mileage/Notes

0.0 **Almar Street.** Highway 1 bends to the right at the three-way traffic light. Safeway lies to the southwest (left) of Highway 1. As we head north, note the steep slope on the right (northeast), which is the erosionally modified, ancient seacliff at the back edge of the Santa Cruz terrace (see figure 1.4 for an explanation of terrace terminology). Two wave-cut platforms have been tentatively identified within the Santa Cruz terrace in this area (fig. 1.5). Fossil mollusks exposed in the seacliff at Point Santa Cruz have yielded an average U-series age of 86,500 years B.P. (Bradley and Addicott, 1968) and an amino-acid racemization age of about 85 ka for the lower, Davenport platform. These dates on fossil material suggest that the Davenport platform was created during the sea-level high stand corresponding to oxygen isotope stage 5a, dated 80 to 83 ka by most workers (see discussion of Stop 1, below). In contrast, shell fragments from a basal lag recovered in a boring near the inner edge of the terrace displayed a cold water fauna and an amino-acid racemization age estimate of 103 ka. This suggests that, in west Santa Cruz, the upper wave-cut platform within the Santa Cruz terrace is the so-called Highway 1 platform, created during the sea-level high stand corresponding to oxygen isotope stage 5c (103 to 105 ka). The two wave-cut platforms within the Santa Cruz terrace are apparently separated by a 1-to-2 meter seacliff, which is buried by the continuous alluvial apron that forms the topographic surface of the terrace.

Because the Cement terrace is absent in the Santa Cruz area, the next highest terrace surface here is the Western terrace of Bradley and Griggs (1976), visible northeast of Highway 1 as a series of erosionally dissected topographic flats above the 103 to 105 ka seacliff. The age of the Western terrace is estimated to be approximately 213 ka (oxygen isotope stage 7). Between Santa Cruz and Point Año Nuevo, the marine terraces of Ben Lomond Mountain lie within a single structural block, the Santa Cruz Mountains structural block (Weber and Lajoie, 1979; Weber, 1980), which lies east of the San Gregorio Fault Zone. Marine terraces within this structural block are undeformed except for a broad, shallow anticlinal flexure in the terrace near Greyhound Rock.

1.0 **Moore Creek.** This creek and other large streams along this segment of the Santa Cruz County coast eroded their bedrock canyons to the Wisconsin low stand of sea level, 100 to 115 meters (300 to 350 feet) below present sea level. The Holocene rise in sea level flooded the lower reaches of these streams, resulting in alluviation of the stream valleys. Small lagoons formed at the mouths of these streams as they became dammed by a combination of storm berms and small aeolian dunes.

Coastal Erosion Rates. Measured rates of cliff retreat along this section of coast are generally less than 1 foot per year (Griggs, 1979). Along the Santa Cruz County coast from Almar Street north to the San Gregorio Fault Zone at Point Año Nuevo, the modern seacliff has formed in the late Miocene Santa Cruz Mudstone. Consequently, the rock type under wave attack in the surf zone is essentially uniform along this entire stretch of coastline, except for a few scattered sandstone dikes.

2.7 **Sandy Flat Gulch.** Late Miocene Santa Margarita Sandstone is quarried for construction sand on the northeast (right) side of the road. The roadcut exposes Quaternary colluvium overlying Santa Cruz Mudstone, as Highway 1 is built just above the Santa Cruz terrace on the colluvial wedge at the base of the 103 to 105 ka seacliff. Between here and Davenport the first three marine terraces and occasionally the fourth terrace are visible from the highway.

5.3 Stop 1—Ben Lomond Mountain Marine Terraces

Information on Stop 1

Introduction

We will be walking up the road beyond the gate to examine the Western, Wilder, and Blackrock terraces. Upon reaching the Wilder terrace, take the right fork in the road and note the intricate flow structures in the asphalt: this is one of the oldest paved roads in Santa Cruz County, utilizing locally quarried bituminous sandstone. For a brief history of these asphalt quarries, which date back to the late 1880's, see the discussion below on Majors Creek (milepost 5.8 on the road log).

Since the initial study of Rode (1930), the exceptionally well-preserved Ben Lomond Mountain marine terrace sequence has been the subject of numerous studies and reinterpretations. These include Bradley (1957, 1958), Bradley and Griggs (1976), Lajoie and others (1979), Hanks and others (1984), Lajoie (1986), Weber (1990a, b), Anderson (1990, 1994), Anderson and Menking (1994), Anderson and Weber (1990), Lajoie and others (1991), and Weber and others (1995).

To summarize briefly, the terrace sequence consists of six marine terraces cut into the slowly rising coastline by successive high stands of sea level during the Pleistocene. Terrace names, elevations, estimated ages and estimated uplift rates for the Davenport area are shown in table 1.1.

Table 1.1. Marine terraces on Ben Lomond Mountain (Santa Cruz Mountains structural block)—elevations, estimated ages and estimated uplift rates.

Marine terrace	Elevation (m)	Estimated age (ka)	Paleosea level (m)	Tectonic uplift (m)	Uplift rate (m/k.y.)
Santa Cruz					
DAV	17	80	-19	36	0.45
Hy 1	32	105	-9	41	0.39
GRX	40	sp			
Cement	58	125	+ 6	52	0.42
Western	92	213	- 5	97	0.46
Wilder (p)	140	320	0	140	0.44
Blackrock	190	430	0	190	0.44
Quarry	240	545 ?	0	240	0.44

DAV, Davenport wave-cut platform;
Hy 1, Highway 1 wave-cut platform;
GRX, Greyhound rock wave-cut platform;
p, shoreline angle elevation projected

Bradley and Griggs (1976) describe the lowest emergent terrace (Santa Cruz terrace) as containing three separate wave-cut platforms and shoreline angles named, from youngest to oldest, the Davenport, Highway 1, and Greyhound Rock wave-cut platforms (note: only one terrace, but three abrasional surfaces). Although not specifically stated, Bradley and Griggs (1976) imply that each of these platforms was formed by surf erosion during a separate sea-level high stand. More recent investigators have concluded that the Greyhound Rock abrasional surface is simply a localized shore platform associated with the Highway 1 wave-cut platform (Weber and others, 1995).

The areal extent of the terraces on the flank of Ben Lomond Mountain is shown in figure 1.3. The Santa Cruz terrace forms the broad, extensively cultivated bench closest to the ocean. Highway 1 lies along the back edge of this terrace between Santa Cruz and Waddell Creek. The Santa Cruz terrace is late Pleistocene in age, probably having formed during the Sangamon interglacial (oxygen isotope stage 5). The higher terraces are all older, ranging in age from about 213 ka for the Western terrace to possibly 545 ka for the Quarry terrace. The older terraces are not continuous along the entire coastline and show successively greater erosional modification and dissection with age and elevation. Note that the Wilder terrace is not preserved north of Laguna Creek, and the Cement terrace is restricted to the immediate vicinity of Davenport.

Determination of Marine Terrace Ages

Despite their excellent geomorphic expression and preservation, there are no indisputable absolute age determinations for any of the terraces (the previously cited dates on fossil material notwithstanding). We know that each terrace must have formed in response to a period of sea-level rise culminating in an interglacial high stand, but we cannot unambiguously correlate this particular sequence of terraces with the known high stands in sea level. Traditionally, any attempt to date a succession of marine terraces has required an assumed age for at least one terrace in the sequence, coupled with an

unknown but *constant* rate of uplift throughout the late Quaternary. These assumptions allow the researcher to match, by trial and error, the spatial sequence of the terraces with the independently derived, temporal sequence of sea-level high stands. The best fit yields both the ages of the terraces and an estimate of the uplift rate. This procedure is analogous to the way magnetic stripes on the sea floor could be correlated with the known sequence of geomagnetic polarity reversals, thus providing an estimate of the spreading rate (see Glen, 1982).

Accordingly, we have estimated the ages of the terraces by comparing their shoreline angle elevations to the known high stands of sea level in the Pleistocene, using the method described by Lajoie (1986). Because each episode of terrace cutting must be linked with a period of rising sea level, each shoreline angle must be associated with a high stand (strandline). Consequently, dating a particular strandline is reduced to correlating it with a peak in an established sea-level curve (fig. 1.6). In our analysis, we have used what is probably the most detailed datum from which to determine terrace ages, the sea-level curve obtained by subtracting tectonic uplift from the record of emergent coral-reef strandlines (terraces) on the Huon Peninsula of Papua, New Guinea. This terrace sequence, accurately dated using U-series techniques on corals, provides a reliable estimate of global sea-level fluctuations back to about 340 ka (Bloom and others, 1974; Chappell, 1983).

We approximated the ages of terraces on Ben Lomond Mountain using the simple graphic technique of Lajoie (1986) and the New Guinea sea-level curve. Shoreline angle elevations are plotted on the vertical axis, and lines are drawn between the shoreline angle elevations and the sea-level high stands. If uplift rates have been constant, all the lines connecting shoreline angle elevations to sea-level high stands will be parallel (see fig. 1.6). If uplift has not been constant during the late Pleistocene (the last 0.5 to 1.0 m.y.), the lines should diverge and not be parallel.

Discussion: Terrace Ages and Uplift Rates

The graphic technique described above does not produce a unique solution for terrace ages and uplift rates on Ben Lomond Mountain. This stems from the absence of an indisputable, independently determined age date for at least one of the terraces. Two contrasting interpretations of terrace ages and uplift rates are shown in table 1.2. A low uplift rate (0.21 m/k.y.) is envisioned by Lajoie and others (1991), whereas both Hanks and others (1984) and Weber and others (1995) suggest a higher uplift rate, 0.41 to 0.44 m/k.y. The Lajoie and others (1991) assignment of terrace ages is similar to that of Bradley and Griggs (1976), with the Highway 1 platform 125 ka in age and the Western terrace about 430 to 450 ka in age. (The Greyhound Rock wave-cut platform would represent the 213 ka strandline in their scheme.) Anderson and Menking (1994), using a more formal analysis, indicate that either of the uplift rates can be used to explain the coast-parallel pattern of shoreline angle elevations for the terraces. We prefer the higher uplift rate interpretation, because it appears that the Greyhound Rock wave-cut platform is a shore platform and not a paleo-strandline as envisioned by Lajoie and others (1991).

Table 1.2. Marine terraces of Ben Lomond Mountain—alternative interpretations of terrace ages and uplift rates in the Davenport area.

Marine terrace	Hanks and others, 1984 Uplift rate: 0.41 m/k.y.	Lajoie and others, 1991 Uplift rate: 0.21 m/k.y.	Weber and others, 1995 Uplift rate: 0.42 to 0.44 m/k.y.
Santa Cruz Hy 1	104 ka	124 ka	105 ka
Cement	120 ka	320 ka	125 ka
Western	230 ka	430 ka	213 ka
Wilder (proj.)	370 ka	800 ka	320 ka
Blackrock	450 ka	1000 ka	430 ka
Quarry	650 ka?	1300 ka	545 ka?

Recently, a completely different approach to dating the Ben Lomond Mountain marine terraces has been taken by Perg and others (in press), leading them to postulate dramatically higher uplift rates in the range of 1.1 m/k.y. Utilizing the relatively new technique of "surface-exposure dating," they sampled the five successive terraces northwest of Santa Cruz and measured the concentrations of two cosmogenic radionuclides, beryllium-10 and aluminum-26, in the soil profiles developed on the terrace deposits. Cosmogenic radionuclides (CRNs) are produced at constant rates in the upper atmosphere and accumulate steadily on any exposed surface that remains undisturbed (such as a marine terrace). Knowing the atmospheric production rate and the half-life of a CRN makes it possible to date the surface in question, provided that several additional parameters are taken into account. Foremost among these complicating factors are the initial concentration of the CRN in the parent material and subsequent mixing in the upper soil horizons.

The preliminary CRN dates suggest that the Ben Lomond Mountain terraces are significantly younger than previously thought. Perg and her colleagues, for instance, correlate the Santa Cruz terrace with oxygen isotope stage 3 (about 60 ka) rather than stages 5a, 5c, or 5e (80 to 125 ka), and they shift the entire sequence of terraces accordingly. The resulting uplift rates are two to three times higher than those proposed by researchers using conventional methods for estimating the terrace ages. Methodology aside, the CRN data cited above may be subject to alternative interpretations requiring a less drastic revision of the older models. Conceptually, the ultimate goal is to correlate a given shoreline angle with an independently documented high stand in sea level, but the CRN technique provides only a minimum age for this purpose since the surface being dated is not the wave-cut platform itself but the top of the terrace deposits. Moreover, CRN dating simply indicates when a terrace surface became *stabilized*, raising questions regarding the extent to which the terrace deposits might have been reworked as sea level dropped. Until these issues are resolved—and until the initial CRN terrace dates are either corroborated or refuted by additional data covering a wider area—we will continue advocating a more traditional view of the terrace ages and have written this guide accordingly.

Correlating Marine Terraces between the Santa Cruz Mountains and Pigeon Point Structural Blocks

Six marine terraces are clearly recognizable on the Pigeon Point structural block, which lies west of the SGFZ. The names of these terraces, their probable ages, and estimated uplift rates are shown in table 1.3. Prior to re-mapping of the terraces by Weber and others (1995), none of the terraces older than the Western terrace had been successfully correlated across the fault zone. Based on this re-interpretation, however, it now appears that the Pigeon Point terrace sequence can be correlated with the Ben Lomond Mountain terrace sequence as shown in table 1.4. Note that, except for the Cement terrace, there is one-to-one correlation between the terraces east and west of the SGFZ (see also fig. 1.7). The absence of the Cement terrace west of the fault zone is not surprising, since it occurs along only 3 km of coastline east of the fault zone, near Davenport, where it is both discontinuous and narrow. This correlation of marine terraces across the SGFZ allows estimation of late Quaternary crustal uplift rates, as well as both horizontal and vertical slip rates along the SGFZ. However, we emphasize the highly interpretative nature of both the terrace ages and uplift rates.

Table 1.3. Marine terraces in the Pigeon Point structural block—elevations, estimated ages and estimated uplift rates.

Marine terrace	Elevation (m)	Estimated age (ka)	Paleosea level (m)	Tectonic uplift (m)	Uplift rate (m/k.y.)
Año Nuevo	7 to 9	80	- 19	28	0.35
Pigeon Pt.	24	105	- 9	33	0.31
Bolsa	61	213	- 5	66	0.31
Gazos	90	320	0	90	0.28
YJ	122	430	0	122	0.28
Mesa	153	510 ?	0	153	0.30

Table 1.4. Correlation of marine terraces and/or wave-cut platforms (wcp) across the San Gregorio Fault Zone

Santa Cruz Mountains Structural Block	Pigeon Point Structural Block
Santa Cruz Terrace	
Davenport wcp	Año Nuevo Terrace
Highway 1 wcp	Pigeon Point Terrace
Cement Terrace	(absent)
Western Terrace	Bolsa Terrace
Wilder Terrace	Gazos Terrace
Blackrock Terrace	YJ Terrace
Quarry Terrace	Mesa Terrace

Uplift Rates

Quaternary uplift rate of the Santa Cruz Mountains structural block, as deduced from terrace elevations on the flank of Ben Lomond Mountain, is not uniform. Anderson and Menking (1994) discuss possible explanations for nonuniform rates, including the hypothesis that the coastline is being transported horizontally past a localized area of uplift. In our analysis we calculated uplift rates in the vicinity of Davenport, where the uplift has been uniform parallel to the coast and has averaged between 0.42 and 0.44 m/k.y. The uplift rate is slightly higher to the northwest, near Greyhound Rock, and somewhat lower to the southeast of Davenport. Another reasonable interpretation of the uplift rate in the Davenport area is 0.21 m/k.y., as suggested by Lajoie and others (1991) and Anderson and Menking (1994). The uplift rate for the Pigeon Point structural block (across the SGFZ) is most likely about 0.3 m/k.y. near Pigeon Point, decreasing slightly to the north and increasing slightly to the south. Another reasonable interpretation of uplift rate in this area is 0.15 m/k.y., which also explains the vertical spacing of the terraces. Figure 1.8 shows our preferred interpretation of these geographic variations on a "tilted shoreline" plot (after Lajoie and others, 1991).

Mileage/Notes

5.8 **Majors Creek.** The black-colored cliffs to the right (up Majors Creek) are composed of bitumen-saturated sandstone that was injected into the overlying Santa Cruz Mudstone in a liquid state. Numerous sandstone dikes and sills, most of which contain some bituminous material, are exposed in the modern seacliff between Wilder Creek and Greyhound Rock. The Santa Margarita Sandstone, the source of these intrusions, contains varying amounts of bitumen throughout its outcrop area, from Santa Cruz to the vicinity of Big Basin State Park. The hydrocarbons are believed to have migrated into the Santa Margarita Sandstone from the underlying Monterey Formation.

The bituminous sandstones in this area have been mined since the late 1880's for paving material. The asphaltic content of the sand ranges from about 4 percent to as much as 18 percent by weight. These oil-impregnated layers vary from 1 to 40 feet in thickness and range in character from dry and brittle to soft and gummy. In some outcrops, tar will drip or flow out of the bituminous sands when sufficiently warmed by the sun. San Francisco streets were reportedly paved in the 1890's with bituminous sandstone mined near Majors Creek and transported to San Francisco by boat. An estimated 614,000 tons of asphaltic paving material, worth approximately $2,360,000, was produced from this area between 1888 and 1914 (Page and Holmes, 1945). Production was intermittent after the 1920's, with the last of the quarries (Calrock Quarry) ceasing operations in the 1940's. Page and Holmes (1945) estimated reserves of approximately 9.8 million cubic yards of asphaltic sand in the area west of Santa Cruz. This sand contains approximately 10 million barrels of asphalt. In oilfield terms, this is about 24 gallons of bitumen per ton, or equivalent to a tar sand with 38 percent porosity, 53 percent oil saturation, and a recovery factor of 1,562 barrels of oil per acre-foot.

Oil and Gas Production at Majors Creek

In 1955, Husky Oil Company, in partnership with the Swedish Shale Oil Company, began an experimental project to adapt the Swedish company's Ljungstrom method to the recovery of hydrocarbons. It was a thermal recovery experiment, utilizing down-hole, gas-fired burners to perform in-situ retorting. In the fall of 1957, Union Oil Company of California joined in the project. During the next 3 years, a total of 228 burner-producer wells, 78 temperature observation wells, 31 gas wells, and 32 miscellaneous wells were drilled (most of them on the Blackrock and Quarry terraces, where the oil-saturated sandstone was encountered immediately below the terrace deposits). The bituminous sandstone in these locations generally lay 8 to 10 feet below the surface and was about 40 feet thick in its saturated section, averaging about 8 percent by weight of 4-degree gravity tar throughout.

Wells were typically drilled in a triangular pattern on a ten-foot spacing to an average depth of 53 feet. They were completed with 14 feet of 4-inch surface pipe and 50 feet of 2-7/8 inch casing. Underground heaters fueled by propane were used in the heating phase of the test, with down-hole temperatures reaching 600 degrees F. The test area was heated from a depth of 15 to 45 feet, with much of the crude oil vaporizing. Products produced in a vapor form were condensed using a water-cooled condenser. The heating phase was completed in January of 1959, with a total production of 2,665 barrels of oil, 4,520 thousand cubic feet (Mcf) of gas, and 9,232 barrels of water. Average gravity of the recovered oil was 27 degrees. The operator reported that in zones 30 feet thick, a recovery of about 18,000 barrels per acre could be achieved—a recovery of 38 percent of the oil in place. Although this is a respectable recovery factor (similar to some steam stimulation projects), it is doubtful that such an operation could be economical because of high heat losses and high fuel costs.

Mileage/Notes

6.1 **Back Ranch Road.** Private road to the right (under the suspended pipe). Note the bituminous sandstone dikes exposed in the road cut; one of the larger, abandoned asphalt quarries in Santa Cruz County is located along Back Ranch Road. Until recently, Santa Cruz Biotechnology operated a large goat ranch up this road for medical research, but the California Coastal Commission shut down the operation amid concerns about runoff contaminated by manure.

To the left, an isolated hill near the edge of the modern seacliff is a stabilized Holocene sand dune (Sand Hill Bluff). It is capped by a 1-meter-thick midden deposit containing remains of an extinct flightless scoter (*Chendytese*, a type of sea duck). The dune is dated at 3,500 to 5,000 years old by ^{14}C analysis of marine shells from the midden deposit. It is possible that the bird became extinct as a result of hunting by the coastal Native Americans.

The development near the hill is Pacific Mariculture's Abalone Farm. The project will ultimately consist of 400 abalone grow-out tanks under 2.5 acres of shade cloth structure. Raising abalone to commercial size (4 inches) takes about 3 to 4 years. Production is projected to reach 500,000 red abalone per year, yielding about 170,000 pounds of meat. The abalone will be fed a mixture of kelp and commercial feed, with the kelp harvested by hand from kelp beds off the coast.

As we drive past the intersection of Old Coast Highway and Highway 1, note the vertical contact zone in the road cut on the north side of Highway 1 (and also in the cut along Old Coast Highway). Hard siliceous bedrock of the Santa Cruz Mudstone is juxtaposed against moderately dipping colluvial deposits along a nearly vertical contact. This is the old 103 to 105 ka seacliff associated with the Highway 1 platform of the Santa Cruz marine terrace. The basal portion of the old seacliff is preserved by the accumulation of talus and colluvium at the base of the cliff. The upper half of the ancient seacliff has been eroded back. It is along this section of coast where Hanks and others (1984) used the profiles of the ancient seacliffs between terraces to develop their paper on scarp degradation.

North of this point the Wilder terrace is no longer preserved, having been destroyed by subsequent erosion during the formation of the Western terrace. Refer to figure 1.3.

7.7 **Yellow Bank Creek.** Large, complex sedimentary intrusions of Santa Margarita Sandstone, injected into the Santa Cruz Mudstone, are exposed in the seacliff near the mouth of the creek. Two higher terraces are visible out the window to the right (northeast).

8.5 Intersection of Highway 1 with Bonny Doon Road. We continue north on Highway 1. Bonny Doon Beach, to the left, is clothing optional, as are most north county beaches.

9.6 **Town of Davenport.** One of several historic, land-based whaling stations that existed along the central California coast during the late 1800's. Grey whales migrating from the Bering Sea to Baja California (and back again) each year pass close to shore at this location. During the whaling days, a lookout stationed at the top of the cliff watched for passing whales. When whales were spotted, an alarm was sounded and the whalers launched their skiffs from the shore. Slain whales were hauled to the beach where they were cut up and the blubber rendered locally in try pots. This method of hunting allowed the whalers to live on shore rather than spending the better part of each year at sea.

Just south of the town of Davenport, the Davenport and Highway 1 wave-cut platforms of the Santa Cruz terrace are exposed in the modern seacliff (see figure 8 of Bradley and Griggs, 1976). Recently, a careful examination of the Davenport wave-cut platform in its type locality suggests that it is actually a stream terrace of San Vicente Creek (Weber and others, 1995). Elsewhere, however, the original concept of the Davenport platform remains the most plausible explanation.

9.8 **RMC Pacific Materials Cement Plant.** Now operated by RMC Pacific Materials (formerly RMC Lonestar), this plant was built between 1905 and 1907, and has been a major producer of cement in the San Francisco Bay area. Limestone and siliceous mudstone are both quarried locally. The relatively pure limestone (actually marble) is quarried about 2 miles northeast of the plant and transported to the plant on a 2-mile-long enclosed conveyor belt. Energy for producing Portland cement is derived from low-sulfur bituminous coal mined in eastern Utah and shipped to the plant by rail. The plant was extensively remodeled in the 1970's, resulting in a great reduction in stack emissions, and is now one of the most advanced cement manufacturing operations in the world.

The railroad tracks are part of a rail system originally intended to connect Santa Cruz and San Francisco (Ocean Shore Railroad). In the early 1900's, the stretch between Davenport and Tunitas Creek (about 30 miles to the north) was graded, but the tracks were laid no farther north than Swanton siding (3 miles north).

10.4 **Molino Road.** We are now paralleling Cement Plant Road, to the right. The private side road off Cement Plant Road leads to the Molino Creek Farm and the old, now abandoned, limestone (marble) quarry operated by the predecessor of RMC Pacific Materials. Portland cement for the Golden Gate Bridge was allegedly produced from this quarry.

10.7 **Davenport Landing Road.** The road to Davenport Landing intersects Highway 1 on the left. It leads to a small group of residences at Davenport Landing and Silverking Oceanic Farms.

Water wells in the Davenport Landing area produce sizable amounts of methane gas with the water. Analysis of gas samples collected from a well at Davenport Landing indicated the gas contained 74 to 91 percent methane, <1 percent ethane, 7 to 23 percent nitrogen, and 2 percent carbon dioxide (Mullins and Nagel, 1982). The sampled well was drilled to a depth of 655 feet, with a standing water table near 330 feet. The gas is produced along with hot water (90° F, 32°C). The Silverking Oceanic Farms well may produce as much as 200 Mcf per day. At present, the gas is simply discharged to the atmosphere and is not used. The gas apparently originates in the Santa Cruz Mudstone, a siliceous organic mudstone, and is thought to be of thermogenic origin.

Cement Terrace. Note the narrow bench between the Santa Cruz and Western terraces. This marine terrace, called the Cement terrace, is present only between San Vicente Creek and Molino Creek (about 2 miles), near Davenport. As discussed earlier, it probably corresponds to the 125 ka high stand of sea level.

11.1 Swanton Road to the right; north end of the Davenport Landing Road loop to the left.

11.3 **El Jarro Point.** The terrace on both sides of the road was the proposed site of a Pacific Gas & Electric nuclear power plant in the late 1960's. The site was abandoned largely because of the close proximity of the active San Gregorio Fault Zone.

12.2 **Scott Creek.** Here we can observe a large drowned valley with a lagoon confined by sand dunes and a well-developed berm. The dune area near the mouth of the creek was once the site of a mushroom farm that was abandoned in the 1960's and torn down in the 1970's. At that time, the dunes were stabilized by extensive growths of thick beach-dune vegetation. However, off-road vehicles, such as 4-wheelers and dirt bikes, started using this beach, destroying the vegetative cover in about 2 years. This allowed the dunes to remobilize, and sand soon started to drift once again across Highway 1 (much to the "delight" of Caltrans). The beach was then closed to off-road vehicles. It is ironic that the vehicles barred from the beach are what returned the back berm to its original condition—drifting sand.

As we drive north out of the valley of Scott Creek, the road again climbs up onto the Santa Cruz terrace, following almost exactly the back edge (shoreline angle) of the Greyhound Rock platform of the Santa Cruz terrace. The terrace platforms in this area are covered with a thick wedge of colluvial and alluvial cover. From here north to Waddell Creek, there is only one higher terrace present—the Western terrace. Note that the gently sloping Santa Cruz terrace surface lies to the left (southwest) and that the roadcuts expose Santa Cruz Mudstone to the right (northeast).

North of Scott Creek, the Santa Cruz terrace is postulated to contain two wave-cut platforms, the Greyhound Rock platform (upper) and the Highway 1 platform (lower) of Bradley and Griggs (1976). We believe that this interpretation is incorrect. The Greyhound Rock platform is a shore platform or storm-wave platform, formed at the back edge of the Highway 1 wave-cut platform.

The seacliff is 140 to 160 feet high and nearly vertical along this portion of coast. The views are spectacular, but the cliff is dangerous. The local Davenport Voluntary Fire Department and Rescue Team rescues numerous unfortunate individuals each year who get "stuck" on the cliff face or are injured trying to climb the cliffs.

13.6 **Colluvium Filled Gullies.** At about 6 locations between Scott Creek and Greyhound Rock, small "V" shaped gullies filled with colluvium are present in road cuts. Fluvial deposits are absent and the colluvial deposits are crudely stratified subparallel to the sides of the "V" shaped channel. These gullies apparently formed following the culmination of the sea-level rise that formed the Highway 1 platform (103 to 105 ka). As erosion modified the original seacliff, some of the initial gullies expanded their drainage networks, developing into the small present-day streams. As the drainage system evolved, the smaller gullies—those that had lost the battle for drainage area—were abandoned and eventually filled with colluvium. Note there is no surface evidence (geomorphic or vegetative) of their presence, as the ground surface passes unbroken over these gully fills.

14.1 **Texas Oil Co. Poleti No. 1 (Optional Stop).** Immediately west of this point near the edge of the seacliff is the site of the deepest exploratory oil well drilled in Santa Cruz County: the Texas Oil Co., Poleti No. 1. Drilled between June and December of 1956 to a depth of 9,201 feet, the well penetrated 9,135 feet of sedimentary rocks (mostly Santa Cruz Mudstone) before entering granitic basement. The target of the drilling was the Santa Margarita Sandstone, about 300 feet thick near the bottom of the hole, which proved to be dry. Apparently, the Texas Oil Co. was looking for the up-dip edge of a stratigraphic pinchout of the Santa Margarita Sandstone on the west limb of the Davenport syncline—or for a bowing of beds against a branch of the SGFZ.

The Santa Cruz Mudstone presents one of the most striking stratigraphic contrasts across the SGFZ: the mudstone is 8,850 feet thick (more than 2,700 meters) in Poleti No. 1, east of the fault zone, but is totally absent less than a mile offshore, west of the fault zone. Farther north, near Bolinas in Marin County, a lithologically similar section of Santa Cruz Mudstone is exposed in the seacliffs west of the juncture of the SGFZ and the San Andreas Fault. There, a composite section is estimated to be as thick as 2,000 meters (6,560 ft.) and has yielded benthic foraminifers including *Bolivina obliqua*, diagnostic of the late Miocene (Clark and others, 1984). Restoration of about 44 to 50 miles (70 to 80 km) of right slip on the SGFZ would juxtapose these thick Santa Cruz Mudstone sections.

Additional stratigraphic contrasts across the SGFZ are depicted in figure 1.9. Along the south shore of Point Año Nuevo, the missing late Miocene formations (Santa Margarita Sandstone and Santa Cruz Mudstone) are represented by an angular unconformity separating the siliceous Monterey Formation of middle Miocene age from Purisima Formation mudstone of early Pliocene age (Clark and Brabb, 1978). As much as 76 meters of Purisima Formation mudstone is exposed between this unconformity and the Green Oaks fault trace; farther east, between the Green Oaks and Coastways traces, sandstone beds of the Purisima Formation are discontinuously exposed in the seacliffs. These sandstone beds are folded and extensively faulted and are separated into two faunally distinct sections by the Frijoles Fault trace. The molluscan fauna from the section west of the Frijoles was believed by Branner and others (1909) to be similar to the type Purisima; in contrast, the section between the Frijoles and Coastways traces has yielded mollusks and echinoids diagnostic of the late Pliocene (Clark, 1981). The distinctiveness of this younger molluscan assemblage led Arnold (*in* Branner and others, 1909) to assign these sandstone beds to the Merced Formation instead, which in seacliff exposures south of San Francisco ranges in age from Pliocene (3.2 Ma) to Pleistocene (200 ka; A. M. Sarna-Wojcicki, written commun., 1996).

15.2 **Greyhound Rock (Optional Stop).** Time permitting, the bus will stop in the large, dirt parking area south of the actual turnoff for Greyhound Rock, and we will walk to the edge of the seacliff for a nice view to the northwest of Greyhound Rock, in the foreground, and Año Nuevo, in the distance. Greyhound Rock is a *tombolo*, an offshore rock connected to the beach by a sand spit. As exposed in the seacliff below the paved parking lot, the Highway 1 wave-cut platform is offset by the Greyhound Rock strand of the SGFZ. The Greyhound Rock strand actually consists of two discrete zones of faulting that offset the 103 to 105 ka wave-cut platform and the overlying terrace

deposits. The "eastern fault zone" lies almost directly below the parking lot and consists of three closely spaced, steeply dipping fault planes that offset the Highway 1 platform about 10 meters, with apparent normal motion. These faults are also exposed along the beach access road north of and below the parking lot, where they cut the marine terrace deposits.

A second, "western fault" is exposed below the access road to the beach, about 60 meters west of the eastern fault zone, and offsets the wave-cut platform and overlying marine terrace deposits about 1.5 meters vertically. However, the western fault is truncated by fluvial sediments overlying the marine terrace deposits. This fault was well exposed in the cut for the access road until it was buried by a small landslide in the early 1990's. Both the western fault and the eastern fault zone have been traced more than 300 meters to the northwest. Unfortunately, poor exposures away from the seacliff preclude conclusive demonstration that these are eastern branches of the main SGFZ. Nevertheless, it appears that the SGFZ consists of at least seven faults that offset the wave-cut platforms of the Santa Cruz terrace in a zone about 4.7 km (3 miles) wide.

Looking north toward Año Nuevo in the distance, the entire SGFZ is visible from this vantage point (fig. 1.10). The area of low cliffs delineates the small graben filled with the deposits of Año Nuevo Creek. The Frijoles Fault lies along the western side of this low area, forming the east-facing fault scarp. The Año Nuevo Creek Fault lies along the eastern side of the low area, in the valley of Año Nuevo Creek. The Coastways Fault lies in the next seacliff reentrant to the east. To the west of the Frijoles Fault, the Green Oaks Fault lies at the west end of the tall sandstone cliffs, and the Año Nuevo Thrust Fault lies west of the white cliffs. The westernmost faults, with demonstrable late Quaternary ground rupture, lie in the channel between Point Año Nuevo and the island. Their presence is confirmed by the Año Nuevo terrace, which lies some 3 to 4 meters (10 to 13 ft) higher in elevation on the island than on the point.

16.0 Swanton Road/Laguna de Las Trancas. Near the top of this ridge, east of Highway 1, a small pond (Laguna de Las Trancas) on a rotational landslide was cored and studied by Adam and others (1979). A piece of pine wood from a depth of 3.12 meters at the base of the core yielded a ^{14}C age of 29,500±560 years before present (B.P.). The core represents the period between roughly 5,000 and 30,000 years B.P. Pollen studies indicate that the flora and climate were significantly different during the Wisconsin glaciation that ended about 15,000 to 17,000 years ago. The presence of grand fir pollen suggests a southward displacement of floral zones by about 150 km. This was probably equivalent to a mean monthly temperature depression of 2 to 3°C and precipitation about 20 percent higher than at present. These changes apparently are valid only for the coastal area, reflecting the ameliorating effect of the ocean (but not the orographic effect of the Santa Cruz Mountains).

More recent pollen studies of two cores from Clear Lake, north of San Francisco Bay, indicate that Wisconsin climatic changes were far greater at inland locations. At Clear Lake temperatures were 7 to 8°C cooler during the Pleistocene, and precipitation was probably 300 to 350 percent of present (Adam and West, 1983). Wisconsin precipitation levels and temperatures in the Santa Cruz Mountains were probably somewhere between the values of Clear Lake and Laguna de Las Trancas.

16.4 Big Creek Lumber Company. The lumber mill on the right processes timber that has been selectively cut in the Santa Cruz Mountains. The lumber mill is built on the crest of a large, recently stabilized, late Holocene aeolian dune. This is part of a large stabilized dune ramp that extends from the beach at the mouth of Waddell Creek up onto the Santa Cruz terrace. Photographs from about 1900 indicate that the dune was active at that time.

17.0 Waddell Creek. This is another drowned valley. Just north of the creek, the high cliffs of Santa Cruz Mudstone (Waddell Bluffs) were originally undercut by waves. The highway, built in the 1940's, is entirely on artificial fill. These bluffs formed a natural barrier to coastal travel in the 1800's, when stagecoaches could pass the bluffs only during low tide on the wet beach. The southern tip of present-day San Mateo County was originally part of Santa Cruz County, but because access to the county seat in Santa Cruz was often impeded by this barrier, this land north of Waddell Bluffs was annexed by San Mateo County in 1868.

Debris that ravels down the cliff collects behind the cable netting on the eastern side of the road. This debris is periodically removed by Caltrans, stockpiled on the western side of Highway 1 and eventually dumped into the ocean to become part of the longshore drift of sediment to the south. Large rock falls are uncommon, probably because of the manner in which the Santa Cruz Mudstone weathers—by the raveling of small blocks and chips less than several inches in dimension. Occasionally, blocks the size of a small car fall and bounce onto Highway 1. About two decades ago, a passenger in a truck traveling north was killed by a rock that bounced through the front window, and litigation against Caltrans ensued for improperly maintaining the debris trap on the eastern side of Highway 1 (then a simple trench and berm). To reduce potential liability, Caltrans recently installed the Geobrugg steel wire rope net barrier, which seems to be working satisfactorily.

A resistant bed of siliceous mudstone is exposed in the surf zone and forms a natural groin at this location. The result is a protective beach up coast and active erosion down coast. Riprap was placed here in 1946 to protect Highway 1, then under construction. Because of its placement on a bedrock platform, this riprap has successfully protected the road for more than 50 years.

Poorly exposed at the top of the bluffs is the narrow remnant of a marine terrace, intermediate in elevation between the Santa Cruz and Western terraces, which is probably the Cement terrace. Exposed in the bluff is a broad anticlinal fold in the Santa Cruz Mudstone. The fold extends for several miles to the northwest, parallel to the trend of the San Gregorio Fault Zone. An unsuccessful exploratory oil well was drilled on this structure several miles north of here in 1956 (Seaboard Atkins No. 1, T.D. 3535).

18.7 Stop 2—Quaternary Faulting at Point Año Nuevo

Information on Stop 2

We will leave the bus and hike down the dirt road to the beach. From there we will hike north about 1.5 miles along the beach, examining the evidence for late Pleistocene and Holocene faulting. Bring your packs, water, and cameras. We will meet the bus in the parking lot for the Año Nuevo State Reserve. Please note that the road is on private property. If you are taking this trip at any time other than September 15, 2001, you must obtain a permit from Coastways Ranch to enter the property. Once we enter the State Reserve, sample collecting is prohibited.

Coastways Fault of the San Gregorio Fault Zone. The Coastways Fault crosses the highway at the small dip in the road just before Coastways Ranch. This fault has long been considered the primary trace of the SGFZ because of the obvious bedrock offset across a small reentrant in the coastline.

STOP 2A. When we reach the beach, examine the rocks on either side of the reentrant in the seacliff. West of the reentrant, fine-grained silty sandstones and sandy siltstones of the Purisima Formation are exposed in near-vertical seacliffs. The sandstones and their fauna are described in more detail above (see milepost 14.1). Bedding strikes approximately east-west and dips 10° to 20° to the south.

East of the reentrant are poorly exposed outcrops of the Santa Cruz Mudstone (also described above, milepost 14.1). Bedding, although hard to find, strikes about N 50° E, dipping about 40° NW. This discordant juxtaposition of two units differing greatly in age, lithology, and structure can be explained only by the presence of a major, Neogene-active fault running along the brush- and colluvium-covered drainage (figs. 1.10 and 1.11).

The fault is obscured by thick wedges of colluvium and dense vegetation, so it is not exposed anywhere in this drainage. Neither the 103 to 105 ka wave-cut platform nor the younger terrace deposits are exposed near the fault; however, leveling across the reentrant indicates that the marine terrace is offset about 5 meters (16 feet), with the northeast side up (W.C. Bradley, personal commun., 1974). Recently, several exploratory trenches were excavated across this fault trace on the Finney Creek alluvial fan, about 300 to 400 meters to the north (see fig. 1.11). The fault clearly juxtaposes well-sorted shallow marine sands with fluvial deposits composed almost entirely of Santa Cruz Mudstone fragments. Apparent fault separation in the trench exposures is west side up, east side down, but this offset may reflect right-lateral transport of the axis of the fan toward the northwest, thereby forming an east-facing scarp.

Walk northward along the beach. From here to the mouth of Año Nuevo Creek, the seacliff is cut in the Purisima Formation. In this area, away from the Coastways Fault, bedding strikes roughly north-south and dips gently 4° to 7° to the east. Exposed in the seacliff are numerous, hard, calcite-cemented layers of fossiliferous sandstone that form resistant ledges and concretions. The fossil fauna is largely shallow marine mollusks.

Age of the Marine Terrace at Point Año Nuevo

At this stop we will examine late Quaternary faulting exposed along the south shore of Point Año Nuevo, within the Año Nuevo State Reserve. We are in the SGFZ (figs. 1.7, 1.9, 1.10 and 1.11). The broad, gently sloping surface of the first emergent marine terrace is visible to the northwest and at the top of the seacliff directly above us. Although this terrace has been mapped as the Año Nuevo terrace, which is correlative with the Davenport wave-cut platform of the Santa Cruz terrace east of the SGFZ (Weber and others, 1995), the terrace here is probably actually equivalent to the Highway 1 platform, with an age of 103 to 105 ka.

This circumstance is a consequence of our inability to distinguish and definitively map the terrace surfaces within the SGFZ. At Pigeon Point the separation between the Pigeon Point terrace (103 to 105 ka) and the Año Nuevo terrace (80 to

83 ka) is clear. South of Whitehouse Creek we can no longer map the two terraces separately. The outer edge of the terrace at Point Año Nuevo can be traced northward into what is clearly the Año Nuevo terrace at Pigeon Point. Based on faunal assemblages and amino-acid racemization data, it appears that the central portion of the broad terrace at Point Año Nuevo is actually the Pigeon Point terrace (103 to 105 ka).

At Point Año Nuevo the first emergent terrace is unquestionably a compound terrace, containing two wave-cut platforms (analogous to the situation in westside Santa Cruz, illustrated in figure 1.5). Although mapped as one terrace surface, the outer portion of the terrace is probably underlain by the 80 to 83 ka wave-cut platform, normally associated with the Año Nuevo terrace. The inner portion of the terrace is underlain by the 103 to 105 ka wave-cut platform, associated with the Pigeon Point terrace west of the fault zone and the Highway 1 wave-cut platform east of the fault zone. Unfortunately, the hypothesized vertical discontinuity in the wave-cut platform of this compound terrace cannot be identified unambiguously in the seacliffs along the south shore of Point Año Nuevo. However, a small, 2-meter-high step in the wave-cut platform, exposed in the seacliff about 100 to 120 meters east of the Año Nuevo thrust fault, may represent the break between the two wave-cut platforms.

The 103 to 105 ka wave-cut platform at the base of the marine terrace deposits is visible near the top of the seacliff. It appears to be unbroken between the Coastways Fault reentrant and the mouth of Año Nuevo Creek. Continue north, toward the mouth of Año Nuevo Creek, until you reach the near-vertical contact between pebble conglomerates and the Purisima Formation.

Note: The locations of the field trip stops discussed below are shown on figure 1.12.

STOP 2B. Exposed in the seacliff is the contact (buttress unconformity) between fluvial deposits of Año Nuevo Creek and the upper sandstone member of the Purisima Formation (fig. 1.13). Detrital charcoal fragments collected near the base of the Año Nuevo Creek deposits have yielded a ^{14}C age of 10,200 ± 300 years B.P. This date, combined with ^{14}C dates on charcoal collected from the top of these deposits near the Frijoles Fault, would suggest that these sediments were deposited between 10,500 and 8,000 years B.P. The presence of abundant charcoal in these fluvial deposits is probably related to the seasonal burning of grasslands and undergrowth by Native Americans to promote growth of grasses and to aid in the capture of small game. Naturally occurring forest fires as a result of lightning are exceedingly rare in the Santa Cruz Mountains because of the lack of convection in the atmosphere during the dry summer season. Air masses are stable during the summer and fall because of temperature inversions in the atmosphere related to the seasonal formation of advection fogs.

Southeast of the mouth of Año Nuevo Creek, the 100-foot-high, near-vertical seacliff in the Purisima Formation is capped by about 20 feet of Quaternary marine terrace deposits. This terrace correlates with the main terrace at Point Año Nuevo, which has been identified as the 103 to105 ka terrace on the basis of amino-acid racemization studies and the cold-water aspect of the fauna. The base of the terrace deposits (the wave-cut platform) is about 70 to 80 feet in elevation southeast of the mouth of Año Nuevo Creek.

Approximately 30 meters to the southeast, a small fault offsets bedding in the Purisima Formation. Poor exposure near the top of the cliff, as a result of overhanging vegetation, makes it difficult to determine if this fault offsets the overlying marine terrace.

Hike northwest, crossing the mouth of Año Nuevo Creek. Exposed in the seacliff are the interbedded pebble conglomerates, poorly sorted sandstones, siltstones, and clays deposited by Año Nuevo Creek. The discontinuous strata are typically channeled and cross-bedded, with thin layers of silt, silty sand, and clay separating thick packages of pebble conglomerate. Some of the fine-grained layers appear to have relict soil structure. Charcoal is quite common in both the conglomerates and the fine-grained deposits. These strata are clearly the channel and overbank deposits of a small stream. The channel deposits are typically imbricated conglomerates, which are clast supported and contain pebbles and cobbles of Santa Cruz Mudstone. The matrix is clay and silty clay. The presence of abundant (>99 percent) Santa Cruz Mudstone clasts indicates a fluvial origin, as mudstone bedrock is present only in the drainage basins of streams that originate northeast of the Coastways Fault. Santa Cruz Mudstone bedrock is not present southwest of the Coastways Fault in San Mateo County, so the mudstone clasts must have been transported into this area from the east. Transport along the coast by littoral drift is not a viable hypothesis because the relatively soft mudstone does not stand up to abrasion by harder clasts derived from the Pigeon Point Formation. Note, for instance, the relative paucity of mudstone pebbles on the beach compared with the Año Nuevo Creek deposits.

Año Nuevo Creek deposits are continuously exposed along 500 to 550 meters (~1,700 feet) of seacliff from the mouth of Año Nuevo Creek northwest to the Frijoles Fault. These beds dip gently 3° to 5° to the northwest along this section of coastline (fig. 1.13), grading from predominantly pebble conglomerates on the southeast (near the mouth of the creek) to predominantly silts, clays, and sandy clays at the northwest end of the beach. The topographically expressed depositional surface on these fluvial sediments also slopes 3° to 5° to the northwest, mimicking the underlying bedrock surface. This northwest dip is, therefore, interpreted to be the result of post-depositional tilting in the late Holocene.

The contact between the Año Nuevo Creek deposits and the Purisima Formation is exposed intermittently for about 300 meters west of the mouth of Año Nuevo Creek, after which the contact lies below the level of the beach. This unconformable contact is typically highly irregular, exhibiting deeply cut channels and irregular bedrock highs. Careful examination of the contact indicates that it is a buttress unconformity, except as noted below.

STOP 2C. Here, in a small cove along the seacliff (fig. 1.12), deposits of Año Nuevo Creek overlie Purisima Formation. Examine the contact between the fluvial sediments and the Purisima Formation (see figs. 1.13 and 1.14). Note the presence of numerous pholad (a variety of clam) borings in the Purisima Formation along this contact. The pholad borings conclusively demonstrate that the surface between the Año Nuevo Creek deposits and the Purisima Formation is a former wave-cut platform—an ancient ocean floor—and is therefore associated with a marine terrace. Careful examination of the outcrop reveals a small wedge of well-sorted sand of marine origin (not composed of Santa Cruz Mudstone detritus) on the old wave-cut platform (fig. 1.14). This thin wedge of sediment, which fills some of the pholad borings, is a remnant of the near-shore marine deposits that once covered the wave-cut platform.

Apparently, the near-shore marine sediments originally deposited on the wave-cut platform were eroded away by ancestral Año Nuevo Creek, thereby exhuming the old wave-cut platform. The creek then deposited fluvial sediments on this exhumed surface originally formed by wave erosion. Examination of the seacliff outcrops west of the mouth of Año Nuevo Creek reveals that the contact between the fluvial deposits and bedrock usually follows the old wave-cut platform, although the creek channeled into the bedrock in several areas, thus destroying the wave-cut platform. The intensely bored surface of the wave-cut platform, stripped of its deposits, is exposed in several areas northwest of this cove.

Along the northwest side of the cove, a small, branching fault offsets the Purisima Formation, the wave-cut platform, remnants of the near-shore marine sediments, and the basal layers of the fluvial deposits (figs. 1.11, 1.13 and 1.14). However, the fault is truncated by younger beds within the creek deposits and does not extend to the surface. The fault is active, as it apparently offsets the basal deposits of Año Nuevo Creek, which are about 10,000 years old, yet there is no surface evidence of this fault. The obvious offset is vertical, northeast side up and southwest side down, but it is probable that this fault also experienced right-lateral strike-slip movement. NOTE: Consider the problem of trying to identify this Holocene-active fault using standard engineering geologic techniques. Without the luxury of a seacliff exposure it would be impossible even to find this fault, much less determine its activity.

Finally, note that directly east of this small fault lies a mudstone unit of the Purisima Formation, in depositional contact with an overlying sandstone unit of the Purisima Formation (fig. 1.14). The contact appears to be conformable and gradational. Bedrock faults on the eastern side of the cove offset the Purisima Formation but not the 103 to 105 ka wave-cut platform.

Age of the Wave-Cut Platform West of Año Nuevo Creek

As indicated earlier, the inner portion of the broad, low terrace at Año Nuevo State Reserve is interpreted to be 103 to 105 ka, based on amino acid racemization data and the presence of a cold-water fauna (Ken Lajoie, personal communication), and is thus correlative with the Highway 1 platform of the Santa Cruz terrace. The 80 to 83 ka platform is present near the actual point, about 1,300 meters (4,000 feet) west of here.

The age of the wave-cut platform exposed at Stop 2C, however, is not known. Which of the wave-cut platforms does it correspond with? Fossils are not present on the platform, and it is overlain by 10,000-year-old deposits. This feature is obviously not a product of the modern sea-level high stand, but it could have formed during the 103 to 105 ka high stand or perhaps one of the younger Pleistocene sea-level high stands.

The position of this localized, low-lying wave-cut platform, apparently on a down-dropped fault block between extensive outcrops of the 103 to 105 ka terrace, suggests it also represents the 103 to 105 ka wave-cut platform (fig. 1.13). Although it could have conceivably formed during one of the younger Pleistocene sea-level high stands, these alternatives can seemingly be eliminated by removing 400 to 500 meters (~1,500 feet) of slip from the Frijoles Fault. Sliding the Pigeon Point block back to the southeast along the Frijoles Fault would isolate the wave-cut platform in question from wave attack by surrounding it with 103 to 105 ka terrace.

The Año Nuevo Creek Fault

The elevation of the wave-cut platform immediately northwest of Año Nuevo Creek, at Stop 2C, is about 3 to 6 meters (10 to 20 feet) above sea level. This is about 18 meters (60 feet) lower than the 103 to 105 ka wave-cut platform

southeast of Año Nuevo Creek (see figs. 1.12 and 1.13). This discrepancy in elevation requires the presence of a fault near the mouth of Año Nuevo Creek, offsetting the 103 to 105 ka wave-cut platform. Apparent fault offset is down to the west, up to the east. Based on regional geomorphology and the trend of other faults in the seacliff, it is probable that the fault lies near the axis of Año Nuevo Creek, trending roughly north-south. It apparently connects the Frijoles and Coastways Fault strands (see fig. 1.11) and appears to act as the east side of a small graben filled with the fluvial deposits of Año Nuevo Creek.

Interpretative History of Año Nuevo Creek. The Holocene deposits of Año Nuevo Creek lie in a small graben, late Pleistocene to Holocene in age, bounded by the Frijoles Fault and the Año Nuevo Creek Fault. Prior to approximately 12,000 years ago, Año Nuevo Creek flowed northwestward along what is now the course of Green Oaks Creek, entering the ocean on the north side of the point (fig. 1.15). About 12,000 years ago, Año Nuevo Creek was captured, probably by headward erosion of a high-gradient stream flowing along the trace of the Año Nuevo Creek Fault. After this capture, the short, high-gradient stream must have experienced a dramatic increase in both discharge and sediment load. Sea level was still on the order of 30 meters (100 feet) or more lower than at present, and the newly energized and redirected Año Nuevo Creek proceeded to erode the existing marine terrace deposits within the graben, thus partially exhuming the 103 to 105 ka wave-cut platform.

As the creek cleansed the graben of marine terrace deposits, sea level continued to rise, the graben continued to sink, and the climate gradually became warmer and drier. These combined processes interacted to change the stream from an erosional regime toward a depositional regime. Between about 11,000 and 8,000 years ago, as sea level slowly rose, Año Nuevo Creek deposited a sequence of fluvial sediments in the graben, which it had stripped of marine sediments just a few thousand years earlier.

The slow rise in sea level during the mid-Holocene was accompanied by rapid surf-zone erosion and seacliff retreat in the unconsolidated fluvial sediments. Seacliff retreat apparently was rapid enough to essentially lower base level for Año Nuevo Creek. After about 8,000 years ago, Año Nuevo Creek reverted to an erosional regime and began to incise the sediments it had deposited between 11,000 and 8,000 years ago. The return to an erosional regime was accompanied by a decrease in precipitation and runoff, thereby reducing the erosional ability of Año Nuevo Creek. Following the stabilization of sea level about 5,500 years ago, Año Nuevo Creek has continued to slowly incise its channel into the fluvial deposits, largely in response to the slow lowering of base level brought about by coastal retreat due to wave erosion.

Onward. Continue to hike northwest along the beach. In at least two other areas, small faults in the seacliff offset the exhumed wave-cut platform and the basal 3 to 6 feet of fluvial deposits (figs. 1.11, 1.13 and 1.14). Again, these faults are truncated by younger depositional units and do not extend to the surface. The Año Nuevo Creek fluvial deposits become finer grained to the northwest. Several weakly to moderately developed paleosols (buried soils) can be found in the fine-grained overbank deposits exposed in the seacliff outcrop northwest of Stop 2C.

Waddell's Wharf, Coastal Erosion, and Littoral Drift

A large wet area in the seacliff represents seepage from a poorly sealed reservoir (pond) that lies several hundred feet north of the seacliff. This seepage approximately marks the location of Waddell's Wharf, built in 1864 by William Waddell. The wharf, about 700 feet long, was used for loading lumber cut in Waddell Creek and transported to the wharf on flatbed cars hauled by horses along a three-mile-long wooden railway. The wharf operated until about 1877, serving several small mills, but business declined after Waddell was killed by a grizzly bear in 1875. The wharf burned in the early 1880's. The shallow excavation for the roadway to the wharf, now filled with dark gray soil, can be identified by comparing the disturbed and undisturbed soil profiles near the top of the seacliff.

In 1974, a single piling from this wharf was found in place on the beach at the base of the modern seacliff. The piling was about 3 feet from the face of the cliff, indicating that through 1974 little if any erosion had occurred in the 110-plus years since the wharf was built. However, a period of extensive cliff erosion was initiated in the winter of 1977-78, when 10 feet of cliff retreat occurred in a single storm season. In the following 5 to 6 years, more than 50 feet of cliff retreat occurred along the coast between Año Nuevo Creek and the steep cliffs that form the south shore of the point. The piling was ripped out of the beach and destroyed during a large storm on December 21, 1979. Since then, the rate of seacliff retreat has slowed and become more intermittent, but active surf erosion still occurs along this seacliff almost every winter. The apparent absence of cliff erosion along the coast north of Año Nuevo Creek for 113 years, followed by almost yearly wave erosion and cliff retreat during the past 24 years, suggests a major change in the erosional equilibrium along this section of coast. Consider for a moment that the coast from west of the Frijoles Fault to Año Nuevo Creek has retreated between 60 and 80 feet during the

past 24 years. This change may reflect a decrease in the littoral drift moving northwest to southeast down the coast, resulting from the gradual depletion of the wide beach that lay north of Point Año Nuevo before the channel between the mainland and the island opened up in the 1700's (Weber, 1981). In other words, it may have taken two centuries for the littoral cell to reequilibrate, and in the interim the cliffs along the south shore were protected somewhat from surf attack by the extra sand.

STOP 2D—Frijoles Fault. Exposed in the seacliff is one of the two primary fault strands of the SGFZ, the Frijoles Fault. It juxtaposes moderately to steeply dipping fluvial deposits of Año Nuevo Creek, to the southeast, with crushed Purisima Formation, to the northwest (fig. 1.13).

The Holocene fluvial deposits, which we first encountered in the seacliff near the mouth of Año Nuevo Creek, dip uniformly to the northwest about 3° to 5° for a distance of roughly 500 meters (1,600 feet). Approaching the Frijoles Fault, however, these Holocene beds are abruptly folded upward, forming a small syncline. This drag fold has formed in response to movement on the Frijoles Fault. The fold plunges to the north, suggesting right-lateral strike-slip movement with a vertical component (southeast side down, northwest side up). Projecting the 103 to 105 ka wave-cut platform into the fault from both sides suggests that the vertical offset of the platform is approximately 30 to 35 meters (100 to 110 feet). The amount of strike-slip displacement cannot be approximated at this outcrop.

Northwest of the main fault exposure lies a broad zone of crushed Purisima Formation, or fault gouge, about 75 meters (250 feet) wide (figs. 1.12 and 1.13). Upon closer examination, the active movement within this shear zone appears to be concentrated in three areas. The crushed rock is weak and susceptible to both erosion and slope failure. The landslides on this slope typically reactivate and enlarge their headscarps each rainy season, depositing debris on the beach that is usually removed each year by wave erosion. The height and angle of the cliff face also reflect the effect of the intense bedrock shearing on slope stability and resistance to erosion.

Landslides of the type present in this shear zone (slumps) are not typically found in seacliffs formed in the sandstone of the upper Purisima Formation. These sandstone cliffs generally fail as block falls and topples controlled by steeply dipping joint sets and triggered by the undercutting action of waves. Large slump landslides are found only in the shear zones at Point Año Nuevo and 15 miles to the north near San Gregorio Creek, where the SGFZ goes offshore. Walk northwest to the end of the beach. Note the difference in hardness, bedding, and internal structure of the intact Purisima Formation bedrock at this location compared to the shear zone along the Frijoles Fault.

Onward. Hike up the stairs to the top of the cliff and out onto the levee that dams the small pond. The levee is porous, permeable, and leaks badly. Compaction is inadequate, and the dam is not stable. During the heavy rains in 1982-83, a 150-foot-long slab of this dam failed and slid off of the face of the dam into the reservoir. Although the main scarp formed down the centerline of the levee, the dam was not breached, and water did not escape from the reservoir. The levee was repaired the following summer, but its stability remains questionable.

Note that the dam for the reservoir lies across the axis of a northwest-trending depression representing the locus of the Frijoles Fault. The steep slope to the west is the northeast-facing Frijoles Fault scarp, heavily modified by erosion. To the east and southeast is the depositional surface on the Año Nuevo Creek fluvial sequence that we observed earlier in the seacliff. A broad linear valley has formed along the trace of the Frijoles Fault. This linear valley and a well-developed set of northeast-facing scarps mark the trace of the Frijoles Fault to the northwest, where the fault crosses the surface of the marine terrace.

Hike west, following the trail up onto the marine terrace. Hike off the trail (fight your way through the Coyote brush) and across the field to the top of the seacliff near the first small headland west of the main beach.

STOP 2E. This is an excellent vantage point from which to view the geology described in this guide, and to put it in perspective (fig. 1.12). To the west and northwest, the Año Nuevo terrace is visible as a broad, nearly planar surface sloping gently to the west. The vegetated remnants of the Año Nuevo dune field (Holocene) overlie this terrace. To the north, the surface trace of the Frijoles Fault is marked by the linear topographic trough. The alluvial fan of Año Nuevo Creek and the depositional surface on the Año Nuevo Creek deposits form the surfaces east of the small reservoir, and further to the southeast lies the graben formed between the Frijoles and Año Nuevo Creek Faults. The Dickerman Barn, which houses the visitor center, lies on fluvial deposits of Año Nuevo Creek within the graben. Farther east, the base of the west-facing slope of the Santa Cruz Mountains marks the trace of the Coastways Fault. Higher, forested marine terraces are visible southeast of Año Nuevo Creek. The surface of the Santa Cruz terrace is visible southeast of Año Nuevo Creek, gradually thinning and finally disappearing just north of the Waddell Bluffs. Looking south, the Santa Cruz and Western terraces are visible in the distance as far south as Scott Creek. Highway 1 lies at the back edge of the Santa Cruz terrace and below the

Western terrace. The headland jutting out from the coastline just south of Scott Creek is El Jarro Point, the proposed site of the Davenport Nuclear Power Plant in the 1960's.

Resume hiking to the bus. Hike back to the northeast toward the parking lot that lies just north of the Dickerman Barn. Along the path you will walk down the scarp of the Frijoles Fault, and after crossing the fault you will walk up the tilted depositional surface of the Holocene graben-filling deposits of Año Nuevo Creek.

Late Quaternary Slip Rates on the San Gregorio Fault Zone

Measurements of late Quaternary fault slip rates are difficult even under the most ideal conditions. Discussion below describes measurement of offset in both the horizonal and vertical directions. Horizontal slip rates in the late Quaternary were determined using offset marine terrace shoreline angles, along with offsets of late Pleistocene streams on alluvial fans near Point Año Nuevo. Although both of these techniques are fraught with assumptions, it appears that the original estimates of late Quaternary slip by Weber (1980), Weber and Cotton (1981), and Weber (1990 a, b) are probably the most reasonable.

The horizontal slip rate determined from the offset of the Santa Cruz and Western terrace shoreline angles across the SGFZ is 6 to 11 mm/yr, with the best estimate being 8 mm/yr. Figure 1.7 is a plot of shoreline angles (or paleostrandlines) on opposite sides of the SGFZ; figure 1.16 is a more detailed map of offset shoreline angles at Point Año Nuevo. Although higher and older marine terraces can be correlated across the fault zone, their shoreline angle positions and fault offsets cannot be accurately determined. Nevertheless, the distribution of the terrace remnants (fig. 1.7) suggests continuous horizontal slip on the SGFZ of 6 to 11 mm/yr during the past 500 k.y.

The late Quaternary slip rate across the fault zone, determined from offset streams on alluvial fans at Point Año Nuevo, is 4 to 10 mm/yr (see fig. 1.15). This is comparable to the rate determined from offset marine terrace shoreline angles (above) and to the slip rate of 6 mm/yr postulated by Clark (1997) for the past 3.0 m.y.

Vertical slip rates are measured by geographic variations in the uplift rates of marine terraces. If the marine terraces record the long-term, late Quaternary uplift rates of both the Santa Cruz Mountains and Pigeon Point structural blocks, the difference between these uplift rates must represent the late Quaternary slip rate across the fault zone. The interpretation most strongly supported by field data is that, over the past 500,000 years, the Ben Lomond Mountain terrace sequence has been uplifting at 0.42 to 0.44 m/k.y., while the Pigeon Point terrace sequence has risen 0.3 m/k.y. (see discussion of Stop 1). The difference is 0.13 m/k.y., a very low rate of vertical displacement.

It is possible that these estimated uplift rates are incorrect; however, using alternative uplift rates generally results in even lower rates of vertical displacement across the SGFZ. If we arbitrarily assume that the highest uplift rate for Ben Lomond Mountain (0.44 m/k.y.) and the lowest rate for the Pigeon Point structural block (0.15 m/k.y.) are valid, then the long-term vertical displacement rate would be 0.29 m/k.y.

Both of these hypothetical displacement rates of vertical offset across the SGFZ are extremely low, lying within the range of long-term uplift rates for the central California coast as a whole. A vertical slip rate of 0.13 to 0.29 m/k.y. indicates that any vertical component of slip on the SGFZ is relatively small.

Road Log for Those Not Hiking

Mileage/Notes

19.2 **Año Nuevo Creek.** Strath terraces of Año Nuevo Creek are visible in the agricultural fields to the east, where the creek is deeply incised into its fan. Both north and south of Año Nuevo Creek, Highway 1 cuts through the alluvial fan formed by the creek. The basal portions of these Highway 1 road cuts expose clean quartzose beach sands, whereas the upper portions of the cuts expose fluvial pebble conglomerates (with clasts derived from the Santa Cruz Mudstone). If you plan to examine these deposits, you should be prepared to dig into the face of the road cut.

19.5 **Entrance to Año Nuevo State Reserve:** Turn left and enter reserve. For trips other than September 15, 2001, pay the ranger and proceed to the main parking lot. Restrooms are available. Exhibits and a natural history bookstore are usually open in the Dickerman Barn, one of the remaining buildings of the historic Steele Ranch.

End of Trip

References

Adam, D.P., Byrne, R., and Luther, E., 1979, A late Pleistocene and Holocene pollen record from Laguna de Las Trancas, northern coastal Santa Cruz County, California: U.S. Geological Survey Open File Report 79-545, 29 p.

Adam, D.P., and West, G.J., 1983, Temperature and precipitation estimates through the last glacial cycle from Clear Lake, California, pollen data: Science, v. 219, p. 168-170.

Anderson, R.S., 1990, Evolution of the northern Santa Cruz Mountains by advection of crust past a San Andreas Fault bend: Science, v. 249, p. 397-401.

Anderson, R.S., 1994, Evolution of the Santa Cruz Mountains, California, through tectonic growth and geomorphic decay: Journal of Geophysical Research, v. 99, no. B7, p. 14013-14029.

Anderson, R.S., and Menking, K.M., 1994, The Quaternary marine terraces of Santa Cruz, California: Evidence for coseismic uplift on two faults: Geological Society of America Bulletin, v. 106, p. 649-664.

Anderson, R.S., and Weber, G.E., 1990, Marine terraces and dating of the Santa Cruz terrace sequence, *in* Schwartz, D.P., and Ponti, D.J., editors, Field Guide to Neotectonics of the San Andreas Fault System, Santa Cruz Mountains, in Light of the 1989 Loma Prieta Earthquake: U.S. Geological Survey Open File Report 90-274, p. 8-11.

Bloom, A.L., Broecker, W.S., Chappell, J., Matthews, R.K., and Mesolella, K.J., 1974, Quaternary sea-level fluctuations on a tectonic coast: New 230Th/234U dates from the Huon Peninsula, New Guinea: Quaternary Research, v. 4, p. 185-205.

Bradley, W.C., 1957, Origin of marine-terrace deposits in the Santa Cruz area, California: Geological Society of America Bulletin, v. 68, p. 421-444.

Bradley, W.C., 1958, Submarine abrasion and wave-cut platforms: Geological Society of America Bulletin, v. 69, p. 967-974.

Bradley, W.C., and Addicott, W.O., 1968, Age of first marine terrace near Santa Cruz, California: Geological Society of America Bulletin, v. 79, p. 1203-1210.

Bradley, W.C., and Griggs, G.B., 1976, Form, genesis, and deformation of central California wave-cut platforms: Geological Society of America Bulletin, v. 87, p. 433-449.

Branner, J.C., Newson,J. F., and Arnold,R., 1909, Description of the Santa Cruz quadrangle, California: U.S. Geological Survey Atlas, Folio 163, 11 p., 3 map sheets, scale 1:125,000.

Burnham, K., 1998, The Point Reyes Conglomerate: A segment of the Carmelo Formation, displaced 150 to 185 km by the San Gregorio Fault, in west-central California [abstract]: American Association of Petroleum Geologists Bulletin, v. 82, n. 5A, p. 843-844.

Chappell, J.M., 1983, A revised sea-level record for the last 300,000 years from Papua New Guinea: Search, v. 14, p. 99-101.

Chappell, J.M., and Shackleton, N.J., 1986, Oxygen isotopes and sea level: Nature, v. 324, p. 137-140.

Clark, J.C., 1981, Stratigraphy, paleontology, and geology of the central Santa Cruz Mountains, California Coast Ranges: U.S. Geological Survey Professional Paper 1168, 51 p.

Clark, J.C., 1997, Neotectonics of the San Gregorio Fault Zone: Age dating controls on offset history and slip rates: U. S. Geological Survey Final Technical Report, 30 p.

Clark, J.C., 1998, Neotectonics of the San Gregorio Fault Zone: Age dating controls on offset history and slip rate [abstract]: American Association of Petroleum Geologists Bulletin, v. 82, no. 5A, p. 844-845.

Clark, J.C., and Brabb, E.E., 1978, Stratigraphic contrasts across the San Gregorio Fault, Santa Cruz Mountains, *in* Silver, E.A., and Normark, W.R., editors, San Gregorio-Hosgri Fault Zone, California: California Division of Mines and Geology Special Report 137, p. 3-12.

Clark, J.C., Brabb, E.E., Greene, H.G., and Ross, D.C., 1984, Geology of Point Reyes Peninsula and implications for San Gregorio Fault history, *in* Crouch, J.K., and Bachman, S.B., editors, Tectonics and Sedimentation Along the California Margin: Society of Economic Paleontologists and Mineralogists, Pacific Section, v. 38, p. 67-86.

Dickinson, W.R., 1996, Kinematics of transrotational tectonism in the California Transverse Ranges and its contribution to cumulative slip along the San Andreas transform fault system: Geological Society of America Special Paper 305, 46 p.

Glen, W., 1982, The Road to Jaramillo: Critical Years of the Revolution in Earth Science: Stanford University Press, Stanford, CA.

Graham, S.A., and Dickinson, W.R., 1978, Apparent offsets of onland geologic features across the San Gregorio-Hosgri fault trend, *in* Silver, E.A., and Normark, W.R., editors, San Gregorio-Hosgri Fault Zone, California: California Division of Mines and Geology Special Report 137, p. 13-23.

Greene, H.G., Lee, W.H.K., McCulloch, D.S., and Brabb, E.E., 1973, Faults and earthquakes in the Monterey Bay region, California: U.S. Geological Survey Miscellaneous Field Studies Map MF–518, 14 p., 4 map sheets, scale 1:200,000.

Griggs, G.B., 1979, Erosion along the northern Santa Cruz County coastline, *in* Weber, G.E., Lajoie, K.R., and Griggs, G.B., editors, Coastal Tectonics and Coastal Geologic Hazards in Santa Cruz and San Mateo Counties, California: Geologic Society of America, Cordilleran Section Annual Meeting, Field Trip Guidebook, p. 2-24.

Hanks, T.C., Bucknam, R.C., Lajoie, K.R., and Wallace, R.E., 1984, Modification of wave-cut and faulting-controlled landforms: Journal of Geophysical Research v. 89, p. 5771-5790.

Lajoie, K.R., 1986, Coastal tectonics, *in* Studies in Geophysics, Tectonics: National Academy Press, Washington D.C., p. 95-124.

Lajoie, K.R., Weber, G.E., Mathieson, S.A., and Wallace, J., 1979, Quaternary tectonics of coastal Santa Cruz and San Mateo counties, California, as indicated by deformed marine terraces and alluvial deposits, *in* Weber, G.E., Lajoie, K.R., and Griggs, G.B., editors, Coastal Tectonics and Coastal Geologic Hazards in Santa Cruz and San Mateo Counties, California, Geological Society of America, Cordilleran Section Annual Meeting, Field Trip Guidebook, p. 61-80.

Lajoie, K.R., Ponti, D.J., Powell, C.L., II, Mathieson, S.A., and Sarna-Wojcicki, A.M., 1991, Emergent marine strandlines and associated sediments, coastal California: A record of Quaternary sea-level fluctuations, vertical tectonic movements, climatic changes, and coastal processes, *in* Morrison, R. B., editor, Quaternary Nonglacial Geology: Conterminous U.S. [The Geology of North America, Volume K-2]: Geological Society of America Decade of North American Geology, p. 190-213.

Muhs, D.R., Kennedy, G.L., and Rockwell, T.K., 1994, Uranium-series ages of marine terrace corals from the Pacific coast of North America and implications for last-interglacial sea level history: Quaternary Research, v. 42, p. 72-87.

Muhs, D.R., Rockwell, T.K., and Kennedy, G.L., 1992, Late Quaternary uplift rates of marine terraces on the Pacific coast of North America, southern Oregon to Baja California Sur: Quaternary International, v. 15/16, p. 121-133.

Mullins, H.T., and Nagle, D.K., 1982, Evidence for shallow hydrocarbons offshore northern Santa Cruz County, California: American Association of Petroleum Geologists Bulletin, v. 66, p. 1055-1075.

Page, B.M., and Holmes, C.N., 1945, Bituminous sandstone deposits near Santa Cruz, Santa Cruz County, California: U.S. Geological Survey Oil and Gas Investigation, Preliminary Map 27, with text.

Perg, L.A., Anderson, R.S., and Finkel, R.C., in press, Use of a new 10Be and 26Al inventory method to date marine terraces, Santa Cruz, California, USA: Geology.

Petersen, M.D., Bryant, W.A., Cramer, C.H., Cao, T., Reichle, M.S., Frankel, A.D., Lienkaemper, J.J., McCrory, P.A., and Schwartz, D.P., 1996, Probabilistic seismic hazard assessment for the State of California: California Division of Mines and Geology Open-File Report 96-08 and U.S. Geological Survey Open-File Report 96-706, 33 p., 2 appendices.

Rode, K., 1930, Geomorphogenie des Ben Lomond (Kalifornien), eine Studie uber Terrassenbildung duch marine Abrasion: Zeitschrift fur Geomorphologie, v. 3, p. 16-78.

Sedlock, R.L., and Hamilton, D.L., 1991, Late Cenozoic tectonic evolution of southwestern California: Journal of Geophysical Research, v. 96, p. 2325-2352.

Silver, E.A., 1978, The San Gregorio-Hosgri Fault Zone: An overview, *in* Silver, E.A., and Normark, W.R., editors, San Gregorio - Hosgri Fault Zone, California: California Division of Mines and Geology Special Report 137, p. 1-12.

Simpson, G.D., Thompson, S.C., Noller, J.N., and Lettis, W.P., 1997, The northern San Gregorio Fault Zone: Evidence for the timing of late Holocene earthquakes near Seal Cove, California: Bulletin of the Seismological Society of America, v. 87, no. 5, p. 1158-1170.

Stanley, R.G., and McCaffrey, R., 1983, Extent and offset history of the Ben Lomond Fault, Santa Cruz County, California, *in* Andersen, D.W., and Rymer, M.J., editors, Tectonics and Sedimentation Along Faults of the San Andreas System: Society of Economic Paleontologists and Mineralogists, Pacific Section, p. 79-90.

Weber, G.E., 1980, Recurrence intervals and recency of faulting along the San Gregorio Fault Zone, San Mateo County, California [Ph.D. dissertation]: University of California, Santa Cruz, 204 p.

Weber, G.E., 1981, Physical environment, *in* Le Boeuf, B.J., and Kaza, S., editors, The Natural History of Año Nuevo: Boxwood Press, Pacific Grove, Calif., p. 61-121.

Weber, G.E., 1990a, Pleistocene marine terraces and neotectonics of the San Gregorio Fault Zone (p. 1-12); Marine terraces, a brief introduction (p. 50-63); and Late Pleistocene slip rates on the San Gregorio Fault Zone at Point Año Nuevo, San Mateo County, California (p.64-79), *in* Griggs, G.B., and Weber, G.E., editors, Field Trip Guide: Coastal Geologic Hazards and Coastal Tectonics, Northern Monterey Bay and Santa Cruz and San Mateo County Coastlines, Association of Engineering Geologists, March 3, 1990, 146 p.

Weber, G.E., 1990b, Late Pleistocene slip rates on the San Gregorio Fault Zone at Point Año Nuevo, San Mateo County, California, *in* Garrison, R.E., Greene, H.G., Hicks, K.R., Weber, G.E., and Wright, T.L., editors, Geology and Tectonics of the Central California Coast Region, San Francisco to Monterey, Volume and Guidebook, Pacific Section, American Association of Petroleum Geolologists, Bakersfield, California, p. 193-204.

Weber, G.E., and Cotton, W.R., 1981, Geologic investigation of recurrence intervals and recency of faulting along the San Gregorio Fault Zone, San Mateo County, California: U.S. Geological Survey Open File Report 81-263, 99 p. with appendices, 18 plates.

Weber, G.E., and Lajoie, K.R., 1979, Evidence for Holocene movement on the Frijoles Fault near Point Año Nuevo, San Mateo County, California, *in* Weber, G.E., Lajoie, K.R., and Griggs, G.B., editors, Coastal Tectonics and Coastal Geologic Hazards in Santa Cruz and San Mateo Counties, California: Geological Society of America, Cordilleran Section Annual Meeting, Field Trip Guidebook, p. 92-100.

Weber, G.E., and Lajoie, K.R., 1980, Map of Quaternary faulting along the San Gregorio Fault Zone, San Mateo and Santa Cruz counties, California: U.S. Geological Survey Open File Report 80-907, 3 map sheets, scale 1:24,000.

Weber, G.E., Nolan, J.M., and Zinn, E.N., 1995, Determination of late Pleistocene-Holocene slip rates along the San Gregorio Fault Zone, San Mateo County, California: Final Technical Report, National Earthquake Hazard Reduction Program, Contract No. 1434-93-G-2336, 70 p., 4 oversize map sheets.

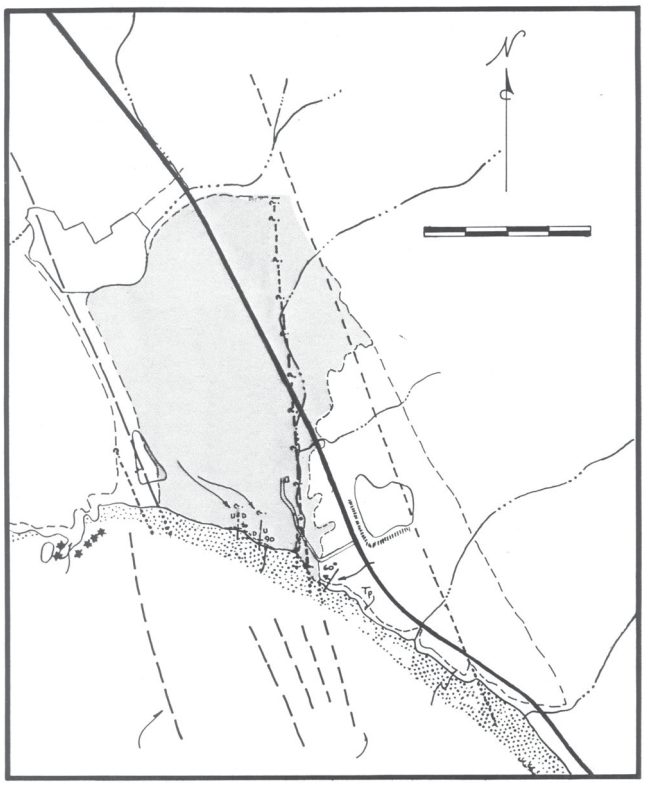

Figure 1.1. Regional map of central California showing major faults.

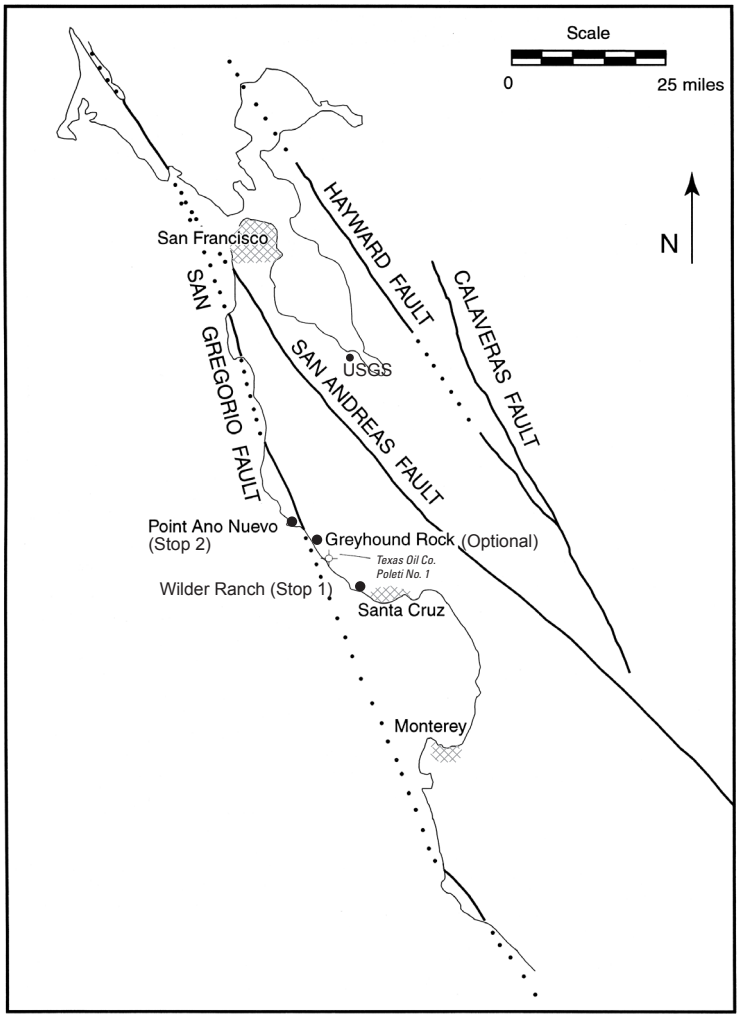

Figure 1.2. Stops of National Association of Geoscience Teachers field trip to the San Gregorio Fault and Pleistocene marine terraces, originating at the Geological Survey in Menlo Park. Faults dashed where approximate.

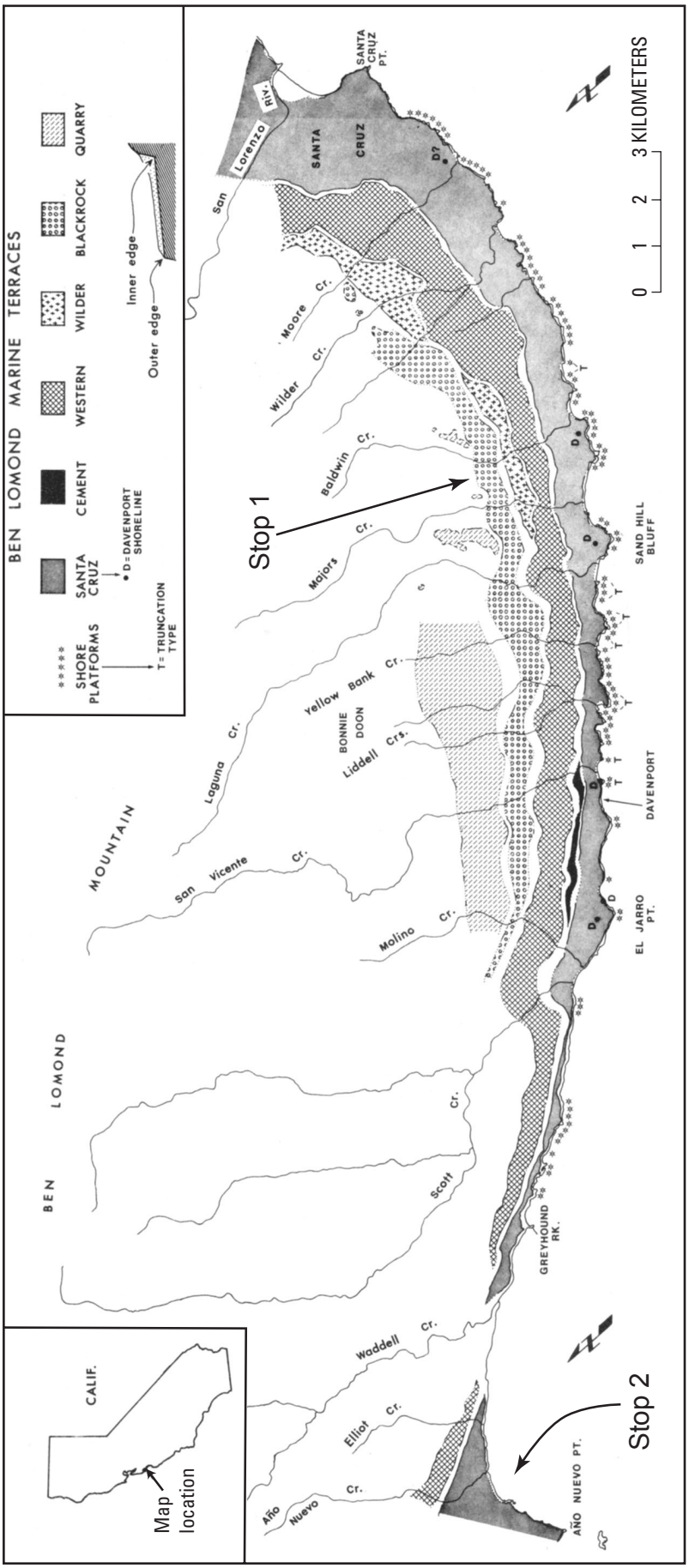

Figure 1.3. Map of marine terraces on the flank of Ben Lomond Mountain; modified from Bradley and Griggs (1976).

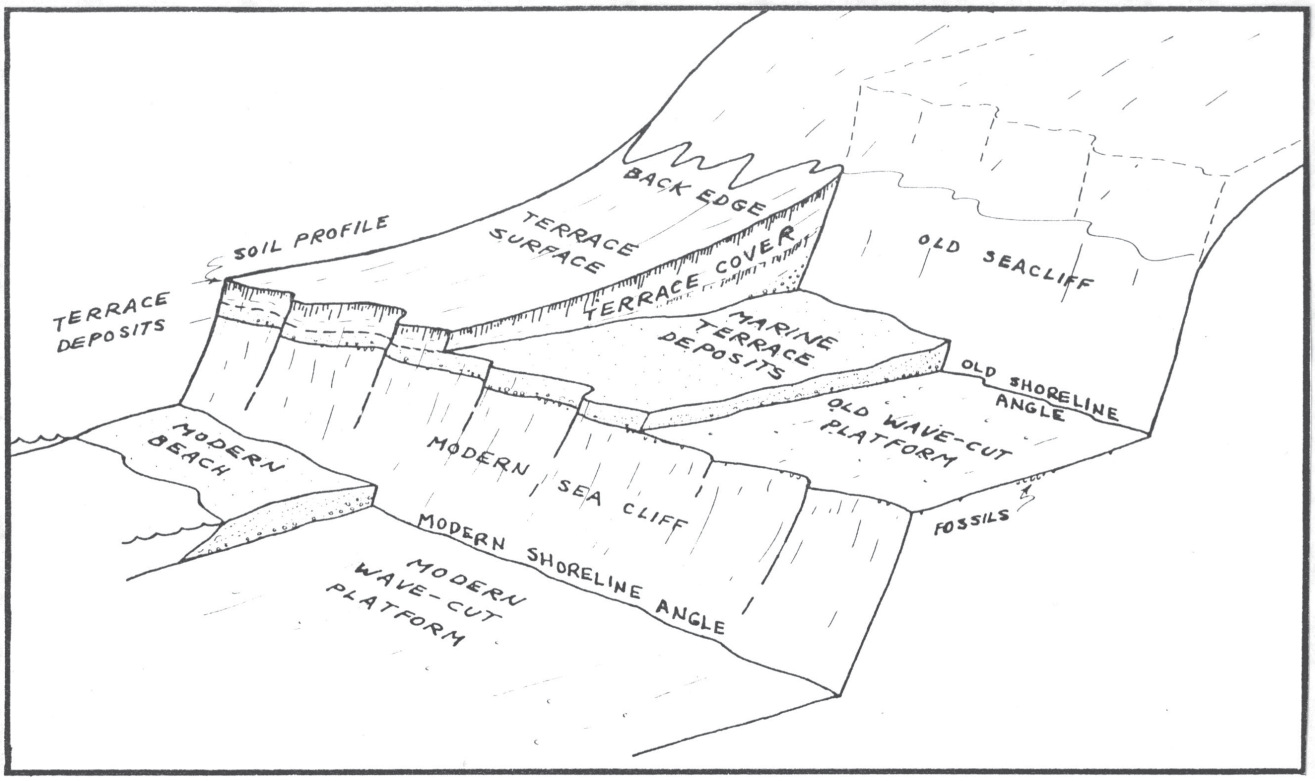

Figure 1.4. Schematic diagram of a marine terrace, indicating the relationship of the wave-cut platform to the shoreline angle and the overlying terrace deposits.

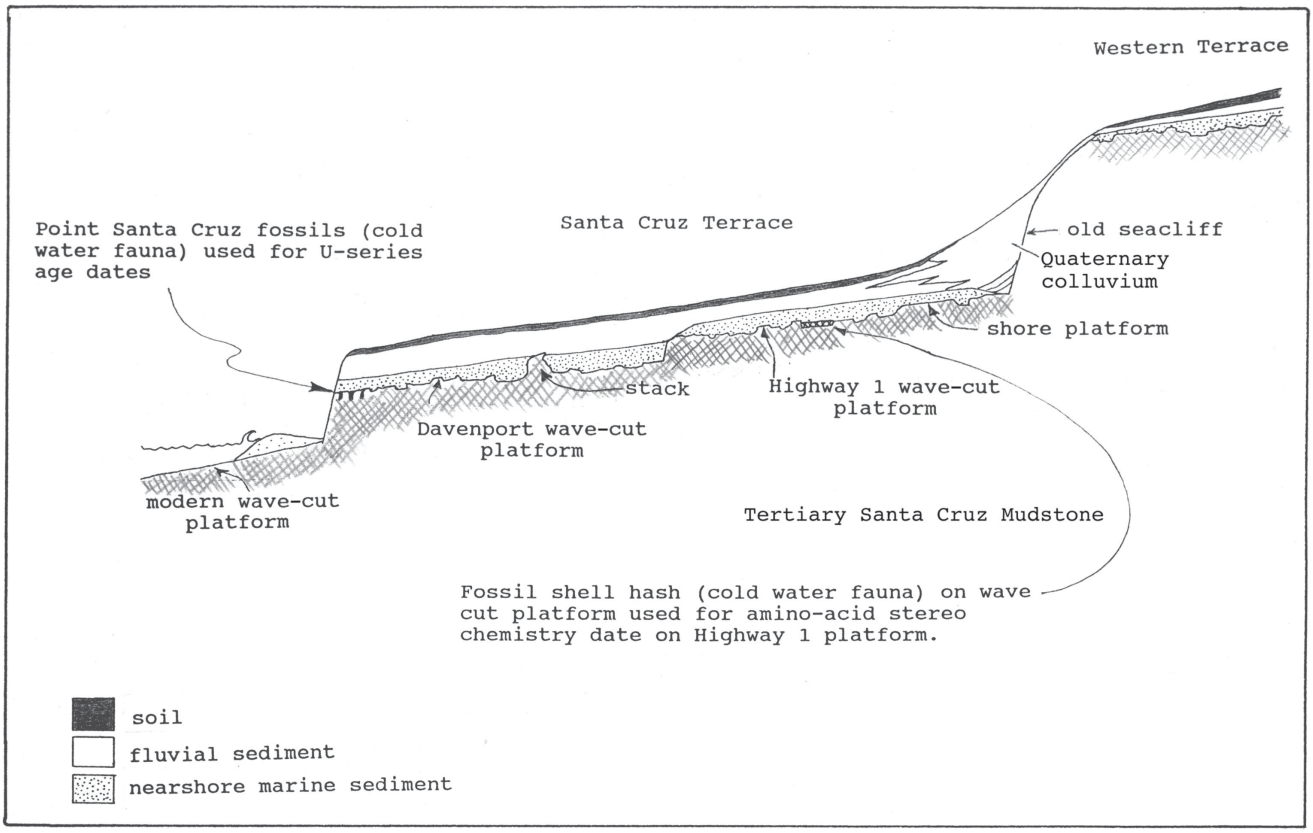

Figure 1.5. Diagrammatic cross section of the Santa Cruz terrace on the west side of Santa Cruz, showing the relative positions of the Davenport and Highway 1 wave-cut platforms.

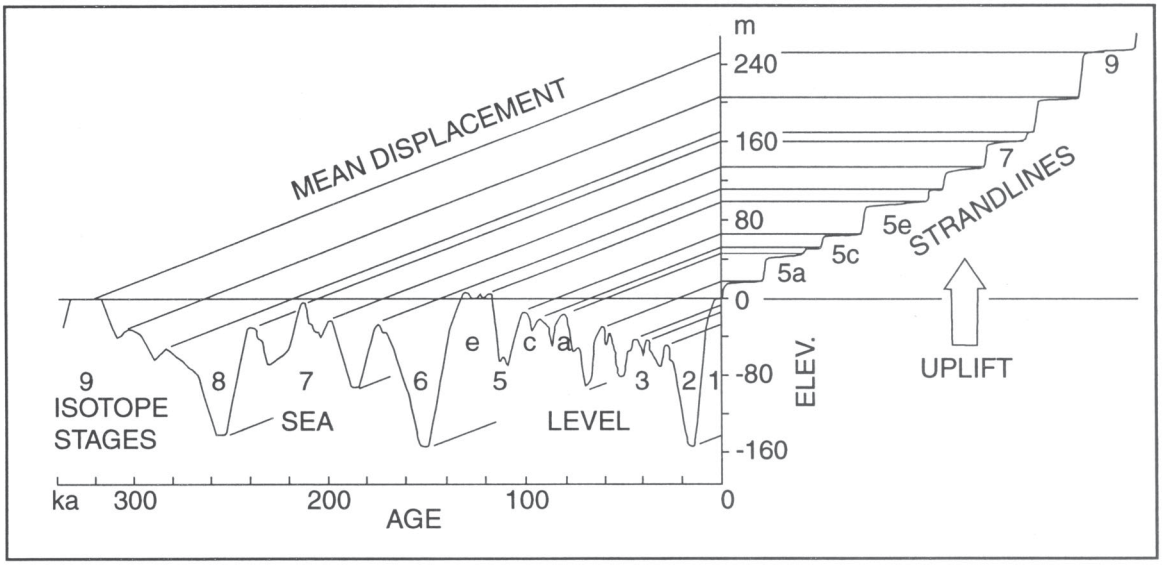

Figure 1.6. Graphic technique for determining the ages of marine terraces and uplift rates. On a rising coastline, the shoreline angle of each terrace (strandline) records a sea-level high stand. Consequently, the slope of the line connecting a shoreline angle elevation with the corresponding sea-level high stand is the average uplift rate. If the uplift rate has been constant, then (1) all of the lines connecting shoreline angle elevations with sea-level high stands will be parallel, (2) knowing the age of one terrace will allow the ages of the other terraces to be determined, and (3) trial and error can be used to approximate the ages for all of the terraces even if the age of one terrace is not known. Sea-level curve from U-series dated corals in the terraces on the Huon Peninsula, Papua New Guinea (Chappell, 1983); diagram from Lajoie (1986).

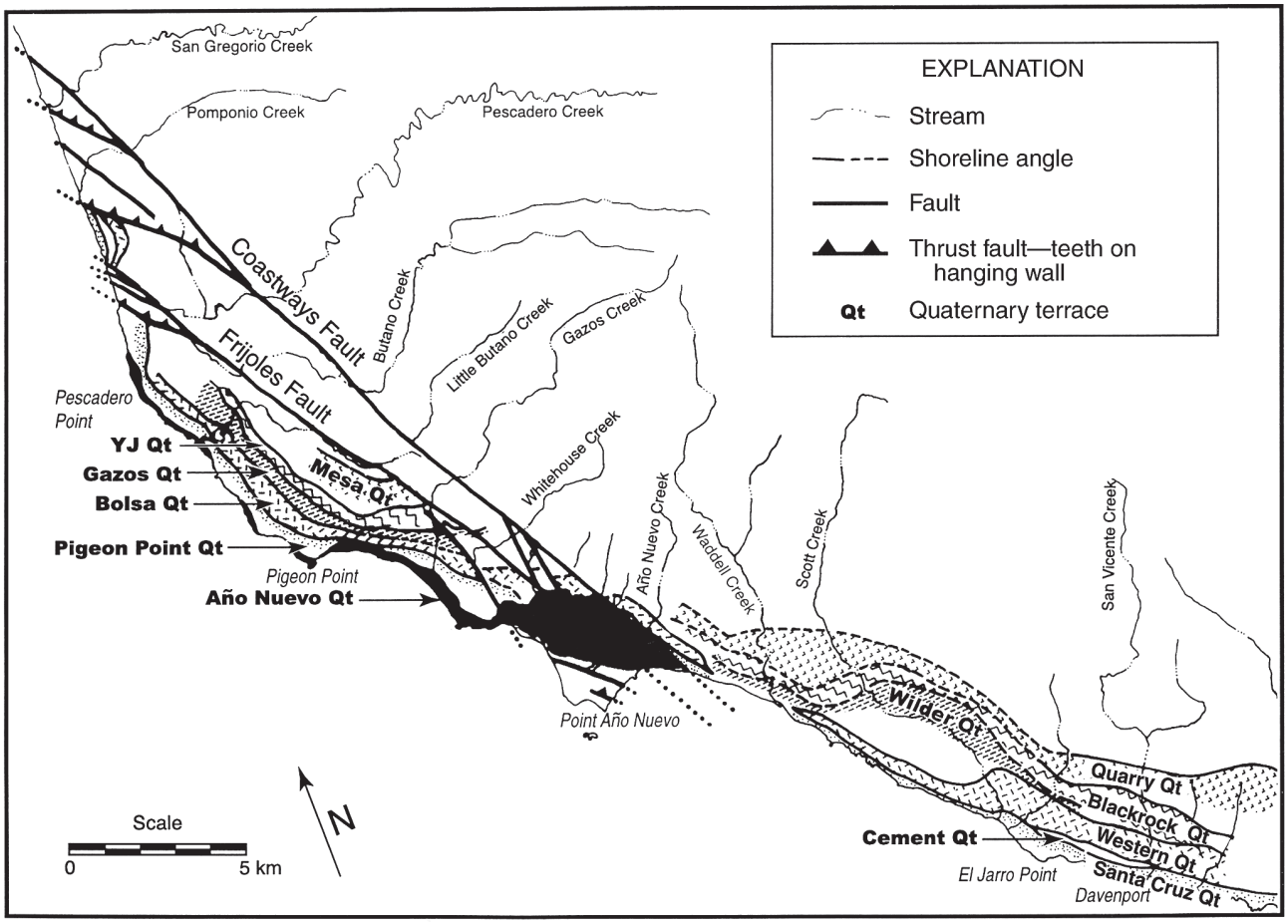

Figure 1.7. Offset Pleistocene strandlines across the San Gregorio Fault Zone; modified from Weber and others (1995). Refer to table 1.4 for the specific terrace correlations across the fault zone.

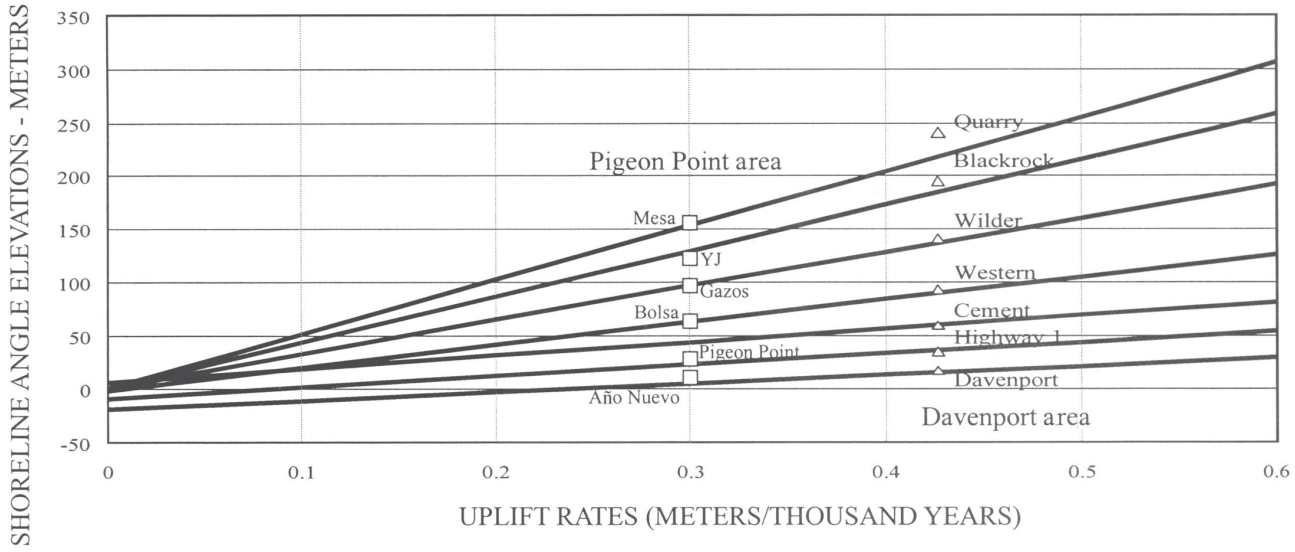

Figure 1.8. Diagram showing proposed correlations and tectonic uplift rates of the emergent marine terraces on opposite sides of the San Gregorio Fault Zone—the Pigeon Point structural block to the west and the Santa Cruz Mountains structural block (Davenport area) to the east. The solid black lines represent theoretical shoreline angle profiles produced by sea-level high stands on a tilted shoreline.

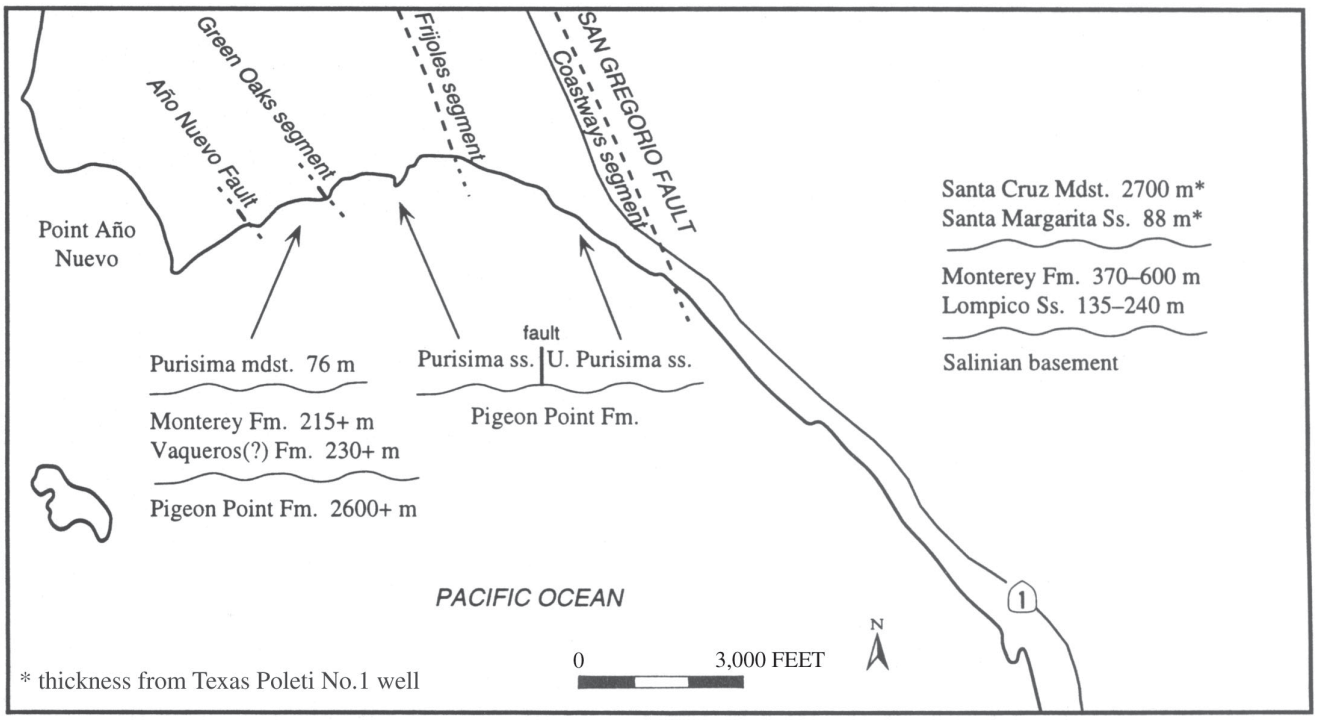

Figure 1.9. Pre-Quaternary stratigraphic contrasts across the San Gregorio Fault Zone at Point Año Nuevo.

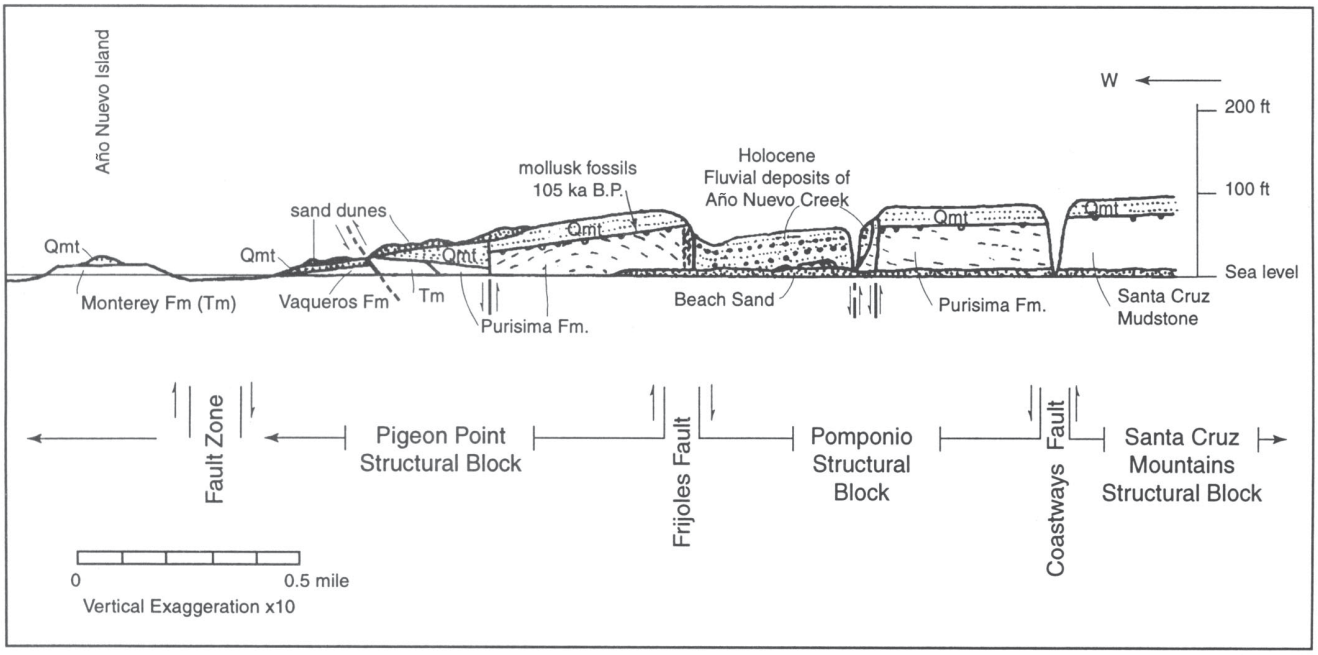

Figure 1.10. Schematic sketch of seacliff geology along the south shore of Point Año Nuevo; modified from Lajoie and others (1979).

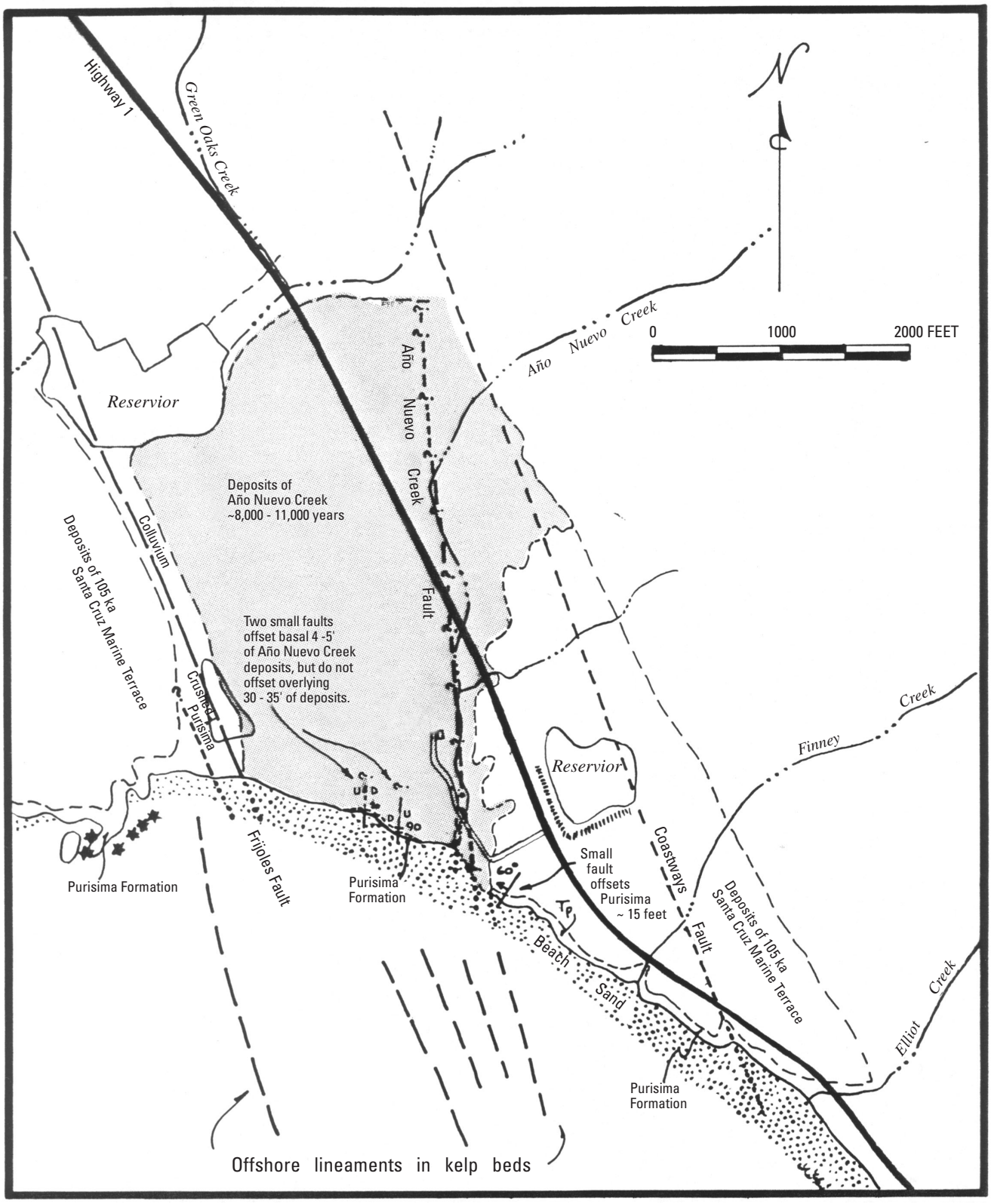

Figure 1.11. Generalized geologic map of the eastern portion of Point Año Nuevo; modified from Weber and Lajoie (1980). Note: The Santa Cruz terrace depicted here is equivalent to the Año Nuevo terrace of Weber and others (1995).

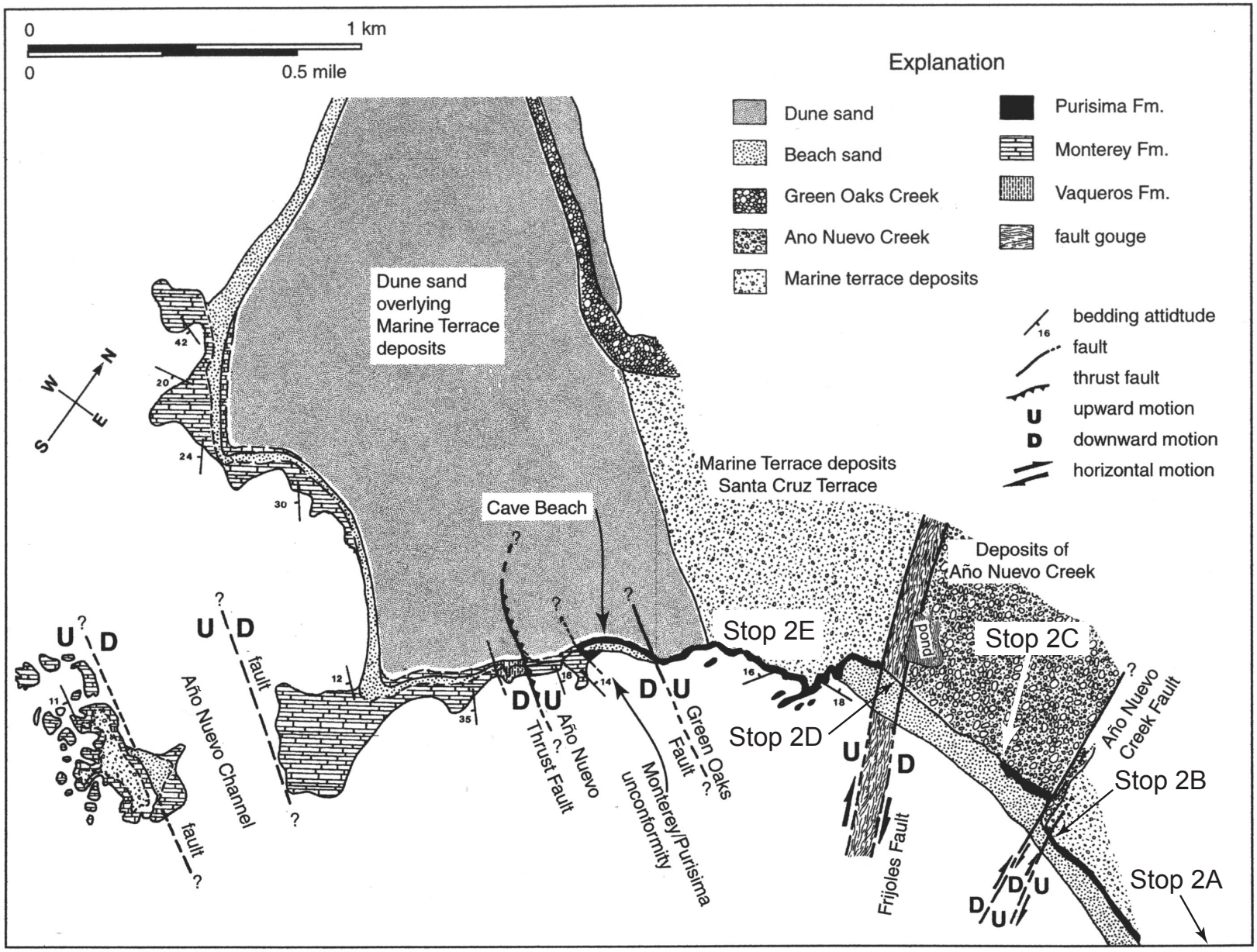

Figure 1.12. The San Gregorio Fault Zone at Point Año Nuevo, showing field trip stops 2B through 2E; see text for discussion. Note: The Santa Cruz terrace depicted here is equivalent to the Año Nuevo terrace of Weber and others (1995).

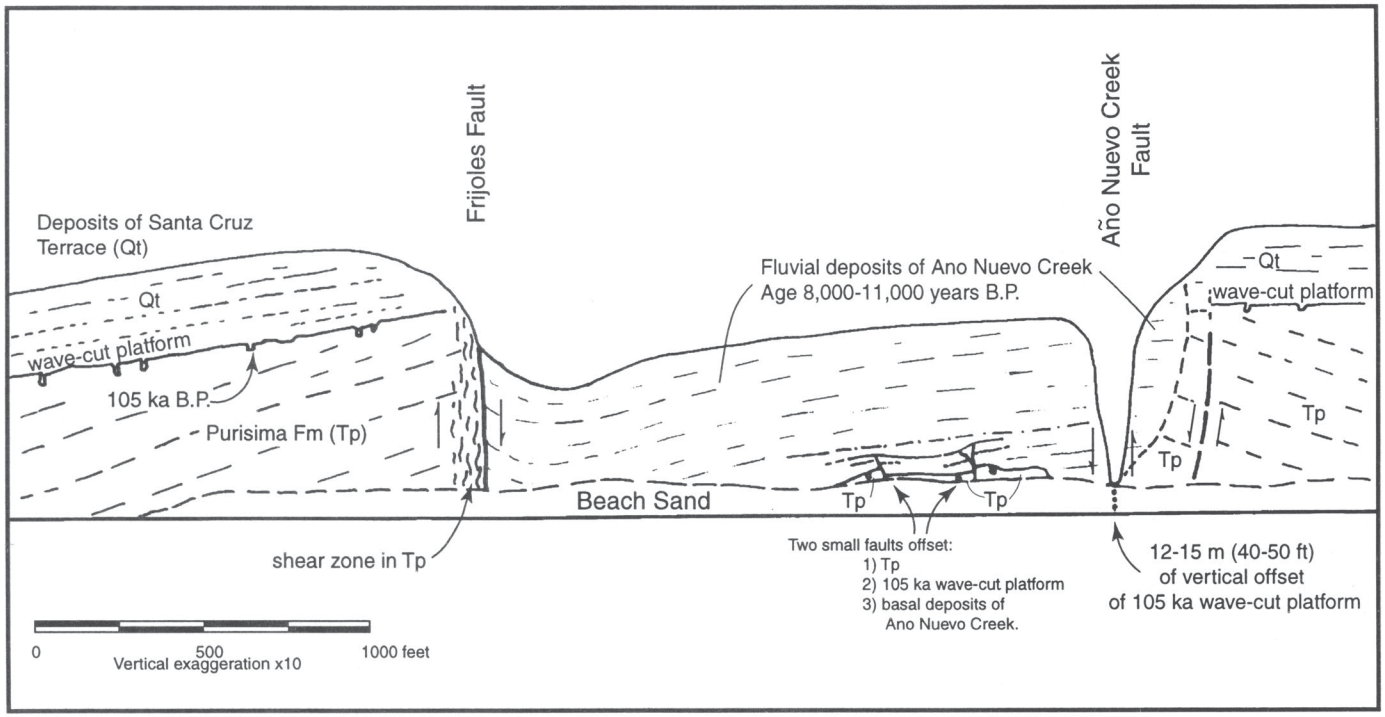

Figure 1.13. Highly schematic sketch of the seacliff geology west-northwest of Año Nuevo Creek, showing Holocene fluvial deposits of Año Nuevo Creek occupying a graben bounded by the Frijoles and Año Nuevo Creek Faults. Note the westward tilt of these fluvial deposits, except where a small drag fold has formed adjacent to the Frijoles Fault. Several minor Holocene faults offset the basal beds of the Año Nuevo Creek deposits (see also fig. 1.14). Note: The Santa Cruz terrace depicted here is equivalent to the Año Nuevo terrace of Weber and others (1995).

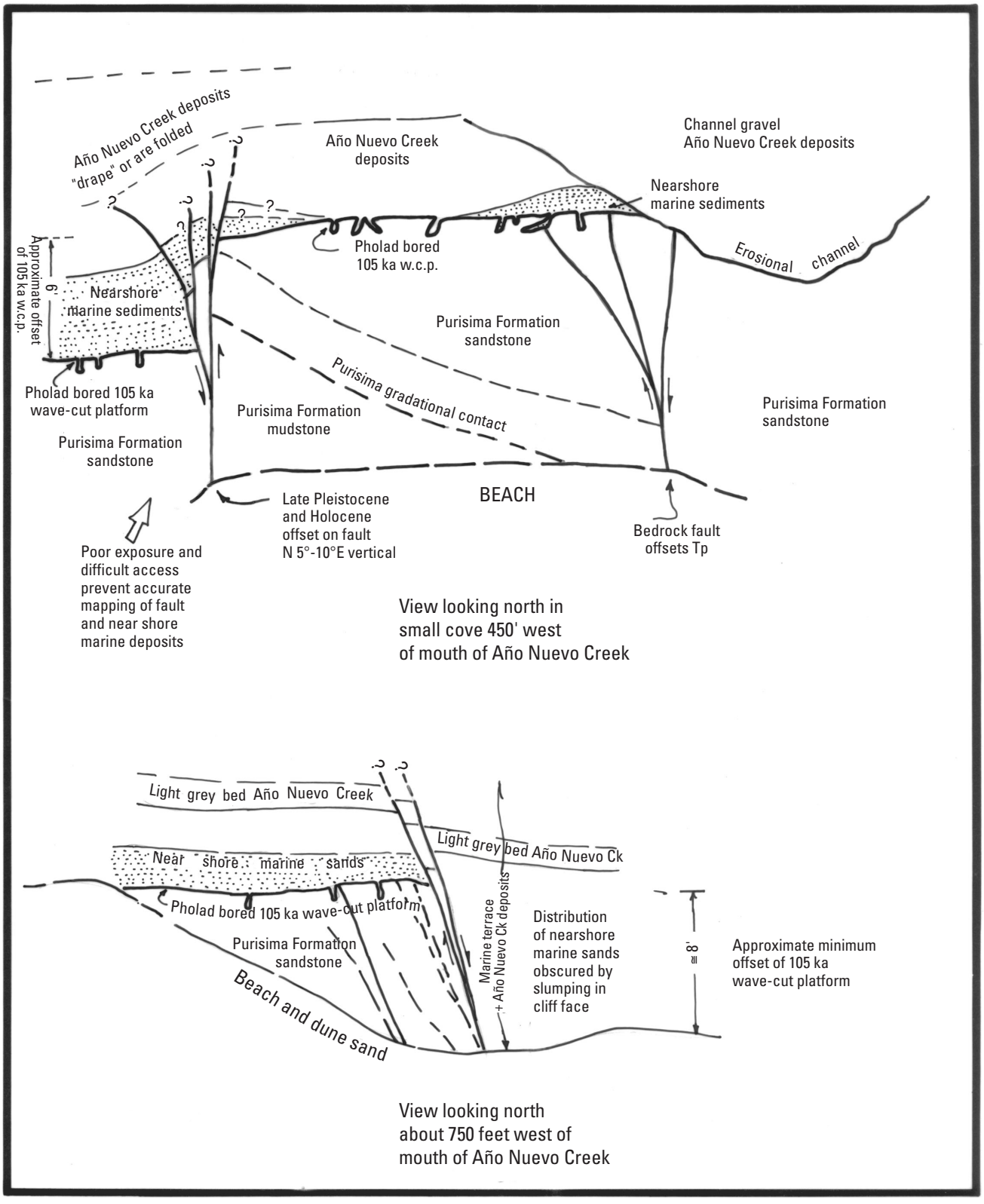

Figure 1.14. Field sketches of seacliff exposures west-northwest of the mouth of Año Nuevo Creek.

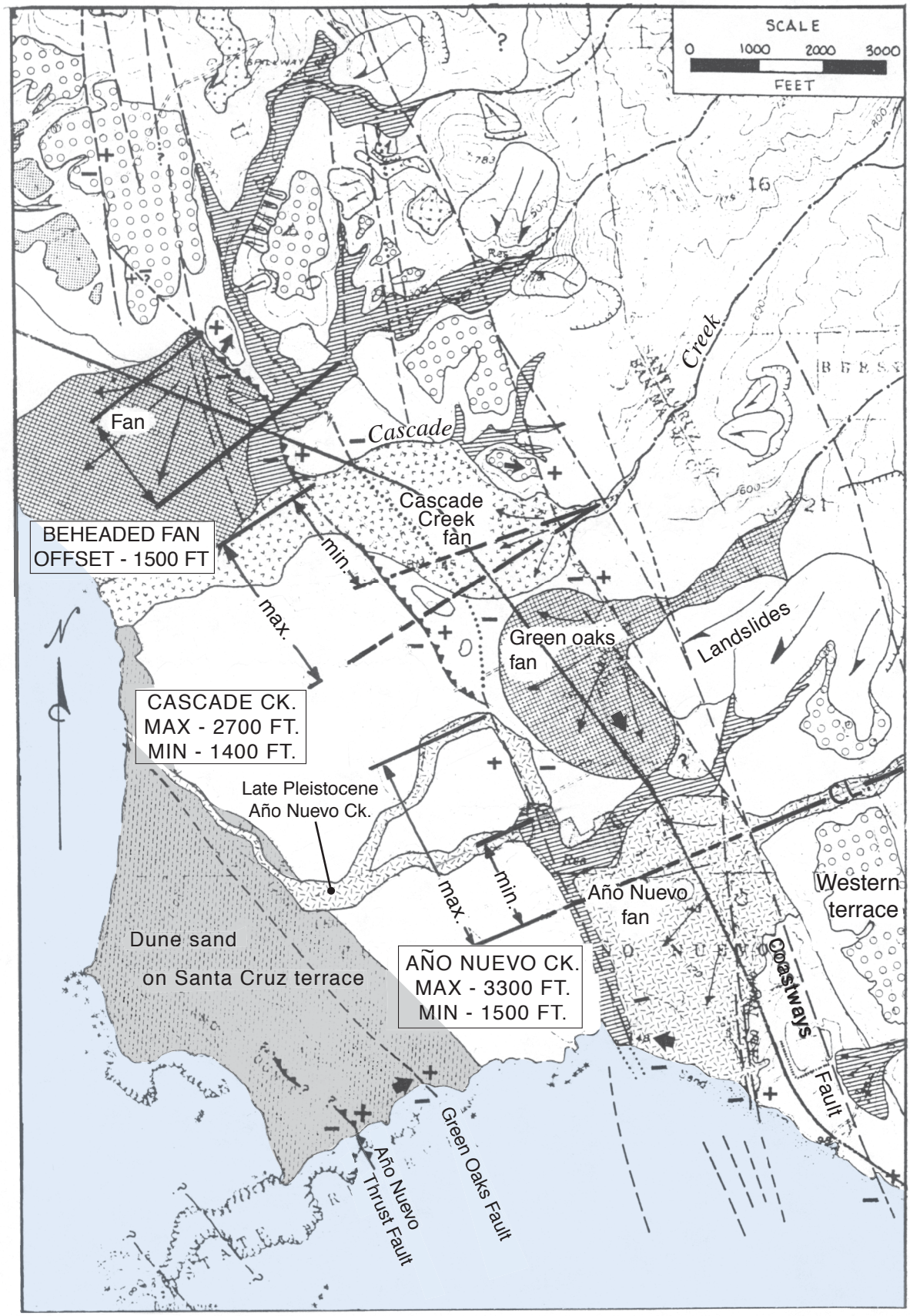

Figure 1.15. Interpretive map showing the probable offset of late Pleistocene drainages near Point Año Nuevo. Refer to text for a discussion of the assumptions employed in these reconstructions. Note: The Santa Cruz terrace depicted here is equivalent to the Año Nuevo terrace of Weber and others (1995).

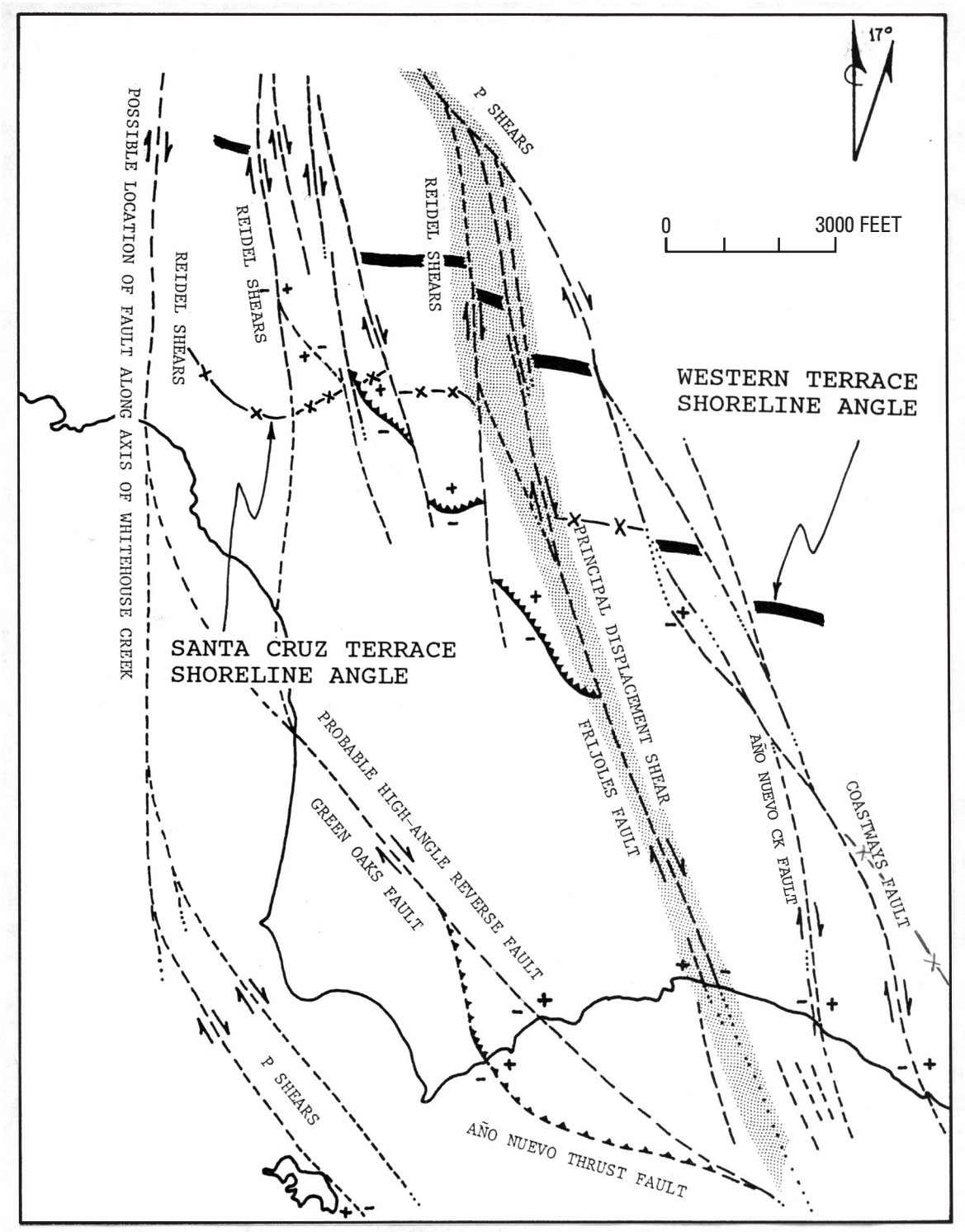

Figure 1.16. Preferred interpretation of displaced marine terrace shoreline angles in the San Gregorio Fault Zone at Point Año Nuevo. Note: The Santa Cruz terrace depicted here is equivalent to the Año Nuevo terrace of Weber and others (1995).

A Geologic Excursion to the East San Francisco Bay Area

Russell.W. Graymer
U.S. Geological Survey, Menlo Park, Calif.

Fieldtrip Overview

This fieldtrip serves two purposes. First, we will take a look at some of the interesting geology that characterizes the San Francisco Bay region. This will be a "hands-on" look that I think offers a better feel for the role of geology in the shaping of the landscape, and the impact of geology on society, than can be obtained in a purely classroom environment. Second, and probably more important, we will have a chance to practice the technique of observational science, following the fundamental principles of the scientific method (observe, hypothesize, test). Geology, perhaps more than any other science, is based on deductive reasoning, because many of the geologic features we work with probably formed over thousands or millions of years. We see only the end product, and we have to deduce how it got that way. Understanding how those features developed and evolved requires looking at the normally very slow (though occasionally catastrophic) processes that are going on today, and extending those processes by thousands or millions of times. However, just a few basics will allow the careful observer to start to understand how the world around us took on the shape it now has and how ongoing geologic forces can impact our lives.

Each of our three stops has three sections in this fieldtrip guide—a short introductory section, an exercise for you to do in the field, and a longer section of material related to the geology seen at that stop. We will be discussing most of what is covered while we are in the field, so the longer section will be mostly useful for you after the trip is over. There is also a road log that lists mileage between the stops and indicates various geologic features along the way.

The point of each exercise is to put you into the field boots of a geologist. Remember that all science starts with an observation, and this is never more true than in geology. Be prepared to take a look at the world in a new way. Any observation may hold the key to understanding the geology at each stop.

If you think that geology is just about looking at rocks and minerals, this fieldtrip may be a bit of a shock. We will not talk much about different kinds of rocks until the third stop, and will hardly mention minerals at all. Geology is about understanding the Earth and how it works. Rocks and minerals can provide a lot of information about the geology (as we will see at the third stop), but they are only a part of the story.

I hope that the information and figures contained in this guide will also be useful to you in your classroom. If you want to know more, the U.S. Geological Survey and the National Park Service maintain web-pages where additional information is available. An excellent introductory page is available at: http://www.nature.nps.gov/grd/usgsnps/project/interp.html. Information about the San Francisco Bay region is available from http://sfbay.wr.usgs.gov, with field geology being emphasized at http://sfgeo.wr.usgs.gov.

I hope you enjoy the trip, and that you come away with an expanded idea of what geology is all about.

Road Log

Mileage/Notes

0.0 **Trip start—U.S. Geological Survey, Menlo Park.**

South on Middlefield Rd., LEFT onto Willow, RIGHT onto Bayfront Expressway (Highway 84), cross Dumbarton Bridge.

7.5 The freeway cuts through the south end of Coyote Hills. This ridge of Franciscan mélange was probably lifted up by a fault thought to be long inactive that runs under the flat area on the west edge of the hills. The hills are now in the process of being buried by young sediments as the Bay Block sinks down. (A block is a large crustal rock mass bounded by faults that moves or behaves as a single unit within a greater tectonically active region.)

EXIT onto I-880 South, EXIT at Mission Blvd., proceed northeast on Mission Blvd.

20.2 You just crossed the most active strand of the Hayward Fault. Did you notice it? Much more about the Hayward Fault and how to recognize faults as we go along.

Right on Stanford Ave., drive to the end of the street and park.

21.3 STOP 1—Mission Peak Landslide, Fremont

Return on Stanford Ave., LEFT on Mission Blvd., RIGHT onto I-680 North.

24.5 Notice the ridge on the right. The highland is underlain by early Pleistocene (about 0.5 to 1.5 million years old) Irvington Gravel (this is where the mammal fossils indicative of early Pleistocene age were first described in North America). The ridge has a very straight west side (see fig. 2.1) cut by the Hayward Fault. Just judging by this ridge, which way would you say the fault was moving?

EXIT at Mission Blvd., LEFT onto Mission Blvd.

27.5 The ridge to the right was formed by motion on the Mission Fault similar to that on the Hayward Fault, but the Mission Fault is thought to be inactive. Why do you think the ridge is still there?

30.1 To your right is Niles Canyon (see fig. 2.2). On the map you can see that Niles Canyon meanders back and forth in large curves. Normally a deep canyon like this is pretty straight, but this one has retained curves from a time before the hills were here. The hills have lifted up over the past million years or so, and Alameda Creek, curves and all, has just eroded its channel through the rocks to form the canyon as the hills were going up.

33.4 To your right the Hayward Fault has formed benches in the sides of the hills. Did you notice there is more than one level of benches? Faults like the Hayward Fault often form zones of deformation with multiple breaks at the surface.

Stay on Mission Blvd. to downtown Hayward, park at B Street.

39.3 STOP 2—Hayward Fault Zone, Hayward

RIGHT onto A Street, LEFT onto Foothill Blvd., merge onto I-580 West.

43.2 Notice the dropoff to the left. This scarp is formed by a strand of the Hayward Fault Zone that was until recently thought to be inactive. Recent studies have documented that it is active, though. The Hayward Fault Zone through here is made up of at least three active strands in a zone almost a kilometer (0.6 miles) wide!

48.8 Notice the white rock in the quarry to the right of the freeway. The rock exposed is a Jurassic (about 160 million years old) volcanic rock called the Leona Rhyolite. Today it is used for construction, but earlier in the 20th century it was mined for pyrite (iron sulphide, also called fool's gold). The sulphur was used to make chemicals. This area was listed as a potential copper mining area because of the high percentage of copper in the pyrite (many minerals are impure, with one element replacing a percentage of another element, like copper for iron in pyrite. Sometimes the impurity is what you're really after!). However, the copper potential never worked out. Imagine a big open-pit copper mine in the Oakland hills!

EXIT onto Highway 13.

52.7 This long, narrow valley was formed when rocks ground up by the motion of the Hayward Fault were more easily eroded than the surrounding rocks. Linear valleys like this can be a good indicator of a fault.

54.3 On the left is Lake Temescal (now a regional park). This long, narrow reservoir takes advantage of the long, narrow valley carved along the Hayward Fault Zone. Unfortunately, the Hayward Fault is still here, and still very active. This reservoir probably would never be built today.

EXIT onto Highway 24 East, go through the tunnel, just past the tunnel exit at Fish Ranch Road, turn RIGHT back over the freeway, turn RIGHT again onto the frontage road, and park in the large open area just before the freeway entrance

56.7 STOP 3—Caldecott Tunnel between Oakland and Orinda

Information on Stops

Stop 1—Mission Peak Landslide, Fremont

Introduction

In March 1998, after two consecutive years of heavy rainfall, a large portion of the northwest flank of Mission Peak detached from the mountain and began to slide down towards the newly constructed neighborhoods of luxury homes below (fig. 2.3). The huge body of displaced material moved slowly, only a few centimeters each day, but when motion finally ceased months later, a mass more than one mile long and a quarter mile wide had moved several hundred feet down the mountainside. Fortunately, only one home was affected by the slide, because its path took it along the side of one neighborhood and stopped just short of another.

Exercise

Geology is an observational science; our conclusions are based on features we see in the landscape, the soil, and the underlying rocks. Look at the 1998 slide (fig. 2.4*A*). How would you describe the shape of the land inside the slide? How would that show on a topographic map? Look at the map (fig. 2.4*B*) to see if there are other areas nearby with similar topography. What does that suggest?

More About It

Normally, the gravitational force that is continually trying to pull material downhill is countered by cohesion and friction in and among the rocks that make up the hillside. However, when conditions are created where the cohesion and friction are reduced enough, material will move downhill. The constant breaking down of rock to form soil by weather, plants, and animals is one way cohesion and friction are reduced, and some material is constantly moving downslope at a very slow rate, much less than a millimeter per day. This slow process is called hillside creep. At times, however, conditions exist when masses of rock can move relatively quickly (for rocks), a process called landsliding.

Several things can lead to landsliding—earthquake shaking, poorly engineered construction, natural erosion, and rainfall. Although landsliding is caused by any of these, and by combinations of them as well, rainfall is by far the most important factor. Heavy rainfall can increase the tendency for landsliding in several ways: by increasing the weight of a body of rock, by providing lubrication between and within the rocks of a hillside, and by raising water pressure sufficiently to lift bodies of rock away from the hillside (this is discussed below).

The Mission Peak Landslide is a very large example of a bedrock, or deep-seated, slide (the technical term is slump earthflow), one of several different kinds of landslides. Bedrock landslides happen where a weak zone below the surface of a hillside allows a large mass of rock to slide downslope all at once. After one or more years of heavy rain, the groundwater in the rock under the hillside is fully charged (all the space within the rocks that can contain water is filled up), and additional incoming water from rainfall creates increased water pressure. The water pressure can begin to lift the rocks near the surface up and away from the hillside, reducing the friction. If water pressure reduces the friction enough, and a weak zone exists in the rocks, a mass of rock will become detached and slide downward. Usually the pace of the slide, while fast for rocks, is slow in human terms, centimeters per day, so bedrock landslides seldom pose a threat to human life. The size and mass of these landslides, however, make them a substantial threat to buildings, roads, and other construction. In 1998, more than $140 million of landslide damage occurred in the San Francisco Bay region, most of it caused by bedrock slides.

Bedrock slides create a collection of unique landscape features (shown and described in fig. 2.5). The place the material is moved from (the zone of depletion) is characterized by features related to extension, whereas the place the material is moved to (the zone of accumulation) is characterized by features related to compression. The main scarp of the Mission Peak landslide is very prominent because of the light-colored rocks exposed there (fig. 2.6).

Over geologic time, the landscape features formed during a landslide are worn down by the effects of weather and hillside creep, leaving progressively more subtle, but still visible signs of older landslides (see fig. 2.7). The 1998 Mission Peak landslide was a reactivation of part of a much larger, older landslide (see fig. 2.8) that was still visible in the landscape prior to 1998.

Almost all hillsides in the San Francisco Bay region show some trace of old landslides (some 90,000 landslides have been mapped in the Bay area!), but some areas are more prone to new landsliding than others (geologists call the greater

or lesser tendency to slide "landslide susceptibility"). Three main factors contribute to a hillside's susceptibility to bedrock landslides—the kind of rock that underlies the hillslope, the steepness of the hillside, and the presence or absence of previous landslides. Weak rock, steep slopes, and the presence of previous landslides all make the area of the Mission Peak landslide very susceptible to bedrock landslides. Research is being conducted right now to quantify the susceptibility to bedrock landslides in the San Francisco Bay region. We are working to provide a tool that can be used for informed land-use planning, so that regions of very high susceptibility can be identified and rejected for development. The community on the flank of Mission Peak was lucky in 1998, the area affected by the slide was for the most part undeveloped. Informed planning can, hopefully, insure that new developments are kept out of harm's way.

In addition to bedrock landslides, another common type of landslide deserves mention, the debris flow (more commonly called a mudslide, but this name is misleading because the mass is made of rocks, trees, and other debris, as well as mud, and because the mass does not move by sliding!). Debris flows occur during very intense rain storms, when the layer of soil that covers the hillslope is saturated. A small slump occurs in the soil, causing the saturated material to liquefy, and flow quickly down slope, carrying rocks, trees, and other debris with it (see fig. 2.9). This type of landslide is small, but very fast-moving, up to 50 km/hour. The speed of these "slides" makes them very dangerous to human life. In 1998, three people were killed by a comparatively few debris flows in the San Francisco Bay region, but in 1982 an intense storm throughout the region caused 18,000 debris flows that killed 25 people.

Stop 2—Hayward Fault Zone, Hayward

Introduction

In 1868, a length of the Hayward Fault Zone stretching from Oakland to Fremont broke, and the rocks west of the fault suddenly jumped several feet to the northwest with respect to those east of the fault. The energy released by this sudden motion produced a large earthquake, causing destruction throughout the San Francisco Bay region (fig. 2.10). Until the earthquake of 1906, the Hayward Fault Zone quake was known as the Great San Francisco Earthquake. Although the effects of this earthquake were well studied at the time, the work was for the most part lost, thought to have been suppressed by local government officials concerned that scientific studies of earthquakes could dampen growth and development in the region!

Since 1868, however, the Hayward Fault Zone has been relatively quiet, and has not generated a large earthquake. The forces that lead to earthquakes have not stopped, though. The rocks underlying San Francisco Bay continue to move northwest with respect to those east of the Hayward Fault Zone, but most of the fault zone itself is stuck, and pressure is slowly building up in the rocks near the fault zone. Eventually the pressure will overcome the friction and other forces that are causing the fault zone to stick, and the accumulated energy will be released in another big earthquake.

While almost all of the fault zone is stuck, in some places conditions within the rock allow the portion of the fault at the surface to slowly slide along in response to the pressure building up on the stuck fault. This slow sliding is called fault creep. Although the motion of creep is very slow (on the Hayward Fault Zone, the maximum creep rate is 9 mm/yr, or about 1/1000 mm/hr!), over the years the effects of the offset can be seen, especially in man-made structures. It is important to note that while creep does allow that part of the fault near the surface to slide along without pressure building up, most of the fault at depth is still stuck, so creep doesn't do much to help reduce the next big earthquake. However, creep does help us find some of the parts of the fault zone where pressure is building up.

Exercise

Look for evidence of creep in the manmade structures (curbs, streets, parking lots, and buildings) in the area. Remember that the rocks west of the fault are moving north with respect to those east of the fault. Mark the position of the fault creep on the detailed map (fig. 2.11*A*)**.** Use your observations of fault creep to make a map of the surface trace of the creeping fault. Transfer your fault trace to the map of the larger area (fig. 2.11*B*). Do you see any other features in the map that look like they might be related to the motion of the fault?

More About It

Major fault zones, like the Hayward Fault Zone, are fractures in the upper crust, formed when very large blocks of the Earth's lithosphere slide along, over, or under other blocks (the lithosphere is the rigid outer part of the Earth composed of the

crust and the upper mantle). The force that drives the motion of these blocks is provided by the continual formation, motion, and destruction of huge pieces of lithosphere called plates. The collective motion of the plates (fig. 2.12), called plate tectonics, is the driving force for most of the earthquakes, volcanoes, and mountain uplifts in the world. Where plates interact by sliding past one another, like they do in California, the upper crust near the plate boundary is broken into large blocks that are separated from each other by fault zones, like the Hayward Fault Zone. Driven by the northwest motion of the Pacific Plate with respect to the North American Plate, the blocks in the San Francisco Bay region are in motion. Each block moves northwest with respect to the one east of it.

Although most people, including many geologists, tend to think of a fault as a single crack in the Earth's crust, the major fault zones are actually very complex systems composed of many faults (fig. 2.13), not all of which are moving at the same time or in the same way. Through the long history of a fault zone (the Hayward Fault Zone is probably about 12 million years old), the sliding motion between the moving blocks is sometimes focused in one area, later in another area. The creeping part of the Hayward Fault Zone has probably moved only about 5 km, roughly 1/20 of the total offset of the Hayward Fault Zone as a whole.

Just as the long history of the fault zone is complex, the active part of the fault zone also involves more than a single crack. In the area near our stop, at least three different faults have evidence of recent activity (perhaps you spotted one in the exercise). Geologists look for evidence of recent fault motion because we believe those parts of a fault zone that have moved most recently are most likely to move again. Remember that although the moving parts of the fault zone have changed, those changes took place over millions of years.

Recent fault activity, like landsliding, produces unique landscape features (fig. 2.14) that can be used to locate active parts of a fault zone. In the Hayward area, linear ridges, linear valleys, fault scarps, and offset streams all mark the active parts of the Hayward Fault Zone (fig. 2.15). It is important to note that not all active parts of the fault zone are creeping, although creeping parts are all active.

It is important to know which parts of the fault zone are currently active because one of the hazards during an earthquake is fault rupture (fig. 2.16). Any structure built across a fault that suddenly moves with offsets up to several feet will suffer extreme damage. In California, the U.S. Geological Survey (USGS) cooperates with the California Division of Mines and Geology (CDMG) to make special maps showing all faults known to be active, and special geologic studies are required before any structure can be built within 50 feet of one of the active faults. Because of the regulatory nature of the maps, though, only those faults known to be active are shown. In Hayward, only the creeping part of the Hayward Fault is shown. The other two faults that have features related to recent movement are not shown because their activity is not proven (though proof for one has recently been discovered, so it will probably be added to the next version of the maps).

Even more important than the fault-rupture hazard is the hazard from earthquake shaking and related effects (the 1989 Loma Prieta earthquake occurred deep in the crust, there was no fault-rupture damage, all the damage was caused by shaking and related effects). Shaking occurs in response to waves of energy that are released by and move away from the rupturing fault. In general, the intensity of the energy waves decreases as they move away from the fault, so the farther from the fault rupture, the less shaking is felt. However, shaking can be magnified by the geologic or man-made material under the surface. Loose materials like artificial fill, bay mud, and sand dunes tend to amplify shaking the most, whereas bedrock tends not to amplify shaking at all. In addition, loose materials saturated with water can be converted to "quicksand" by shaking, a process called liquefaction. Shaking can also trigger landslides, especially if there has also been heavy rainfall. Although these hazards have long been recognized (the danger of artificial fill was noted after the 1868 earthquake!), maps of these hazards have only recently begun to be produced. USGS is currently cooperating with the CDMG to produce maps showing areas of liquefaction and earthquake induced landslide hazard. Regional maps showing predicted shaking intensity for large earthquakes on several faults in the San Francisco Bay region are available from the Association of Bay Area Governments: their informative earthquake website is http://www.abag.ca.gov/bayarea/eqmaps/eqmaps.html.

The Holy Grail of earthquake study is, of course, earthquake prediction. Accurate prediction of earthquakes is at present impossible, because irregularities in the fault surface, differences in properties of the rocks cut by the fault, and the interplay of pressure buildup and release on every fault in the region, all affect the exact amount of pressure that needs to build up to overcome the resisting friction on any given part of a fault. Perhaps one day geologists will be able to measure tiny changes in some property of the fault zone, such as electrical, magnetic, acoustic, production of various gasses, to give an early warning of an earthquake. For now, scientists at USGS and elsewhere are using more general techniques to try to determine where and when an earthquake is likely to occur. Information about when the last major earthquake was, how fast pressure is building up, and how large an earthquake to expect are combined to give a probability of an earthquake on active faults over a 30-year time period. At the same time, engineers are using seismic data to design earthquake resistant structures.

It may be interesting to note that the idea of plate tectonics that all our understanding of earthquakes and major faults is now based on is a relatively new concept. The first observations that ultimately led to the modern ideas of plate tectonics were made mostly after World War II, and the theory was only fully accepted by the scientific community in the late 1960's.

Stop 3—Caldecott Tunnel Between Oakland and Orinda

Introduction

In the San Francisco Bay region, vegetation and soil obscure much of the detail about the underlying rocks. Geologists make the most of those few areas where the rocks are well exposed, either by natural processes like canyon erosion, or by man, such as in the roadcut at this stop (figs. 2.17 and 2.18). When Caldecott Tunnel was expanded, the steep and deep cuts here exposed a body of rock that otherwise would have been for the most part obscured. The complete exposure allows us to make important observations that can tell us what the environment was when the rock formed, where material that was deposited here came from, how old the rocks are, and what has happened to the rocks since they were formed.

Exercise

The work of the geologist in the field is much like the work of a detective, making careful observations and trying to put all the information together to make a coherent story that explains what we observe. Use the map (fig. 2.19) to record your observations about the rocks at this stop (Are they all the same color? Texture? Are they made up of the same things? Are they layered?). Try to think of a story that explains what you see.

More About It

The first thing to look at here is the big picture. As we look north, we see that there are two very different kinds of rock bodies (fig. 2.18). On the left, the rocks are green, light gray, and in some places red: they are distinctly layered, and some layers are harder than others. This body of rocks is called the Orinda Formation. On the right, the rocks are dark brown, hard, with thicker layers that are less distinct. This body of rocks is called the Moraga Volcanics. Geologists name rock bodies after the place where they were first discovered or described, or where they are best exposed. Naming rock formations helps geologists communicate with each other our observations about various rock bodies, although misuse of names sometimes leads to confusion.

A closer look at the Orinda Formation reveals that it is made up of layers of broken up pieces of other kinds of rock (fig. 2.20). Rocks made up of pieces of other rocks are called sedimentary. Some layers are made of large pebbles and cobbles (geologists call rocks like these conglomerate), other layers are made of tiny grains too small to see (geologists call that mudrock), others are in between, made up of sand (sandstone). A very close look at the pieces reveals that there are many different kinds of rocks among the pieces, all mixed together here. The pieces were broken off a variety of rock bodies somewhere else, mixed together during their transport here, and then dropped off to form the layers you see. But how?

There are several different forces on the Earth's surface that can move rock fragments, such as glaciers, wind, landslides, ocean currents, and rivers. Because the pieces in the layers here are sorted out into different sizes in different layers, we can eliminate glaciers and landslides. Why? Because observations by geologists have shown that glaciers and landslides deposit all different sizes of fragments mixed together. And wind does not have enough force to move the large cobbles we see in some of the layers here. So, that leaves ocean currents and rivers, which can form very similar-looking layers. We need a little help here, but the fossils of land mammals discovered here and elsewhere in the Berkeley Hills (fig. 2.21) reveal that the layers were deposited by rivers. The conglomerate layers formed in stream beds, where fast moving water could bring the large pieces, and floods formed the sandstone and mudrock as the river overflowed its banks and dropped out sediments in the floodplain as the moving water slowed down.

The Moraga Volcanics, as the name suggests, are an entirely different kind of rock body, not made up of broken pieces of other rocks brought here. A closer look at the rock body reveals that it is fairly uniform, dark and heavy. A very close look shows that it is not made of pieces, but is, instead, a solid mass. In some places, though, we can find parts of the rock body that are full of holes, and in others the solid mass is punctuated by well-formed crystals of a white mineral called plagioclase. Geologists know that a solid mass like this can only form when molten rock cools and crystallizes, forming an igneous rock. Igneous rocks can form deep within the earth, slowly cooling and crystallizing, producing rocks made of large crystals like granite (fig. 2.22), or can form when molten rock flows or erupts out onto the surface of the earth, cooling quickly with no time to form large crystals. The lack of large, interlocking crystals here shows us that this rock formed from molten rock on the surface (lava), which flowed out of volcanoes to make volcanic rocks (hence the name Moraga Volcanics). The holes we see in some places (fig. 2.23) are actually the remnants of bubbles, produced by gas released from the lava, and trapped when the lava hardened. The plagioclase crystals are large crystals that formed slowly deep below the volcano, and were brought to the surface with the lava during eruptions. The dark color of the volcanic rock reveals that it is rich in iron and magnesium, a

kind of rock called basalt. The volcanoes that produced the lava were long ago eroded away, although you can still see the remnants of one at Sibley Volcanic Regional Park nearby.

The place where the two bodies meet is called a contact (fig. 2.24). There are two ways a contact between different rock bodies can form. One is by sliding two rock bodies next to each other along a fault, which would form a fault contact. Fault contacts are usually recognizable by the grinding and stretching in the rocks on either side. The absence of grinding and stretching here says that this is not a fault contact. The other way a contact can form is when a younger rock body is formed next to an older body, a depositional contact. A closer look at the contact here reveals a thin, bright red layer of mudrock. The brick-red color is the result of baking, the hot lava cooking the layer of mud that it flowed onto. So, here, we can tell that this is a depositional contact, the lava flowed onto the sedimentary layers, and the volcanic rocks formed there. Geologists are very interested in contacts, because they tell us a lot about the history of the formation of the rocks. We make geologic maps that show where the contacts between different rock bodies are. However, in the San Francisco Bay region, it is very unusual to be able to see a contact as well as this.

Another thing you notice right away about this roadcut is that all the layers are steeply tilted (figs. 2.17 and 2.18). One of the earliest observations by geologists was that sedimentary and volcanic layers are almost always formed close to horizontal. This is called the Law of Original Horizontality, a fancy name for a simple idea—rock layers start out flat. The Grand Canyon is a perfect example of a place where the layers are still flat, but not so here. The plate tectonic forces that are driving the Hayward Fault Zone have also tilted and folded the layers of the Orinda Formation and the Moraga Volcanics. The roadcut has exposed the tilted layers of part of one side of a U-shaped structure called a syncline (fig. 2.25). As we leave this stop, we will drive east on the freeway to see the other side of the syncline, where the layers are tilted the other way. The tilting makes it hard to visualize the place these layers originally formed, everything is now standing on its edge. Even if the volcanoes that produced the lava flows were preserved, they too would be tipped entirely onto their sides!

Nevertheless, we can start to put together the history of these rocks. We start with a river system that over thousands of years of geologic time builds up a thick pile of sedimentary layers. At some point volcanoes erupt nearby, filling the river valleys with lava, flow after flow to build up a thick pile. Later, the originally flat sedimentary and volcanic layers are tilted and folded. This kind of story reveals the sequence, or relative age of events associated with these rocks. The idea of relative age is another of the earliest ideas of geology. All of the geologic periods that you may have heard of (like Jurassic, as in "Jurassic Park") were divided up using the ideas of relative age, including those involving fossils. Over the last few decades, though, we have been able to deduce the numeric age of certain kinds of rocks by measuring the decay of certain radioactive elements in the minerals within the rock (radiometric dating). Sedimentary rocks are not very good for this technique, but volcanic rocks are much better. The Moraga Volcanics here are about 10 million years old. You can see how numeric age and relative age can be combined. Clearly the Orinda Formation is older that 10 million years, the folding of the layers is younger than 10 million years.

And there's more! The way the cobbles in the conglomerate stack on one another tell us that the sediments in the Orinda Formation came from the west, the large size of the cobbles tells us the rivers were energetic and flowed down a steep slope, and the rounding-off of the edges and corners of the cobbles and pebbles tells us the sediments were only brought a moderate distance. It is hard to imagine now, but the hills we are in here were once a low river valley, and where San Francisco Bay is now were once pretty high hills and mountains!

So what happened? One clue is that the Hayward Fault Zone is between us and the Bay, so the mountains and hills that provided the sediment have been moved northwest by the fault motion, but how far? The answer is only now being unraveled, and the Moraga Volcanics play a big part. That is because the Moraga Volcanics are only half of the lava flows that were produced by volcanoes 10 million years ago. The other half is now found about 45 kilometers to the northwest (fig. 2.26), moved there by offset on the Hayward Fault Zone, so the mountains and hills must also have been moved that far (actually, there is another part of the Hayward Fault system that branches west of the volcanics, the total offset on the Hayward Fault Zone is about 90 kilometers). In addition to sliding northwest, the rocks of the San Francisco Bay block have also been pushed down by the same plate tectonic forces that folded and tilted the layers and lifted up the hills.

A geologist is trained to understand all the complexities of the story that the rocks can tell us and can draw on the observations and experiments of many geologists working before him or her, but we all start with careful observations of the rocks. Knowing just a few of the basics will allow anyone to begin to unravel the history of the landscape around us and the rocks under our feet. We can look at the world with a new point of view. Did any of us think about where the flat layers of the Grand Canyon came from before now? Have they been exposed to the same kind of plate tectonic forces that the rocks here have?

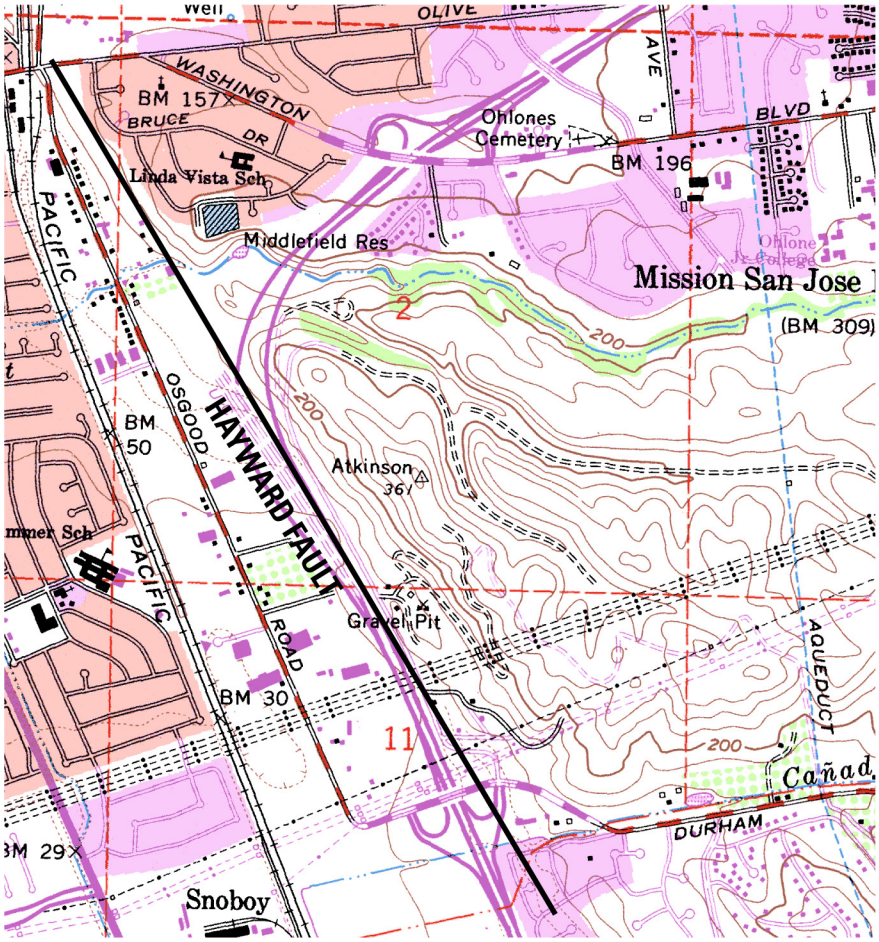

Figure 2.1. The ridge to the east of the freeway in the Irvington District of Fremont has a straight west face carved by the Hayward Fault (marked by the thick black line). This kind of face is called a scarp. (The map from the a portion of the Niles 7.5-minute quadrangle USGS topographic map.)

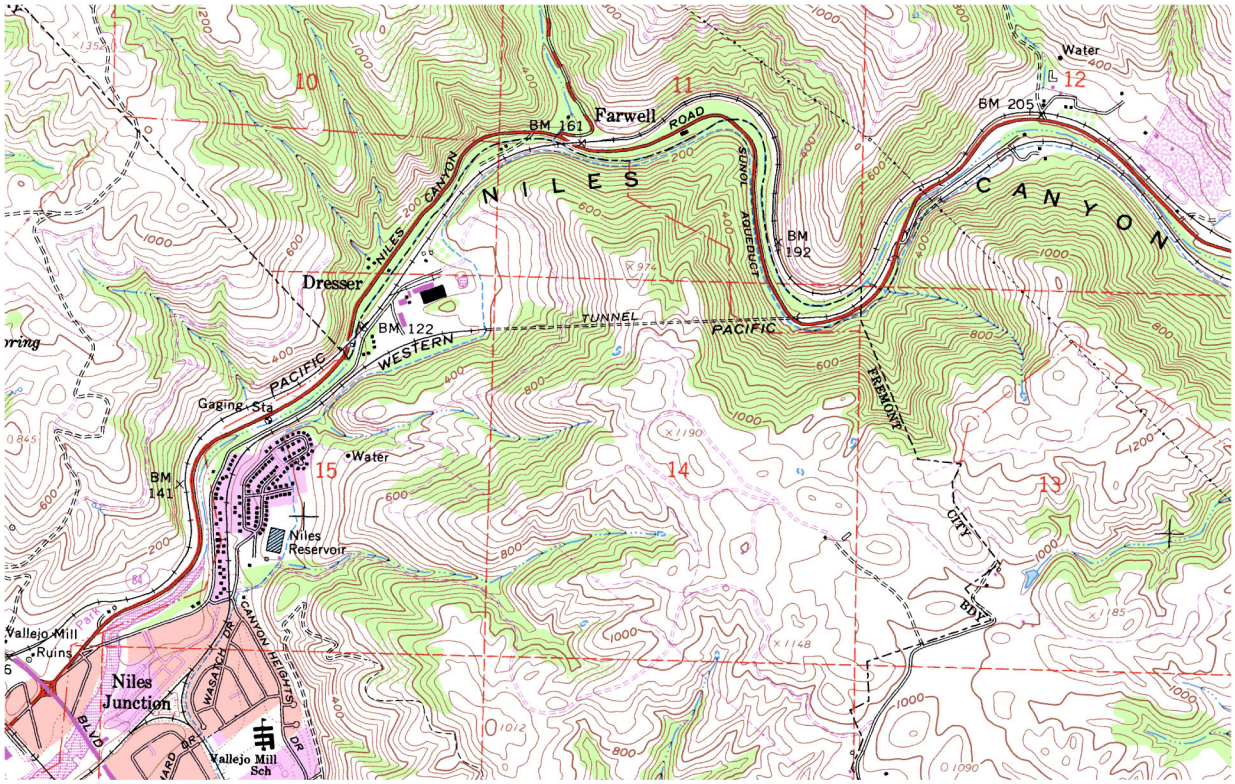

Figure 2.2. Notice the meandering path of Alameda Creek in Niles Canyon. These meanders were probably formed before the hills, and were trapped in the shape of the canyon which formed as the stream eroded through the hills being lifted up. (The map from the a portion of the USGS Niles 7.5-minute quadrangle topographic map.)

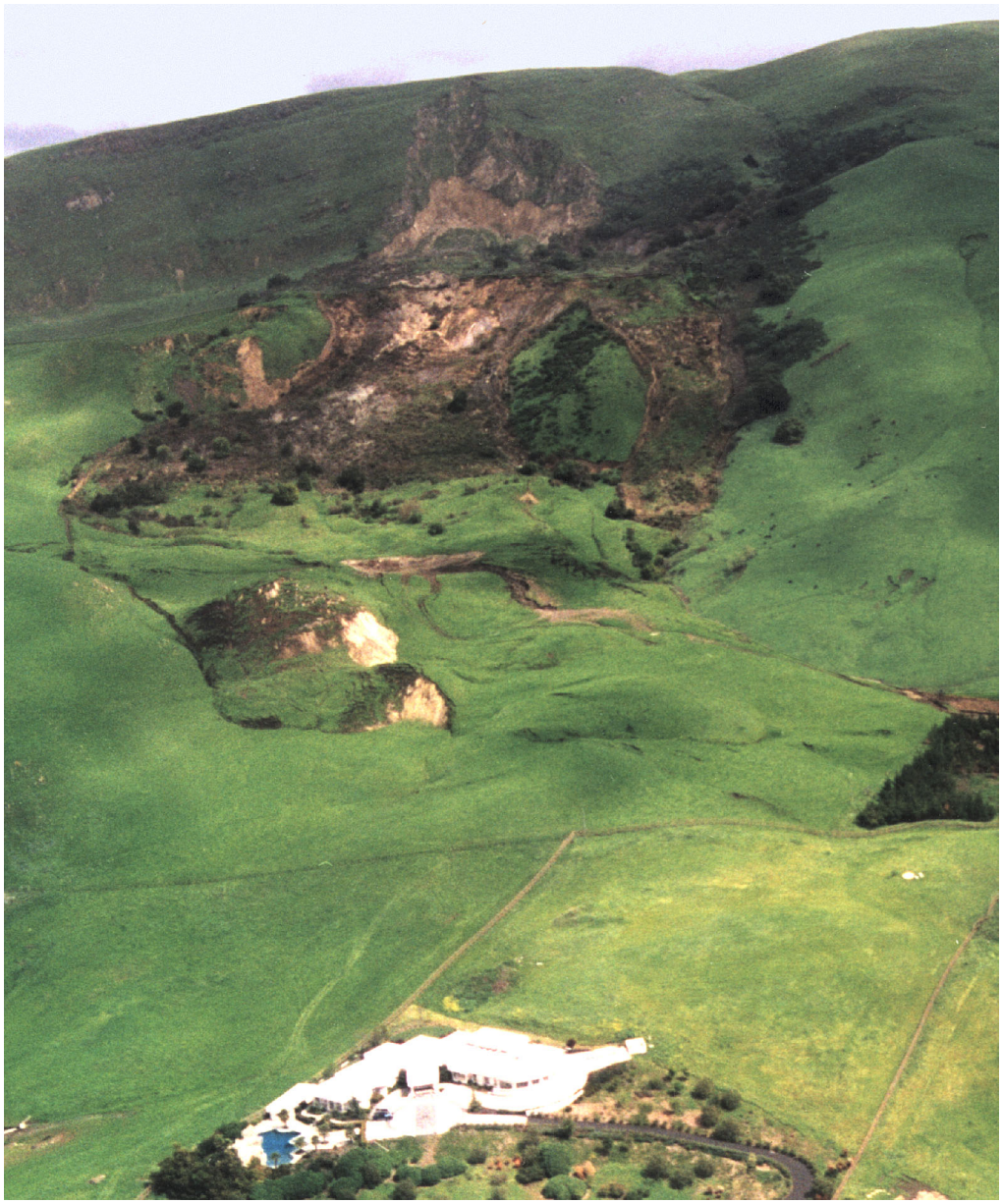

Figure 2.3. An aerial view of the Mission Peak Landslide (photo by Jeff Coe, U.S. Geological Survey).

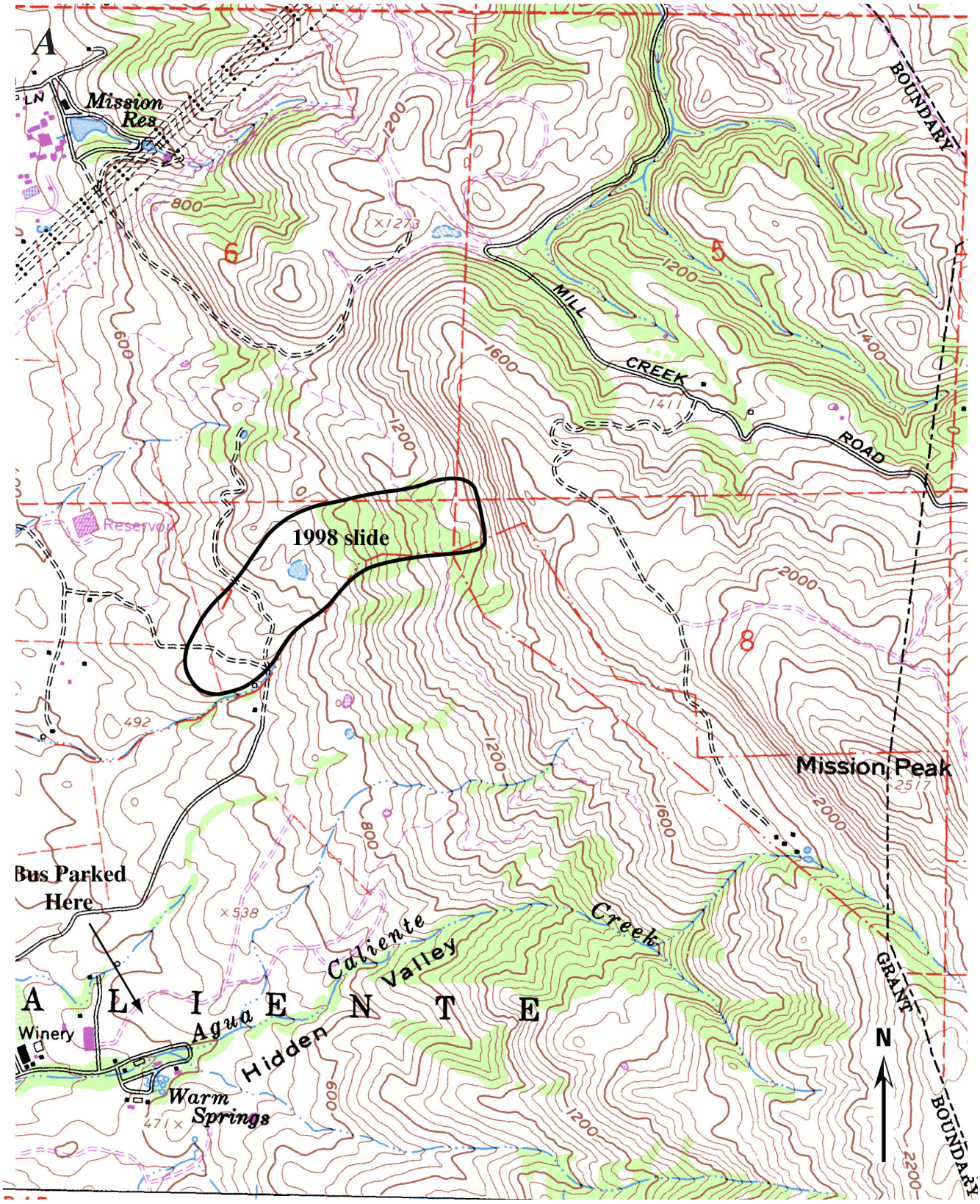

Figure 2.4*A* and *B*. Exercise maps for Stop 1 (portions of the USGS Niles 7.5-minute quadrangle topographic map).

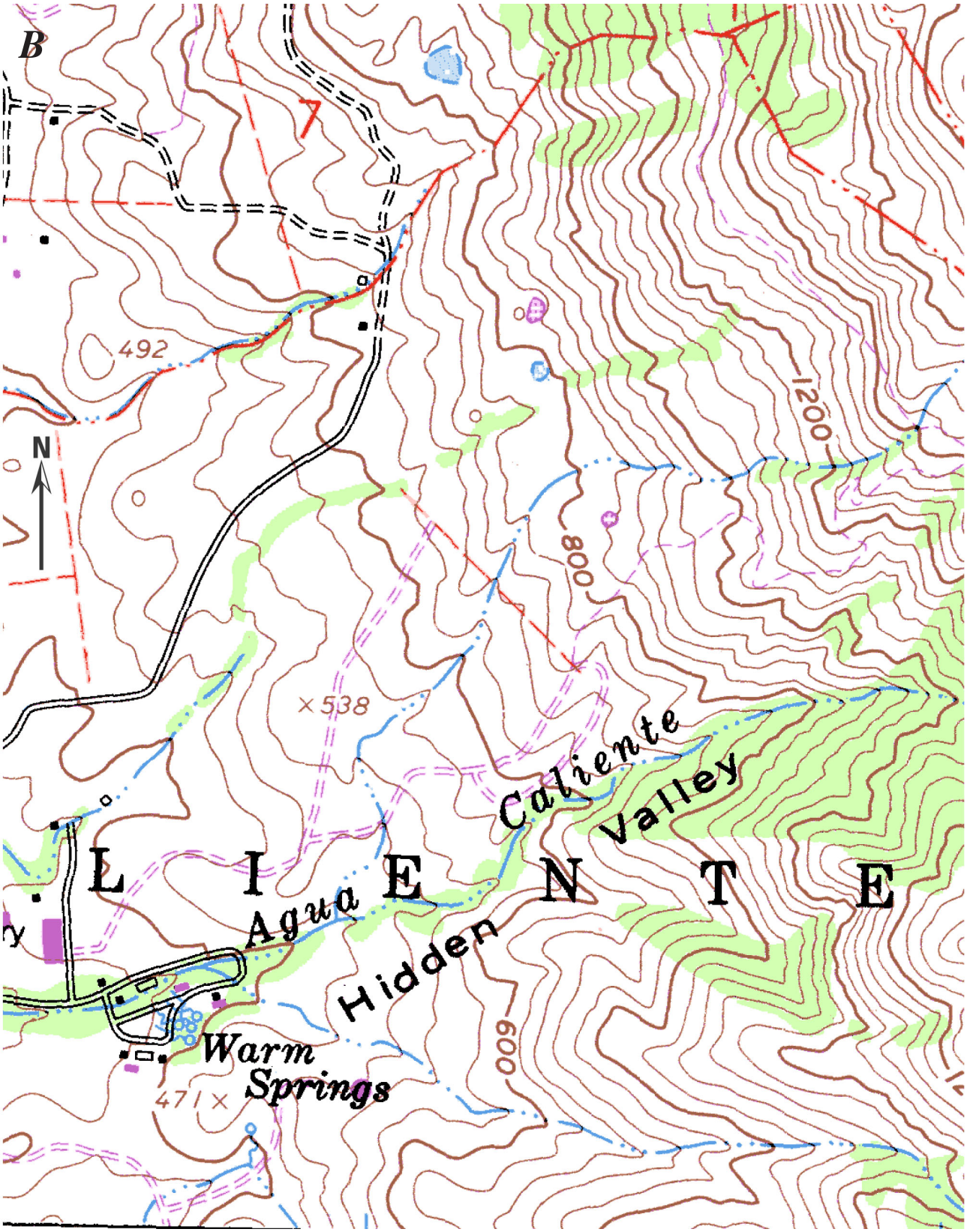

Figure 2.4*A* and *B*—Continued. Exercise maps for Stop 1 (portions of the USGS Niles 7.5-minute quadrangle topographic map).

MAIN SCARP—A steep surface on the undisturbed ground around the periphery of the slide, caused by the movement of slide material away from undisturbed ground. The projection of the scarp surface under the displaced material becomes the surface of rupture.

MINOR SCARP—A steep surface on the displaced material produced by differential movements within the sliding mass.

HEAD—The upper parts of the slide material along the contact between the displaced material and the main scarp.

TOP—The highest point of contact between the displaced material and the main scarp.

TOE OF SURFACE OF RUPTURE—The intersection (sometimes buried) between the lower part of the surface of rupture and the original ground surface.

TOE—The margin of displaced material most distant from the main scarp.

TIP—The point on the toe most distant from the top of the slide.

FOOT—That portion of the displaced material that lies downslope from the toe of the surface of rupture.

MAIN BODY—That part of the displaced material that overlies the surface of rupture between the main scarp and toe of the surface of rupture.

FLANK—The side of the landside.

CROWN—The material that is still in place, practically undisplaced and adjacent to the highest parts of the main scarp.

ORIGINAL GROUND SURFACE—The slope that existed before the movement of interest occurred. If this is the surface of an older landslide, that fact should be stated.

LEFT AND RIGHT—Compass directions are preferable in describing a slide, but if left and right are used they refer to the slide as viewed from the crown.

SURFACE OF SEPARATION—The surface separating displaced material from stable material, but not known to be a surface of failure.

DISPLACED MATERIAL—The material that has been moved from its original position on the slope. It may be in a deformed or undeformed state.

ZONE OF DEPLETION—The area within which the displaced material lies below the original ground surface.

ZONE OF ACCUMULATION—The area within which the displaced material lies above the original ground surface.

VC—Vertical component of slump.

HC—Horizontal component of slump.

L— Length of displaced zone along the slope.

LC—Length of slump along the slope.

D—Depth to rupture surface.

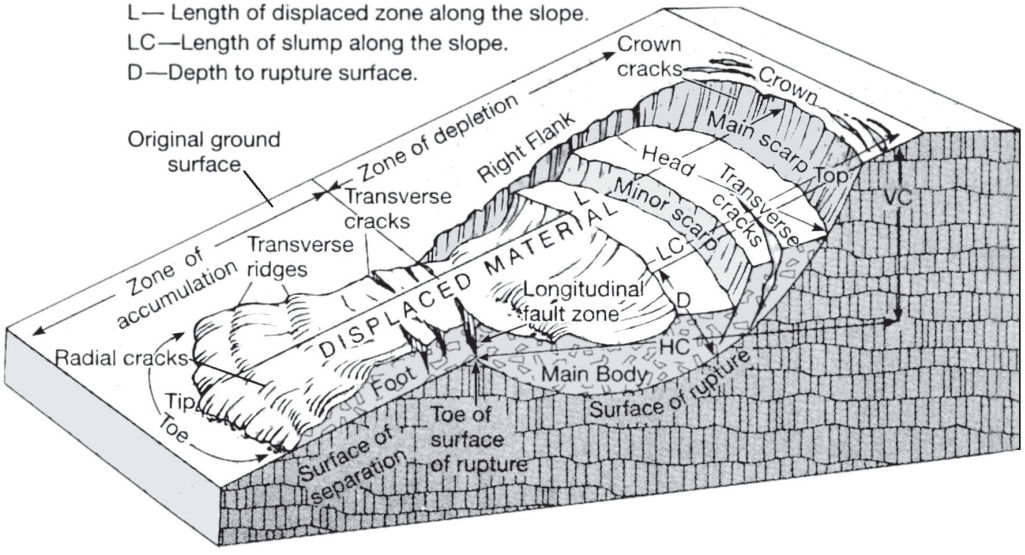

Figure 2.5. Anatomy of a landslide, showing landscape features produced by a bedrock landslide. Notice especially the different kinds of features at the top and the bottom of the landslide. This difference reflects the different forces at work in the area where rock is being piled up (the bottom, or zone of accumulation) and where the rock is being moved away (the top, or zone of depletion). Can you see some of these features in the Mission Peak slide? See fig. 2.3. (Diagram modified from West, T.R., 1995, Geology applied to engineering: Englewood Cliffs, New Jersey, Prentice-Hall, p. 294)

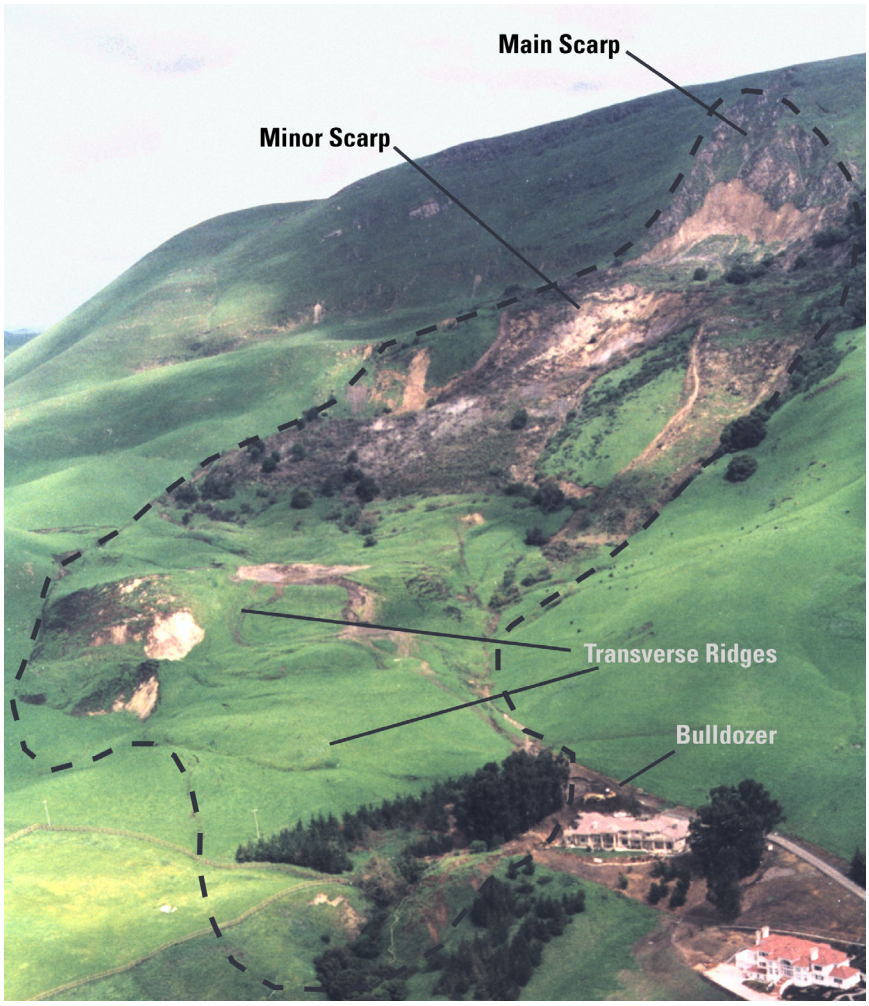

Figure 2.6. The outline of the slide is shown by the dashed line. The house nearest the slide experienced some damage during the slide, despite strenuous efforts to divert sliding material (note the large bulldozer beside the house!). Several of the landscape features formed during the slide are also marked (see fig. 2.5 for more about landscape features formed by bedrock landslides) (photo by Jeff Coe, U.S. Geological Survey).

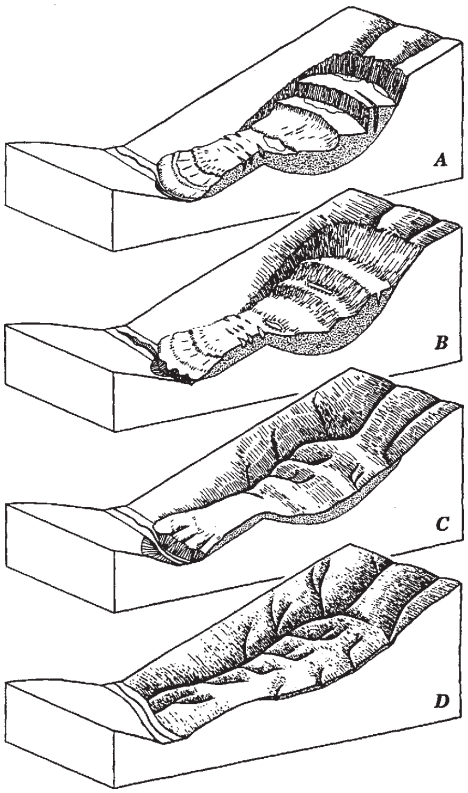

Figure 2.7. The effects of erosion on landscape features formed by landslides, from ***A***: a very recent slide, to ***D***: a very old slide.

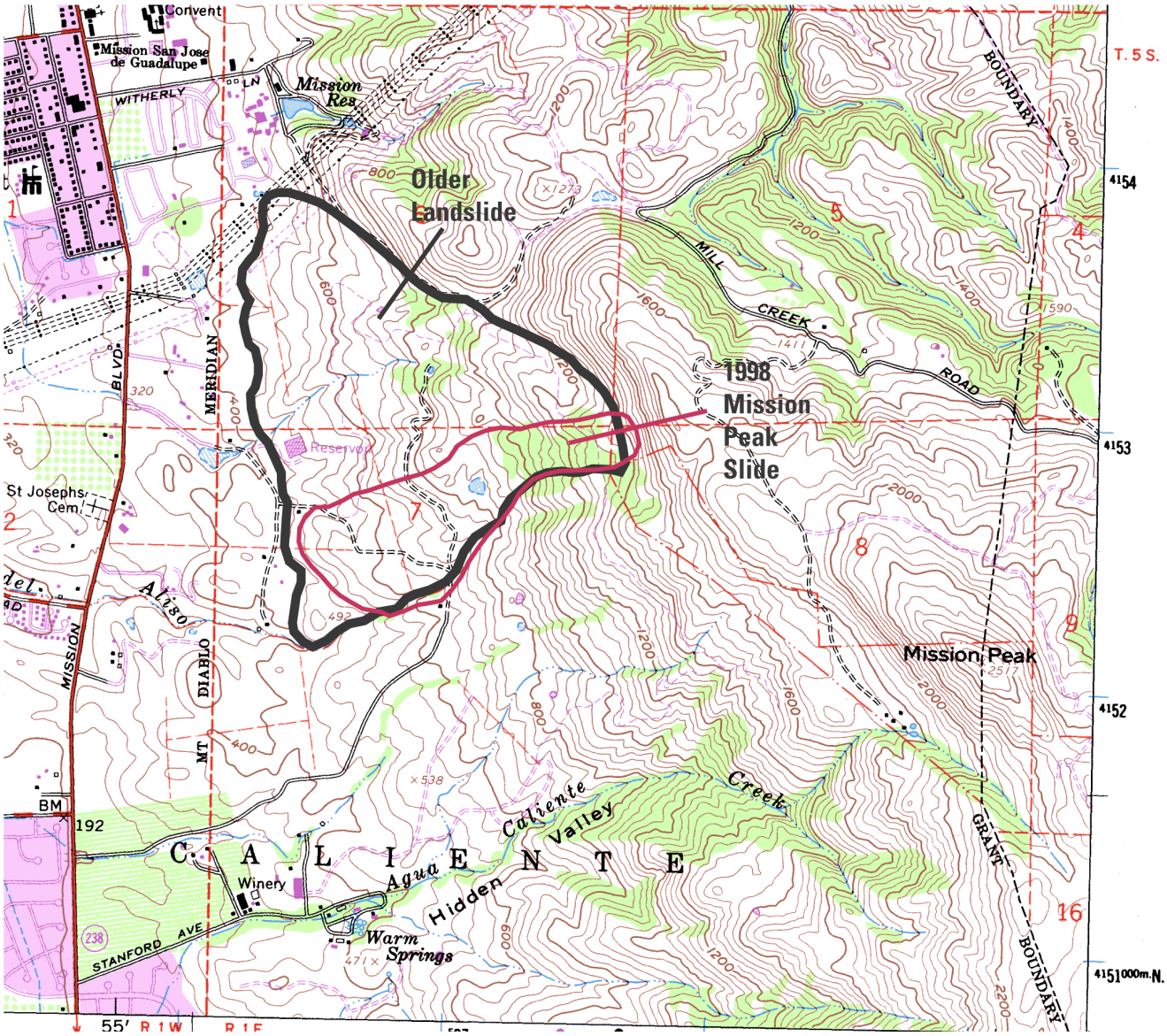

Figure 2.8. Map showing the approximate outline of both the 1998 Mission Peak landslide and the much larger, older landslide that contains it. Note the irregular appearance of the contour lines within the older landslide. Do you see other areas on the map that could be older landslides?

Figure 2.9. Debris flows: small, shallow, fast-moving landslides that commonly occur during very heavy rainstorms. Photo ***A*** shows a natural hillside scarred by many debris flows in 1998. Photo ***B*** shows the impact of a single debris flow on a home in Marin County in 1998.

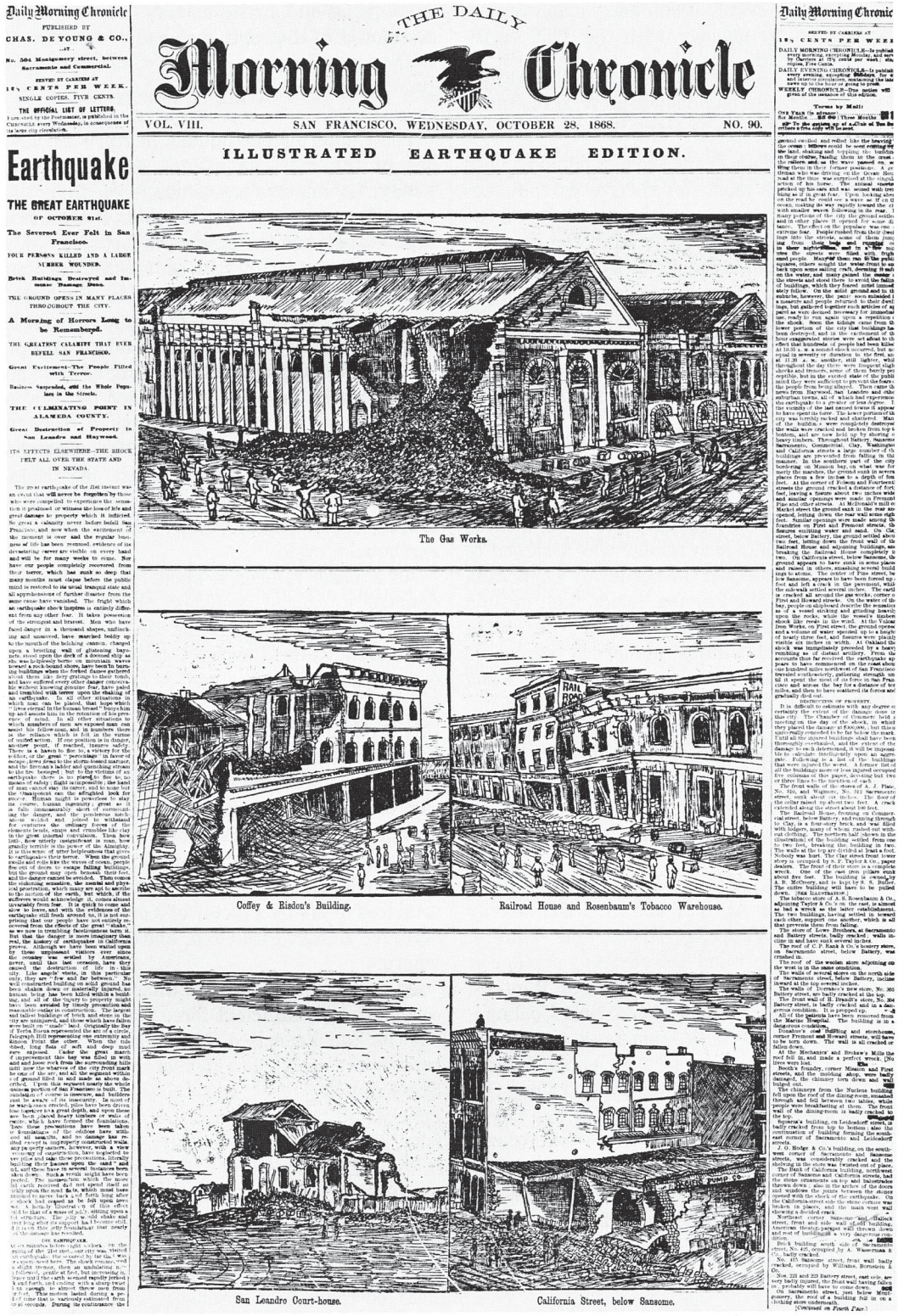

Figure 2.10. The front page of the San Francisco Chronicle following the 1868 earthquake on the Hayward Fault Zone.

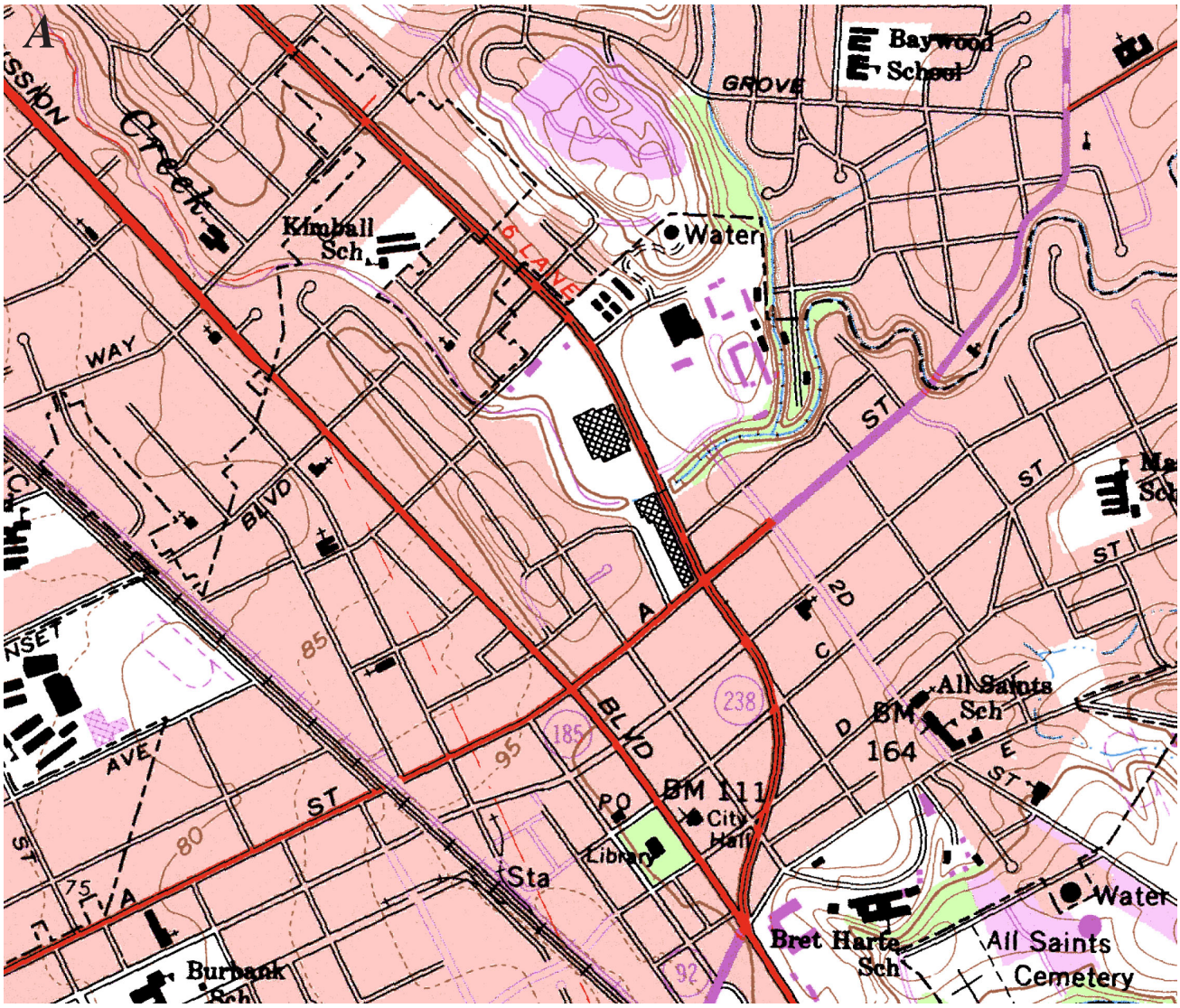

Figure 2.11*A* and *B*. Exercise maps for Stop 2 (portions of the USGS Hayward 7.5-minute quadrangle topographic map).

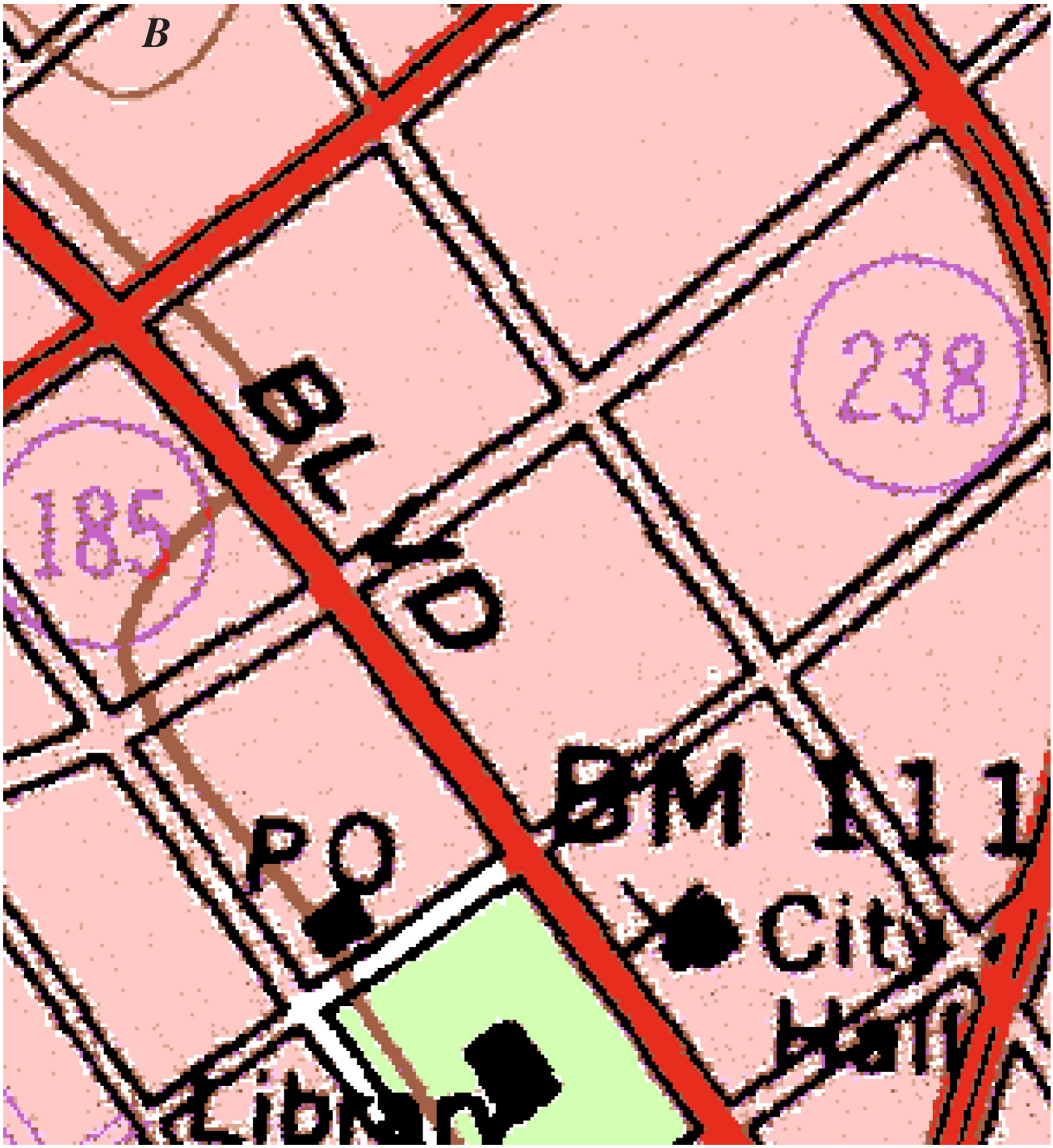

Figure 2.11*A* and *B*—Continued. Exercise maps for Stop 2 (portions of the USGS Hayward 7.5-minute quadrangle topographic map).

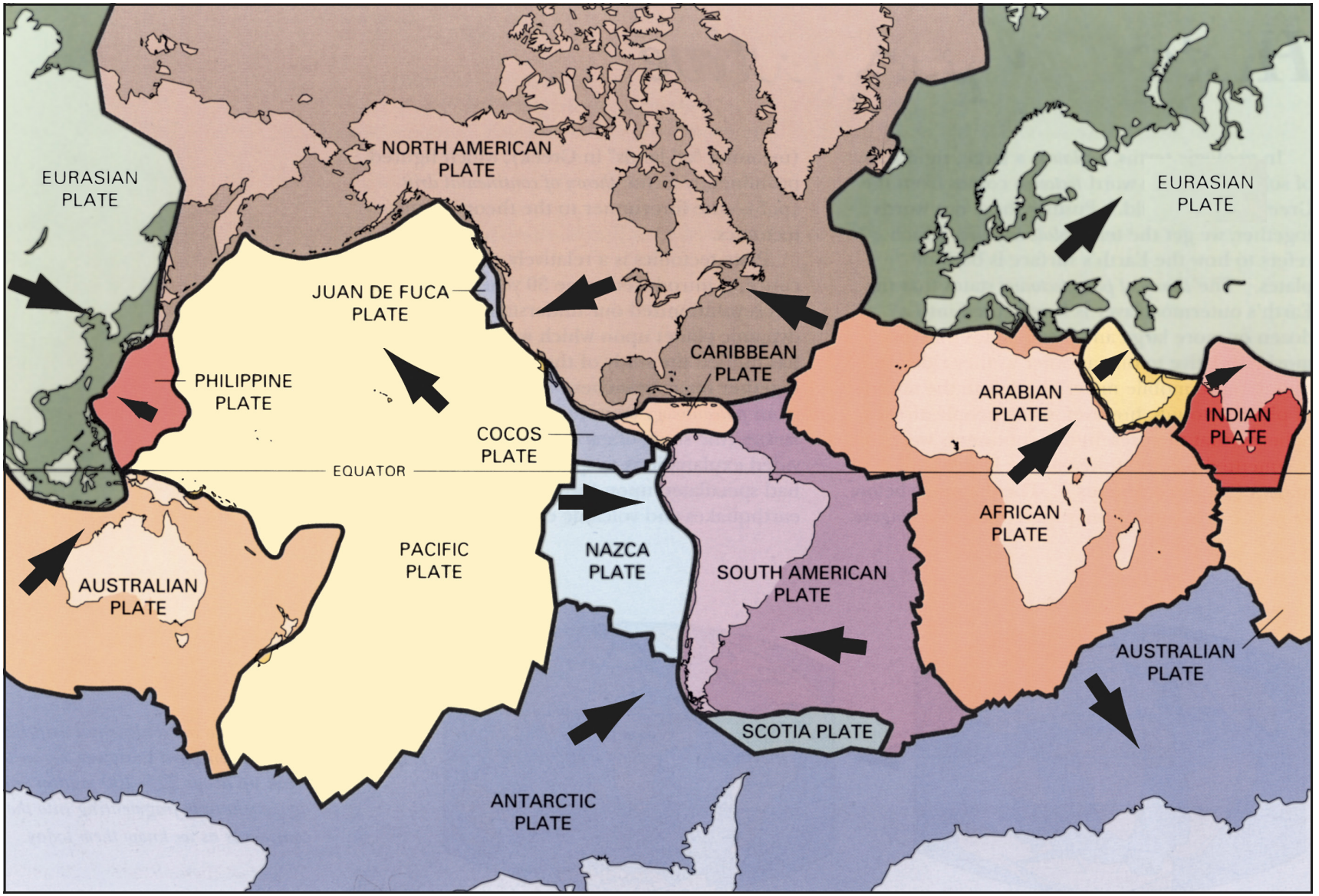

Figure 2.12. Map of the Earth's lithospheric plates, showing the direction of the relative motion of some of the largest. The motion of the Pacific and North American Plates is the driving force for the faults in California, like the Hayward fault. The U.S. Geological Survey and the National Park Service have excellent web-pages with more information about plate tectonics and links to detailed descriptions at http://pubs.usgs.gov/publications/text/dynamic.html and http://www2.nature.nps.gov/grd/usgsnps/pltec/pltec1.html.

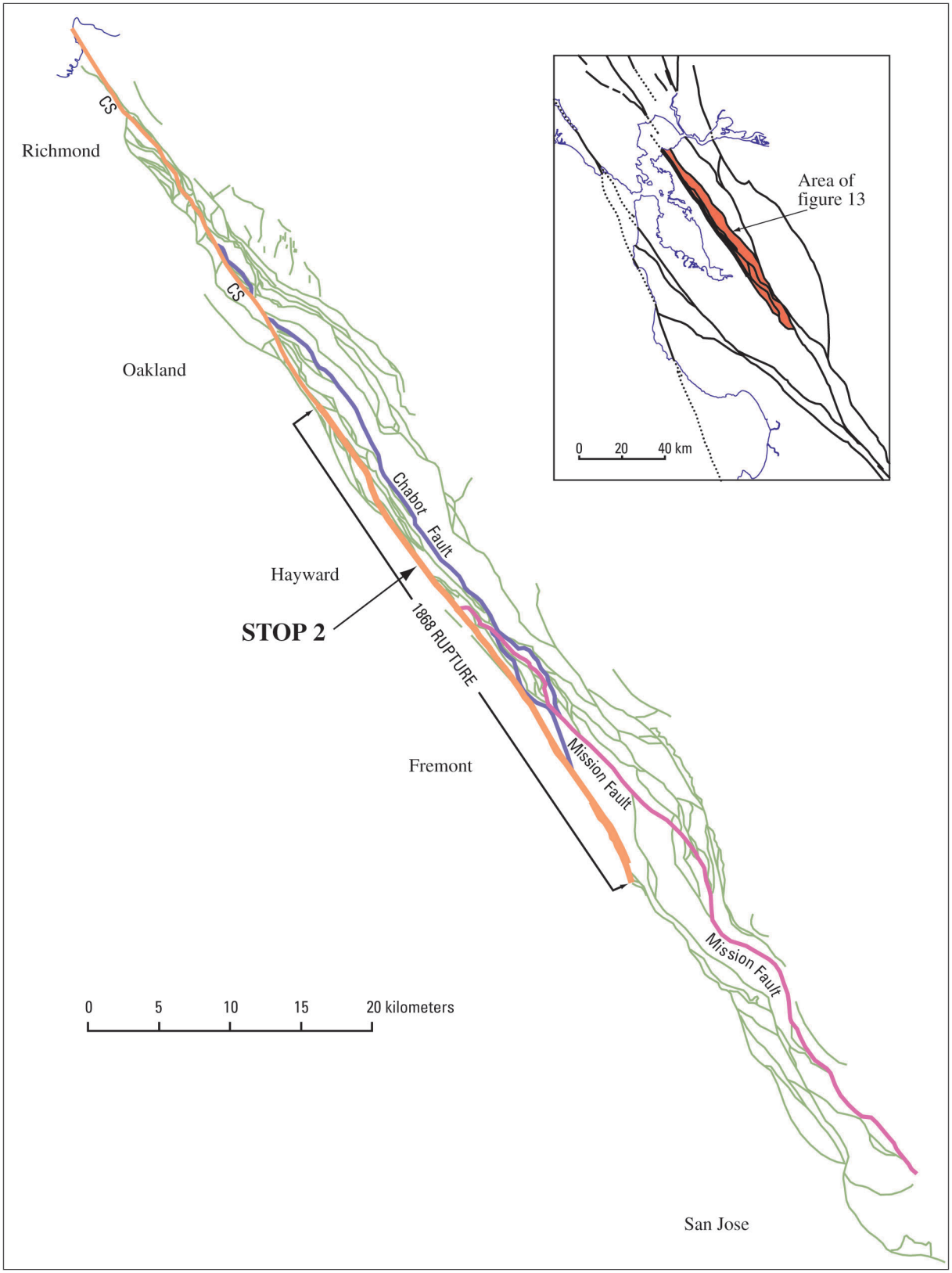

Figure 2.13. Generalized map showing all the known faults in the Hayward Fault Zone. Note that most of the faults are not presently active, but all have played a part in the 12-million-year history of the fault zone. The creeping part of the fault zone is shown by the thick line marked CS, and other named faults in the fault zone are labeled. The length of the fault rupture in 1868 is also shown.

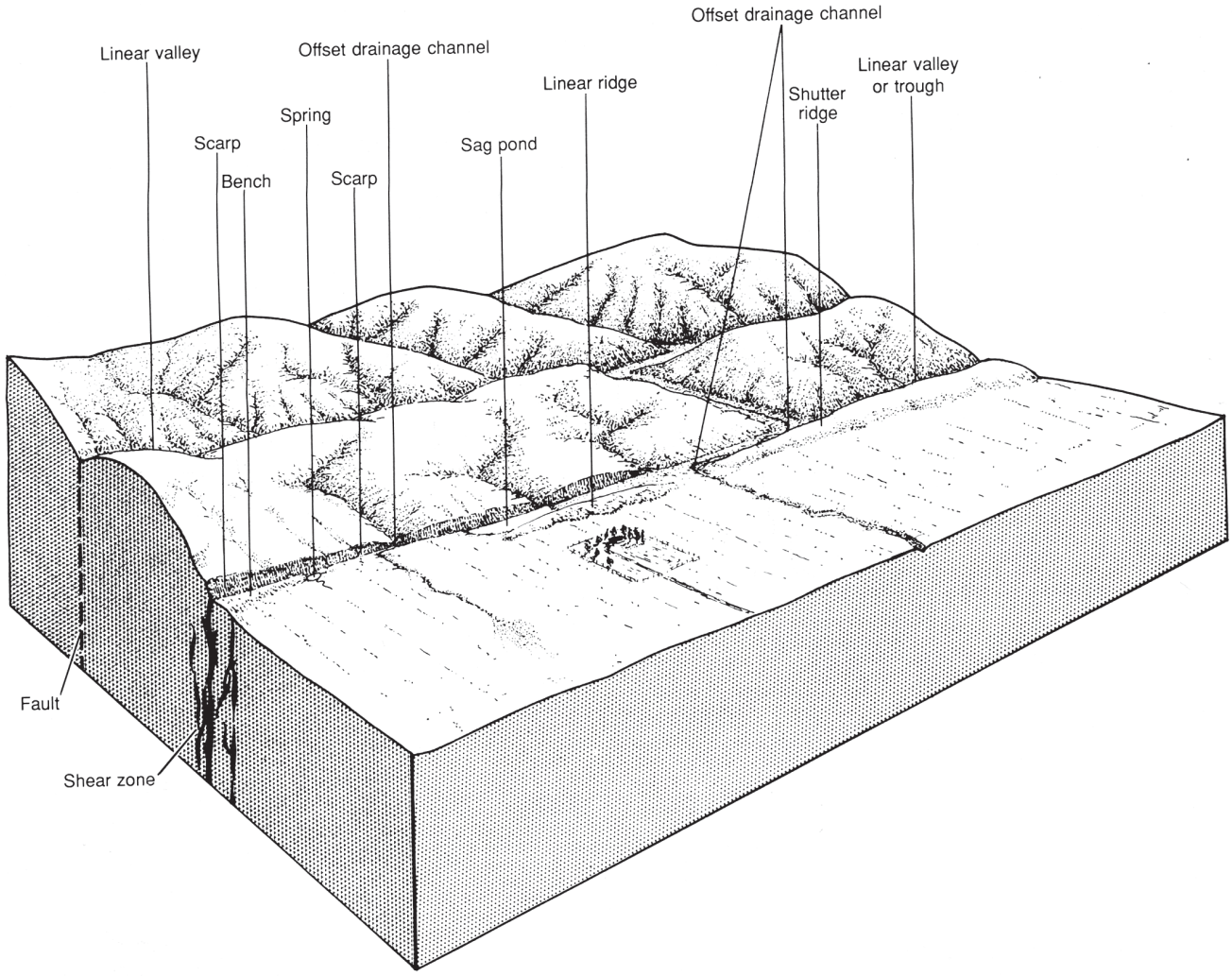

Figure 2.14. A block diagram of part of the upper part of the crust showing the landscape features associated with fault offset. Recognizing the presence of these features can help geologists locate faults that might be active even if they are not creeping. (Diagram from Wallace, R.E., ed., 1990, The San Andreas Fault System, California: U.S. Geological Survey Professional Paper 1515, p. 17.)

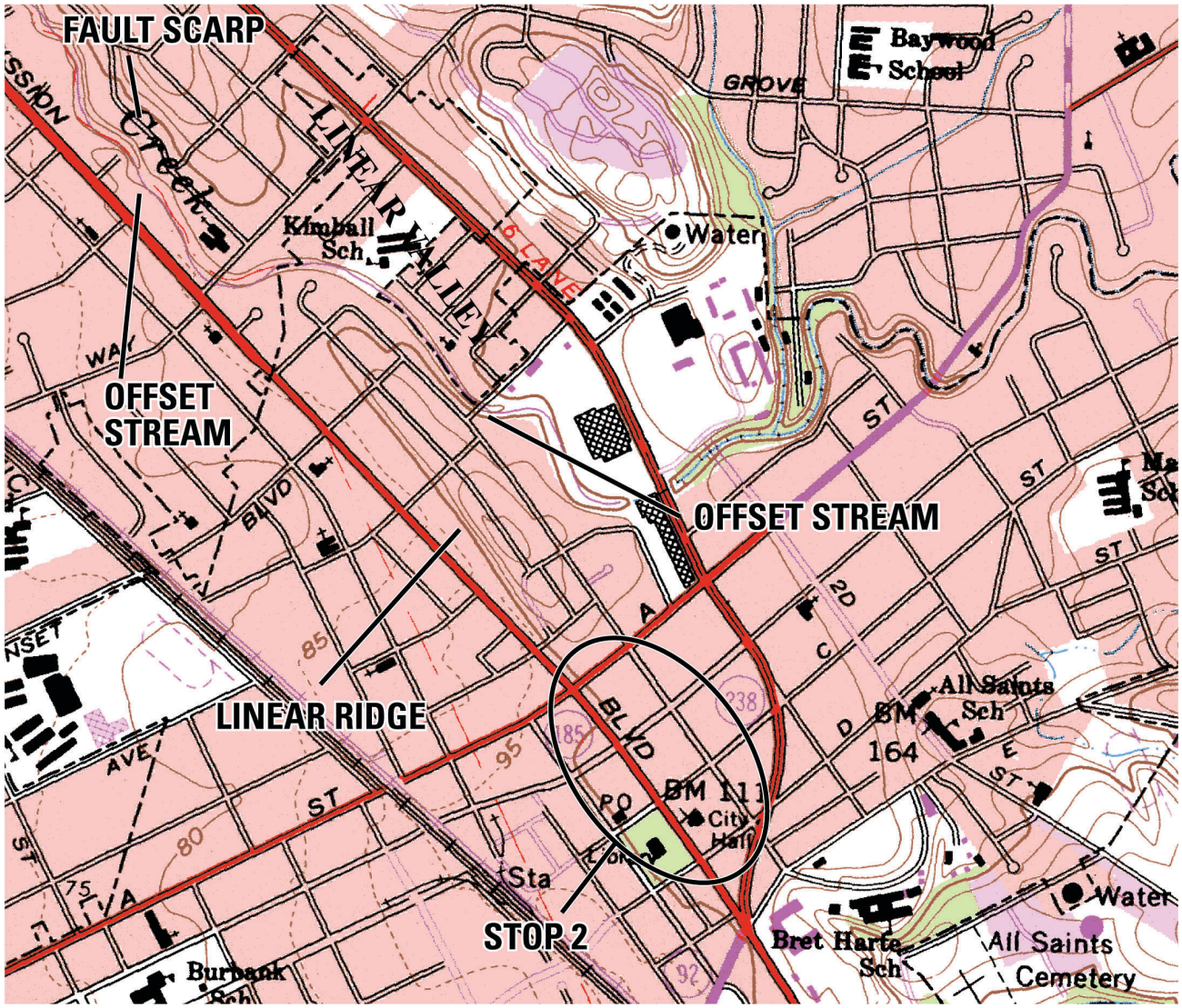

Figure 2.15. Topographic map of northern Hayward showing the landscape features associated with the Hayward Fault in the area of Stop 2.

Figure 2.16. Two photos showing the effects of fault rupture. During an earthquake, the Earth's surface along a fault can be suddenly and permanently offset by many meters. Photo ***A*** shows the result of 6 meters of offset that occurred during the 1940 Imperial Valley earthquake in southern California. Photo ***B*** shows the crack left by 6 meters of offset that occurred near Point Reyes during the 1906 San Francisco earthquake. Imagine what would happen to anything built across the fault. (Photos from Wallace, R.E., ed., 1990, The San Andreas Fault System, California: U.S. Geological Survey Professional Paper 1515, p. 163.)

Figure 2.17. Photo looking west from the parking area at the deep roadcut east of Caldecott Tunnel. Exposure like this is very rare in the San Francisco Bay region.

Figure 2.18. Another view of the roadcut east of Caldecott Tunnel. Notice the two very different kinds of rocks—the lighter rocks on the lower-left are the Orinda Formation, the darker rocks on the upper-right are the Moraga Volcanics.

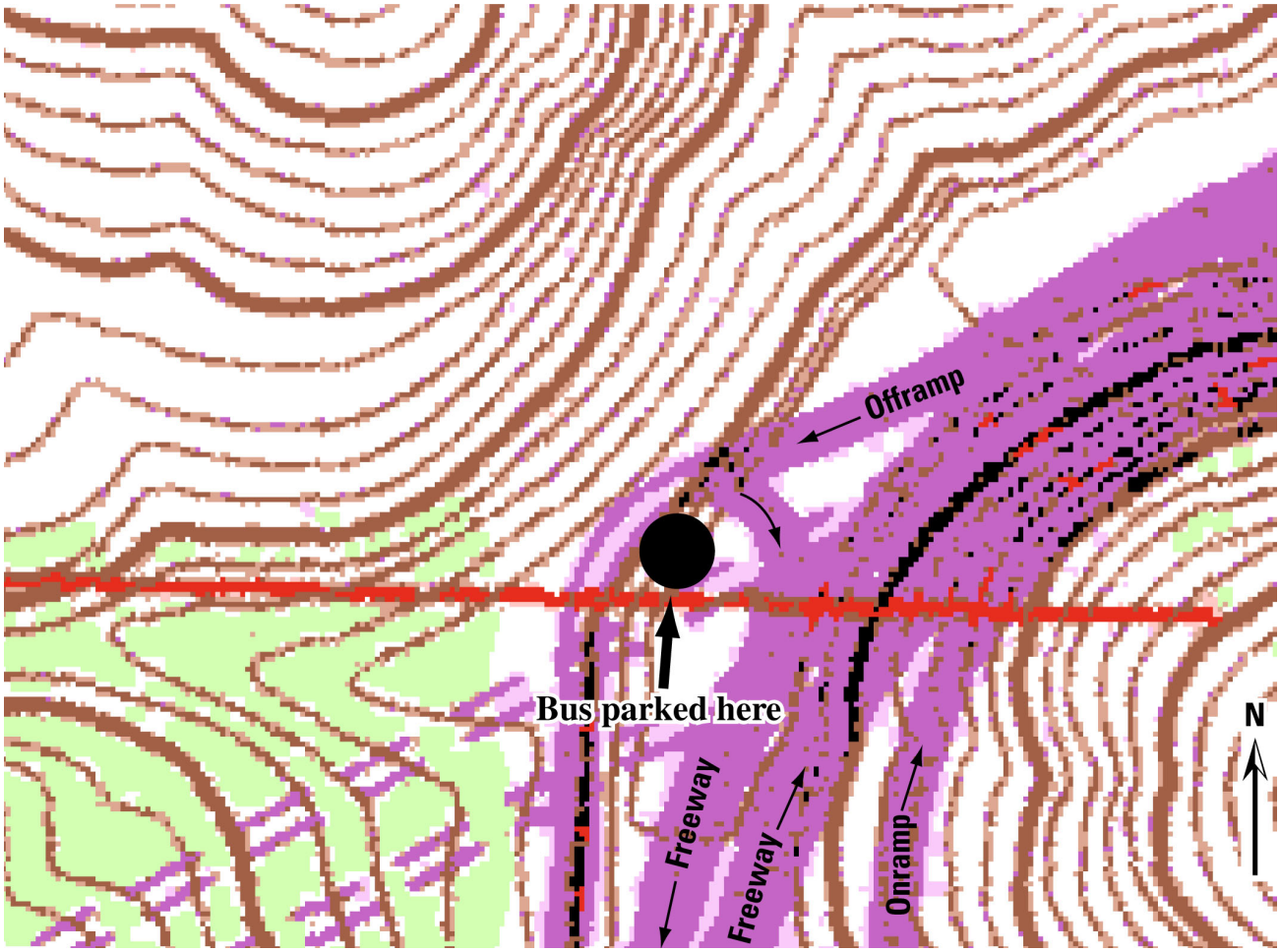

Figure 2.19. Exercise map for Stop 3 (a portion of the USGS Oakland East 7.5-minute quadrangle topographic map).

Figure 2.20. Two close-up views of the Orinda Formation. In the upper photo, notice how the rock is made up of fragments of many other kinds of rocks mixed together. In the lower photo, notice the layers, and how the different sized pieces are sorted into separate layers, cobbles and pebbles in the layer on the left, sand in the layer on the right, and mud in the red and green layers in the middle. Geologists use information like this to deduce how rocks were formed, in this case by deposition of eroded material by a river.

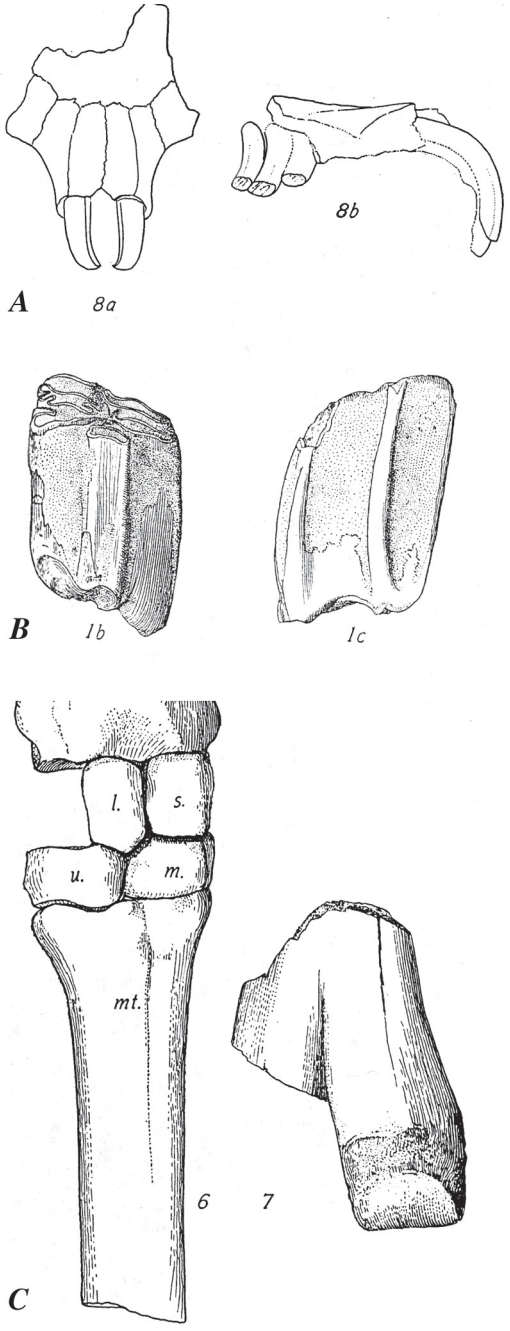

Figure 2.21. Sketches of fossils found in the Berkeley Hills. ***A*** is part of a beaver skull, ***B*** shows two horse teeth, and ***C*** shows two parts of a camel leg. Fossils from rabbits, hippos, and various plants have also been found. Notice the difference between the teeth of a beaver more than 10 million years ago and the teeth of a beaver today! These fossils show that the sedimentary rocks here formed in rivers, not in the ocean. What sort of fossils would you expect from rocks formed in the ocean? (Sketches reproduced from Merriam, J.C., 1913, Vertebrate fauna of the Orindan and Siestan beds in Middle California: University of California, Bulletin of the Department of Geology, v. 7, no. 19, p. 373-385.)

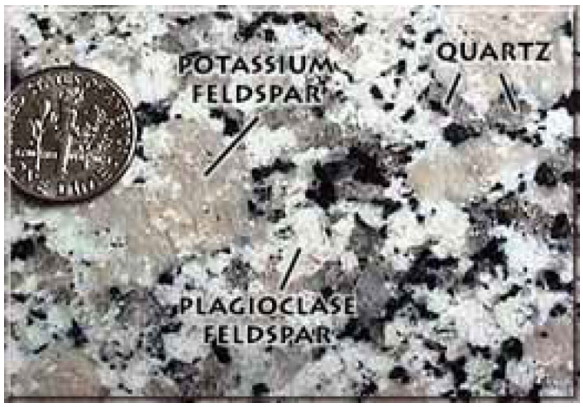

Figure 2.22. A close-up photo of granite. Notice that it is made up of interlocking large crystals. The large crystals form when molten rock is allowed to cool slowly deep within the earth. When molten rock is erupted onto the surface by volcanoes, it cools quickly, so volcanic rocks mostly lack large crystals. The labels show the names of some of the minerals in granite.

Figure 2.23. A close-up view of part of the Moraga Volcanics. Notice the many holes in the rock. These are vesicles, bubbles of gas released from the lava as it erupted (like carbonation is released when a bottle of soda is opened) and trapped when the lava hardened into rock.

Figure 2.24. The south face of the roadcut east of Caldecott Tunnel. The depositional contact between the Orinda Formation on the right and the Moraga Volcanics on the left is marked.

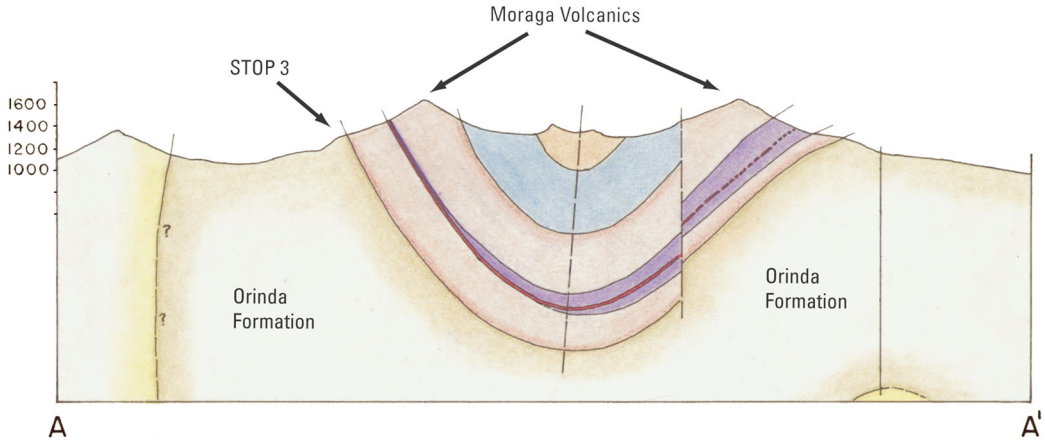

Figure 2.25. A hand-drawn diagram of the tilted and folded geologic units in the Berkeley Hills. The diagram looks at the layers in the Earth's crust from the side, as if you could slice the crust like a layer cake (geologists call that a cross section). The Orinda Formation and Moraga Volcanics are labeled, as well as the general location of Stop 3. The numbers on the left side mark feet above sea-level. This U-shaped fold in the layers of rock is called a syncline. Remember that all the layers were originally flat. The same plate tectonic forces that are driving the Hayward and San Andreas Faults today have bent and warped the layers in the rocks here, and have also pushed up rocks that were formed in a river valley to make the hills we see now. (Diagram drawn by A. Sarna-Wojcicki, U.S. Geological Survey.)

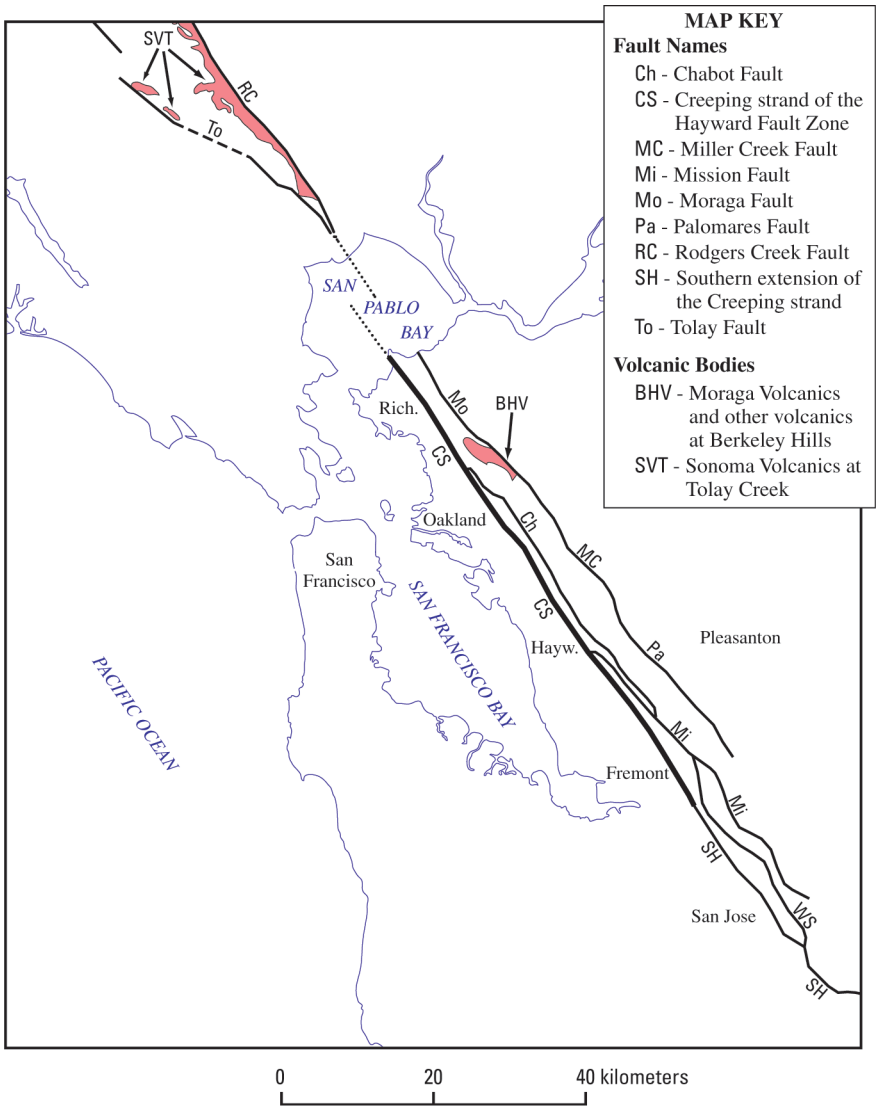

Figure 2.26. Map showing the area of the Moraga Volcanics and other volcanics at the Berkeley Hills and their offset equivalent north of San Pablo Bay, as well as the faults of the Hayward Fault Zone and the next fault zone to the east. Note that the Tolay Fault passes west of the northern volcanics. 45 more kilometers of offset have taken place on that part of the Hayward Fault Zone. Note also that the volcanics at the Berkeley Hills are bounded on the east by a fault zone. Do you think the Berkeley Hills Volcanics could have been moved northwest by those faults too?

Geology of the Golden Gate Headlands

William P. Elder
National Park Service, Golden Gate National Recreation Area, Calif.

Introduction

This field trip focuses on the rocks of the peninsular headlands found just north and south of the Golden Gate, on lands of the Golden Gate National Recreation Area. Exposed in dramatic seacliffs, these rocks not only form a spectacular backdrop for the Golden Gate Bridge, but also provide a detailed geologic record of Pacific Basin and active continental margin processes going back 200 million years. This is arguably one of the longest records of its type in the world. The significance of these rocks, however, goes beyond the geologic history that they tell, for they, and others of the Franciscan Complex associated with them, played a critical role in developing our current understanding of subduction zone mechanics and processes. Although the serpentine of the headlands, and its relationship to mountain building, was recognized as early as 1821 (see VanderHoof, 1951; Wahrhaftig, 1984a), it was not until the late 1970's to early 1980's that these rocks were understood in the light of modern tectonic concepts. This led to the publication of the volume edited by Blake (1984), which placed the Franciscan Complex into a modern plate tectonic framework. A detailed chronology of these geologic advances is provided by Wahrhaftig (1984a).

The following article draws heavily upon the many excellent publications that the late Clyde Wahrhaftig wrote on the rocks of the San Francisco area, both for the professional geologist and the general public (for example, Wahrhaftig, 1984a, 1984b; Wahrhaftig and Murchey, 1987; Wahrhaftig and Sloan, 1989). In this paper, I will describe the characteristics of the rocks and geologic processes observed at the six field trip stops, interpret their geologic story, and place them into a regional geologic context. The primary focus will be on geology of the Franciscan Complex, but other aspects, such as the Quaternary geology and the relationship between the geology and the plant communities, will be discussed.

During the field trip, please keep in mind that the sites we are visiting all lie within a national park and that sample collecting of any kind is prohibited. Please leave your rock hammers at home, but be sure to bring your camera—the rocks are beautifully photogenic at many places.

Geologic Setting

Transform Faulting (Stop 1)

San Francisco and the Golden Gate headlands are located on the boundary between two of the Earth's great tectonic plates, the North American and Pacific Plates. Today, this plate boundary is a transform fault (the plates are sliding past each other) and is formed by what is perhaps the best-known geologic feature of California, the San Andreas Fault Zone. Movement, totaling about 1 inch (2.5 cm) a year, along the San Andreas and its subsidiary faults, the Hayward and Calavaras (fig. 3.1), is infamous for producing the large earthquakes that periodically rock California and also is responsible for the area's youthful and beautifully rugged terrain. Major earthquakes occur several times each century on these or less well-known faults in the San Francisco Bay area, releasing strain built up between the creeping plates.

In the San Francisco Bay area, the current mountains of the California Coast Ranges, the Santa Cruz Mountains and the Diablo Range, started to uplift only about 3 to 4 million years ago (Page, 1989), when pressure increased across the plate boundary due to a slight shift in relative plate motions (Cox and Engebretsen, 1985); this same shift caused the Isthmus of Panama to rise from the sea and connect North and South America. The Santa Cruz Mountains are forming where the San Andreas Fault makes a slight bend to the left. This bend produces compression, folding and thrust faulting at the plate boundary, as the Pacific Plate tries to slide northward past the North American Plate. In contrast, valleys between the ranges, such as the San Francisco Bay/Santa Clara Valley, lie in stable or slowly downdropping areas formed between the major faults, in this case the San Andreas, Hayward and Calavaras Faults (fig. 3.1) (Page, 1989).

Right lateral movement on the San Andreas Fault system may be responsible for a major structural break developed under the Golden Gate Straits (Wakabayashi, 1999). This tectonic feature is indicated by a dramatic shift in the direction that the strata and thrust planes dip on opposite sides of the Golden Gate, from northeasterly on the San Francisco Peninsula to southerly in the Marin Headlands (fig. 3.2). Based on structural and paleomagnetic evidence, the Marin Headlands have undergone 130 degrees of clockwise rotation (Curry and others, 1984). The timing of this rotation is poorly constrained, but it postdates emplacement and folding of Franciscan Complex rocks in the area and is likely the result of transform tectonics.

Making San Francisco Bay

Although the valley in which San Francisco Bay resides probably began to form 2 to 3 million years ago, when the surrounding mountains and hills started to rise on either side, the first known estuarine (marine influenced) rocks were laid down only about 600,000 years ago, as dated by the Rockland ash bed which overlies the earliest marine rocks (Sarna-Wojcicki; personal commun., 2001). Cores taken during bridge-foundation studies and construction record up to seven different estuarine periods over the past half million years, corresponding to times of high sea level during interglacial periods (Atwater, and others, 1977; Sloan, 1989). During the glacial periods, when vast quantities of ocean water were stored in continental glaciers, the Bay floor became a valley and experienced erosion and downcutting. At those times, the huge, glacial-fed ancestral Sacramento River flowed through the Bay valley and out the Golden Gate Straits. Ocean water started flooding into the present San Francisco Bay only about 8,000 years ago, when the sea reentered the Golden Gate following the last glaciation (Wisconsin).

The Franciscan Complex (Stops 2 to 6)

The San Andreas Fault system is a relatively new geologic feature in the San Francisco Bay area, originating to the south 28 million years ago, but extending through the Bay area only 6 to10 million years ago (Page and Wahrhaftig, 1989). In contrast, older rocks of coastal California indicate that, before the Pacific Plate started slipping northward past the North American Plate on the San Andreas Fault system, the Pacific Ocean floor was subducted (moved) beneath the western edge of the North American Plate (fig. 3.3). The distinctive rocks of the world-famous Franciscan Complex, named at San Francisco and underlying much of coastal northern California, formed in this subduction zone.

In the Bay area, rocks of the Franciscan Complex form the basement for the Coast Ranges east of the San Andreas Fault. The Franciscan primarily consists of graywacke sandstone and argillite, but also contains lessor amounts of greenstone (altered submarine basalt), radiolarian ribbon chert, limestone, serpentinite (altered mantle material), and a variety of high-grade metamorphic rocks such as blueschist (high-pressure), amphibolite, and eclogite (high-temperature). These rocks are typically highly fractured and disrupted and may be mixed together on a local scale to create what is called a *mélange* (French for “mixture” or “blend”).

Franciscan Complex rocks in the Bay area range in age from about 200 to 80 million years old. They represent an accretionary wedge, a complex body of rock that accumulates in a subduction zone. The Franciscan Complex is composed of an amalgamation of semicoherent blocks, called tectonostratigraphic terranes, that were episodically scraped from the subducting oceanic plate, thrust eastward, and shingled against the western margin of North America (fig. 3.3). This process formed a stacking sequence in which the structurally highest rocks (on the east) are the oldest, and in which each major thrust wedge to the west becomes younger. Within each of the terrane blocks, however, the rocks become younger upsection, but the sequence may be repeated multiple times by thrust faults.

Franciscan Terranes in the Bay Area

Franciscan terranes are composed of oceanic rocks that may include igneous basement material and marine sedimentary rocks. Zones of mélange separate the terranes. In the Bay area, the Franciscan Complex is divided into the eastern and the central belts, with the older eastern belt lying structurally higher and being of higher metamorphic grade than the central belt (Blake and others, 1984). This field trip will focus on central-belt rocks, which Blake and others (1984) divided into eight terranes in the Bay area (fig. 3.2). This division is based on differences in basement types and ages, in the age and types of overlying sedimentary sequences, and in their metamorphic grade.

San Francisco and the Marin Headlands contain three of these terranes, from oldest to youngest, the Alcatraz, Marin Headlands, and San Bruno Mountain. Separating the terranes are the Hunters Point and City College mélange zones, which are primarily composed of sheared serpentinite and shale with scattered blocks of greenstone, chert, graywacke, and high-grade metamorphics (fig. 3.2). The Alcatraz terrane is characterized by graywacke turbidite deposits containing fossils indicating that the sediments were deposited between 130 and 140 million years ago (Early Cretaceous) (Blake and others, 1984, Elder, 1998). The Marin Headlands terrane, which is discussed in more detail below, contains an oceanic sequence including basaltic crust covered by open-ocean chert deposits and overlying continental-derived sandstone. Fossils in these units indicate that the chert was deposited from about 200 million to 100 million years ago (Early Jurassic to Late Cretaceous) and the sandstone between 100 and 90 million years ago (Murchey and Jones, 1984). The San Bruno Mountain terrane is composed predominately of sandstone and has yielded no fossils. Although its age is unknown, the block is thought to be Late Cretaceous in age, based on its position west of the Marin Headlands terrane (fig. 3.2).

Marin Headlands Terrane

On this field trip, we will be looking at rocks of the Marin Headlands terrane and the Hunters Point mélange zone, which bounds it to the east (figs. 3.2, 3.4, 3.5). The thick sequence of rocks preserved in the Marin Headlands terrane has received much attention by geologists in the last few decades, yielding a detailed record of their transport history (fig. 3.6). Tropical fossils and paleomagnetic evidence indicate that the terrane originated in the central Pacific near the equator. It then moved northeastward with the oceanic plate towards the North American Plate, finally colliding with North America at the latitude of today's Mexico (Murchey, 1984; Murchey and Jones, 1984). After this oceanic fragment became attached to the North American margin, rather than being subducted under it, right-lateral faulting produced by northeasterly directed subduction transported it northward along the western edge of the continent. Finally, San Andreas-related transform faulting moved it farther up the coast to the Bay area and rotated the Marin Headlands block into the position the we find it in today (Wahrhaftig 1984a; Curry and others, 1984; Wakabayashi, 1999). The following discussion of rock types and field trip stops will fill in the details of how scientists deciphered this story from the rocks.

Franciscan Rock Types

Basalt (Stop 2)

Basalt makes up about 20 to 25 percent of the exposed rocks of the Marin Headlands terrane. Alteration of Franciscan Complex basalt, presumably by hot seawater circulating through it at the mid-ocean ridge, has resulted in low-grade metamorphism and the development of the minerals chlorite and pumpellyite. These minerals give the basalt a dark green color and hence its common name, *greenstone*. Basalt in the Marin Headlands is typically deeply weathered, forming a zone of orange-brown clays and iron oxides that extends to depths of 5 to 10 m (15 to 30 feet). Most roadcuts do not penetrate this weathered zone to expose fresh rock. When subjected to constant wave action, however, the basalt forms hard, erosion-resistant black to dark green seacliffs like those seen at the Point Bonita.

Most basalt of the Marin Headlands terrane exhibits well-developed pillow forms and is vesicular. A few flows lack internal structure and may represent submarine flood basalts. Tuff and volcanic breccia beds also are present at some localities including Point Bonita.

Typical pillows are a few tens of centimeters to a meter across. They have rounded tops and downward projecting keels that were molded by the tops of the older underlying pillows. These forms provide an upsection indicator and demonstrate an underwater origin for the flows (Moore, 1975). When seen in cross section, some pillows show thin layers of basalt alternating with thicker quartz and calcite layers. These internal features resulted from lava partially draining out of the pillows to form voids that were later filled by quartz and calcite. The thin lava shelves in the pillows coincide with the true horizontal at the time of the flow, providing an accurate paleohorizontal indicator (Moore and Charlton, 1984).

At some places, such as near the tunnel entrance out to Point Bonita lighthouse and near Battery 129, chert can be seen between the pillows (fig. 3.7). Near Battery 129 and at the south end of Rodeo Beach, cream to pink pelagic limestone also is present. The occurrence of these relatively slowly deposited sedimentary rocks indicates periods of volcanic quiescence between pillow lava flows. In addition, the presence of limestone between the pillows demonstrates that the mid-ocean ridge crest was above carbonate compensation depth (CCD), which in today's oceans is typically around 4 km depth, allowing carbonate to be preserved. The lack of limestone in the immediately overlying chert sequence shows that the cooling oceanic plate descended below CCD shortly after it moved away from the ridge crest.

Chemical analysis of the basalts of the Marin Headlands terrane indicates that they are rich in titanium and iron, which is consistent with a mid-ocean ridge basalt (MORB) origin, particularly at a spreading center near a hot spot. However, at Point Bonita, the basalt chemistry is somewhat different, suggesting a seamount or oceanic island site of eruption, although a mid-ocean ridge site near a hot spot is also possible (Wahrhaftig and Wakabayashi, 1989; Shervais, 1989). The difference in composition between the Point Bonita basalt and that elsewhere in the Marin Headlands terrane led Wahrhaftig and Wakabayashi (1989) to establish a separate Point Bonita block.

Chert (Stop 3)

Chert underlies about 50 percent of the Marin Headlands and a small part of the Presidio. Because chert is resistant to weathering, it forms many of the ridge tops. At places, the chert is found in depositional contact with the underlying basalt (fig. 3.8; Battery 129) or with the overlying clastic rocks (Alexander Avenue), but most contacts are formed by faults. The chert is bedded and is composed predominately of 2- to 10-cm thick red chert layers that alternate with

thinner, dark-red shale beds. The red color indicates the oxidized state of the iron in this siliceous rock. Light green to white chert beds also are present, but are much less common and occur in the mid to upper parts of the section. In general, the bedding thickness decreases and the shale content increases upsection. Because of the prominent thin bedding, these rocks are commonly called ribbon chert. Chert lying near the basalt contact has a silvery gray to black manganese-oxide staining. This manganese is probably related to both hydrothermal and hydrogenous Mn associated with the spreading ridge (Karl, 1984).

Locally, the chert is intensely folded, forming complex sharp-crested chevron and isoclinal folds (fig. 3.9). Such folding is well exposed along Conzelman Road. Most likely, the folding occurred when the Marin Headlands terrane was wedged against the continental margin and subsequently faulted to its present position. However, abrupt changes from only slightly deformed sequences to highly folded areas, and unbroken sharply folded beds, have led to speculation that some of the contorted folding reflects submarine slumping on the flank of the mid-ocean ridge prior to final hardening of the layers (Bailey and others, 1964; Wahrhaftig, 1984a).

The chert of the Marin Headlands contains abundant radiolarian fossils that are silt to sand size and that are clearly visible with a hand lens. These tiny siliceous fossil shells provided much of the silica content in these beds. The radiolaria can be extracted from the rock with hydroflouric acid, providing spectacular three-dimensional fossils (fig. 3.10). By studying these fossils, Murchey (1984) determined that the oldest cherts deposited on the basalt contain species that lived about 200 million years ago (Early Jurassic, Pliensbachian Stage) and that the youngest species, at the top of the section near the sandstones, lived about 100 million years ago (Cretaceous, Albian to Cenomanian stages). The chert sequence, therefore, reflects 100 million years of pelagic deposition and is one of the longest stratigraphic sequences of chert in the world (Wahrhaftig and Murchey, 1987).

The cherts contain a number of features indicating that they formed in the equatorial central Pacific (fig. 3.6). Murchey's (1984) study identified radiolarians characteristic of warm tropical to subtropical waters. This finding, coupled with the fact that red, oxidized radiolarian cherts are typically associated with high productivity upwelling zones found just north and south of the equator (Karl, 1984), suggest that the sediments forming these rocks were deposited in near the equator. The observed upsection decrease in bedding thickness also is consistent with a depositional site that was moving northward, out of the equatorial high-productivity zone, thus resulting in progressively thinner bedding cycles (Karl, 1984). The general lack of terrigenous, continental-derived sediments throughout the sequence implies that it was deposited far offshore, probably more than 1,000 km (600 miles), if there was no topographic barrier to impede continental sediment supply (Karl, 1984).

The prominent rhythmic bedding of the cherts is one of their most distinguishing features (fig. 3.11). The contrast between the hard chert beds and the intervening shale beds has been magnified by diagenesis following deposition. Subtle original compositional differences would have been enhanced as silica moved from the less silica-rich zones to the more silica-rich beds during diagenesis, in which opal-A silica from radiolarian shells was transformed into opal-CT silica, and ultimately to quartz (Tada, 1991).

However, the origin of the primary compositional differences is debatable. Karl (1984) concluded that the bedding was produced by periodic submarine landslides (dilute turbidity currents) that occurred on the flank of the mid-ocean ridge. Predominately lenticular bedding and some internal sedimentary features are consistent with this origin. Alternatively, the rhythmic bedding may represent periodic changes in oceanic upwelling and siliceous productivity, possibly developed in response to the Earth's orbital cycles (Decker, 1991). A growing body of literature indicates that the Earth's 21,000, 41,000 and 100,000 year orbital cycles, as well as others, are reflected in biogenic sedimentary sequences (Fischer, 1991). In any case, diagenesis would have enhanced the cycles produced by either turbidite or productivity mechanisms.

Clastic Rocks—Conglomerate, Sandstone, Shale (Stops 4 and 6)

Continentally derived clastic rocks underlie about 25 percent of the Marin Headlands terrane. The clastic rocks weather deeply and are usually exposed only in the coastal bluffs, where they erode to form steep, dangerous cliffs. This trip will visit two good sandstone exposures, one at the north end of Rodeo Beach and the other at the north end of Baker Beach (fig. 3.12). Sandstone is dominant among the clastic rocks and is mainly a lithic arkose wacke, consisting of a poorly sorted mixture of angular plagioclase feldspar, quartz, and volcanic rock fragments. The volcanic component gives the sandstone its characteristic greenish-gray color. This "dirty sandstone" is commonly called graywacke, and is typical of submarine landslide deposits (turbidites) associated with subduction zones along continental margins.

The sandstone intervals are composed of beds typically ranging in thickness from 1 to 2 m to more the 20 m. The beds generally show no internal features other than graded bedding, although internal laminae or cross-bedding are occasionally present. The base of the beds may be pebbly or have small shale and other rock clasts. Beds grade upward to progressively finer sandstone and may be capped by thin shale intervals, usually no more than 10 to 20 cm in thickness.

This grading from cobbles or pebbles at the base to fine sand and silt at the top of beds results from decreasing transport energy after a slide event. As the energy decreased, smaller and smaller particles drop out of suspension and are deposited. Most sandstone beds reflect the A, C, and D facies of the classic Bouma turbidite sequence (Bouma, 1962) with the preservation of the pelagic E facies at the tops of some (Wahrhaftig, 1984b). Locally, carbonized plant material is apparently concentrated at the tops of sandstone beds, perhaps floating to the top of the sand slurry following a turbidite event.

Shale intervals are typically less than 50 cm thick and reflect periods of pelagic deposition between turbidite events. Rarely, shale intervals several meters in thickness are present, such as immediately above the chert sequence on Alexander Avenue. Portions of the mélange at north Baker Beach appear to contain much shale, but the highly disturbed nature of the outcrop prohibits determination of bed thickness.

Conglomerate is rare but has been identified at three localities on the Marin Headlands—two localities at Bonita Cove and one on Wolf Ridge (Wahrhaftig, 1984a). No conglomerate will be seen on this field trip. The two Bonita Cove localities have different compositions: one contains greenstone, limestone, and red chert pebbles, and the other locality has gray quartzite and chert cobbles.

The sandstone of the Marin Headlands terrane has yielded two molluscan fossils, both ammonites (fig. 3.13). One was found near the base of the north tower of the Golden Gate Bridge and identified by Hertlein (1956), and the other came from the south end of Baker Beach and was reported on by Schlocker and others (1954). These Cretaceous ammonites provide quite accurate ages of early Cenomanian and early Albian for the clastic rocks north and south of the Golden Gate, respectively (Elder, 1998). These ages are consistent with the radiolarian-derived Albian to Cenomanian age for the top of the underlying chert sequence. These ammonites lived widely throughout the Pacific and thus provide no evidence regarding the latitude at which the rocks were deposited.

Serpentinite (Stop 5)

Serpentinite is associated with the mélange blocks of the central belt that surround the Marine Headlands terrane (fig. 3.2). Highly fractured serpentinite rocks and associated mélange form hills with broad crests and abundant slumps and landslides. Although serpentinite does not typically form sizable outcrops, soils form slowly over serpentinite, such that disturbed areas may be barren for extended periods before vegetation develops. The bluffs above north Baker Beach provide spectacular serpentinite exposures that also exhibit the landslides and seeps characteristic of this rock type (fig. 3.14).

Serpentinites are rocks composed of the serpentine-group minerals, chrysotile (asbestos), lizardite, and antigorite. These minerals impart a characteristic blue-green color to the serpentinite blocks and the sheared clay zones surrounding them. In outcrop, massive rounded serpentinite blocks, typically 1 to 2 m in diameter, are surrounded by a matrix of sheared, flaky serpentine, called slickentite. The massive blocks may show relict porphyritic textures (bastite replacements of pyroxene) of deep oceanic crust and mantle rocks (dunite and harzburgite). Other blocks may contain a lacy network of 1-5 mm thick asbestos veins (fig. 3.15).

The serpentinites of the Franciscan Complex in the San Francisco Bay area are exotic fragments of oceanic crust and mantle (ophiolite) that were accreted to the active continental margin rather than being subducted under it (Coleman, 1989). Hydrothermal activity in the subduction zone has completely altered the mineralogy of these deep crust and mantle rocks to serpentinite, making them much lighter and more plastic. These serpentinites are probably derived from the base of the Coast Range Ophiolite, a piece of Middle Jurassic oceanic crust that underlies the rocks of the Great Valley Sequence of central California. Extensive faulting, and possibly upward diapiric movement of these relatively light rocks, has led to their ascent to the Earth's surface.

Because serpentinite is altered mantle rock, its chemistry is unlike that of most other continental rocks. Serpentinite is low in potassium and calcium, which are important plant nutrients. It also contains high levels of magnesium, nickel, and chromium that are potentially toxic to plants. Therefore, plants living on serpentine soils are specially adapted to these unusual chemical conditions, and serpentine areas can often be mapped by using the abrupt vegetation change that occurs at their boundaries.

Serpentinite outcrops in California and throughout the world are known to support rare and endangered plant species (Kruckenberg, 1984). Some species are confined to just one or a few outcrop areas. Eight of the twelve rare plants found at the Presidio grow on serpentinite, including the federally endangered Presidio clarkia and Raven's manzanita, the latter of which is represented by a single plant (fig. 3.16).

Quaternary Geology of the Colma Formation (Stop 6)

The Pleistocene Colma Formation locally forms a thin veneer over rocks of the Franciscan Complex on the Golden Gate headlands of San Francisco Peninsula. The formation extends to Angel Island and to the southern peninsula, where

it overlies the Pliocene and Pleistocene Merced Formation from Fort Funston, south (Schlocker, 1974). The Colma Formation is mostly composed of sandy deposits laid down from 80 to 125 thousand years ago during an interglacial period (Sangamonian/Mindel-Riss/Holsteinian Interglacial) when sea level was slightly higher than today. At that time, northern San Francisco Peninsula was an island separated from the southern peninsula by the narrow"Colma Strait" (fig. 3.17).

The predominately poorly consolidated sands of the Colma probably originated in a variety of environments ranging from shallow bay to dune and valley slopes. The formation extends under the San Francisco Bay and is developed up to 500 feet above sea level (Schlocker, 1974). It apparently represents shallow bay deposits below about 200 feet in elevation and valley-slope debris above. The permeable sands of the Colma Formation form a good aquifer, and springs are common at the interface between the Colma Formation and the underlying Franciscan Complex serpentinite at the Presidio.

Holocene Sand Dunes (Stop 6)

Holocene sand dunes mantle the Colma Formation and the Franciscan Complex over large areas of San Francisco (fig. 3.18). These dunes are composed of sand that has blown up and over the hills from Ocean Beach and Baker Beach. The sand probably originated on the broad coastal plain of the Sacramento/San Joaquin River system, which extended from the Golden Gate to the Farallon Islands during the last glacial period (Wisconsin), when sea level was about 100 m (300 ft) lower than at present (Atwater, 1979; Sloan, 1989). Sand from this plain was transported onto the beaches and blown over the coastal hills during the rapid sea level rise that occurred between about 18,000 and 5,000 years ago. Sea level has been relatively stable for the past 5,000 years, rising only 1 to 2 mm/year during that period (Atwater, 1979).

The Holocene sand dunes of this area formed one of the most extensive coastal dune systems on the West Coast, underlying about one-third of San Francisco. The dynamic nature of these dunes, constantly shifting and in different phases of ecological succession, produced a complex mosaic of sandy habitats that once supported many different plant and animal species. Today, only a small remnant of that ancient ecosystem survives, much of it within the Presidio. Preserved and restored dune habitat at Baker Beach (Stop 6) and in more inland areas, such as nearby Lobos Creek Valley, supports a much greater biodiversity than the surrounding urban areas. The coastal dune scrub community here provides food and shelter for insects, reptiles, birds, and mammals and includes several rare plants, such as the Dune gilia and San Francisco lessingia (fig. 3.16).

Road Log

The field trip begins at the National Park Service Visitor Center at the Presidio. The trip crosses the Golden Gate Bridge to stops in the Marin Headlands and then returns south to the Presidio. Figures 3.4 and 3.5 show the location of stops.

Mileage/Notes

0 From National Park Service Visitor Center drive south on Montgomery.

0.1 Turn right on Sheridan Avenue.

0.4 Sheridan Avenue becomes Lincoln Boulevard; continue on Lincoln west.

0.9 Go under Highway 101.

1.3 Turn right on Armistead; immediate left onto Golden Gate Bridge approach; then right onto the bridge.

3.3 Exit right to Vista Point at the north end of the Golden Gate Bridge.

STOP 1—Vista Point provides excellent panoramic views of San Francisco Bay, the Golden Gate Bridge and the Marin Headlands (fig. 3.4). As you stand at the Vista Point, try to visualize what this scene looked like a mere 12,000 years ago, when a rushing, glacially fed river flowed through the grand valley before you, now occupied by bay water. The river flowed through Raccoon Straits, between Angel Island and the Tiburon Peninsula, and out through the gorge of the Golden Gate before crossing a wide coastal plain to the Pacific.

Today San Francisco and the Golden Gate Bridge dominate this view. Built over a 4 year period, the Golden Gate Bridge was completed in 1937. Bridging the Golden Gate was not only one of the greatest engineering efforts of the century, it also acted as a social and economic catalyst that forever changed the San Francisco Bay region. Today more than 40 million vehicles cross the bridge each year. The foundations of the bridge towers extend 110 feet below the water into bedrock. The south tower is anchored in fractured serpentinite rock, leading to some concern about its integrity during a large earthquake.

3.5 Leave vista point onto Highway 101 north.

3.7 Exit immediately onto Alexander Avenue.

3.8 Proceed toward Sausalito on Alexander Avenue.

3.9 Turn left toward Marin Headlands (this is Bunker Road, but there is no sign).

4.1 Proceed through tunnel. The traffic light can last up to 5 minutes.

4.9 First visible chert outcrops are on the left; views encompass coastal scrub plant community typical of the Marin Headlands. No trees are native to this area; the natural landscape contains low, tundra-like vegetation due to the persistent winds and cool foggy conditions.

6.6 Turn left on Field Road.

6.9 Graywacke outcrops are visible on left.

7.0 Nike missile museum is on right.

7.7 Point Bonita Trailhead parking area is on the left (will stop here in a few minutes).

8.0 Lookout vista. From this point you can see Bird Island (covered with white guano), Point Bonita Lighthouse, basalt seacliffs and gun emplacements from the early 20th century.

8.2 Return to Point Bonita Trailhead parking area.

STOP 2—Proceed down Point Bonita Trail to locked tunnel. This stop will be focused on the pillow basalts (now altered to greenstone) of the Point Bonita block (fig. 3.4). On the way down the trail, the first outcrop seen to your right is graywacke sandstone. A prominent fault and sheared zone can then be seen separating the graywacke from greenstone. Greenstone is the predominate rock the rest of the way to the tunnel, except for a small interval of serpentinite and shale just beyond the fault. Near the tunnel entrance, well-developed pillows are seen in the basalt of the cliff face. Pods of red chert, altered to jasper, are present between some pillows (fig. 3.7). The chert was deposited during periods between eruptions. Locally, in the Marin Headlands terrane, interpillow limestone pods also are found, indicating that the sea floor was above calcium carbonate compensation depth (CCD) for at least a short time after forming. The best pillows are seen near the water line below Point Bonita lighthouse, where the waves have beautifully exposed them. The tunnel to the lighthouse is open on weekends and Mondays between 12:30 and 3:30 p.m. The red-looking growth covering the basalt by the tunnel entrance is a type of cyanobacteria (Trentepohlia). Feral cabbage, escaped from the lighthouse keeper's garden, is a common plant here, as well as a many native species, such as cobweb thistle and blue-dicks.

Return to the bus.

9.2 Return and turn left onto Bunker Road toward Rodeo Beach.

9.6 Pull out into gravel parking area just beyond large warehouse building.

STOP 3—This abandoned quarry face provides excellent exposures of the radiolarian ribbon cherts characteristic of the Marin Headlands terrane (fig. 3.4). The chert seen here displays dark steely-gray manganese staining typically developed in rocks near the base of the chert section, probably reflecting manganese-rich hydrothermal and bottom

waters associated with the mid-ocean ridge volcanism. Complex folding is well displayed on the left-hand side of the cliff face, probably produced when the terrane was accreted onto North America (fig. 3.19). Thrust faults formed during the period of accretion have sliced the oceanic sequence up and repeated it ten or more times in the headlands area (Wahrhaftig, 1984a). Prominent chert and shale bedding rhythms also are evident (fig. 3.11). These sedimentary cycles, which have been enhanced by burial diagenesis, reflect either submarine landslides or cyclic changes in radiolaria productivity and (or) clay input. The shells of some radiolaria (fig. 3.10) can be seen on freshly broken surfaces with a handlens.

9.6 Proceed left and on to Fort Chronkhite.

10.2 Proceed to the bus parking at Rodeo Beach at north end of parking area.

STOP 4—From the Rodeo Beach parking lot (fig. 3.4) proceed west onto the gated road and then left, up the path to the cliff top. From the top of this promontory are excellent views of the coast to the north and south. The bluffs in this area are composed of graywacke sandstone. The deep cove just to the north cuts into an area of less resistant, more shaley turbidite beds.

To the south and east, Rodeo Cove and Rodeo Lagoon are visible (fig. 3.20). No other West Coast beaches have the composition or coarse grain size of the beach in Rodeo Cove. The beach is composed predominately of rounded red and green chert and lesser amounts of mafic volcanic rock fragments that fall mostly in the 1 to 4 mm grain size range (Wakeley, 1970). In addition to the brightly colored chert pebbles, the beach contains carnelians, semitranslucent orange chalcedony, that formed in the vesicles of the nearby pillow basalts.

Rodeo lagoon fills a valley drowned by recent sea-level rise following the last glacial period. The lagoon is developed behind a barrier bar formed by the beach. During winter storms, ocean water may overtop the bar during storm tides and high seas, forming landward-dipping washover fans. In addition, rains may increase freshwater flow into the lagoon, causing overtopping and erosion from the landward side (Hill, 1970). The barrier beach reforms during summer dry season conditions, when the coastal beaches build up and out.

Leave Rodeo beach and proceed eastward.

12.4 Turn on to McCullough Road.

13.1 A small slump can be seen on the left.

13.2 Ahead on left, note large graywacke blocks on top of the chert outcrops.

13.3 Turn left onto Conzelman Road.

13.7 Stop bus for great view of folds in chert on left, bay and bridge views on right.

14.0 Manganese stained chert can be seen on left; similar to Stop 3 (above).

14.1 Pillow basalts crop out on left, and contact with overlying chert is visible.

14.5 Take entrance ramp to Highway 101 South, and onto Golden Gate Bridge. Stay in far right lane.

16.5 Turn right on Merchant Road immediately after toll booth.

16.7 Turn right on Lincoln Boulevard.

16.72 Take immediate right on Langdon Court and proceed to bus parking.

STOP 5—From the Coastal Overlook (fig. 3.5) we will walk to the beach where we will examine serpentinite and mélange outcrops. This is a clothing optional public beach that provides excellent exposures. Take the trail from the southwest corner of the parking lot (fig. 3.5, loc. 1), over the bluff edge and into the trees. Spectacular exposures of serpentinite can be seen in the large landslide headwall as the trail descends the bluff (fig. 3.5, loc. 2). The steep coastal bluffs in this area are formed from a series of these landslide headwalls (fig. 3.14). East dipping foliation and flattening of the boulders can be seen in these exposures.

Just south of where the trail meets the beach, a rock promontory juts into the ocean (fig. 3.5, loc. 3). The north side of this exposure is serpentinite and the south is composed of sandstone. This fault contact juxtaposes the large serpentinite block forming the bluffs to the north, against a mélange zone developed to the south at the boundary of the Marin Headlands terrane and the Hunters Point mélange zone (fig. 3.2).

Climb over the promontory and walk south across the low wetlands area formed at the toe of the landslide. A serpentine seep 100 m (320 ft) inland feeds these wetlands. Several rare plants in the area, including the Franciscan thistle (fig. 3.16), are adapted to, and largely restricted to, serpentine seep conditions. Proceed to the edge of the low bluff to the west (fig. 3.5, loc. 4). Here, the bluff is composed of green clay that appears to be slowly oozing onto the beach. The clay contains popcorn-like balls of what may be zeolite minerals (fig. 3.21) and is thought to be an altered volcanic tuff bed, similar to tuffs found in mélange throughout the central and northern Coast Ranges (Wahrhaftig and Sloan, 1989).

Continue south to the large ribbon-chert outcrop at the end of the beach. This chert block is in fault contact with a large sandstone block to the south (we will inspect this block at Stop 6) and a pillow basalt block to the north (fig. 3.22). These blocks are pieces of the Marin Headlands terrane and probably represent the northern boundary of that terrane on the San Francisco Peninsula.

Head back north and, if time permits, continue past the trailhead about 250 m (800 ft) to the north end of the beach, where large rocks extend into the water (fig. 3.5, loc. 6). These are high-grade metamorphic rocks composed of amphibolite. Locally they are garnet-bearing and have textures suggestive of partial melting indicative of high-temperature metamorphism (about 700°C; Wakabayashi, 1999). Quartz- and garnet-rich beds appear to be metachert, probably metamorphosed during the early stages of subduction (Wakabayashi, 1999). High-grade metamorphic blocks of the Franciscan Complex all date to about 160 million years ago, but the Hunters Point mélange zone is probably not older than about 100 million years, based on the age of the Marin Headlands terrane to its west (Wakabayashi, 1999).

Return up the trail to the bus.

17.0 Exit parking lot and turn right onto Lincoln Boulevard.

17.3 Serpentine chaparral restoration site containing last remaining Raven's Manzanita.

17.8 Turn right on Bowley Street, then right onto Gibson Street to Baker Beach.

18.0 Turn right to Battery Chamberlin Road.

18.2 Park in bus parking area at Baker Beach.

STOP 6—From the Baker Beach parking lot, walk through Battery Chamberlin, a coastal defense gun emplacement built in 1904. The battery contains the last "operational" six-inch diameter disappearing rifle on the West Coast. Walk north to the exposures at the end of the beach. This is another clothing optional beach.

The bluffs at the north end of Baker Beach provide an excellent opportunity to observe sandy turbidite deposits of the Marin Headlands terrane close at hand (fig. 3.5, loc. 7). These graywacke sandstone bluffs are composed of massive sandstone beds as much as 5 m (26 ft) in thickness, separated by finely laminated cross-bedded sandstone and shale interbeds from 5 cm to 1 m (2 in to 3 ft) thick. Some of the interbeds contain abundant plant material, now carbonized and coaly, that apparently rose to the tops of the underwater landslide flow deposits (fig. 3.23). The abundance of plant material suggests that there was land nearby. The turbidite beds are cut by numerous small faults, and calcite veins fill many of these faults and fractures.

Walk back south to the nearby tan bluffs fig. 3.5, loc. 8). These bluffs are composed of poorly consolidated silts and sands of the Colma Formation (Pleistocene) that are dipping about 20 degrees south. The Colma Formation weathers to form badlands topography in this area (fig. 3.24). Low angle or planer laminations are evident in the basal Colma Formation exposed on the beach here and suggest a beach foreshore or backshore environment. The overlying finer-grained rocks may represent lagoonal deposits.

The top of the Colma Formation is marked by a prominent gray soil horizon that is overlain by Holocene sand dunes (fig. 3.18). In ravines along the cliff base, high-angle cross beds indicative of sand dune deposits are visible in the slightly consolidated sand present near the base of the Holocene unit (fig. 3.25). The dunes on the bluffs here provide a glimpse into what the northern San Francisco Peninsula looked like before becoming urbanized. These dunes are some of the least impacted in the city, providing critical habitat space for rare plants like Dune gilia and San Francisco wallflower (fig. 3.16).

Return to the bus at the Baker Beach parking lot.

18.4 Turn left on Gibson Street.

18.5 Turn left on Bowley Street.

18.6 Turn left on Lincoln Boulevard.

19.1 Turn right on Kobbe Street.

19.4 Continue straight on Kobbe past Upton Street.

19.7 Turn left on Park Boulevard.

19.8 Turn right on Lincoln Boulevard.

20.5 Turn right on Montgomery Street and back to William Penn Mott Jr., Visitor Center.

End of trip

References

Atwater, B.F., Hedel, C.W., and Helley, E.J., 1977, Late Quaternary depositional history, Holocene sea-level changes, and vertical crustal movement, southern San Francisco Bay, California: U.S. Geological Survey Professional Paper 1014, 15 p.

Bailey, E.H., Irwin, W.P., and Jones, D.L., 1964, Franciscan and related rocks and their significance in the geology of western California: California Division of Mine and Geology Bulletin 183, 177 p.

Blake, M.C., Jr., 1984, Franciscan Geology of Northern California: Pacific Section Society of Economic Paleontologists and Mineralogists, v. 43, 254 p.

Blake, M.C., Howell, D.G., and Jayko, A.S., 1984, Tectonostratigraphic terranes of the San Francisco Bay region, *in* Blake, M.C., Jr., ed., Franciscan Geology of Northern California: Pacific Section Society of Economic Paleontologists and Mineralogists, v. 43, p. 5-22.

Bouma, A.H., 1962, Sedimentology of Some Flysch Deposits—A Graphic Approach to Facies Interpretation: Elsevier Scientific, 167 p.

Coleman, R.G., 1989, Serpentinites, *in* Wahrhaftig, C. and Sloan, D., eds., Geology of San Francisco and Vicinity, 28th International Geological Congress Field Trip Guidebook T105, p.10-11.

Cox, A., and Engebretsen, D.C., 1985, Change in motion of Pacific Plate at 5 Ma: Nature, v. 313, p. 472-474.

Decker, K., 1991, Rhythmic bedding in siliceous sediments—An overview,—*in* Einsele, G., Ricken, W., and Seilacher, A., eds., Cycles and events in stratigraphy: Springer-Verlag, Berlin, Heidelberg, p. 464-479.

Fischer, A.G., 1991, Orbital cyclicity in Mesozoic strata, *in* Einsele, G., Ricken, W., and Seilacher, A., eds., Cycles and events in stratigraphy: Springer-Verlag, Berlin, Heidelberg, p. 48-62.

Elder, W.P., 1998, Mesozoic molluscan fossils from the Golden Gate National Recreation Area and their significance to terrane reconstructions for the Franciscan Complex, San Francisco Bay area, California, *in* Santucci, V.L., and Lindsay, M., eds., National Park Service Paleontological Research: National Park service Technical Report NPS/NRGRD/GRDTR-98/01, p. 90-94.

Hertlein, L.G., 1956, Cretaceous ammonite of Franciscan group, Marin County, California: American Association of Petroleum Geologists Bulletin, v. 40, p. 1985-1988.

Hill, M.R., 1970, Barrier Beach: California Geology, v. 23, no. 12, p. 231-233.

Karl, S.M., 1984, Sedimentologic, diagenetic, and geochemical analysis of Upper Mesozoic ribbon cherts from the Franciscan Assemblage at the Marin Headlands, California, *in* Blake, M.C., Jr., ed., Franciscan Geology of Northern California: Pacific Section Society of Economic Paleontologists and Mineralogists, v. 43, p. 71-88.

Kruckenberg, A.R., 1984, California serpentines—Flora, vegetation, geology, soils, and management problems: University of California Publications in Botany, v. 78, 180 p.

Moore, J.G., 1975, Mechanism of formation of pillow lava: American Scientist, v. 63, p. 269-277.

Moore, J.G., and Charlton, D.W., 1984, Ultrathin lava layers exposed near San Luis Obispo Bay, California: Geology, v. 12, p. 542-545.

Murchey, Benita, 1984, Biostratigraphy and lithostratigraphy of chert in the Franciscan Complex, Marin headlands, California, *in* Blake, M.C., Jr., ed., Franciscan Geology of Northern California: Pacific Section Society of Economic Paleontologists and Mineralogists, v. 43, p. 51-70.

Murchey, Benita, and Jones, D.L., 1984, Age and significance of chert in the Franciscan Complex in the San Francisco Bay region, , *in* Blake, M.C., Jr., ed., Franciscan Geology of Northern California: Pacific Section Society of Economic Paleontologists and Mineralogists, v. 43, p. 23-30.

Page, B.M., 1989, Coast Range uplifts and structural valleys, *in* Wahrhaftig, C., and Sloan, D., eds., Geology of San Francisco and vicinity, 28th International Geological Congress Field Trip Guidebook T105, p. 30-32.

Page, B.M., and Wahrhaftig, Clyde, 1989, San Andreas Fault and other features of the transform regime, *in* Wahrhaftig, C., and Sloan, D., eds., Geology of San Francisco and vicinity, 28th International Geological Congress Field Trip Guidebook T105, p. 22-27.

Schlocker, Julius, 1974, Geology of the San Francisco North Quadrangle, California: U.S. Geological Survey Professional Paper 782, 109 p.

Schlocker, Julius, Bonilla, M. G., and Imlay, R. W., 1954, Ammonite indicates Cretaceous age for part of Franciscan group in San Francisco Bay area, California: American Association of Petroleum Geologists Bulletin, v. 38 p. 2372-2381.

Shervais, J.V., 1989, Geochemistry of igneous rocks from Marin Headlands, *in* Wahrhaftig, C. and Sloan, D., eds., Geology of San Francisco and vicinity, 28th International Geological Congress Field Trip Guidebook T105, p. 40-41.

Sloan, Doris, 1989, San Francisco Bay, *in* Wahrhaftig, C. and Sloan, D., eds., Geology of San Francisco and Vicinity, 28th International Geological Congress Field Trip Guidebook T105, p. 46-47.

Tada, R., 1991, Compaction and cementation in siliceous rocks and their possible effect on bedding enhancement, *in* Einsele, G., Ricken, W., and Seilacher, A., eds., Cycles and Events in Stratigraphy: Springer-Verlag, Berlin, Heidelberg, p. 480-491.

VanderHoof, V. L., 1951, History of geologic investigation in the bay region, *in* Geologic Guidebook of the San Francisco Bay Counties: California Division of Mines Bulletin 154, p. 109-116.

Wahrhaftig, Clyde, 1984a, Structure of the Marin Headlands block, California—A progress report, *in* Blake, M.C., Jr., ed., Franciscan geology of Northern California: Pacific Section Society of Economic Paleontologists and Mineralogists, v. 43, p. 31-50.

Wahrhaftig, Clyde, 1984b, A Streetcar to subduction and other plate tectonic trips by public transportation in San Francisco, revised edition: Washington, D.C., American Geophysical Union, 72 p.

Wahrhaftig, Clyde, and Sloan, Doris, 1989, Geology of San Francisco and Vicinity, 28th International Geological Congress Field Trip Guidebook T105, 69 p.

Wahrhaftig, Clyde, and Murchey, Benita, 1987, Marin Headlands, California—100-million-year record of sea floor transport and accretion: Geological Society of America Centennial Field Guide, Volume 1—Cordilleran Section, p. 263-268.

Wahrhaftig, Clyde, and Wakabayashi, John, 1989, Tectonostratigraphic terranes, *in* Wahrhaftig, C., and Sloan, D., eds., Geology of San Francisco and vicinity, 28th International Geological Congress Field Trip Guidebook T105, p. 6-8.

Wakabayashi, John, 1999, The Franciscan Complex, San Francisco Bay area—A record of subduction complex processes, *in* Wagoner, D.L., and Graham, S.A., eds., Geologic Field Trips in Northern California: California Division of Mines and Geology Special Publication 119, p. 1-21.

Wakeley, J.R., 1970, The unique beach sand at Rodeo cove: California Geology, v. 23, no. 12, p. 238-241.

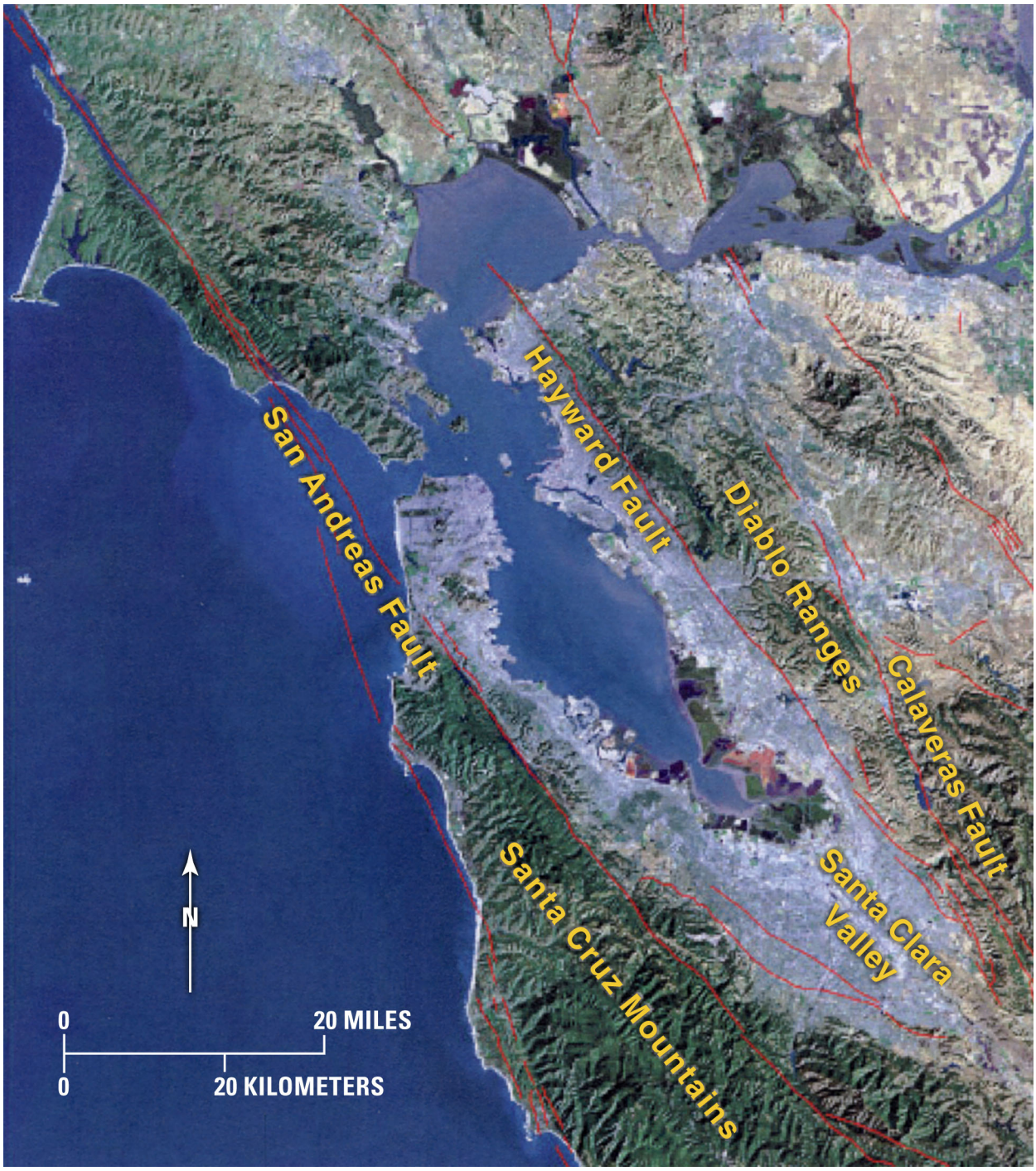

Figure 3.1. Satellite image of San Francisco Bay area showing major faults and geographic features discussed in text (modified from U.S. Geological Survey and Pacific Gas & Electric image).

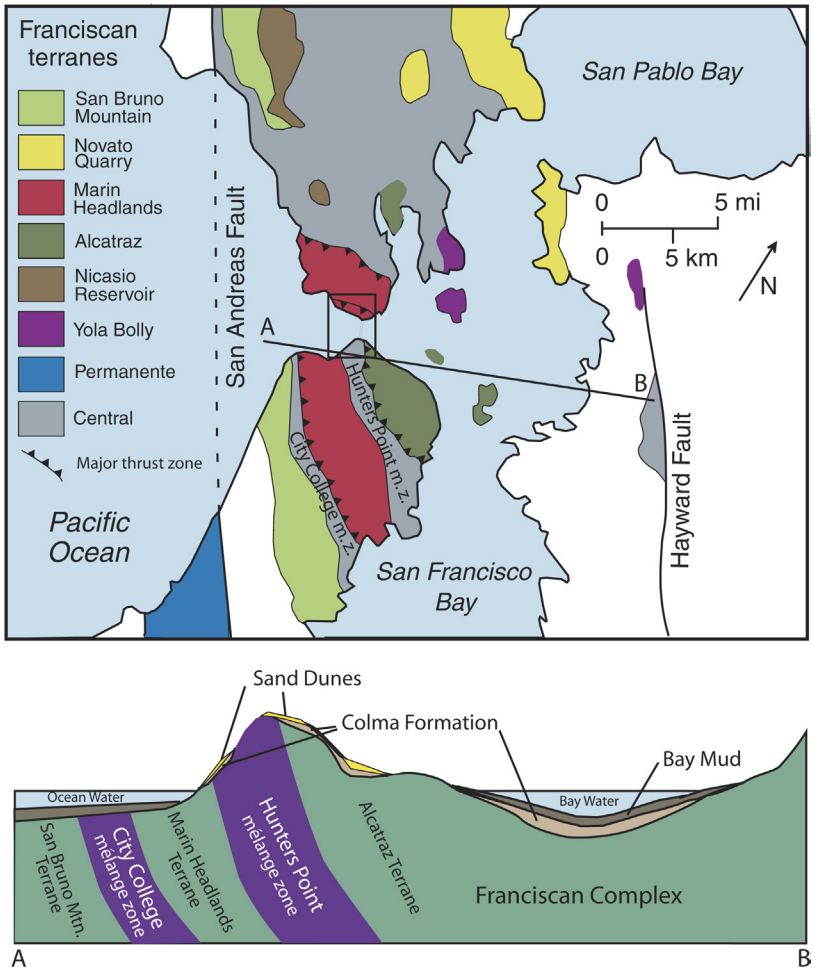

Figure 3.2. Top part of figure shows terranes of the Franciscan Complex in the San Francisco Bay area and dip direction of major thrust faults referred to in text. Cross section A-B for lower part of figure also is indicated (modified from Blake and others, 1984). Bottom part of figure is a schematic cross section through northern San Francisco Peninsula across bay to Oakland (not to scale).

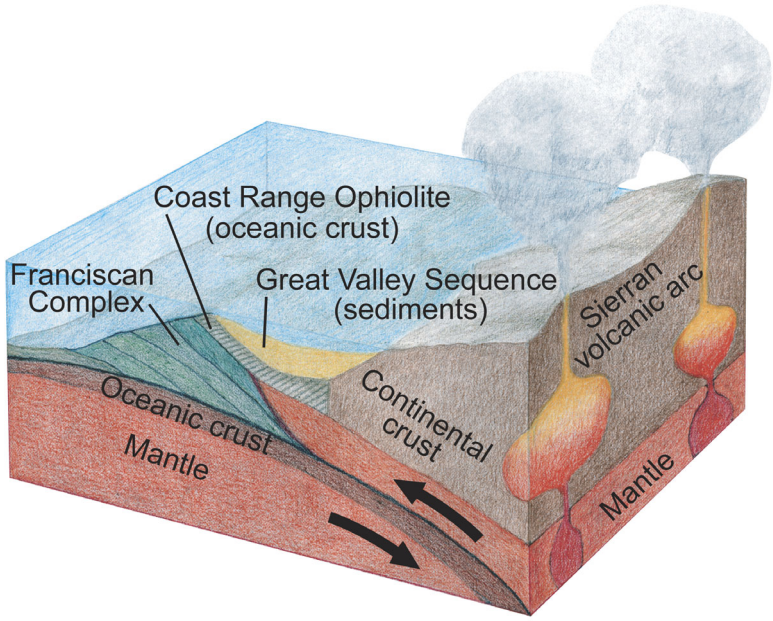

Figure 3.3. Cartoon of the subduction zone present on the West Coast 100 million years ago showing position of the accretionary wedge of the Franciscan Complex.

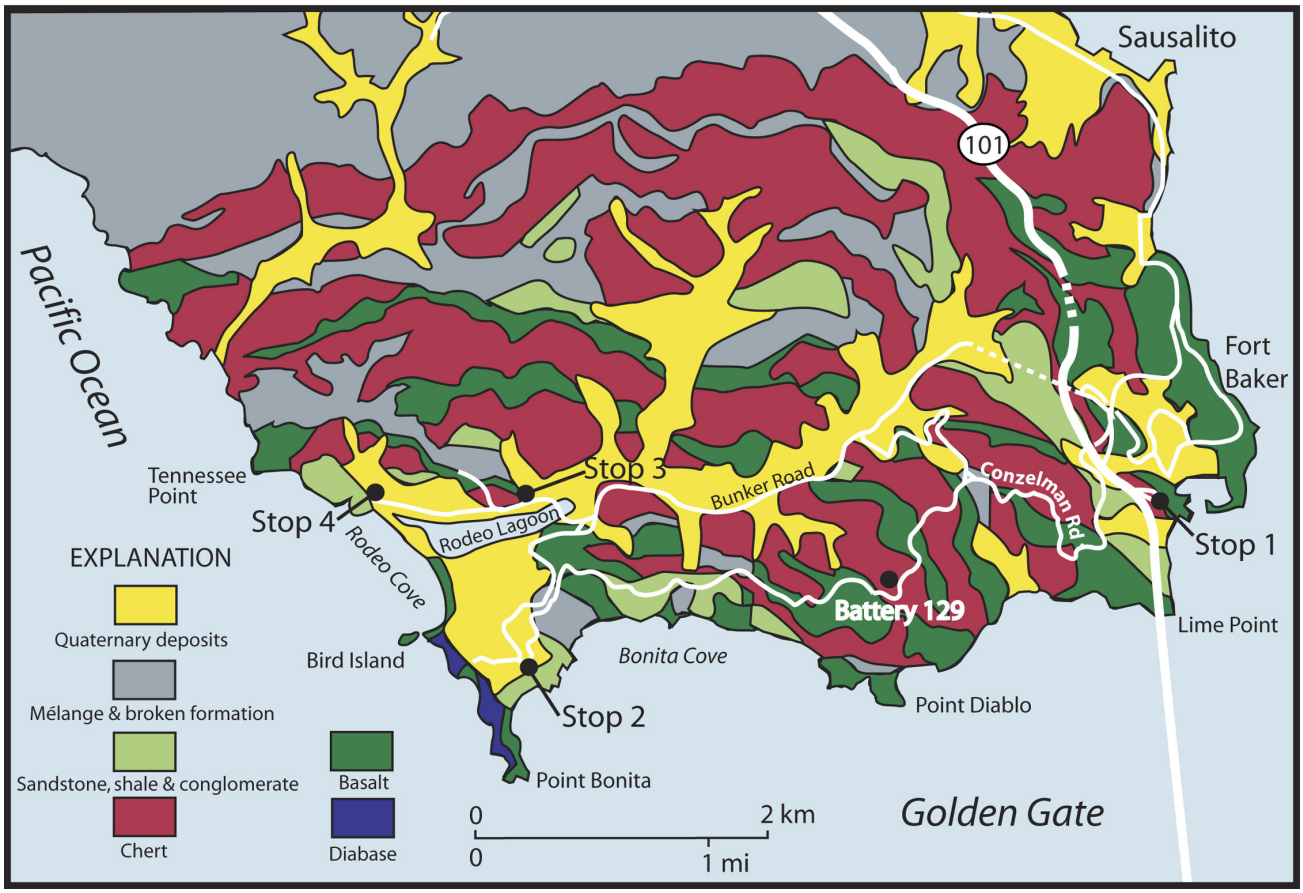

Figure 3.4. Geologic map of the Marin Headlands showing major geologic units, location of field trip stops, and other places referred to in text (modified from Wahrhaftig and Murchey, 1987).

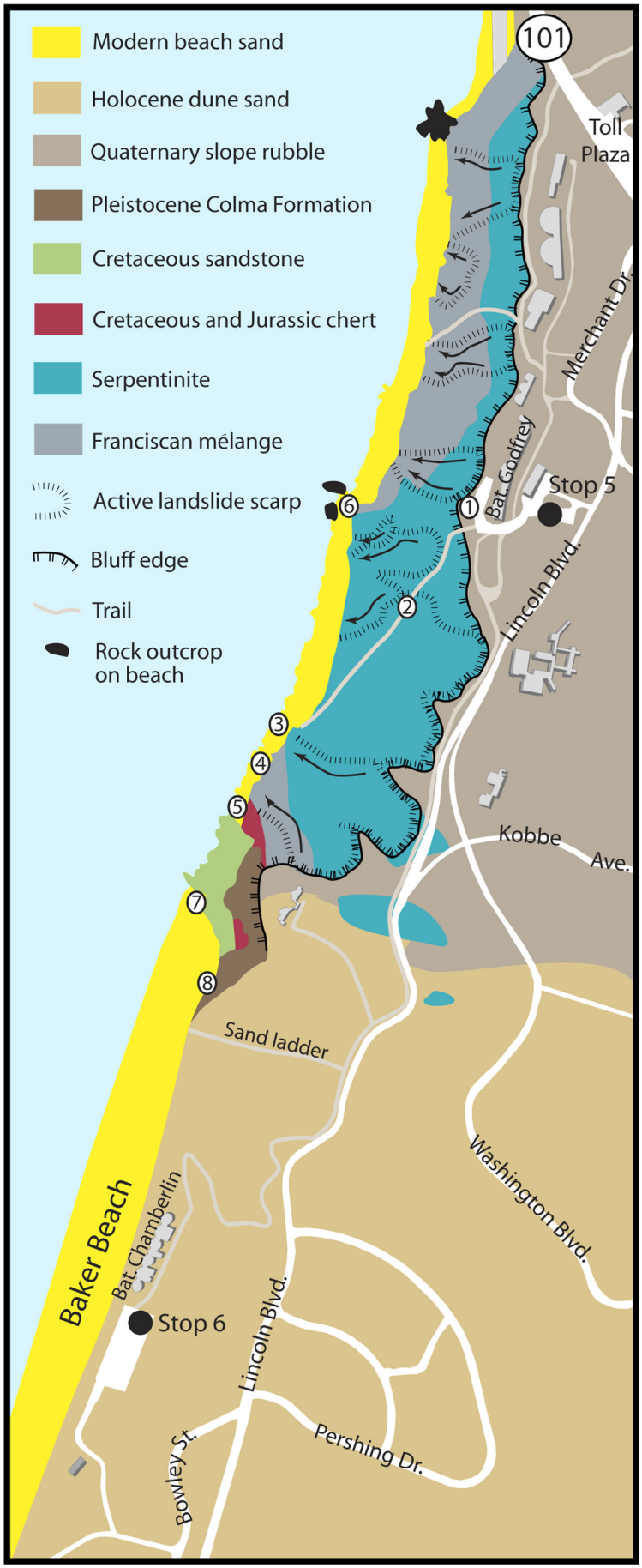

Figure 3.5. Geologic map of coastal bluffs in the Presidio showing major geologic units, location of field trip stops, and locations at stops referred to in text (modified from Wahrhaftig, 1984b; Schlocker, 1974). Arrows indicate the direction of landslide movement.

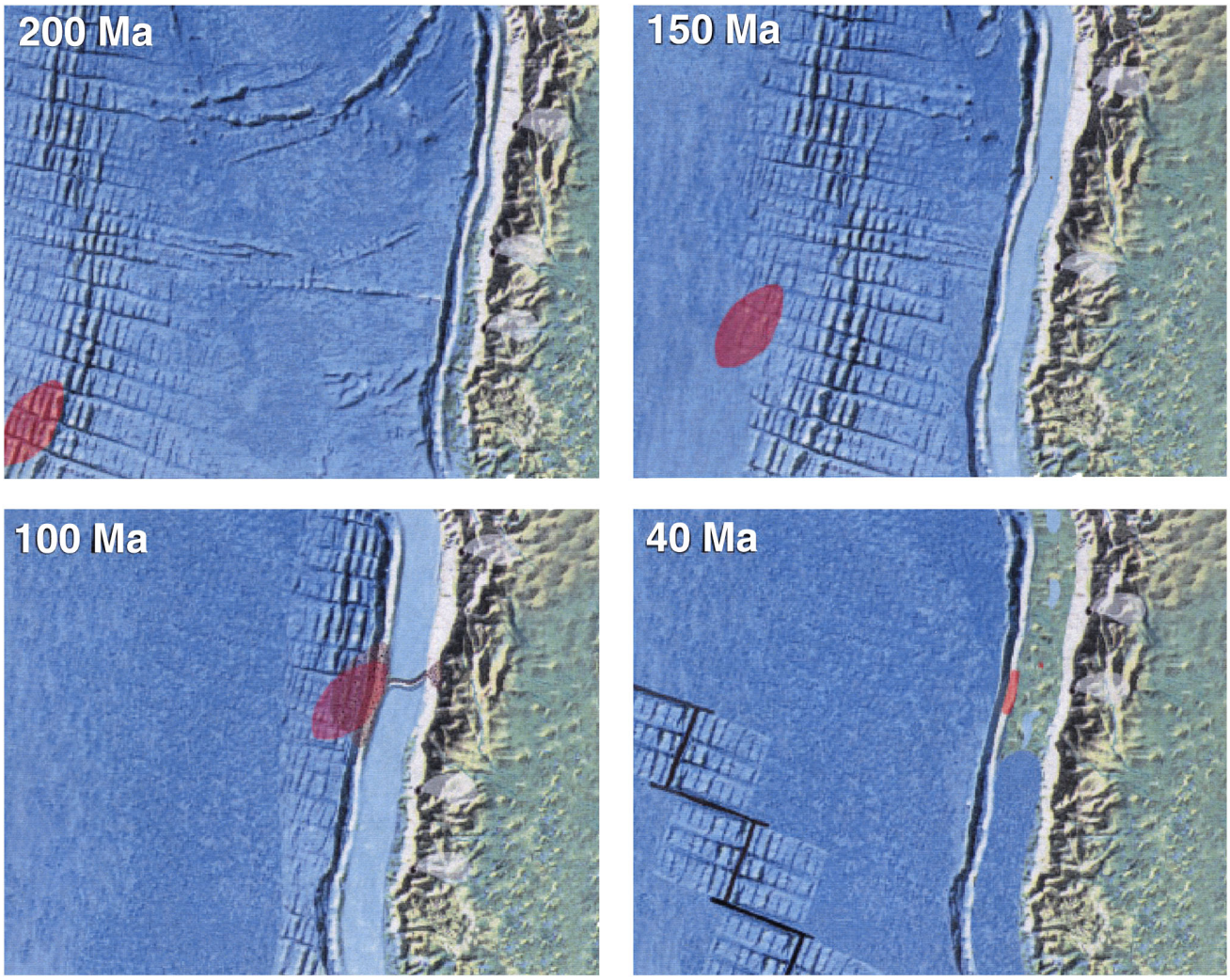

Figure 3.6. Transport history of the Marin Headlands terrane across the Pacific Basin. Panels show approximate geographic position of terrane, shown as red area, at 200, 150, 100, and 40 million years ago (modified from Murchey and Jones, 1984).

Figure 3.7. Pillow basalt with red chert interbeds at Point Bonita. Hat for scale.

Figure 3.8. Ribbon chert in depositional contact with pillow basalt at Battery 129.

Figure 3.9. Folded chert beds on Conzelman Road. Note the lack of fracturing on the tight folds. Knife for scale.

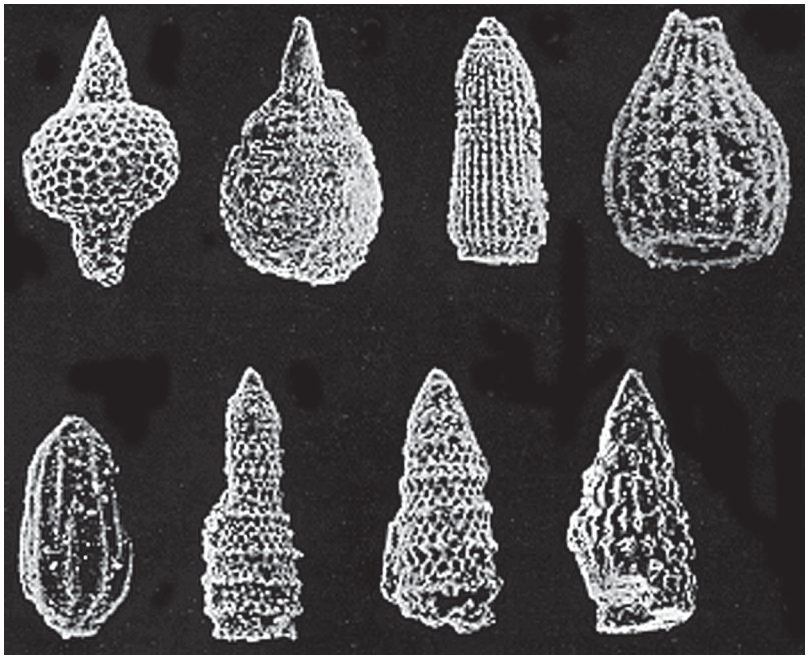

Figure 3.10. Scanning electron micrographs of silica tests (shells) of Radiolaria removed from the Marin Headlands chert by using hydroflouric acid.

Figure 3.11. Bedding rhythms developed in ribbon chert along Conzelman Road. Diagenetic transfer of silica has enhanced the bedding. Knife for scale.

Figure 3.12. Graywacke sandstone turbidite beds at the north end of Baker Beach. Note the darker fine-grained interbeds dipping northeast, away from the camera.

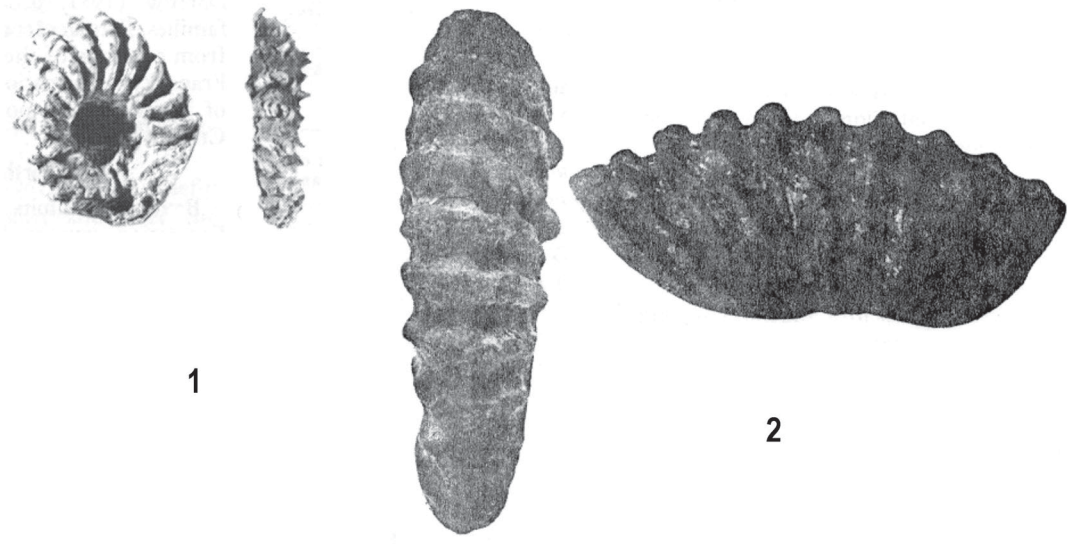

Figure 3.13. Ammonite fossils from turbidite sandstones of the Marin Headlands terrane—(1) *Douvilleiceras* cf. *mammillatum* (Schlotheim) from Baker Beach area, (2) *Mantelliceras* sp. from below the north tower of the Golden Gate Bridge (photos from Hertlein, 1956; Schlocker and others, 1954).

Figure 3.14. Serpentine exposed in landslide headwalls in bluffs of the Presidio. The dark rocks in the ocean below are high-grade metamorphic amphibolite blocks.

Figure 3.15. Lacy network of chrysotile (asbestos) veins in serpentinite boulder on the beach near the Presidio.

Figure 3.16. Rare and endangered plants living on serpentine soils and dunes of the Presidio—(1) Presidio clarkia (*Clarkia franciscana*), serpentine soils; (2) Dune gilia (*Gilia capitata*), coastal dunes; (3) San Francisco wallflower (*Erysimum franciscanum*), serpentine and dunes; (4) San Francisco lessingia (*Lessingia germanorum*), coastal dunes; (5) Raven's manzanita (*Arctostaphylos hookerii* ssp. *ravenii*), serpentine soils; and (6) Franciscan thistle (*Cirsium andrewsii*), serpentine seeps.

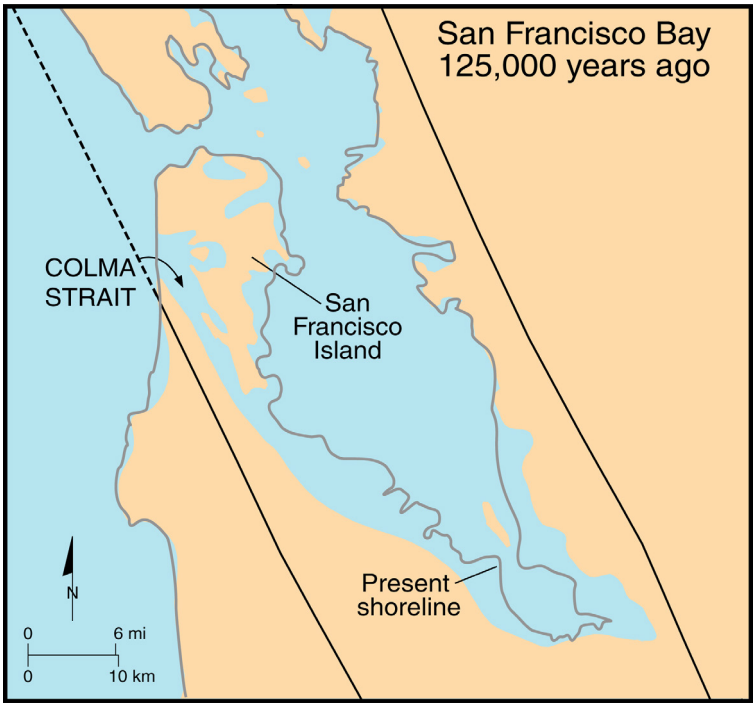

Figure 3.17. Paleogeographic map of the San Francisco Bay area when the Colma Formation was deposited about 125 thousand years ago, during an interglacial period when sea level was slightly higher than today. Note that the area of San Francisco was largely an island at that time (modified from an unpublished map based on data of Ken Lajoie, U.S. Geological Survey).

Figure 3.18. Top of Colma Formation and overlying Holocene sand dunes at Baker Beach. Note the gray soil horizon at paleoerosion surface developed between the two units.

Figure 3.19. Ribbon chert exposed in old quarry at Stop 3 of field trip. Note relatively undeformed beds on right side and folding on left.

Figure 3.20. Rodeo Beach and Lagoon. The barrier bar developed by the beach is overtopped during winter storms.

Figure 3.21. Altered tuff with zeolite nodules in Franciscan Complex mélange on beach (Stop 5, loc. 4).

Figure 3.22. Large blocks in the mélange at the boundary of Marin Headlands terrane on the beach at the Presidio (fig. 3.5, loc. 5). Greenstone blocks are in foreground, ribbon chert in center, and graywacke sandstone in background.

Figure 3.23. Turbidite sandstone with lens of carbonized plant material at the north end of Baker Beach (fig. 3.5, loc.7). Knife for scale.

Figure 3.24. Colma Formation forming small badlands in the bluffs at the north end of Baker Beach (fig. 3.5, loc.8).

Figure 3.25. High-angle crossbeds exposed in a gully in the poorly consolidated Holocene dune deposits at the north end of Baker Beach (fig. 3.5, loc.8). Knife for scale.

San Andreas Fault and Coastal Geology from Half Moon Bay to Fort Funston: Crustal Motion, Climate Change, and Human Activity

David W. Andersen
Department of Geology, San José State University, Calif.

Andrei M. Sarna-Wojcicki
U.S. Geological Survey, Menlo Park, Calif.

Richard L. Sedlock
Department of Geology, San José State University, Calif.

Introduction

The geology of the San Francisco Peninsula reflects many processes operating at time scales ranging from hundreds of millions of years to a fraction of a human lifetime. We can attribute today's landscape in the San Francisco Bay area to three major processes, each operating at its own pace, but each interacting with the others and with subsidiary processes: (1) the slow, long-term motion of the North American tectonic plate as it moves relative to the northwest-moving Pacific Plate, and the smaller but important component of crustal compression between the two plates; (2) the more rapid changes in global climate during the last few million years, which have controlled the rise and fall of sea level and the succession of flora and fauna on land and along the coast; and (3) the very recent, explosive growth of human population and its related activity, as expressed in pervasive ecological impact and urbanization.

The oldest rocks in the region formed nearly 170 Ma (million years ago) under conditions very different from those in the San Francisco Bay area today, and rocks that were formed far apart have been juxtaposed during their later history. On a much shorter time scale, local climatic conditions and sea level have fluctuated dramatically since about 2 Ma during glacial and interglacial times. Very recent processes such as erosion and human activity have significantly affected the landscape on a still shorter time scale. The purpose of this trip is to examine the effects and interplay of these processes in producing some of the geologic features in this part of coastal California.

Mesozoic and Cenozoic Geologic Evolution of California

During the late Mesozoic and early Cenozoic, about 170 to 28 Ma, California lay along a convergent plate boundary. Modern convergent boundaries between a continent and an oceanic plate, such as the western edge of South America, typically include a volcanic arc on the continent, a forearc basin and accretionary complex seaward of the arc, a trench, and the unsubducted part of the oceanic plate farther seaward. The Mesozoic rocks of California reflect their origins in various parts of this setting (fig. 4.1). Granitic rocks of the Sierra Nevada formed below the arc of then-active volcanoes. The Coast Range Ophiolite represents the oceanic basement beneath part of the forearc basin, and sedimentary rocks of the eastern Coast Ranges (which we will not see on this trip) formed above this basement within the forearc basin. The oldest rocks in many parts of the Coast Ranges, called the Franciscan Complex, consist of deformed pieces of the accretionary complex (Page, 1981; Wahrhaftig, 1984).

About 28 Ma, the oceanic spreading ridge that lay west of the convergent boundary encountered the trench, and the North American Plate began to interact directly with the Pacific Plate (Atwater, 1970, 1989). Relative motion between these two plates is dominantly parallel to the plate margin, and the transform fault plate boundary of which the modern San Andreas Fault is a part began to develop and lengthen at that time (fig. 4.2). The northern end of this transform fault system, called the Mendocino triple junction, migrated northward and reached the latitude of Menlo Park about 10 Ma (Dickinson, 1981; Atwater, 1989). The geologic history of the San Francisco Bay area since about 10 Ma largely reflects the development of the San Andreas Fault system as the complex boundary between the North American and Pacific tectonic plates.

San Andreas Fault System

The San Andreas Fault is one of many faults comprising the transform plate boundary in the San Francisco Bay area (fig. 4.3). Most of these faults, such as the San Andreas, Hayward, Calaveras, and Greenville, are right-lateral strike-slip

faults (the block on the west moves northward relative to the block on the east). Average slip rates are shown on figure 4.3. Other Bay-area faults are thrusts, in which one side of the fault moves upward and over the adjacent side. The unlabeled faults south of San José (fig. 4.3) probably are thrusts, and the San Gregorio Fault Zone may have components of both right-lateral strike slip and thrust slip.

The faults of the San Andreas Fault Zone juxtapose rocks with very different characteristics and histories. Throughout most of central California, the San Andreas Fault forms the boundary between areas underlain by Franciscan Complex rocks on the east side of the fault and areas underlain by granitic basement on the west (fig. 4.4). The areas underlain by granitic rocks constitute the Salinian block, which represents a piece of the old volcanic arc that has been transported northward along the San Andreas Fault and placed outboard (west) of the Franciscan Complex rocks.

One somewhat enigmatic fault on the San Francisco Peninsula is the Pilarcitos (fig. 4.3). In this area, Franciscan Complex rocks lie west of the San Andreas, and the Pilarcitos forms the boundary between blocks with Franciscan and Salinian basements. A traditional view is that the Pilarcitos represents a former trace of the San Andreas, and that the presently active trace on the Peninsula formed relatively recently (McLaughlin and others, 1996). The crustal block bounded by the Pilarcitos and the Peninsular strand of the San Andreas would thus be a piece of the former North American Plate that has been captured by the Pacific Plate and now moves to the northwest with the latter. The total amount of offset on the active trace of the San Andreas Fault since this capture is about 25 km. An alternative interpretation proposed by Wakabayashi (1999) is that the Pilarcitos is an old thrust fault not related to the San Andreas, which would require that most of the slip on the transform margin at this latitude has taken place on faults other than the San Andreas.

Many parts of the Bay area have experienced uplift and erosion or subsidence and sediment accumulation in response to compression normal to the San Andreas Fault system. Such vertical displacements would certainly accompany thrusting on the unlabeled faults in figure 4.3 and probably also accompany horizontal slip on the dominantly strike-slip faults. Sarna-Wojcicki and others (1986) estimated that the rate of shortening across the San Andreas Fault system is at least 10 percent of the rate of strike-slip motion over the past 6 m.y.

Sea Level Fluctuations During the Quaternary and Uplift of the Coast Ranges

Superimposed on slow lateral displacement and uplift of the faulted crustal blocks are the effects of the repeated rise and fall of the world oceans in response to changes in the amount of water stored in Earth's ice caps. High stands of the sea level are preserved as marine terraces, cut into the rising Coast Ranges. Multiple marine terraces can be observed on the coast near Santa Cruz and Half Moon Bay. The oldest terrace cut by sea level is now the highest; it has been uplifted the most because it has had time to be uplifted to a higher elevation. The youngest terrace above the modern surf-abrasion platform is the lowest; it has been uplifted only slightly, relative to the older terraces.

During the last major worldwide glacial maximum, about 20 ka (thousand years ago), sea level was as much as 130 m lower than it is now (fig. 4.5). The continental shelf was much more broadly exposed above sea level during this period, with the coastline as much as 35 km west of the present one. The Farallon Islands were then rugged hills rising above a broad, gently sloping plain, with the coastline lying to the west. At that time, there was no San Francisco Bay. The lowland that now forms the bay was a broad, forested valley. Local tributary rivers and streams converged near the center of the modern Bay area to join the huge, swollen river that rushed from eastern California past the present location of San Francisco and out onto the broad alluvial plain (now the continental shelf covered by the ocean). This huge river, bearing the runoff water from about 40 percent of California's land area during a cooler and wetter time than the present, must have been an imposing sight. Once the river met the broad, flat plain west of San Francisco, it meandered to the coast, just south of the Farallon Hills.

At that time, the valley that is now partly filled by San Francisco Bay contained stands of incense cedar, cypress, Douglas fir, and juniper, with an undergrowth of cocklebur and other brushy plants, and horned pond weed, elatine, and potamogeton in the wetlands. Meadows contained composites, chenopods, and grasses, as well as sage. Oak and sequoia, now so common in parts of the Bay area, were scarce or absent. Horse, bison, camel, and mammoth roamed the Bay valley, while smaller vertebrates lived in the brush and grass. Specimens of all of these fossils have been found in sediment exposed in deep pits excavated northwest of San José near Mountain View for San Francisco's garbage in the early 1970's. Fossil wood found in these deposits has yielded radiocarbon ages of 21 to 23 ka (Helley and others, 1972), close to the age of the last glacial maximum at about 18 ka. The pits are now filled and covered, and the area is the site of Shoreline Amphitheater, a large open-air theater where music concerts and other media events are staged. Even today, some spectators amuse themselves by lighting the methane that seeps out of the ground from the buried garbage below.

As the climate warmed after the last glacial period, glaciers began to melt, and the water stored in ice began to be returned to the oceans. Starting about 18 ka and continuing until about 5 ka, world sea level rose (fig. 4.6). The rise was

not uniform, but punctuated by accelerations and slowdowns, and occasional stillstands, accompanied by formation of stable coastlines for perhaps hundreds of years. Sea level rose high enough by ~9 ka to extend into the valley of San Francisco Bay (Atwater and others, 1977). By ~5 ka, the sea level reached near its present position, and ceased to rise. Ages of dated Native American habitation sites around the bay, marked by shell middens (mounds of shells containing artifacts and often also used as burial mounds) date to about 5 ka, but no older. This suggests that older habitation sites are now below sea level, corresponding to earlier, lower stands of the ocean (Helley and others, 1972).

Effects of Human Activity on the San Francisco Landscape

Early Native American inhabitants of the San Francisco Bay area were probably a minor factor in affecting the form of the area's landscape. The human population was small, and the lifestyle of hunting and gathering was not particularly disruptive, but if humans contributed significantly to the late Pleistocene extinction of mammoths and other large animals in North America (Alroy, 2001), then they definitely had an impact on the ecosystem. With the transition from a gathering and hunting lifestyle of the early Native Americans to the agricultural economy and grazing practices of early Spanish and Mexican Californians, the original fauna and flora were gradually diminished, replaced, or eradicated. Rapid acceleration of change began with the influx of population that occurred after the discovery of gold in 1848. Timber harvesting, the expansion and intensification of agriculture accompanying the population influx, the growth of towns and cities, and industrialization all contributed to major changes in the flora, fauna, and landscape. Mining activities accelerated erosion in the hills and mountains, accelerating sediment deposition in the lowlands. Today, environmental issues including the decrease of wetlands in the Bay area (fig. 4.7) continue to be of concern.

The effects of human activity on the landscape in this area are likely to continue and accelerate into the future as population here continues to grow. The Bay area is likely to experience not only the effects derived from local population growth, but also from global effects induced by human activity. For example, continued global warming may result in a rising of sea level, with displacement of population from the lowest elevations (fig. 4.8).

Road Log

The trip begins at the U.S. Geological Survey in Menlo Park. The trip route and locations of the stops are shown on figure 4.9.

Mileage/Notes

0.0 Leave the U.S. Geological Survey parking lot and proceed north to Middlefield Road.

0.1 Turn left onto Middlefield Road.

0.4 Turn left onto Ravenswood Avenue.

1.1 Cross El Camino Real; street name changes to Menlo Avenue.

1.4 Turn left onto University Drive.

1.7 Turn right onto Middle Avenue.

2.5 Turn left onto Olive Street.

2.6 Turn right onto Oak Avenue.

3.2 Turn right onto Sand Hill Road.

4.9 Turn right onto Interstate 280 North.

7.4 Greenish-gray, rocky soil with little vegetation in the road cuts indicates the presence of serpentinite. Note the numerous small landslides in this weak material.

7.9 San Andreas Fault Zone occupies wide valley in left foreground.

11.1 Exit freeway at first Vista Point north of Edgewood Road.

11.5 Park at Vista Point. Proceed up path to the west to view Crystal Springs Reservoir.

Stop 1—San Andreas Fault Overlook—Crystal Springs Reservoir

This reservoir occupies a portion of the San Andreas Fault Zone. About 4 m of right-lateral strike slip was recorded (by offset fences, dams, and other features) in this area during the 1906 San Francisco earthquake. Maximum displacement on the fault was ~6 m farther to the north, and the entire rupture length was 430 km. The magnitude of the earthquake was determined to be ~ 8.3 on the Richter scale, though later moment-magnitude calculations yield a lower value of ~7.8 (Thatcher, 1990). The earthquake was felt from southern Oregon to southern California and as far east as central Nevada (Ellsworth, 1990). Although the dams at Crystal Springs Reservoir and at San Andreas Lake farther north held during this earthquake, the water pipes supplying the city were ruptured in many places, so that water could not be delivered to stop fires that had broken out after the earthquake. It was the fire much more than the ground shaking that contributed to the great damage of the 1906 earthquake (Ellsworth, 1990).

Rocks of the Jurassic-Cretaceous Franciscan Complex occupy the northeast side of the fault, whereas Cretaceous granitic rocks of the Salinian block lie to the southwest. This contrast is part of the basis for interpretations of up to 320 km of cumulative right-lateral displacement along the San Andreas Fault. Clahan and others (1995) estimated an average slip rate of 17±3 mm/yr in this area since 2 ka (fig. 4.3).

Although none of the rocks here are true “in place” outcrops, fragments on the ground and in the rock wall come from bedrock nearby. Blocks of serpentinized ultramafic rock along the path represent metamorphosed oceanic mantle, probably from the Coast Range Ophiolite. Large boulders near the path include Franciscan Complex greenstone (metamorphosed basalt) and radiolarian chert from the accreted oceanic plate.

Exit Vista Point and return to Interstate 280.

11.8 Reenter Interstate 280.

14.7 Exit Interstate 280; take Highway 92 West to Half Moon Bay.

15.9 Cross Crystal Springs Reservoir within San Andreas Fault Zone.

17.9 Cross summit on Highway 92. Valley in foreground is occupied by Pilarcitos Creek, and the Pilarcitos Fault runs parallel to the creek near the bottom of the valley.

18.6 Several terraform-sculpted retaining walls were recently installed in this area in order to help stabilize the slopes with a minimum of right-of-way expansion.

23.1 Turn right onto Highway 1 North.

26.3 Turn left into parking lot at Pillar Point Harbor.

Stop 2—El Granada Beach

This flat coastal area is a marine terrace that formed during a relatively higher stand of the sea about 100 ka. Note the old wave-cut cliffs to the east and partly dissected higher terraces. Although originally incised horizontally into the rising terrane, the ancient terrace surface is gently folded into a northwest-plunging syncline (fig. 4.10). The lowest elevation coincides with the deepest part of the embayment at Half Moon Bay; the terrace surface rises both to the north and to the south (Lajoie, 1986).

The higher elevation of this same terrace west of the Half Moon Bay airport has been caused by uplift on the Seal Cove Fault, one splay of the San Gregorio Fault Zone. The amount of uplift on the Seal Cove Fault is thought to be small compared to its strike-slip displacement, but the rates of modern and recent strike slip on this fault are controversial (Simpson and others, 1997; Sedlock, 1999).

The deformed marine terrace consists of eroded rocks of the Miocene to Pliocene Purisima Formation (about 5 to 3 Ma) overlain by a thin veneer of younger, unconsolidated sediment. The Purisima Formation forms the relatively resistant rocks that make up Pillar Point to the west of the Seal Cove Fault. At El Granada, however, the unconsolidated sediment at the top of the terrace is at sea level, and erosion by waves is much more rapid here. The rate of coastal erosion became even greater after installation of the breakwater in 1960 (Mathieson and others, 1997).

Exit parking lot and return to Highway 1.

26.4 Turn left onto Highway 1 North.

27.9 Half Moon Bay airport on left. This area provides another view of the terrace, old wave-cut cliffs, and Seal Cove Fault described at Stop 2.

30.9 Crossing the marine terrace at Montara Beach.

31.4 First steep outcrops of granitic rocks.

32.1 Turn right into parking area.

Stop 3—Salinian Granitic Rocks

Rocks in this area are Cretaceous (about 90 Ma) granitic rocks of the Salinian block. These quartz-rich plutonic rocks, very similar to granitic rocks of the Sierra Nevada, formed several kilometers below the land surface within what was then an arc of active volcanoes in southern California. The rocks have since been transported northward along the San Andreas Fault and uplifted, and the overlying volcanic, sedimentary, and metamorphic rocks have been eroded. Because these granitic rocks are much more resistant to erosion than the sedimentary materials at Stop 2, the coast is much steeper here.

Leave parking area and return to Highway 1.

32.2 Turn right onto Highway 1 North.

33.1 Highway 1 crosses a large landslide complex here near Devil's Slide. The landslide is mostly or entirely within sedimentary rocks that overlie the Salinian granitic rocks, and it has been active for many years. The most recent repairs were made after a slide in 1995 caused the road to be closed. The road was reopened after 5 months; although it has remained open since then, Caltrans personnel maintain that the repairs must be thought of as temporary (Williams, this volume).

33.6 Rocks on the right are Paleocene turbidites (younger than about 65 Ma).

34.3 Pilarcitos Fault runs through the valley ahead.

36.2 Turn left onto Rockaway Beach Avenue and take immediate right onto Old County Road.

36.4 Turn left at end onto San Marlo Way.

36.5 Park in lot.

Stop 4—Pacifica Quarry

At Pacifica Quarry near Rockaway Beach, Franciscan Complex rock types include limestone, greenstone dikes, and mélange that are part of the Permanente terrane. This discussion is slightly updated from Larue and others (1989).

The greater than 70 m-thick section of Calera Limestone Member of the Franciscan Complex (previously quarried for cement) includes dark gray to black strata overlain by beige to light gray strata; interbedded chert probably formed due to diagenesis (very weak metamorphism). The limestone consists chiefly of planktonic forams and micritic (muddy)

groundmass, with minor coccoliths, and yields early Albian to mid-Cenomanian ages (about 105 to 94 Ma). Black limestones probably accumulated under anoxic conditions. Similar, probably correlative, rocks currently are quarried at Permanente (west of San José).

Greenstone, or metamorphosed basalt, is present only in dikes that cut the limestone on the west wall of the quarry, but similar rocks crop out in large, massive bodies a few kilometers north. Geochemical analysis of immobile elements and relict clinopyroxenes were used to infer that the basalts were emplaced either at a spreading center (MORB) or at an oceanic plateau or island (within-plate tholeiite)—the elemental composition of these basalts more closely match the composition of rocks in these oceanic settings than basalts found in continental interior regions. Some greenstone dikes contain lawsonite and jadeitic clinopyroxene, which indicate that the dikes (and their limestone host) experienced blueschist-facies metamorphism (low temperatures, high pressures).

Mélange, defined as a mixture of blocks in a weaker matrix, here consists chiefly of limestone blocks in shale. Elsewhere in the Permanente terrane, mélange blocks include greenstone, sandstone, and blueschist; matrix is either shale or serpentinite.

A likely geologic history is as follows (fig. 4.11): (1) the limestone accumulated (not as a reef complex) atop basaltic oceanic crust (not exposed here) on a seamount, (2) few basaltic dikes intruded the limestone sequence, perhaps near a transform fault that leaked basaltic magma, (3) the fossil seamount was subducted beneath western North America to depths sufficient for blueschist-facies metamorphism (at least 15 km), and (4) complex faulting juxtaposed the limestone, basalt, and mélange during subduction, exhumation, or both.

Some workers have interpreted paleomagnetic data to indicate that the limestone was deposited at a latitude of 22°N and shifted northward on the Farallon Plate or (after accretion to North America) within the Franciscan Complex (Tarduno and others, 1985). However, others have argued that the Calera Limestone Member, like much of the Franciscan, was remagnetized after its initial magnetization, invalidating the paleomagnetic argument for long-distance transport. The presence of tropical microfauna in the limestone, however, tends to support the initial hypothesis of long-distance northward transport (Sliter, 1984).

Leave parking lot and proceed toward Highway 1.

36.6 Turn right onto Dondee Way.

36.7 Turn left onto Rockaway Beach Avenue.

38.7 Turn left onto Highway 1 North.

39.5 Take Manor Drive exit. Keep left on Oceana Boulevard.

39.9 Turn left onto Manor Drive. Cross Highway 1 and take immediate right onto Palmetto Avenue.

40.8 Turn left onto Westline Drive. Keep left along the coast to parking lot.

41.2 Park and walk northward to view area.

Stop 5—Mussel Rock

The San Andreas Fault crosses the shoreline near here and passes offshore of San Francisco to the north. The steep cliffs on the northeast side of the fault are composed of weakly consolidated sediment of the Merced Formation and related units, which are Pliocene and Pleistocene in age (perhaps about 3 Ma to less than 50 ka).

The Merced Formation and related units are more than 1700 m thick and are composed of sediment deposited in a variety of coastal settings, ranging from shelf through nearshore to nonmarine environments (Clifton and Hunter, 1999). Environments can be determined from the nature of the bedding and other lithologic criteria, and comparison of these features with those found in modern settings. Independent confirmation of depths can also be obtained from fossils present in the sediments by comparing these to the same or similar organisms living today in the corresponding environments and water depths. The sediment exposed in the cliffs contains mostly shelf deposits in the lower part of the Merced Formation near here, and the proportion of shallow-water and nonmarine facies increases farther north in younger layers. However, there is a cyclic, smaller-scale repetition of alternating deeper and shallower environments that is superimposed on the generally shallowing trend (Clifton and Hunter, 1999). These smaller-scale cycles represent packages of sediment deposited during sea-level oscillations caused by climate change during deposition.

The repeated occurrence of shallow-water deposits in this thick sequence indicates that the sediment accumulated in an area that was slowly subsiding over millions of years, and accumulation kept approximate pace with subsidence. The fact that these young strata are now tilted and exposed well above sea level shows that this same area has recently changed to a site of uplift.

There are many examples of slope failure in the weakly consolidated Merced Formation along the cliff face. A narrow bench that crosses the cliff face was originally part of the Ocean Shore Railroad, constructed in 1905 and 1906, then abandoned in 1920. Some time after 1933, the right-of-way was widened to accommodate California Highway 1, the Ocean Shore Highway, which was maintained here with great difficulty, expense, and frequent shutdowns. The road was heavily damaged by landsliding in the March 22, 1957 earthquake (fig. 4.12) and was abandoned in 1958 (Sullivan, 1975).

The area became heavily developed between 1950 and 1960. Much of the rolling topography atop the bluffs was leveled, and subdivisions were put in, extending close to the cliff edges. Many homes close to the cliff were damaged, condemned, and destroyed as a result of landsliding. Landsliding and damage to the houses continues to the present.

Return to parking area and exit toward Westline Drive.

41.5 Turn left onto Skyline Drive (sign is missing; turn at change in pavement) and immediately left again onto Westline Drive.

41.7 Westline Drive closed ahead due to landsliding. Turn right onto Rockford Avenue.

41.9 Turn left onto Longview Drive.

42.0 Former continuation of Westline Drive on left. Homes near the bottom of this hill have been removed recently.

42.1 Turn left onto Skyline Drive.

42.3 Houses that formerly lined this street on the seaward side have been removed because of landslide damage.

42.9 Turn left onto Northridge Drive.

43.2 Northridge Park with view of Wood's Gulch to north.

43.3 Turn left onto Avalon Drive.

43.4 View of Wood's Gulch on left. Recent work on the south side of Wood's Gulch involved extensive terracing and installation of drains.

43.5 Turn right onto Westmoor Avenue.

43.6 Turn left onto Skyline Boulevard.

44.8 Former entrance to Thornton Beach State Park, now closed because of landsliding. More landslide damage is evident ahead.

46.3 At John Muir Drive, make a U-turn and return southward on Skyline Boulevard.

46.6 Turn right into Fort Funston. Keep right and proceed toward hang glider launch area.

47.0 Park in parking lot. Walk toward the ocean, keep to the left of the hang-glider launch area, and hike down the path to the beach. NOTE: this is a fairly strenuous hike. Turn right and hike northward along the beach to outcrops.

Stop 6—Fort Funston

The Merced Formation here is Pleistocene in age (about 0.5 Ma) and includes excellent examples of several different sedimentary environments. Clifton and Hunter (1999) identified 41 distinct stratigraphic divisions within the Merced

Formation and related units; we will be examining exposures in their units R, S, and T. Excellent descriptions of the stratigraphy and the sedimentary features here are presented by Hunter and others (1984) and Clifton and Hunter (1987, 1999).

Marine facies in this part of the section are quite diverse. Subtidal deposits include dark, fossiliferous and bioturbated sand in unit R, parallel laminated and burrowed sand and silt in unit S, and cross-bedded gravel and pebbly sand in unit T. The differences between these shallow-marine facies probably reflect different influences of tidal currents, waves, and biological activity during accumulation of the different units. Intertidal and lower supratidal deposits in each of these units include parallel laminated sand with local concentrations of heavy minerals. The nonmarine deposits in each unit consist mostly of wind-blown sand, locally modified by soil-forming processes. Notable additional elements in the nonmarine facies are pebbly fluvial sediment at the top of unit R, the Rockland ash bed [probably 400 ka (Sarna-Wojcicki and others, 1985) but possibly about 610 ka (Lanphere and others, 1999)] in unit S, and well developed, water-worked backshore deposits, especially in unit T. The part of the Merced Formation exposed here contains a larger proportion of shallow-water and nonmarine deposits than the older part of the formation at Stop 5.

Each of the units in this part of the Merced Formation consists of a shallowing-upward sequence, with shallow-marine deposits at the base that are overlain by intertidal facies and then capped by sediment deposited above sea level. At the top of each unit is an unconformity, which represents a time when sediment was eroded or not deposited. At each unconformity, nonmarine deposits of the lower stratigraphic unit are overlain by marine deposits of the next higher unit.

As at Stop 5, the repetition of marine units shows that this area was subsiding during the deposition of the Merced Formation. At the same time, Pleistocene ice sheets were expanding and melting repeatedly, changing the volume of water in the oceans and causing worldwide fluctuations in sea level exceeding 100 m. We correlate the major unconformities in this part of the section to times of low sea level, and we attribute the marine deposits above the unconformities to flooding as sea level rose. In each of the units, the shallowing-upward sequence formed mainly by progradation of the coast during the sea-level high stand and, perhaps, during the early stages of the next sea-level fall. The punctuated nature of the stratigraphic sequence here is thus the result of repeated worldwide changes in sea level superimposed on long-term local subsidence.

Studies of the mineralogy of sediment in the Merced Formation indicate that the lower two-thirds of the formation contains sediment derived from local sources within the central Coast Ranges. Minerals in the sediment are similar to those found in streams draining various parts of the Coast Ranges within the vicinity of San Francisco Bay. Heavy minerals can be more useful and diagnostic of sediment provenance than fine rock fragments and light minerals. Among the heavy minerals present in the lower units are glaucophane, jadeite, actinolite, omphacite, and pumpelleyite. These are minerals typical of Franciscan Complex metamorphic rocks found in the Coast Ranges. About two-thirds of the way up in the Merced Formation section, however, there is a sudden and dramatic change in mineralogy. A flood of fine volcanic rock fragments and minerals appear that are evidently derived from the Sierra Nevada and the southern Cascade Range, with only a minor percentage of Coast Range-derived sediment. Heavy minerals such as hornblende, hypersthene, and augite predominate. These data indicate that sediment derived from the interior of California was suddenly introduced into the Merced embayment at the time of the change in the mineral assemblage (Hall, 1965). This geological event marks the inception of river drainage from the Great Valley of California through the area of the modern San Francisco Bay. Prior to this event, Great Valley drainage had been channeled through an outlet at the south end of the Great Valley. The change in mineralogy occurs about 115 m below the Rockland ash bed. Thus, by interpolation, this major change in the Great Valley drainage is inferred to have occurred sometime about 650 ka (Sarna-Wojcicki and others, 1985).

Return to parking lot. Exit parking lot and return to Skyline Boulevard.

47.2 Turn right onto Skyline Boulevard.

48.3 Turn left onto John Daly Boulevard.

49.5 Turn right onto Interstate 280 South.

63.9 Crystal Springs Reservoir on right with dam out of view below freeway. The canyon on the left leads to the city of San Mateo.

75.4 Exit Interstate 280 at Sand Hill Road and proceed east toward Menlo Park.

79.6 Turn left onto El Camino Real.

80.4 Turn right onto Ravenswood Avenue.

81.0 Turn right onto Middlefield Road.

81.3 Turn right onto Survey Lane.

81.4 Enter U.S. Geological Survey parking lot. This concludes the road log for this trip.

References

Alroy, John, 2001, A multispecies overkill simulation of the end-Pleistocene megafaunal mass extinction: Science, v. 292, p. 1893-1896.

Atwater, B.F., Hedel, C.W., and Helley, E.J., 1977, Late Quaternary depositional history, Holocene sea-level changes, and vertical crustal movement, southern San Francisco Bay, California: U.S. Geological Survey Professional Paper 1014, 15 p.

Atwater, Tanya, 1970, Implications of plate tectonics for the tectonic evolution of western North America: Geological Society of America Bulletin, v. 81, p. 3513-3536.

Atwater, Tanya, 1989, Plate tectonic history of the northeast Pacific and western North America, *in* Decker, R.W., ed., Decade of North American geology, v. N: The eastern Pacific region: Boulder, Colorado, Geological Society of America, p. 21-72.

Clahan, K.B., Hall, N.T., and Wright, R.H., 1995, Late Holocene slip rate and slip events for the San Francisco peninsula segment of the San Andreas Fault (abs.): Geological Society of America Abstracts with Programs, v.27, no. 5, p. 9.

Clifton, H.E., and Hunter, R.E., 1987, The Merced Formation and related beds: A mile-thick succession of late Cenozoic coastal and shelf deposits in the seacliffs of San Francisco, California, *in* Hill, M.L., ed., Cordilleran Section of the Geological Society of America centennial field guide volume 1: Boulder, Colorado, Geological Society of America, p. 257-262.

Clifton, H.E., and Hunter, R.E., 1999, Depositional and other features of the Merced Formation in seacliff exposures south of San Francisco, California, *in* Wagner, D.L., and Graham, S.A., eds., Geologic field trips in northern California: California Division of Mines and Geology Special Publication 119, p. 89-100.

Dickinson, W.R., 1981, Plate tectonics and the continental margin of California, *in* Ernst, W.G., ed., The geotectonic development of California, Rubey volume 1: Englewood Cliffs, New Jersey, Prentice-Hall, p. 1-28.

Ellsworth, W.L., 1990, Earthquake history, 1769-1989, in Wallace, R.E., ed., The San Andreas Fault system, California: U.S. Geological Survey Professional Paper 1515, p.153-187.

Hall, N.T., 1965, Petrology of the type Merced Group, San Francisco Peninsula, California (M.A. thesis): University of California, Berkeley, 127 p.

Helley, E.J., Adam, D.P., and Burke, D.B., 1972, Late Quaternary stratigraphic and paleontological investigations in the San Francisco Bay area, *in* U.S. Geological Survey Staff, Progress report on the U.S. Geological Survey. Quaternary studies in the San Francisco Bay area: Guidebook for the Friends of the Pleistocene, Oct. 6-8, 1972, p. 19-29.

Hunter, R.E., Clifton, H.E., Hall, N.T., Csaszar, Geza, Richmond, B.M., and Chin, J.L., 1984, Pliocene and Pleistocene coastal and shelf deposits of the Merced Formation and associated beds, northwestern San Francisco Peninsula, California: Society of Economic Paleontologists and Mineralogists Field Trip Guidebook No. 3, p. 1-29.

Irwin, W.P., 1990, Geology and plate-tectonic development, *in* Wallace, R.E., ed., The San Andreas Fault system, California: U.S. Geological Survey Professional Paper 1515, p. 61-80.

Kelson, K.I, Lettis, W.R., and Lisowski, Michael, 1992, Distribution of geologic slip and creep along faults in the San Francisco Bay region, *in* Borchardt, Glenn, and others, eds., Proceedings of the second conference on earthquake hazards in the eastern San Francisco Bay area: California Division of Mines and Geology Special Publication 113, p. 31-38.

Lajoie, K.R., 1986, Coastal tectonics, in Active tectonics: Washington, National Academy Press, p. 95-124.

Lanphere, M.A., Champion, D.E., Clynne, M.A., and Muffler, L.J.P., 1999, Revised age of the Rockland tephra, northern California: Implications for climate and stratigraphic reconstructions in the western United States: Geology, v. 27, p. 135-138.

Larue, D.K., Barnes, I., and Sedlock, R.L., 1989, Subduction and accretion of the Permanente terrane near San Francisco, California: Tectonics, v. 8, p. 221-235.

Mathieson, S.A., Lajoie, K.R., and Hamilton, J.C., 1997, Induced sea-cliff erosion southeast of the Pillar Point breakwater, Half Moon Bay, California: U.S. Geological Survey Open-file Report 97-688, scale 1:200.

McLaughlin, R.J., Sliter, W.V., Sorg, D.H., Russell, P.C., and Sarna-Wojcicki, A.M., 1996, Large-scale right-slip displacement on the East San Francisco Bay Region fault system, California: Implications for location of late Miocene to Pliocene Pacific Plate boundary: Tectonics, v. 15, p. 1-18.

Page, B.M, 1981, The southern Coast Ranges, in Ernst, W.G., ed., The geotectonic development of California, Rubey volume 1: Englewood Cliffs, New Jersey, Prentice-Hall, p. 329-417.

Sarna-Wojcicki, A.M., Meyer, C.E., Bowman, H.R., Hall, N.T., Russell, P.C., Woodward, M.L., and Slate, J.L., 1985, Correlation of the Rockland ash bed, a 400,000-year-old stratigraphic marker in northern California and western Nevada, and implications for middle Pleistocene paleogeography of central California: Quaternary Research, v. 23, p. 236-257.

Sarna-Wojcicki, A.M., Meyer, C.E., and Slate, J.L., 1986, Displacement of a ca. 6 Ma tuff across the San Andreas Fault system in northern California (abs.): EOS, v. 67, no. 44, p. 1224.

Sedlock, R.L., 1999, The San Gregorio Fault Zone: Late Cenozoic destral slip and slip rate, and southward linkage with the Sur, San Simeon, and Hosgri faults (abs.): American Association of Petroleum Geologists Bulletin, v. 83, p. 701.

Simpson, G.D., Thompson, S.C., Noller, J.S., and Lettis, W.R., 1997, The northern San Gregorio Fault Zone: Evidence for the timing of late Holocene earthquakes near Seal cove, California: Bulletin of the Seismological Society of America, v. 87, p. 1158-1170.

Sliter, W.V., 1984, Foraminifers from Cretaceous limestone of the Franciscan Complex, northern California, *in* Blake, M.C., Jr., ed., Franciscan geology of Northern California: Pacific Section Society of Economic Paleontologists and Mineralogists Special Publication 43, p. 149-162.

Sullivan, Raymond, 1975, Geological hazards along the coast south of San Francisco: California Geology, v. 28, p. 27-33.

Tarduno, J.A., McWilliams, M., Debiche, M.G., Sliter, W.V., and Blake, M.C., Jr., 1985, Franciscan Complex Calera limestones: Accreted remnants of Farallon plate oceanic plateaus: Nature, v. 317, p. 345-347.

Thatcher, Wayne, 1990, Present-day crustal movements and the mechanics of cyclic deformation, *in* Wallace, R.E., ed., The San Andreas Fault system, California: U.S. Geological Survey Professional Paper 1515, p. 189-205.

Wagner, D.L., Bortugno, E.J., and McJunkin, R.D., 1990, Geologic map of the San Francisco-San José quadrangle: California Division of Mines and Geology, scale 1:250,000.

Wahrhaftig, Clyde, 1984, A streetcar to subduction and other plate tectonic trips by public transport in San Francisco: Washington, D.C., American Geophysical Union, 76 p.

Wakabayashi, John, 1999, Distribution of displacement on and evolution of a young transform fault system: The northern San Andreas Fault system, California: Tectonics, v. 18, p. 1245-1274.

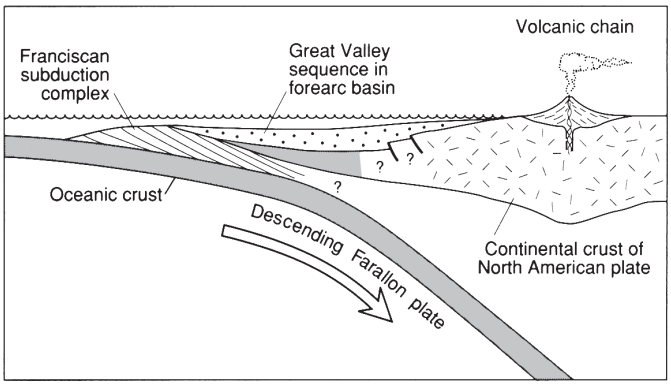

Figure 4.1. Schematic cross section showing California as an Andean-type continental margin during late Mesozoic time (from Irwin, 1990).

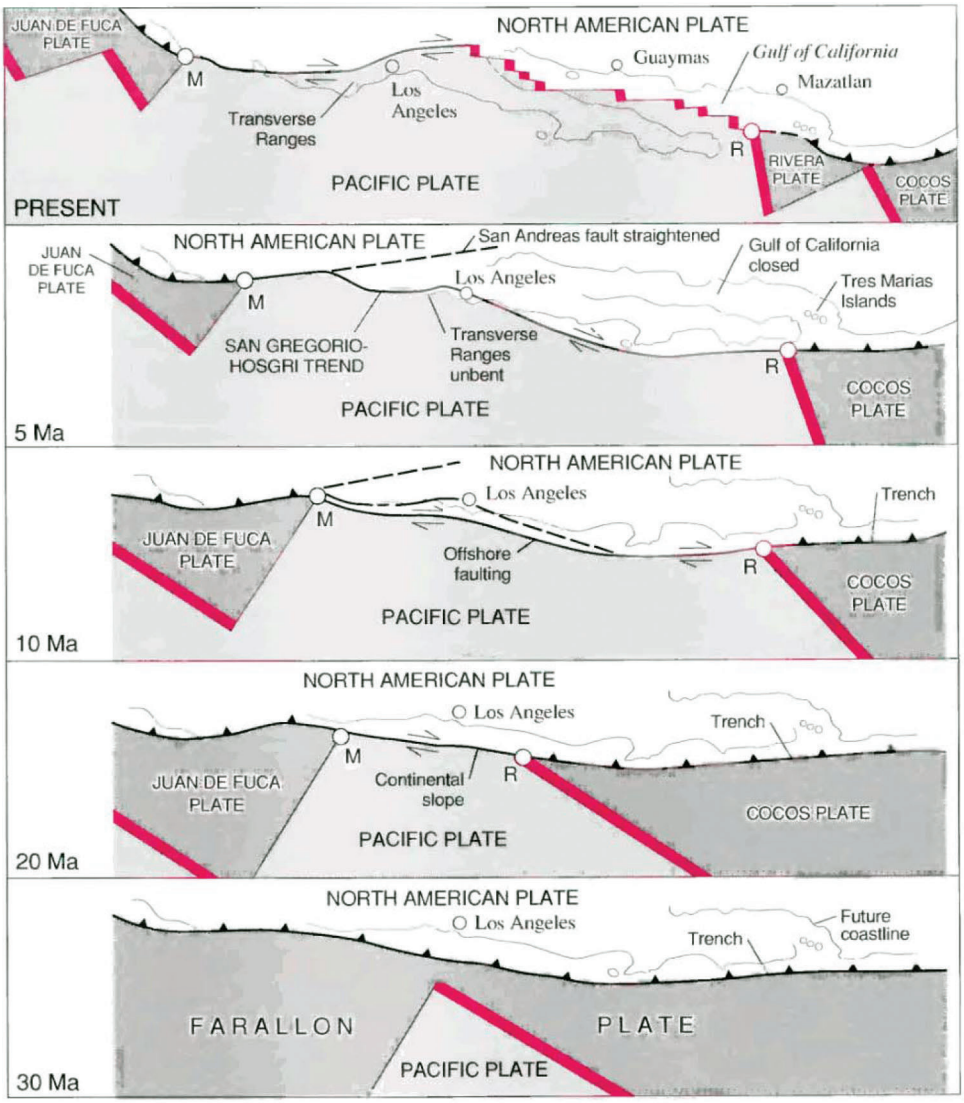

Figure 4.2. Maps showing evolution of the San Andreas transform fault system (from Irwin, 1990).

EXPLANATION

Spreading center

Subduction zone—Dashed where approximately located. Sawteeth on upper plate

Fault—Dashed where approximately located. Arrows indicate direction of relative movement

M **Mendocino triple junction**

R **Rivera triple junction**

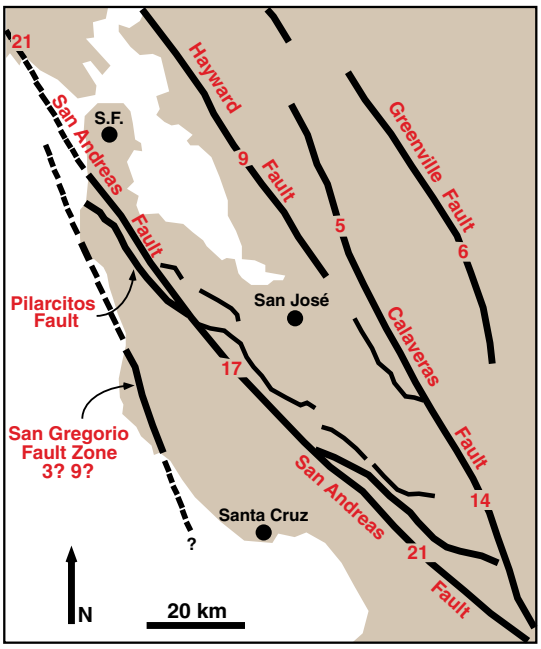

Figure 4.3. Faults of the San Andreas system in the San Francisco (S.F.) Bay area. Average slip rates shown are current estimates in mm/yr based on a wide range of geodetic (primarily GPS) and geologic (stream offset, trench) studies (after Kelson and others, 1992).

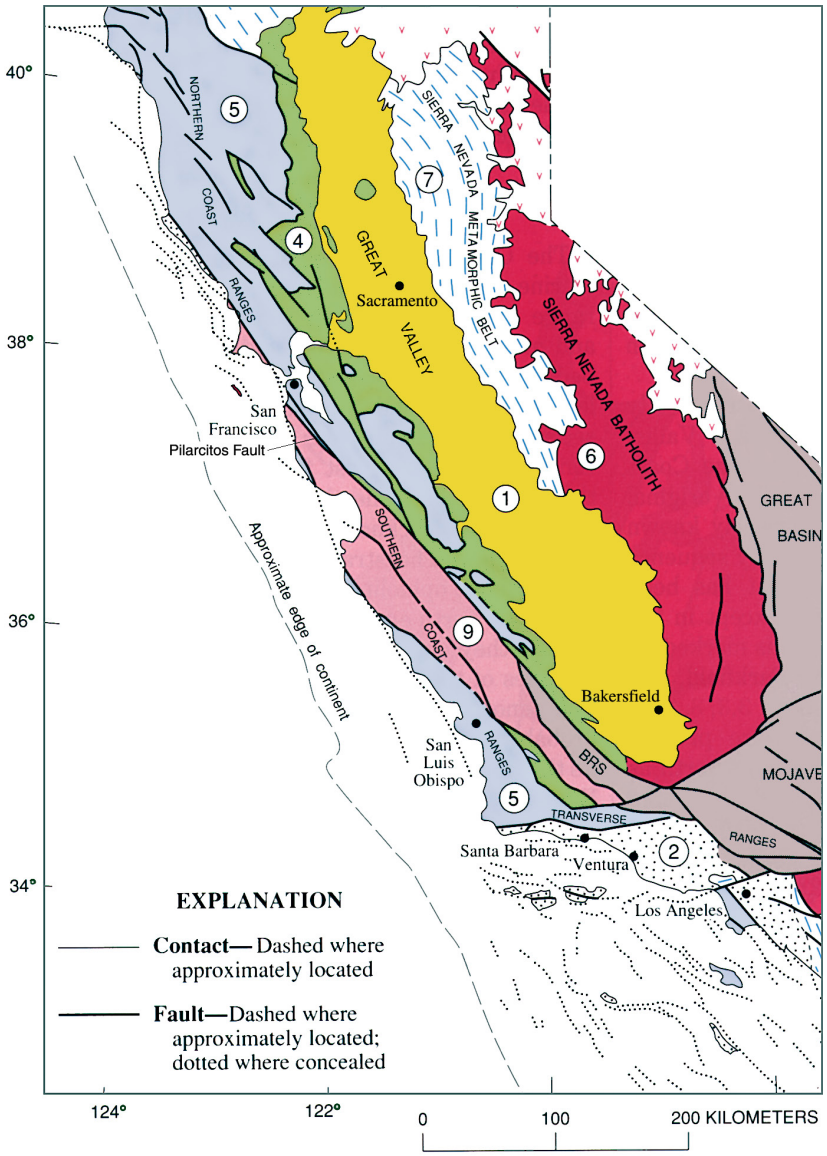

Figure 4.4. Simplified geologic map of part of California, showing distribution of principal basement rock groups (modified from Irwin, 1990). Units shown are (1) Quaternary alluvium, shown only in the Great Valley, (2) area in which older rocks are concealed by overlying Upper Cretaceous and Tertiary deposits, (4) Great Valley sequence of forearc-basin sedimentary rocks, (5) Franciscan Complex, (6) Sierra Nevada granitic batholith, (7) Sierran metamorphic belt intruded by Sierran granitic rocks, and (9) Salinian block.

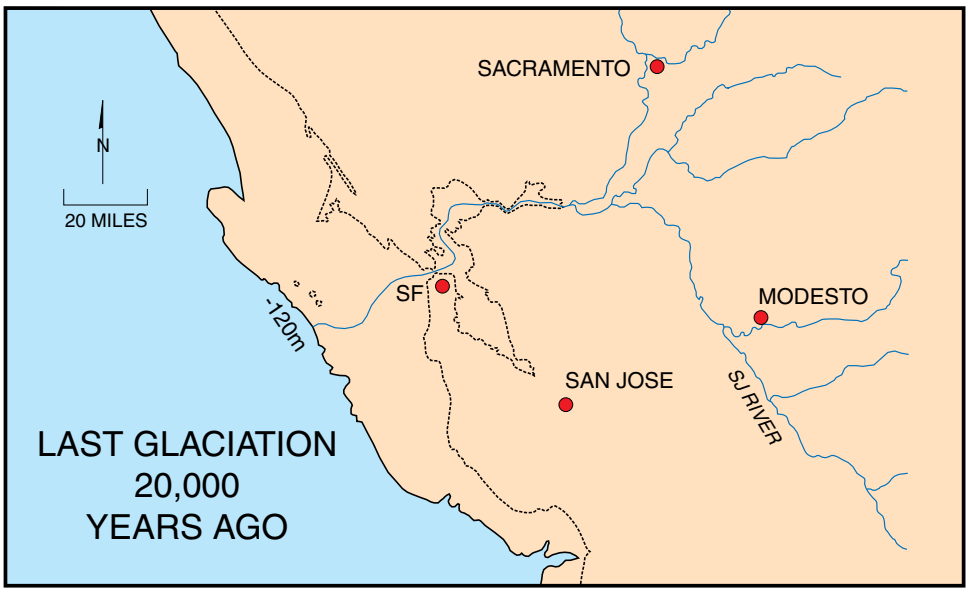

Figure 4.5. Map of the San Francisco Bay area at 20 ka, during the last major glacial period. The coastline was close to the present 120-m bathymetric contour, and areas to the east were exposed above sea level. The present coastline is dashed, including the outlines of the Farallon Islands west of San Francisco (SF). Figure by K.R. Lajoie, U.S. Geological Survey.

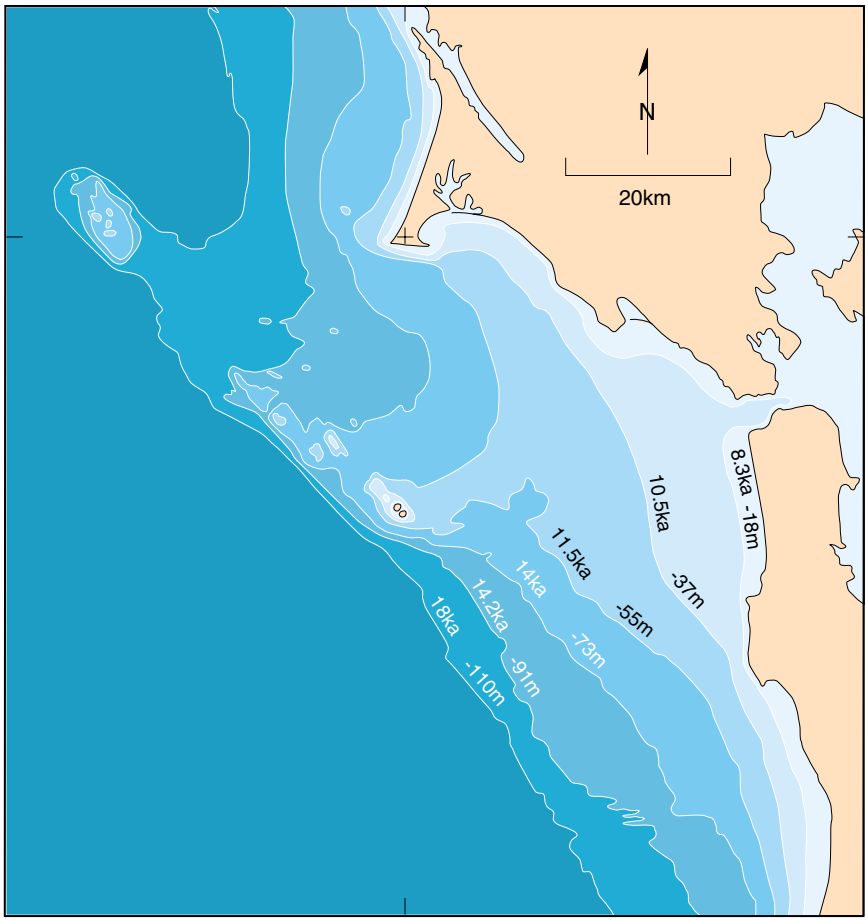

Figure 4.6. The rise of the ocean level on the continental shelf after the last major global glaciation, from ~18 ka until ~8 ka. A long stillstand of sea level occurred during this rise at about 11.5 ka, as indicated by widespread, thick, nearshore deposits of gravel and sand presently at ~55 m depth. Figure by K.R. Lajoie, U.S. Geological Survey.

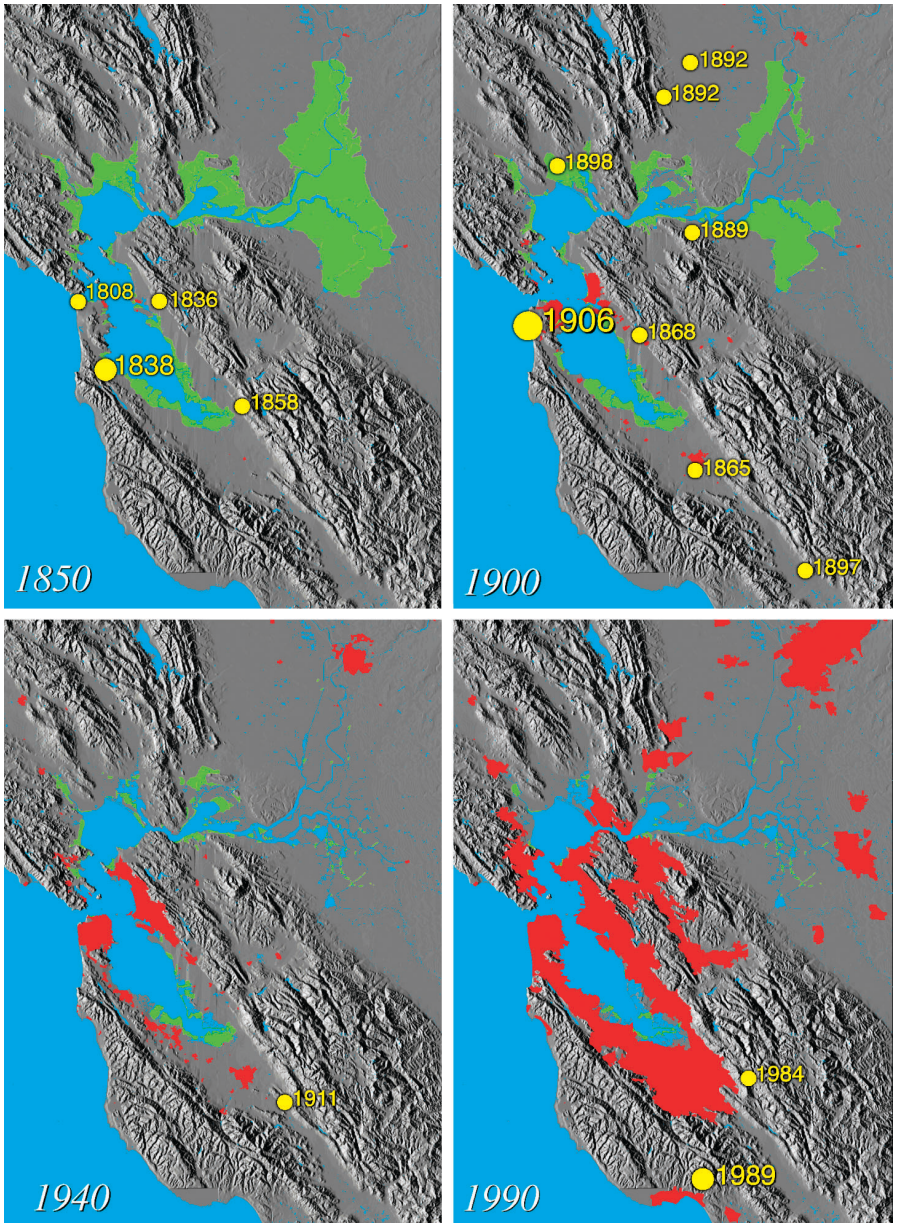

Figure 4.7. Effect of human activity and population growth in the San Francisco Bay area during the period from 1850 to 1990. The green pattern shows open wetlands, and the red pattern shows growing population centers. Also shown are some of the major earthquakes (yellow dots) that have taken place in the Bay area during historical time (from Len Gaydos, U.S. Geological Survey).

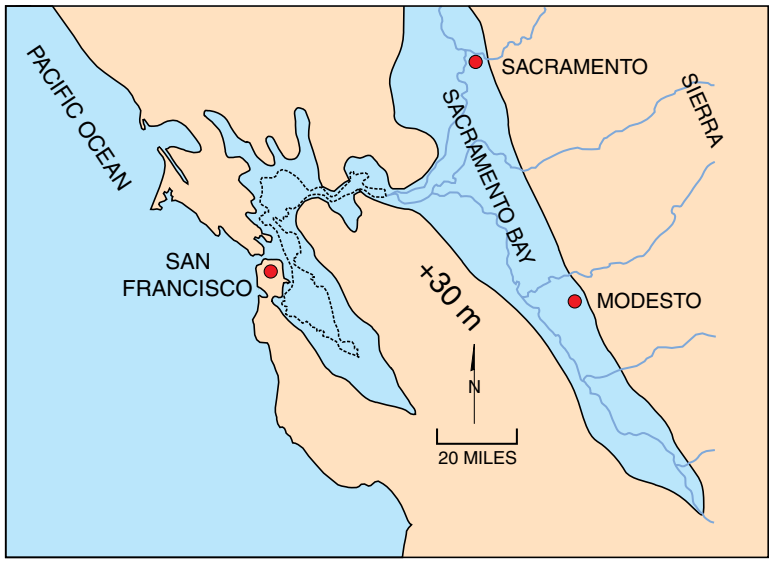

Figure 4.8. Extent of flooding by rising sea level if greenhouse warming continues unabated, and approximately one third of the world's volume of land-bound ice and snow melts (not sea ice). The resulting rise would put sea level at about 30 m above the present sea level. Dashed line shows approximate outline of the present San Francisco Bay. Figure by K.R. Lajoie, U.S. Geological Survey.

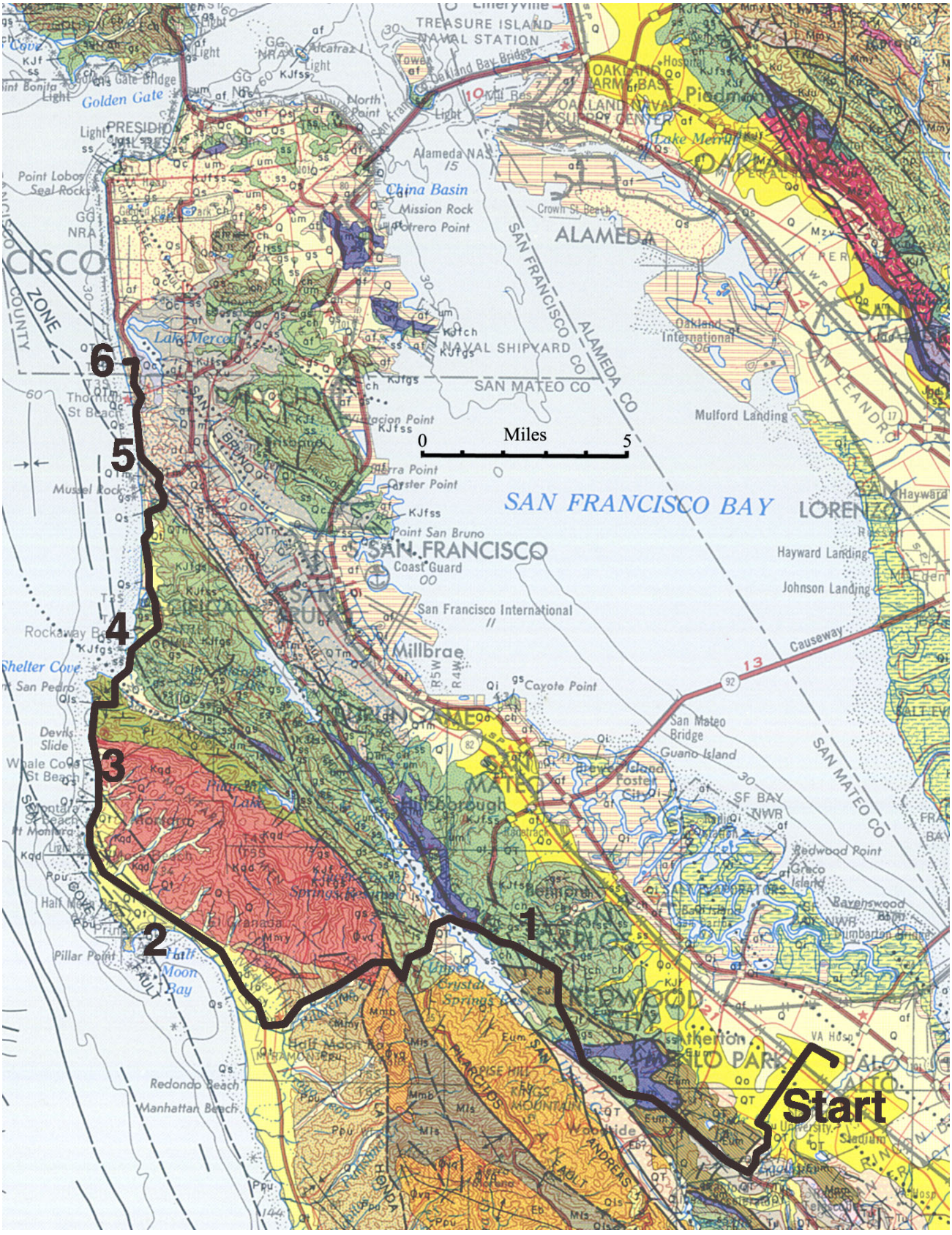

Figure 4.9. A portion of the geologic map of the San Francisco-San José quadrangle (Wagner and others, 1990), showing field-trip route and stops.

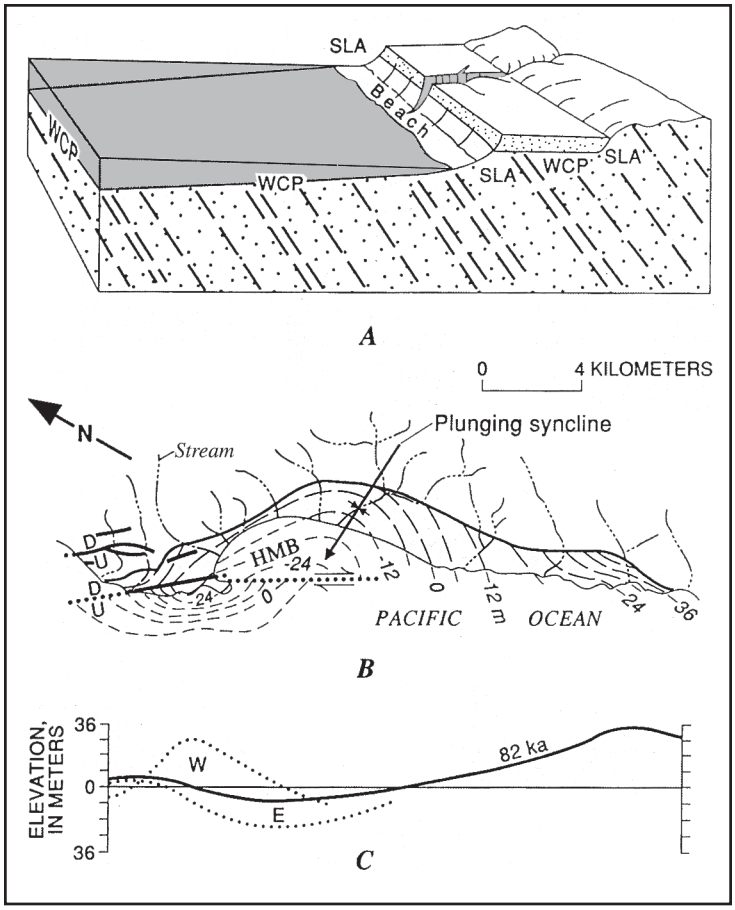

Figure 4.10. Local variability in coastal uplift shown by deformed shoreline angle and wave-cut platform. ***A,*** Coastal geomorphic features used to measure Quaternary deformation. SLA, shoreline angle; WCP, wave-cut platform; WCP' and SLA', elevated surface and shoreline angle of an older wave-cut platform mantled by sediment (stippled). ***B,*** Deformed Pleistocene wave-cut platform at Half Moon Bay (HMB) showing structure contours in meters. Arrows on fault indicate direction of relative movement. U, upthrown side; D, downthrown side. ***C,*** Platform profiles on fault plane (dotted lines: E, east; W, west), showing vertical separation across fault and deformation relative to shoreline angle (heavy line). Modified from Lajoie (1986).

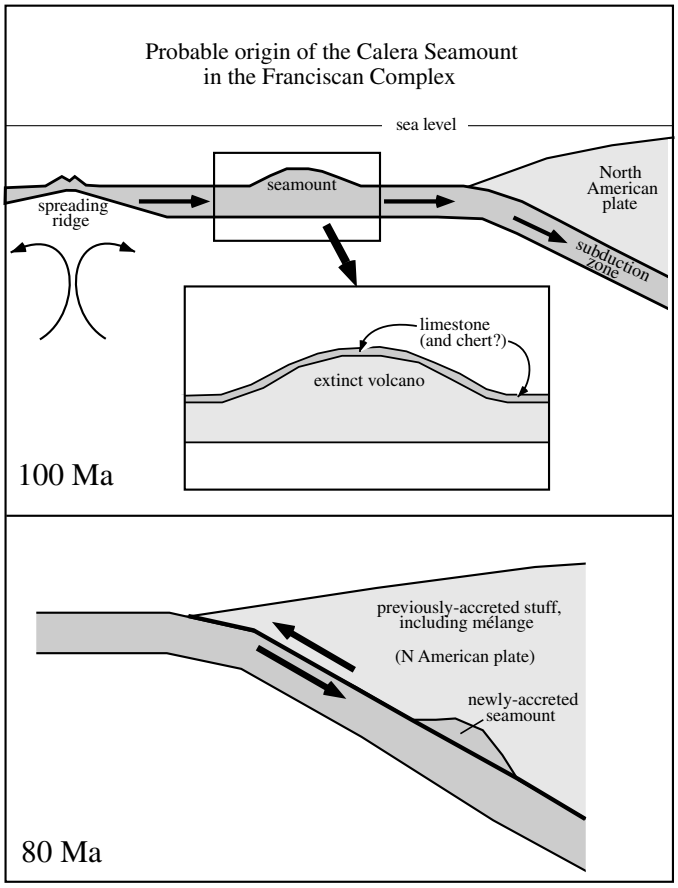

Figure 4.11. Cross-sections showing probable origin of the Calera Seamount in the Franciscan Complex

Figure 4.12. Aerial view looking south along San Francisco Peninsula showing road repairs after the March 22, 1957, earthquake. The photograph, taken in April 1957, shows equipment clearing landslide debris north of Woods Gulch. Photo courtesy of California Division of Highways, as reproduced by Sullivan (1975).

Elements of Engineering Geology on the San Francisco Peninsula—Challenges When Dynamic Geology and Society's Transportation Web Intersect

John W. Williams
Department of Geology, San José State University, Calif.

Introduction

The greater San Francisco Bay area currently provides living and working space for approximately 10 million residents, almost one-third of the population of California. These individuals build, live, and work in some of the most geologically dynamic terrain on the planet. Geologically, the San Francisco Bay area is bisected by the complex and active plate boundary between the North American and Pacific Plates prominently marked by the historically active San Andreas Fault. This fault, arguably the best known and most extensively studied fault in the world, was the locus of the famous 1906 San Francisco earthquake and the more recent 1989 Loma Prieta earthquake. There is the great potential for property damage and loss of life from recurring large-magnitude earthquakes in this densely populated urban setting, resulting from ground shaking, ground rupture, tsunamis, ground failures, and other induced seismic failures. Moreover, other natural hazards exist, including landslides, weak foundation materials (for example, bay muds), coastal erosion, flooding, and the potential loss of mineral resources because of inappropriate land-use planning. The risk to humans and their structures will inexorably increase as the expanding San Francisco Bay area urban population continues to encroach on the more geologically unstable lands of the surrounding hills and mountains.

One of the critical elements in the development of urban areas is the requirement that people and things have the ability to move or be moved from location to location. The list of "things" that have to be moved is extensive and diverse, ranging from people, food products, and building materials to water and energy resources in all forms (solid, liquid, and gas). In California, long known for its love affair with the automobile, many of these items are transported by road although railroads and pipelines play significant roles. These corridors of transport that spread like a web throughout the Bay area are essential to our present way of life. By their very nature, being long continuous features, they must cross a wide variety of terrain including some that is geologically unstable. While avoidance of a potentially threatening geological location is often the best approach, there are many areas in which this approach is not feasible. Further complicating the situation is the fact that many hazardous intersections of transportation lines and geologic hazards were established before the presence and level of geologic risk at a particular location were known or fully appreciated.

Today's brief trip will provide the opportunity to visit and discuss a number of these intersections between society's transportation web and California's dynamic geology. These intersections illustrate past and continuing problems of slope instability (Highway 92, Devil's Slide), coastal erosion (Half Moon Bay Harbor area), active faulting (San Andreas Fault), and the impact of these geological constraints on transportation lines including water supply conduits as well as railroads and roadways (fig. 5.2).

In addition to the geological complexities of these situations, one also must be aware of the complicated and often overlapping roles played by local, state, and Federal agencies and the public as they work together to regulate the planning, the construction, and the operation of these varied construction projects. One of the challenging problems often encountered is that of the situation when a project already exists and functions well, but it was designed and built using older standards that are not equal to those of today. The question that is often difficult to answer is whether it is appropriate to divert the available limited resources to upgrade these older projects away from new projects that may be desperately needed by the public.

The data contained in this field guide are the results of many years of thoughtful and careful work and writing by many geologists, engineers, and land-use planners from government and private practice. No one individual could possibly know all of the information contained in this guide or could have been personally responsible for its development. The author is grateful for the opportunity to draw generously upon the work of many others and to bring some of these data together to provide an overview of one of the many significant roles that geology plays in our society's activities. He is particularly appreciative for access to and use of the work and publications of the Association of Engineering Geologists, Caltrans, the San Francisco Public Utilities Commission, U.S. Geological Survey, California Division of Mines and Geology, Regional Water Quality Control Board, and other organizations and for the assistance of individuals too numerous to mention. It is hoped that this guide will be a starting point and a resource for others wishing to learn and teach about engineering geology.

Road Log

Mileage/Notes

0.0 Bus departure—Exit the U.S. Geological Survey, Menlo Park, by the main entrance, turning right (south) onto Middlefield Road.

0.5 Turn left onto Willow Road.

1.6 Travel northeast along Willow Road to Highway 101, exit Willow Road by north (San Francisco) exit to Highway 101.

11.8 Travel Highway 101 to Highway 92, exit Highway 101 by west (Half Moon Bay) exit.

14.5 Travel Highway 92 west to Interstate 280, (**Rolling Stop** to examine/discuss "Campus Cut" slope stability problem along Highway 92 and general plans for improving the highway from Highway 101 to Highway 1 in coastal community of Half Moon Bay—refer to attached discussion materials.

18.2 Exit Highway 92 south toward San José on Interstate 280; note the complex multi-level interchange between Highway 92 and Interstate 280 located within 1,000 feet of the San Andreas Fault.

21 Continue south on Interstate 280 to Edgewood Road exit. Take exit, turn east under Interstate 280 and use San Francisco entry ramp to reenter 280 going north.

22 Continue north on Interstate 280 to vista point overlook on east side of freeway.

22.2 **STOP 1—**Discussion of general geologic setting, San Andreas Fault, San Francisco water supply, Interstate 280, and engineering geology on the peninsula—refer to attached discussion materials.

25.5 Return to Interstate 280 northbound to Highway 92, take Half Moon Bay exit onto Highway 92.

26.8 Continue on Highway 92 to Half Moon Bay (**Rolling Stop** along Highway 92 to examine/discuss highway widening, slope instabilities and slope stabilization on western slope west of Highway 35—refer to attached discussion materials).

32.3 Ox Mountain /Corinda Los Trancos Landfill site—a landfill site originally permitted in 1976, owned and operated by Browning-Ferris Industries—refer to attached discussion materials.

34.9 Turn right, north, on Highway 1 in Half Moon Bay (at second traffic light). Travel north along the warped coastal terrace—refer to attached discussion materials.

38.1 Pillar Point Harbor—this is the area of Stop 3 to which we shall return later in the trip.

39.4 Half Moon Bay Airport—note the northwest-southeast trending, northeast-facing scarp west of the airport. This scarp, the Seal Cove Fault, is the northeastern segment of the active, right-lateral San Gregorio Fault Zone. Continued seismic activity and documentation of Holocene offset by trenching studies demonstrate its potential for future earthquakes and ground rupture.

40.5 Pass California Avenue and Fitzgerald Marine Reserve (an excellent stop for all, but particularly for geology and biology students, with fine examples of many aspects of geology including good exposures of folds at low tide) and continue to community of Montara.

45.3 Devil's Slide slope stability area—this will be the area of Stop 2 to which we will return after continuing north and turning around so that we may return to park on the west side of the highway.

47.0 Right turn at traffic light onto Linda Mar Boulevard; go east 2 blocks to "Park and Ride" area, and turn around.

Return on Linda Mar Boulevard to Highway 1; turn left at traffic light, south, and return to Devil's Slide area

48.7 **STOP 2**—Devil's Slide slope instability. Use **EXTREME CAUTION** at this site—narrow road with heavy and fast traffic—refer to attached discussion materials for Stop 2. After stop, continue south on Highway 1 toward Half Moon Bay.

56.8 **STOP 3**—Half Moon Bay Harbor, just south of Pillar Point Harbor southern breakwater (See Stop 3 discussion materials about the general geologic setting, coastal issues such as tsunami impact, coastal erosion, etc. with particular emphasis on human-induced coastal erosion—refer to attached discussion materials).

60 Continue south on Highway 1, to Highway 92 in Half Moon Bay; turn left (east) on Highway 92; continue to Highway 101; exit south toward San José onto Highway 101; continue to Willow Road; exit to west; continue to Middlefield Road; turn right; continue to entrance to U.S. Geological Survey; turn left. (This route basically retraces the route to the starting point of the trip.)

84.1 U.S. Geological Survey, Menlo Park, and conclusion of trip.

Introduction to Highway 92 Improvements

State Highway 92 is one of the major east-west traffic corridors in San Mateo County for an increasing number of commuter and commercial vehicles (truck traffic). It is the major link between San Francisco Bay and the Pacific Coast community of Half Moon Bay. Highway 92 links the San Mateo Bridge, north-south Highways 101, 84, 35 and 1, and I-280 (fig. 5.2). In the relatively short distance of 18 miles between San Francisco Bay and the Pacific Ocean, the highway climbs from sea level at the San Francisco Bay to an elevation of 880 feet at its intersection with Highway 35 near the crest of the Coast Range and returns to sea level at the Pacific Coast. Highway 92, often on grades as steep as 7 percent, crosses the complex geology of the California Coast Ranges. To construct the road, numerous road cuts were necessary. Along some of these cuts, slope instabilities have developed, which in turn have periodically resulted in serious disruptions of traffic flow, causing significant economic and emotional hardships on the motoring public.

At present, for much of its route west of Interstate 280, Highway 92 is a two-lane road. Between Interstate 280 and the San Mateo Bridge, it is a four-lane road. The increasing volume of traffic has prompted Caltrans to upgrade the highway. Four phases of improvement of Highway 92 are in progress. The section between Highway 101 and Interstate 280 is being studied to evaluate alternatives. An Environmental Impact Study (Negative Declaration) has been filed on the portion between Crystal Springs Reservoir and Highway 35 (Caltrans, 2000). The widening and slope stabilization have been completed between Highway 35 and Pilarcitos Creek, east of Half Moon Bay. The section of Highway 92 between Pilarcitos Creek and Half Moon Bay is being evaluated for improvement, including widening and adding additional safety features.

Rolling Stop—Mitigation of Highway 92, College of San Mateo, "Campus Cut" Slope Instabilities[1]

The site of interest is in a road cut on Highway 92, between Highway 101 and Interstate 280 in San Mateo County (figs. 5.2, 5.3). It is approximately 7,000 feet in length, topographically below the College of San Mateo, and known as the "Campus Cut." Before highway construction, the area was open farmland with moderately steep, rolling hills. To construct the highway, it was necessary to excavate portions of the hill creating cut slopes on each side of the highway. Construction of the four-lane highway was completed in 1963. The cut slope on the westbound lane (north side) was originally designed with a slope ratio of 1.5 to 1 as were the cut slopes on the eastbound lane (south side). Since the construction of Highway 92, numerous landslides have occurred on the cut slopes.

Brabb and Pampeyan (1972) mapped the bedrock on the site as Jurassic-Cretaceous age Franciscan Complex. Regionally, the Franciscan Complex is variable in composition, and the site is predominately greywacke, siltstone, and shale with substantial portions having been sheared. There are isolated blocks of other Franciscan rock types present.

The USDA Soil Conservation Service (1991) describes the erosion potential on the westbound side as "high to very high" and on the eastbound side as "medium to very high." Groundwater appears to be higher on the westbound side in contrast to the eastbound side, based upon analysis of aerial photographs showing patches of green grass during the dry summer months suggesting water nearer to the ground surface. Irrigation of the football field and other vegetated areas of the College of San Mateo campus probably has contributed to the elevated ground-water levels in the area.

Since construction, slopes of the Campus Cut have failed repeatedly. Slope failures have been a combination of shallow slumps and rotational slides. A hummocky topography has developed that gives the appearance of a single large failure. Depths to the failure planes are estimated to be approximately 10 to 15 feet.

A field review in 1994 was conducted to determine the reason for the concentration of slope failures near the north end of the westbound cut. An earlier study by the Federal Highway Administration concluded that groundwater was the most important factor contributing to the slope instability. The 1994 review supported this earlier conclusion and noted that the failures followed the trend of the gully that had existed on the hill slope before construction. A drainage system (involving pipeline and culvert) was installed to replace the natural drainage path during construction. A subsequent investigation of the drainage system, which was intended to "replace" the gully, showed that although the pipe was in good shape, the concrete culvert was not. Water was able to bypass the culvert and infiltrate the slope. This additional water contributed directly to the slope instabilities.

In 1994, the drainage system on the Campus Cut was repaired reducing the negative impacts of increased pore pressure on the slope stability. Nonetheless, the excessively wet winter in 1998 reactivated many of the landslides, and the Caltrans maintenance department was unable to keep pace with the frequent and severe slides. Following the winter of 1998, a field investigation revealed 14 slides in various stages of development. Three landslides, posing the greatest threat to the highway, were repaired.

Because of the extreme instability of the slope, the lack of funds, and the potential threat to the highway, emergency repairs were completed without the benefit of soil analysis. Caltrans selected-rock slope protection (the placement of large rocks on a partially excavated slope) as the most appropriate mitigation measure. The cost of this repair in 1999 was $120,000.

Stop 1—Vista Point, Interstate 280

From this Vista Point, north of Edgewood Road on the east side of Interstate 280, many important features can be seen, including:

- a portion of the topographically well expressed San Andreas Fault Zone (figs. 5.2, 5.3),
- the reservoirs that have been developed in the fault zone to serve as the terminus for water brought from the Hetch Hetchy Reservoir in the Sierra Nevada, north of Yosemite National Park, to supply San Francisco and many mid-peninsula cities,
- Interstate 280 that parallels the San Andreas Fault as both traverse San Mateo County, and
- the Filoli Estate—famous for its beauty and use in a popular television series—is the location of a number of fault-trenching studies to document the rate of slip along this portion of the San Andreas Fault.

General Geologic and Physiographic Setting of the San Andreas Fault Zone[2]

From the vantage point of the Vista Point north of Edgewood Road along Interstate 280, one can view topography that has been sculpted by dynamic geologic processes. This terrain is dominated by one of the world's most spectacular tectonic features—the San Andreas Fault. For hundreds of miles, the San Andreas Fault is the boundary between basement rocks of the Franciscan Complex and the Salinian Block (figs. 5.4, 5.5). The Franciscan Complex of Jurassic and Cretaceous age is northeast of the fault and consists of mafic and ultramafic basement rocks and sedimentary rocks that were deposited in a deep ocean environment and subsequently accreted to the western margin of the North American plate. Most Franciscan Complex rocks in this area are part of the central tectonic belt (Irwin, 1960; McLaughlin and others, 1988), which is a tectonic mélange of Late Jurassic to Early Cretaceous age. Many of the larger blocks within the central belt mélange are given separate terrane names. The terranes are primarily gently dipping thrust sheets that trend northwesterly and dip northeasterly (Sullivan and Galehouse, 1991).

On the southwest side of the fault zone, Cretaceous and Tertiary sedimentary and volcanic rocks were deposited on a continental block of the Late Cretaceous granitic basement rocks, referred to as the Salinian Block (Clark and Brabb, 1978). The Tertiary section consists predominantly of marine classic sedimentary rocks ranging in age from Paleocene to Pliocene (Clark and Brabb, 1978). These deposits include a thick, early Tertiary sequence that accumulated in deep marine basins and a thick, late Tertiary sequence of predominantly diatomaceous beds that accumulated in sediment-starved basins (Sullivan and Galehouse, 1991). The rocks of the Salinian Block originated south of their present location; however, there has been debate about the distance traveled by the Salinian Block along the transform (strike-slip) system (Page, 1989). Hill and Dibblee (1953) suggested that the Salinian Block was displaced several hundred miles from the southern part of the Sierra Nevada. Evidence for this model includes similarity of the Salinian rocks to granites along the crest of the Sierra Nevada in terms of age, mineralogy, and chemistry.

Approximately 28 million years ago, the Pacific Plate first came into direct contact with the North American Plate, creating a transform boundary. Since that time, there have been slight shifts in both the direction and the rate of movement of the Pacific Plate with respect to the North American plate. Geologists agree that one of the more notable of these changes, a shift to slightly oblique movement, caused convergence between the Pacific and the North American Plates, producing the northwest-oriented mountains of the Coast Ranges beginning approximately 3 to 4 million years ago. The Peninsula segment of the San Andreas Fault is estimated to have been initiated between 1 to 2 million years ago. Several paleoseismic studies of the Peninsula segment have been completed (fig. 5.6). The slip rate estimate determined from the studies at the Filoli Estate near Woodside is 17±3 mm/year (Clahan and others, 1995).

The San Andreas Fault is well defined by seismic activity and conspicuous geomorphic expression. However, contrary to the above discussion, the San Andreas Fault is not the fundamental boundary between the Franciscan Complex rocks and the Salinian Block in the San Mateo County region. The juxtaposition of basement rocks in this region is marked by the Pilarcitos Fault, a fault that extends from Black Mountain to the offshore environment at Rockaway Beach in Pacifica (fig. 5.5). Many geologists have assumed that the Pilarcitos Fault was the principal strike-slip boundary of the San Andreas Fault Zone on the San Francisco Peninsula, and that the San Andreas Fault is the product of a geologically recent (1 to 2 million years ago) eastward shift of tectonism. However, this model has been challenged recently by Wakabayashi (1999), who argues against significant Cenozoic slip on the Pilarcitos Fault, and suggests that the Peninsula Segment of the San Andreas Fault represents a shift from faults located east of the San Francisco Peninsula.

The San Gregorio Fault (mostly offshore) is a major, right-lateral strike slip fault that forms the principal active tectonic structure west of the San Andreas Fault in central coastal California (fig. 5.5). Recent investigation in the Moss Beach/Seal Cove area by Simpson and Lettis (1999) led to recognition of offset alluvial deposits associated with a paleovalley in the uplifted fault block. Simpson and Lettis (1999) estimate a late Pleistocene slip rate of between 3.5 to 4.5 mm/year for the eastern, on-land trace of the San Gregorio Fault, and suggest that an offshore (western) San Gregorio Fault trace may contribute a similar amount of slip. Thus, the total slip across the entire zone may be 6mm/year or greater.

Onshore, along the San Mateo coastline west of the Half Moon Bay Airport, the San Gregorio Fault extends for approximately 1.5 miles, from Pillar Point to Moss Beach. Along this segment, which is sometimes referred to as the Seal Cove Fault, the on-land portion of the fault zone forms the eastern margin of an uplifted fault block. The western margin of this block appears to be bounded by a second trace that has been seismically imaged offshore.

The Coast Range is being uplifted in the modern tectonic regime. The Peninsula portion of the San Andreas Fault was a segment of the fault that ruptured during the 1906 earthquake. This event, the first major seismic event to be so thoroughly studied, was brilliantly reported upon by Andrew Lawson and his colleagues (figs. 5.7, 5.8). Much of our basic understanding of seismic mechanisms was initiated by that study (Lawson and others, 1908). The Santa Cruz Mountains west of the San Andreas Fault were uplifted as much as 4 feet during the Bay area's most recent major earthquake, 1989 Loma Prieta event. The San Francisco Bay region has been and continues to be a dynamic portion of California. This is attested to in part by the data contained on regional maps prepared by the Association of Bay Area Governments showing the intensity of ground shaking during the 1906 and 1989 earthquakes on the San Andreas Fault (figs. 5.9, 5.10).

Filoli Estate[3]

The Filoli Estate, located 30 miles south of San Francisco, is a 654-acre property containing a historic house and 16 acres of formal garden (fig. 5.3). From 1917 until 1937, the house was occupied as the private residence of its original owners, William Bowers Bourn II and his wife. The property was sold in 1937 to the Roth family, owners of the Matson Navigation Company, who donated the house and 125 acres to the National Trust for Historic Preservation in 1975. Within the last decade, the estate has been the location of several important geologic studies involving trenching of the 1906 trace of the San Andreas Fault to determine earthquake recurrence intervals and rates of fault slip (fig. 5.6).

The Filoli house was built for the Bourn family, whose chief source of wealth was the Empire Mine, a hard-rock gold mine in Grass Valley, California. Bourn was the owner and president of the Spring Valley Water Company comprising Crystal Springs Lake and the surrounding watershed areas that are now part of the San Francisco Water Department (fig. 5.3). He selected the southern end of Crystal Springs Reservoir (then known as Crystal Springs Lake) as the site for his estate, in part, to escape the dangers experienced during the 1906 earthquake by the population of the City of San Francisco. (It is interesting to note that the site selected for the house is within a few hundred feet of the 1906 San Andreas Fault rupture trace.) He created the name "Filoli" by combining the first two letters of the words of his credo: Fight for a just cause; Love your fellow man; and Live a good life.

Bourn chose his longtime friend, the San Francisco architect Willis Polk, to design the house. In addition to the Filoli Mansion, Polk designed the Pulgas Water Temple, which is the western terminus of the Hetch Hetchy Water System for

water flowing into Crystal Springs Reservoir, and a number of important structures in San Francisco, including Kezar Stadium. Polk had played a major role as the city architect in the rebuilding of San Francisco following the 1906 earthquake. Construction of the Filoli mansion began in 1915, and the Bourn family moved into the house in 1917.

History and Construction of the Hetch Hetchy Water Distribution Project[4]

In 1900, San Francisco Major James Phelan directed the City Engineer Carl Grunsky to study 14 possible water sources for San Francisco. Of these possible sites, Grunsky selected the Tuolumne River system for its high quality and large supply of water, good reservoir sites, and hydroelectric production potential.

Later renamed Hetch Hetchy, the Tuolumne System was believed to be the best answer to San Francisco's problem of providing safe, reliable drinking water to a growing number of residents. However, political conflicts within the San Francisco city government and with the managements of the Modesto and Turlock Irrigation Districts developed. The management of these districts feared that San Francisco would threaten their established rights to use Tuolumne River water. As a result of these conflicts, in early 1906, the city dropped the Tuolumne System proposal.

In the early morning of April 16, 1906, a devastating earthquake struck San Francisco. The earthquake was followed by fires that destroyed much of the downtown area. The city lacked an adequate quantity of water to fight the fires primarily because of earthquake damage to the water distribution system. The earthquake and resultant fires reinforced the city's need to construct a more reliable water system with a higher capacity. After several years of political bickering at local, state, and national levels, on September 3, 1913, the Raker Act was adopted by the U.S. House of Representatives.

As the Raker Act moved to the floor of the Senate, controversy ensued between environmentalists and the City of San Francisco. Many people, including the noted environmentalist John Muir, feared that the Hetch Hetchy system would destroy Yosemite Valley and other natural resources of the area. Eventually, after much debate, the Senate passed the bill on December 2, 1913.

Also known as the Hetch Hetchy Act, the Raker Act included provisions that met the objections of the Turlock and Modesto Irrigation Districts by allowing them to retain their already existing water rights. The act also granted San Francisco the use of public land to construct, operate, and maintain dams, tunnels, and other structures necessary to develop a water and power system. One important element of the act was the provision that no water or power generated by the system could be sold to private companies for resale.

Work on the Hetch Hetchy system began in 1914. The system was to bring water from 650 square miles of watershed in Yosemite National Park and the Stanislaus National Forest to San Francisco. Water moves from the source area to the terminal reservoirs exclusively by gravity flow. Ultimately the elements of the system included the following:

- major reservoirs: O'Shaughnessy (360 thousand acre feet), Eleanor (27 thousand acre feet), Cherry (270 thousand acre feet),
- five dams,
- four hydroelectric plants with a total capacity of 380,000 kw,
- a total storage capacity of 659,600 acre feet (The San Francisco Public Utilities Commission maintains an additional 238,700 acre feet of storage in the Bay area.)

The Hetch Hetchy System has the ability to meet a peak demand for water of 400 million gallons a day. Construction took place in separate, simultaneous, construction projects across a distance of 150 miles (fig. 5.11). The main dam (O'Shaughnessy) was completed in 1923 and was in full operation by 1934. Today the system provides San Franciscans with about 85 percent of their water. The remaining 15 percent of their supply comes from a watershed on the San Francisco Peninsula, which is mostly west of the Crystal Springs Reservoir and San Andreas Lake, and a watershed in portions of Alameda County surrounding, in part, the Calaveras Reservoir.

Interstate 280—"The World's Most Beautiful Highway"

Interstate 280 was approved for California's Interstate system on September 15, 1955, and was opened to traffic in the mid-1970's (figs. 5.2, 5.3). This Interstate, named the Junipero Serra Freeway, honors Father Junipero Serra, the Spanish missionary who established nine of the missions along the El Camino Real during the colonization of California by the Spanish in the 1700's and 1800's. Many individuals who travel this highway consider it one of the more beautiful roadways in the world, and the portion of the Interstate in San Mateo County has received a number of national awards for its design. Each direction is on a separate grade to minimize grading and excavation, and some bridges were designed to blend with the surrounding terrain.

The engineers and designers working on the highway faced many challenges including:
- the environmentally sensitive road alignment,
- the potential for generating a significant and unwanted visual impact,
- the proximity to the active San Andreas Fault with its history and potential for great earthquakes accompanied by intense ground shaking and the generation of secondary ground failures,
- the varied and often unstable bedrock materials of the Franciscan Complex underlying the highway's alignment, and
- hydrologic factors including concern for the potentially contaminated runoff from the paved surfaces.

Rolling Stop—Modification of Highway 92 Between Crystal Springs Reservoir and Highway 35

Caltrans has proposed to improve Route 92 between the Crystal Springs Reservoir and Highway 35 (fig. 5.2). These 2.1 miles of highway have been the location of an increasing number of accidents and significant traffic delays as the result of increasing vehicular traffic, including a significant increase in heavy trucks traveling between the Peninsula and Half Moon Bay. The annual average daily traffic flow was 24,400 vehicles in 1998, and is projected to increase to 39,300 vehicles daily by 2020. Truck traffic increased by 4.5 percent between 1995 and 1997 (Caltrans, 2000).

In 1993, an Initial Study/Environmental Assessment was approved for a proposed westbound, up-hill, slow-vehicle lane and safety improvement. Since the initial assessment, there have been a number of suggested changes, and a new and more comprehensive environmental document has been prepared (Caltrans, 2000). Currently, the project includes:
- an interchange at Highway 92 and Highway 35,
- a median barrier,
- realignment and curve correction,
- a bridge across a small canyon to allow wildlife to cross under the highway, and
- an undercrossing to allow San Francisco Water District personnel access to their corporation yard.

One of the more important environmental issues associated with the project is the potential for increased storm-water runoff because of the increase in paved surface area and the increased number of disturbed cut slopes. There is the need to restrict the flow of turbid water (particularly storm runoff) into the Crystal Springs Reservoir, the City of San Francisco's water supply. Currently, there is no turbid-water collection system, and any runoff from the highway moves into natural drainage ways and eventually into the reservoir.

The proposed turbid-water collection system consists of a series of interconnected ditches and pipes capable of handling a 50-year design flow (Caltrans, 2000). Beginning at the ridge crest, near Highway 35, the system will collect approximately two-thirds of the runoff from the paved road surface and the disturbed slopes. This flow will be transferred downhill where it will enter the proposed Highway 92 detention basin and pump-plant storage box. After appropriate dentition time, this flow will be released back to the turbid water collection system, where it will combine with the remaining one-third of road and slope runoff. This combined flow will be piped across the existing causeway to a pump plant, where it will be collected and pumped up to Basin no. 3 which is part of the Interstate 280 turbid water collection system. The Interstate 280 turbid water pipeline connects a series of seven basins that ultimately drain into San Mateo Creek and then into San Francisco Bay.

A separate, clean-water collection system is also proposed to collect and pass natural runoff from the undisturbed areas to the natural drainages that lead to the Crystal Springs Reservoir (Caltrans, 2000). Any abandoned segments of Highway 92 generated by realignment will be removed and the slopes restored to as near a natural state as possible.

Five major active faults are located within 50 miles of this section of Highway 92 between Crystal Springs Reservoir and its intersection with Highway 35. The closest is the San Andreas Fault at the eastern margin of the project (fig. 5.5). Caltrans has estimated that this fault has the potential for a maximum credible earthquake magnitude of 8.0 and a maximum peak bedrock acceleration of 0.73 g (Caltrans, 2000). During the 1906 earthquake, approximately 8 feet of right-lateral offset occurred in the causeway crossing Crystal Springs Reservoir (fig. 5.1). The causeway currently carries Highway 92 across the reservoirs.

Rolling Stop—Improvement of Highway 92 Between Highway 35 and Pilarcitos Creek (East of Half Moon Bay)

Key Elements and Background of the Project[5]

Highway 92 is the primary east-west route between the San Francisco Peninsula and Half Moon Bay serving an increasing volume of commuter and truck traffic (fig. 5.2). The two-lane road between Highway 35 and Pilarcitos Creek

on the western-facing slope of one of the ridges of the Coast Ranges long has been a bottleneck to efficient traffic flow. Steep grades of as much as 7 percent and sharp curves contribute to significant traffic delays. The project provides for a continuous uphill lane for slow vehicles. Other safety improvements include standard lane and shoulder widths and a concrete median barrier. Construction began in March 1997, and was completed in October of 2000 at a cost of $21.5 million (Caltrans, 2000b). Of the total cost, approximately $4.5 million was for repairing storm-induced landslide damage (15 slides) during the El Niño events.

Topographically, the project area rises from the alluvium-filled valley of Pilarcitos Creek at 210 feet elevation to 880 feet at the intersection between Highway 92 and Highway 35, near the crest of the ridge. Structurally and lithologically, the project area is complex, in large part because of its location within the San Andreas Fault system (fig. 5.5). The main trace of the San Andreas Fault is approximately 1.5 miles east of the project area. The Pilarcitos Fault, a subsidiary branch of the San Andreas Fault, passes through the project area just west of the ridge crest along which Highway 35 runs.

This section of Highway 92 crosses five distinctly different bedrock formations—Jurassic-Cretaceous Franciscan Complex, Cretaceous Montara Granite (quartz diorite), and an Oligocene through lower Miocene sequence of rocks including the Vaqueros Sandstone, Mindego Basalt and Lambert Shale. Generally, these formations are overlain by surficial deposits consisting of varying thickness of alluvium, colluvium, and (or) residual soil derived from the underlying bedrock (Caltrans, 1996). Geological investigations for the project included:

- literature review,
- field investigations to include geologic mapping,
- 16 seismic refraction survey lines,
- vertical and horizontal borings, and
- laboratory tests on collected samples for shear strength and corrosion properties.

The subsurface exploration for the proposed retaining walls required for the widening of this section of Highway 92, consisted of seventeen 2-inch diameter vertical and twelve 2.5 to 3-inch subhorizontal, diamond rock core borings. Depths of the subhorizontal borings ranged from 17.5 to 66.5 feet. Depths of the vertical borings ranged from 40 to 45 feet (Caltrans, 1996).

A shallow seismic refraction investigation was conducted using a 12-channel exploration seismic unit. Because of the widely differing geologic conditions and rock materials, seismic velocities varied greatly. Overlying the weathered bedrock are several feet of unconsolidated rock and (or) soils characterized by seismic velocities ranging from 624 to 1,639 feet per second. In the underlying weathered bedrock, the velocities varied between 1,549 and 5,805 feet per second and, for less weathered bedrock, varied between 5,141 and 15,108 feet per second.

The original plans specify cut slopes to accomplish the needed road widening. Based in part upon results of subsurface exploration, the construction of soil-nailed retaining walls was recommended to minimize the right-of-way expansion, environmental impacts, and material disposal costs (Con-Tech Systems, Ltd. [CTS], 2001). (See “Elements of Soil Nailing,” below.) ”The major structures associated with the retaining wall component of this Highway 92 improvement project include nine land-sculpted soil-nailed retaining walls and 14 soldier-pile retaining walls (figs. 5.12, 5.13).

Elements of Soil Nailing

Soil nailing as a slope stabilizing technique has become increasingly popular in the past two decades. Until recently, it was more frequently used in Europe compared to its use in the United States. It is a technique by which untensioned rods are placed in a closely spaced grid pattern into material that needs to be reinforced to remain stable. The rods may be placed in predrilled holes or emplaced by direct push; commonly, the rods are grouted in place. Generally, the daylighting ends of the rods are embedded in a facing to help minimize interrod slope erosion. Figure 5.14 illustrates some of the fundamentals of the technique (CEN Technical Committee 288, 2000).

Ox Mountain (Corinda Los Trancos) Municipal Refuse Disposal Site[6]

Browning-Ferris Industries of California owns and operates a Class III municipal refuse disposal site in Corinda Los Trancos Canyon, San Mateo County, approximately 2 miles northeast of Half Moon Bay, immediately north of Highway 92 (fig. 5.2). The Ox Mountain landfill originated as a small, 33 acre, Class-III landfill in the upper portion of Corinda Los Trancos Canyon. The initial landfill received approximately 7.5 million cubic yards of waste from 1976 to 1993. In 1992, the discharger was issued waste discharge permits for a 140-acre landfill expansion that has led to the present landfill configuration. The 1992 permit design extended the landfill approximately 2,700 feet down canyon and required

a composite liner with an underdrain, a leachate collection system, and 2 feet of soil with permeabilities less than $1x10^{-7}$ cm/sec. Construction began in 1992. Recently, the landfill operator received approval to expand the permitted area by approximately 9 acres. The landfill receives non-hazardous municipal solid waste including:

- household wastes,
- construction debris,
- sewage sludge,
- autoclaved medical waste,
- demolition wastes,
- green waste,
- treated auto shredder waste,
- clean-fill materials, and
- petroleum contaminated soils with concentrations below or at specified levels.

The landfill's current permitted capacity is 37.9 million cubic yards. With the recent expansion, the capacity will increase to 48.2 million cubic yards. The discharger estimates that the useful life of the landfill is 28 years starting January 1, 1999.

The surface and subsurface geology at the site was evaluated by geologic consultants based on field mapping, literature reviews, a seismic-refraction survey, and review of the geologic logs of over 80 borings totaling more than 4,000 linear feet of drilling. The disposal area is underlain by granitic rocks, alluvial and colluvial units, and landslide and debris-flow deposits. A number of shear zones were mapped in cut slopes and through borings, but as recent displacements were not noted, these zones are not considered active faults. Some of the alluvial deposits underlying the facility were considered susceptible to liquefaction and were stabilized through a ground improvement program in 1992. None of the observed landslides was considered active, but they could be reactivated as the result of heavy rains and (or) seismic activity.

Groundwater movement in the area occurs in two hydraulically connected hydrostratigraphic units. The upper unit includes the alluvial and colluvial deposits, the deeply weathered granite, and the moderately weathered granite. This unit can be considered an aquifer with hydraulic conductivities of $3.8x10^{-4}$ to $13.8x10^{-6}$ cm/sec based on pumping tests. The second unit is the slightly-weathered to fresh granite. The hydraulic conductivity of this unit is so low ($8.0x10^{-7}$ to $1.0x10^{-4}$, averaging ~10^{-6} cm/sec based on packer tests) that it is not considered an aquifer although it might serve as a recharge source area and contribute groundwater to regional aquifers.

Along Corinda Los Trancos Canyon, depth to groundwater during the wet season rises to within a few feet of the ground surface. Along the ridge tops, depth to groundwater is about 85 feet with as much as 20 feet of seasonal variation.

A Brief History and the Geologic Setting of the Half Moon Bay Area

Half Moon Bay, originally known as Spanishtown, is the oldest settlement in San Mateo County, dating back to the 1840's (fig. 5.2). The level, relatively narrow coastal terrace on which Half Moon Bay is built has had a colorful history. This history includes the exciting but failed attempt to build and operate a coast side railroad, the Ocean Shore Railroad, between San Francisco and Santa Cruz. Geologic problems played a large role in the failure of the railroad. Excitement generated by rum runners enlivened the prohibition era of the 1920's and 1930's. As a legacy of that period, one of the local restaurants is reported to have at least one ghost in residence.

Half Moon Bay, with a current population of 11,000, is the only incorporated city along this portion of the coast; being incorporated in 1959. All of the other coastal communities, such as El Granada, Miramar, Pescadero, and La Honda, are unincorporated areas governed by the San Mateo County Board of Supervisors. The region is a sought-after housing location for those working in San Francisco and in the Peninsula communities. Currently, the median-priced home in Half Moon Bay is in the $700,000 range, with those on golf courses costing between $900,000 and $1,500,000 (Half Moon Bay, 2001).

The largest industry in the area is agriculture, primarily floriculture (flowers), followed by tourism and commercial fishing. The beauty and climate of this scenic coastal area have stimulated tourism and the building of a number of hotels, motels, and restaurants.

Because of the recent rapid growth of the community, commuting and visitor traffic have become important economic and political issues. As an example of the impact of visitors, the Pumpkin Festival during the fall of each year has become a Bay area landmark event, attracting thousands of individuals (along with their cars) to this coastal community. At present, north-south Highway 1 along the coast and east-west Highway 92 provide the only significant routes for vehicular traffic into and out of the community. The competition for space on the these roadways has created hotly contested debates adding to the complexity of trying to resolve the Devil's Slide issue. Geologically, the area has a

number of interesting features (figs. 5.15, 5.16) including:

- warped marine terrace,
- landslides on the western slopes of the Coast Ranges,
- landslides along the coastal bluffs and cliffs,
- topographic expressions of active faulting,
- well-exposed geologic structures, in particular, folded and faulted units,
- evidence of accelerated rates of coastal erosion, and
- varied geologic bedrock units.

Given what is known about the types and severity of geologic hazards along some portions of the coast, it is interesting that it was to this area that a number of residents of the City of San Francisco moved to seek a safer living environment following the 1906 earthquake and fire.

Stop 2—Devil's Slide—A Slope Instability in a Stranglehold Location[7]

Highway 1—The Present Road

After a major landslide in January 1995 closed Highway 1, Caltrans began a $1.5 million construction project to repair and stabilize the road (figs. 5.2, 5.17). Grouted and post-tensioned rock bolts were installed under the highway. A steel net was bolted to the slope above the road to catch detached rocks. Although the road was reopened after approximately 150 days and has remained intact through subsequent winters, Caltrans personnel maintain that the repairs are only temporary measures. Following extensive litigation and public debate, the construction of a tunnel east of Devil's Slide was determined to be the most feasible permanent solution to the problem of providing reliable north-south access along Highway 1 to the Half Moon Bay area.

Devil's Slide Tunnel Project—The Bypass

Projected Coast: $165 million

Environmental Report: Approval by the Federal Highway Administration of the environmental report is expected in 2001.

Schedule: If the environmental impact report is finalized in 2001 and no significant delays are caused by the lack of funding, Caltrans and its consultant can complete the design of the tunnel project by spring of 2003. Construction will start in the summer of 2003 and is expected to take 3 years.

Design: The tunnel plan specifies two 30-foot wide bores with one directional lane and standard 8-foot shoulders per bore. Each bore will be about 4,000 feet long. A bridge approximately 1,000 to 1,500 feet long will be constructed at the north portal. The primary purpose of the bridge will be to protect the red-legged frog habitat and other environmentally sensitive areas.

Bicycle Path: Upon completion of the tunnel, Caltrans expects to deed the original section of Highway 1 at Devils Slide to the County of San Mateo for bicyclists, hikers, and other nonmotorized traffic.

Alignment: Highway 1 will diverge from its present alignment near Gray Whale Cove north of Montara, pass through a tunnel, and exit at Shamrock Ranch in Pacifica.

Funding: This project will be primarily funded by Federal emergency funds. Less than 5 percent of the funds will come from the State Transportation Improvement Program.

Measure T: Measure T is the San Mateo County initiative that was approved by 76 percent of the voters in November 1996. It changed the local coastal plan to designate the tunnel as the chosen alternative to bypassing Devil's Slide. Before this initiative, an overland bypass to the east of Devil's Slide had been the preferred alternative.

Historical Perspective on the Devil's Slide[8]

Devil's Slide is a large bedrock landslide complex, extending from the ridge crest, at approximately 900 feet elevation down to at least sea level on the San Mateo County coastline located just south of Pacifica. The complex has a width of approximately 4,000 feet (fig. 5.17). Highway 1 crosses the landslide between elevations 450 and 300 feet. Local

geologic conditions are complex, involving steeply dipping Paleocene and Cretaceous sedimentary rocks and underlying Jurassic-Cretaceous granitic rocks. The relationship between the two rock types is complex because of past faulting, folding, and landslide movement. The most active landslide failure surface is approximately 150 feet below the ground surface. A number of discrete failure zones have been identified within the landslide complex by the monitoring of slope change using inclinometers. It appears that the granitic rocks are not involved in the landsliding (figs. 5.18, 5.19). The exact details of this complex slide, particularly the exact depths of the critical failure surfaces, are still a matter of debate.

The landslide complex is readily recognized in an 1866 topographic map of the area. Since 1897, the landslide area has frustrated road builders, repair crews, and the traveling public, disrupting in turn a county road, a railroad, and a State highway. The first county road crossed Devil's Slide at approximately elevation 400 feet. Because of numerous failures, this road was abandoned in 1914, and replaced with a bypass road to the east over San Pedro Mountain (fig. 5.22).

The Ocean Shore Railroad Company was incorporated in the early 1900's with the intent of constructing a double-track, electric railroad from San Francisco to Santa Cruz. The railroad alignment began near 12th and Mission streets in San Francisco, and reached the Pacific coast near Thornton Beach in Daly City. Farther south near Devil's Slide, the railroad alignment penetrated San Pedro Point with a 400-foot-long tunnel at approximately an elevation of 50 feet, and then began a long 2 percent grade. From that point southward, the railroad grade climbed to its highest point at the "saddle cut" of present Highway 1. Severely damaged in the 1906 earthquake and by subsequent chronic landsliding, the railroad was abandoned in the 1920's. Remnants of the railroad grade are still visible near Devil's Slide.

In 1933, 1,600 miles of county roads were incorporated in the State highway system. The State Division of Highways acquired the Ocean Shore Railroad right-of-way by condemnation and constructed Highway 1 (then known as Route 56) in its present location. Construction and maintenance of the highway were difficult because of the continuing slope instabilities.

Since the opening of the roadway in 1936, landsliding and road closures have plagued the route. Major road closures occurred in every subsequent decade. In the late 1950's, the State Highway Department determined that the alignment across Devil's Slide should be abandoned, and that a new bypass should be constructed around the inland margin of landsliding. By 1970, a 6.8-mile bypass was ready for construction. The construction contract was halted by a lawsuit filed by the Sierra Club and others, invoking provisions of the recently passed legislation: California Environmental Quality Act and National Environmental Policy Act. The litigation was successful, and the State Highway Department was directed to conduct environmental studies for the bypass.

In the early 1980's, landsliding and $50 million in Federal funding prompted renewed design studies of the highway realignment. In 1986, the Martini Creek Alignment (a proposed road alignment east of the Devil's Slide area) was selected as the preferred alignment by the Federal Highway Department as a solution to road failures at Devil's Slide. The bypass was designed to be a 4.5-mile-long, two-lane roadway with slow up-hill lanes. This alignment would require extensive grading in environmentally sensitive areas. For the next decade, the question of whether the Martini Creek alignment would be built or not was the subject of legal argument and was not resolved until 1996.

The Marine Disposal Alternative was studied as an alternative to the inland bypass. This proposal consisted of unloading the driving force at the top of the landslide and buttressing at the bottom of the slide (fig. 5.20). The project would require the removal of an estimated 1 million cubic yards of material from the head of the landslide and placing the material offshore into a nonerodible buttress constructed behind a concrete, reinforced, tetrahedral breakwater (fig. 5.20). This technique has been used at a number of locations along the California coastline but never of the scale proposed for Devil's Slide. Although considered feasible, this proposal left many critical issues unanswered. Eventually, the creation of a national marine sanctuary by the Federal government immediately offshore eliminated this alternative.

In January 1995, heavy rains again caused the roadway to fail at Devil's Slide, closing the road for 150 days and created many traffic problems for the coastal communities to the south. For all practical purposes, all vehicular traffic from the Half Moon Bay area was forced to use the only remaining highway, Highway 92, to reach the urbanized portion of the Bay area, thus creating numerous traffic delays. Caltrans worked aggressively to repair the road (see figs. 5.21-5.26). In 1996, the voters of San Mateo County overwhelmingly passed Measure T. This measure identified the preferred alternative to be a tunnel bypass, and eliminated the Martini Creek alignment alternative (figs. 5.27, 5.28).

The final environmental document is expected to be approved in 2001, and tunnel design will then begin. The tunnel is planned to be a 4,000-foot long, double-bore facility with one lane in each direction. The north approach will leave the existing alignment of Highway 1 onto an approximately 1,000- to 1,500-foot-long bridge structure that crosses the valley at Shamrock Ranch, entering the tunnel facility beneath San Pedro Mountain. The south approach will exit on the south side of San Pedro Mountain onto a 1,000-foot approach fill that rejoins Highway 1 south of Devil's Slide.

In November 1997, Caltrans evaluated the feasibility of stabilizing the landslide complex using dewatering wells in conjunction with existing horizontal drains. The study concluded that the rock mass has a low hydraulic conductivity and transmissivity. There is no evidence of a pressurized aquifer that could be relieved, and the shallow and moderately deep failure surfaces are located above the average groundwater-table level. In addition, slow landslide movements appear to

continue regardless of rainfall patterns and dewatering activities. Consequently, it was determined that dewatering would not be an effective, long-term mitigation measure. However, as part of an ongoing effort to maintain the Highway 1 roadway bench until the tunnel project is completed, continual near-surface and deep dewatering is performed though the use of horizontal drains and the existing drainage wells. The roadway and the slope face directly above the roadway bench are constantly monitored, and the roadway will be closed in the event of significant movement.

Geologic Setting of the Devil's Slide Bypass Tunnel[9]

The proposed tunnel will pass through Montara Mountain and San Pedro Mountain. The proposed tunnel alignment crosses at least two geologic formations—the Montara Granite and a series of folded and faulted Paleocene sedimentary rocks (turbidites) that overlie the granite (fig. 5.29). The granitic mass that makes up Montara Mountain covers about 30 square miles along the coast. The northernmost outcrop is in the cliff face at Devil's Slide. Franciscan Complex rocks crop out about 1 mile to the northeast, separated from the granitic complex by the Montara and Pilarcitos Faults. At the south end of the alignment, for approximately the first 1,500 to 1,600 feet, the tunnel alignment is in granitic rock. The remainder of the tunnel alignment is in the Paleocene sedimentary rocks. Because of the current uncertainty about the geologic structure at depth, it is unclear as to whether the tunnel will encounter Cretaceous sedimentary rocks. While not penetrated by the proposed tunnel alignment, alluvial deposits exist within the valley north of the north portal. These deposits will be crossed by the proposed roadway between the north portal and where the new roadway will join existing Highway 1. Small local slides have occurred near the north and south portals.

The Devil's Slide area is within a seismically active area. The San Andreas Fault is less than 4 miles east of the study area. The San Gregorio Fault and the associated Seal Cove Fault are about 1.5 miles offshore to the west. No known active faults, however, pass directly through the tunnel alignment.

The effects of earthquakes on underground structures such as tunnels can be broadly grouped into two general classes, displacement (rupture) or shaking. Sympathetic fault displacement in the rock mass along the tunnel alignment would result in relatively minor structural damage. The Devil's Slide bypass tunnel will be subject to shaking during its useful life. In general, worldwide experience shows that tunnels survive earthquakes significantly better than surface structures. Damage to tunnels is not likely if horizontal acceleration at the ground surface above the tunnel does not exceed 0.5g (Caltrans, 1999). The effect of an earthquake is to impose deformations on the underground structure that cannot be overcome by strengthening the structure. The object of an effective earthquake-resistant design is, therefore, to produce a structure of sufficient ductility to absorb the imposed deformation without losing the capacity to carry static loads.

Stop 3—Coastal Erosion Accelerated by Human Activity in the Half Moon Bay Area (Pillar Point Harbor)

Along the San Mateo County coastline, cliff erosion and retreat by wave erosion, landslides, block falls, and debris slides occur at different rates. Wave erosion is the primary erosive process. All waves, but particularly storm waves, erode the shore, oversteepening and destabilizing the slopes. Landslides, block falls, and surface erosion move the weakened and detached material to the beach where it is reworked by wave action. Along many parts of the San Mateo County coastline, augmenting the destabilizing action of the waves is the movement of groundwater out of the cliff and bluff faces, softening, and detaching materials in the cliffs and bluffs (Lajoie and Mathieson, 1998).

The U.S. Geological Survey has prepared a series of geologic and erosion maps for the coast of San Mateo County depicting the general geologic relationships and the relative amounts and types of erosion occurring (Lajoie and Mathieson, 1998) (figs. 5.30 to 5.33). For the region near Half Moon Bay, these maps record the influence of human intervention and construction in modifying the natural patterns of erosion. Human actions have contributed significantly to acceleration of the rate of coastal erosion in a localized area adjacent to the Pillar Point Harbor breakwater.

Aerial photographs of the area show the wave-refraction patterns around the resistant headland, Pillar Point, produced by the prevailing northwesterly winds (fig. 5.34). Before the construction of the breakwater-protected harbor, the energy of the waves refracted around Pillar Point was dissipated uniformly over a length of beach that was in equilibrium—neither eroding nor growing seaward.

Because of the marine-oriented economy of the Half Moon Bay area and the fact the Half Moon Bay area is the only good safe harbor along this section of the California coastline between Santa Cruz and San Francisco, the community has had a long history of interest in the quality of the harbor. During times when southwesterly storms strike the coast, boats in the Half Moon Bay anchorage had been at risk. A number of them sank, and others were damaged by being driven onto the coastal rocks (McLaughlin and Sarna-Wojcicki, 1997). To provide protection for the boats, the U.S. Army Corps

of Engineers completed a breakwater in 1960. The impact of this breakwater was immediate and significant. It did provide protection for the boats, but at the same time it also altered the wave-refraction patterns. The refocused wave energy was concentrated on a small segment of the coastline south of the breakwater, El Granada Beach, and it dramatically accelerated the rate of erosion. For the period between 1861 and the completion of the breakwater in 1960, the rates of erosion were somewhat variable, but they averaged about 0.03 meters (approximately 1 inch) per year. These relatively stalemate conditions suggest that the shoreline essentially was in equilibrium. Following construction of the breakwater, the rate of coastal erosion increased sharply to 1.1 meters per year, slightly more than 3 feet per year (Mathieson and others, 1997) (fig. 5.35). This increase in erosion damaged and has caused the removal of coastal buildings, railroad tracks, and roads. Currently, Caltrans is constructing and repairing existing rip-rap to protect Highway 1 (Caltrans, 1999b).

Notes

[1]Data for this section of the field guide have been taken from two reports prepared by Anne Rosinski, 2000, 1994, currently a geologist at the California Division of Mines and Geology and a graduate student in engineering geology at San José State University. The text of her reports has been abstracted and slightly revised by the author.

[2]This brief overview of the general characteristics of the San Andreas Fault system is taken from the paper, *Living with Moving Ground – Landslides and Coastal Erosion in San Mateo Country*, by Cole and others (2000). Minor modifications and editorial changes have been made to the text by the author.

[3]Material for this section is based on information contained in the web site for the Filoli Center and has been abstracted and edited by the author.

[4]The material for this section is based on information contained in the web site of the San Francisco Public Utilities Commission.

[5]The data for this section are from reports prepared by Caltrans (2000, 1996), slightly abstracted and edited by the author.

[6]Data for this portion were taken from the California Regional Water Quality Control Board San Francisco Bay Region Order No. 99-067 (San Francisco Bay Area Regional Water Control District, 1999). The text has been abstracted and slightly modified by the author. The Regional Water Quality Control Board has the responsibility for permitting these facilities. As an element of that responsibility, both water-control boards require specific elements for the geologic investigations done in support of the permit requests. The Boards also review all materials submitted in support of the permit requests to determine their completeness.

[7]Data for this portion are from a Caltrans Summary Statement (Caltrans 2001).

[8]This historical perspective of Devil's Slide is a slightly modified version of a portion of a paper on Devil's Slide prepared by Cole and others (2000).

[9]This section is a portion of the Environmental Impact Study (1999) by Caltrans which has been slightly modified by the author.

References

Association of Bay Area Governments (ABAG), 1999, Ground shaking intensity maps: http://www.abag.ca.gov/cgi-bin/pickmapx.pl.

Barnes, Nancy, (ed.), 1995, Engineering geology and tectonic setting of the Point San Pedro– Devil's Slide Area, San Mateo County, California: Association of Engineering Geologists, San Francisco Section, Field Trip, 18 November 1995.

Brabb, E., and Pampeyan, E., 1972, Preliminary Geologic Map of San Mateo County, California: US Geological Survey Basic Data Contribution no. 41.

California Department of Conservation, Division of Mines and Geology, 1976, State of California special studies zones, Woodside Quadrangle, July 1, 1974.

Caltrans, 2001, Devil's Slide at Route 1 and Devil's Slide Tunnel Project: http://www.ca.gov/dist4/dslide.htm.

Caltrans, 2000, Route 92 Uphill slow vehicle lane/safety improvements initial study (CEQA)/environmental assessment (NEPA): State of California, Department of Transportation.

Caltrans, 2000 b., Route 92 in San Mateo County from Pilarcitos Creek to Route 35 South, slow vehicle lane project: State of California, Department of Transportation.

Caltrans, 1999, Devil's Slide 1999 Environmental Impact Statement, Devil's Slide improvement project—Route 1 from Half Moon Bay Airport to Linda Mar Boulevard in Pacifica San Mateo County, California: http://www.dot.ca.gov/dist4/dslide/dsdeis_htm.

Caltrans, 1999 b, Project plans for construction on State Highway in San Mateo County near Half Moon Bay at 2.1 kilometers south of Capistrano Road: State of California Department of Transportation.

Caltrans, 1996, Geotechnical design and materials report (from Pilarcitos Creek Bridge to Route 35): State of California, Department of Transportation Engineering Services Center.

CEN Technical Committee 288, 2000, Reinforced Soil: http://person.Dundee.ac.uk/~amcjones/cen/fd/FDPPart1.doc.

Clahan, K.B., Wright, R.H., and Hall, N.T., 1995, Paleoseismic investigation of the San Andreas Fault on the San Francisco Peninsula, CA, Final Technical Report, Award No. 14-08-001-G2081, National Earthquake Hazards Reduction Program, U.S. Geological Survey, Reston, Virginia.

Clark, J., and Brabb, E., 1978, Stratigraphic contrasts across the San Gregorio Fault, Santa Cruz Mountains, West Central California, *in* Weber. G.E., and Griggs, G.B., Coastal Geologic Hazards and Coastal Tectonics, Northern Monterey Bay and Santa Cruz/San Mateo County Coastlines, Field trip guide for San Francisco Section of the Association of Engineering Geologists.

Cole, W.F., Sayre, T.M., Smelser, M.G., Hay, E., Wallace, J. M., Velsor, J.V., Whitman, T.G., Snell, C., and Kieffer, D.S., 2000, Living with Moving Ground—Landslides and Coastal Erosion in San Mateo County, California *in* Alvarez, Leonardo (ed.), 2000 AEG-GRA 2000 Field Trip Guidebook—From the Pacific Ocean to the Sierra Nevada: Taming Shaky Ground: Association of Engineering Geologists, p. 1-31.

Con-Tech Systems, Ltd. [CTS], 2001, Con-Tech Projects: http://www.contechsystems.com/Projects/H-92.html.

Filoli Center, 2001, The History of Filoli: http://www.filoli.org/history.html.

Griggs, G. and Savoy, L., eds., 1985, Living with the California coast, Duke University Press, North Carolina, 394 p.

Half Moon Bay, 2001, Our community, coastside profile: http://halfmoonbaychamber.org.

Hall, N.T., Wright, R.H., and Clahan, K.B.,1995, Final Technical Report: Paleoseismic Investigations on the San Andreas Fault on the San Francisco Peninsula, California: for U.S. Geological Survey National Hazards Reduction Program, by Geomatrix Consultants, September 1995, Award No. 14-08-0001-G2081.

Hall, N.T., R.H. Wright, and K.B. Clahan, 1994, Final technical report: Paleoseismic Investigations on the San Andreas Fault on the San Francisco Peninsula, California: for U.S. Geological Survey National Hazards Reduction Program, by Geomatrix Consultants, July 1994, Award No. 14-08-0001-G2081.

Harden, D.R., 1998, California Geology, Prentice Hall, Inc., New Jersey, 479 p.

Heyes, D.G., 1984, Engineering geology of Devil's Slide, San Mateo County, California in 35th Annual Highway Geology Symposium Field Trip Guide, p. 14-41.

Hill, M.L., and Dibblee, T.W., Jr., 1953, San Andreas, Garlock, and Big Pine faults, California—a study of the character, history, and tectonic significance of their displacements: Bulletin of the Geological Society of America, v. 64, no. 4, p. 443-458.

Irwin, W.P., 1960, Geologic reconnaissance of the northern Coast Ranges and Klamath Mountains, California: California Division of Mines and Geology Bulletin 179, 79 p.

Jachens, R.C., Roberts, C.W., and Zoback, M.L., 1996, Total Offset And Right-Stepping Geometry of The San Francisco Peninsula Segment of The San Andreas Fault, California, Defined By Aeromagnetic Anomalies: Eos Transactions (American Geophysical Union) v. 77, p.46.

Lajoie, K. and Mathieson, S.A. 1998, 1982-83 El Niño coastal erosion: San Mateo County, California: http://elnino.wr.usgs.gov/elnino/SMCO-coast-erosion/coaststabl-lg.html.

Lajoie, K. and Mathieson, S., 1985, San Francisco to Año Nuevo, *in* Griggs, G., and Savoy, L., eds., Living with the California Coast: National Audubon Society, Duke University Press, Durham, North Carolina, p. 140-177.

Lawson, A.C., ed., 1908, Report of the State Earthquake Investigation Commission: Publication 87: Washington, D.C., Carneigie Institute of Washington, v. 2, no. 12.

Mathieson, S. A., Lajoie, K. R., and Hamilton, J.C., 1997, Induced sea-cliff erosion southeast of the Pillar Point breakwater, Half Moon Bay, California: U.S. Geological Survey Open File Report 97-688, scale 1:200.

McLaughlin, R., and Sarna-Wojcicki, A., 1997, Coastal geology of the Half Moon Bay Area and vicinity, San Mateo County, California: U.S. Geological Survey, unpublished field trip guide.

McLaughlin, R, and others, 1988, Tectonics of formation, translation, and dispersal of the Coast Range Ophiolite of California: Tectonics, 7(5), p. 1033-1056.

Montara Press, 2001, Aerial Photograph of Devil's Slide Bypass Tunnel Alignment: http://plants.montara.com/frontpix/ds.jpeg.

Page, B.M., 1989, The Salinian Block, in Wahrhafiig, C. and Sloan, D., (eds.), Geology of San Francisco and vicinity: Field Trip Guidebook T 105, 28th International Geological Congress, American Geophysical Union, Washington, D.C., p. 16-20.

Rosinski, A., 2000, Slope stability and mitigation for Campus Cut, Highway 92, San Mateo County, California: unpubl. manuscript, Engineering Geology Class, , San José State University, Department of Geology.

Rosinski, A., 1994, Slope stability study of two cut slopes along a portion of Highway 92 in San Mateo County: unpubl. B.S. thesis, San Francisco State University, 53 p.

San Francisco Public Utilities Commission, 2001, Map of the Hetch Hetchy distribution system: http://www.ci.sf.ca.us/puc/html/hetchy.htm.

San Francisco Public Utilities Commission, 2001, History and construction of Hetch Hetchy: http://www.ci.sf.ca.us/puc/html/hetchy.htm.

San Francisco Bay Regional Water Control Board, 1999, Order No. 99-067 Updated Waste Discharge Requirements and Recision of Order No. 92-087 for Browning-Ferris Industries of California, Inc. Corinda Los Trancos Landfill/Ox Mountain Sanitary Landfill, Half Moon Bay, California: http://www.swrcb.ca.gov/rwqcb2/Order_Nos_99-025/99-034/6appendixb/Orde…/5ddmp.htm.

Simpson, G., and Lettis, W.R., 1999, The northern San Gregorio Fault Zone, Pillar Point to Moss Beach, *in* Weber, G.E., and others, eds., Neotectonics and Quaternary Geology of the San Gregorio Fault Zone, Santa Cruz and San Mateo Counties, California: Geological Society of America, Cordilleran Section Annual Meeting, June 2-4, 1999.

Sullivan, R., and Galehouse, J.S., 1991, Geological setting of the San Francisco Bay area, *in* Sloan, D., and Wagner, D.L., eds., Geologic Excursions in Northern California—San Francisco to the Sierra Nevada: Field Trip Guidebook for the Joint Meeting of the Geological Society of America Cordilleran Section, Special Publication 109, California Department of Mines and Geology, 130 p.

U.S. Department of Agriculture, Soil Conservation Service, 1991, Soil survey of San Mateo County, eastern part, and San Francisco County, California: United States Department of Agriculture Soil Conservation Service, 120 p.

U.S. Geological Survey, 1999, Portfolio of images of landscapes, seascapes, and faults of the San Francisco Bay area: http://www.sfbayquakes.org/.

Wahrhaftig, C., and Sloan, D., 1989, eds., Geology of San Francisco and Vicinity: Field Trip Guidebook T 105, 28th International Geological Congress, American Geophysical Union, Washington, D.C.

Wakabayashi, J., 1999, Distribution of displacement on and evolution of a young transform fault system: The northern San Andreas Fault system, California: Tectonics, v. 18, no. 6, p. 1245-1274

Wakabayashi, J., and Hengesh, J.V., 1995, Distribution of late Cenozoic displacement on the San Andreas Fault system, northern California, *in* Sangines, E.M., Andersen, D.W., and Buising, A.V., eds., Recent Geologic Studies in the San Francisco Bay: Society of Economic. Paleontologists and Mineralogists, Pacific Section, v. 76, p.19-30.

Woodward Clyde Consultants, 1996, Devil's Slide tunnel study: unpubl. consultant report California Department of Transportation.

Wright, R., and Hall, T., 2001, Paleoseismic investigations of the San Andreas Fault Zone—Old Canada Road Site, San Mateo County, California: http://erp-web.er.usgs.gov/reports/annsum/vol40/nc/g3167.htm.

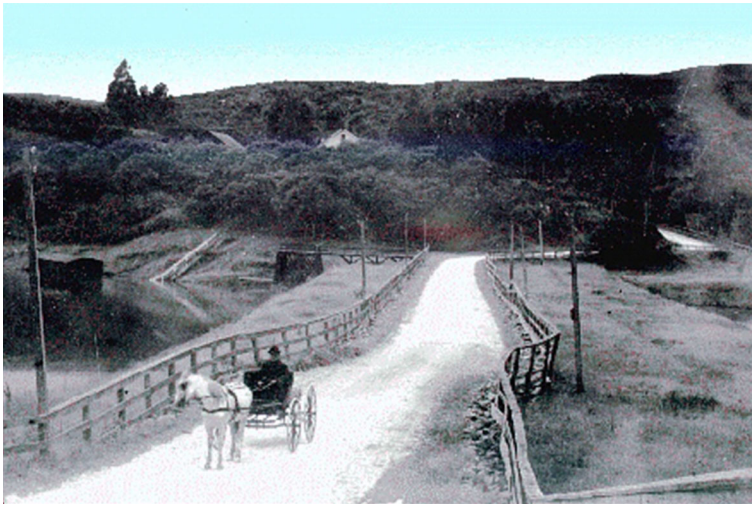

Figure 5.1. Offset of road across Crystal Springs Reservoir causeway following the 1906 San Francisco Earthquake (Bancroft Collection, University of California, Berkeley).

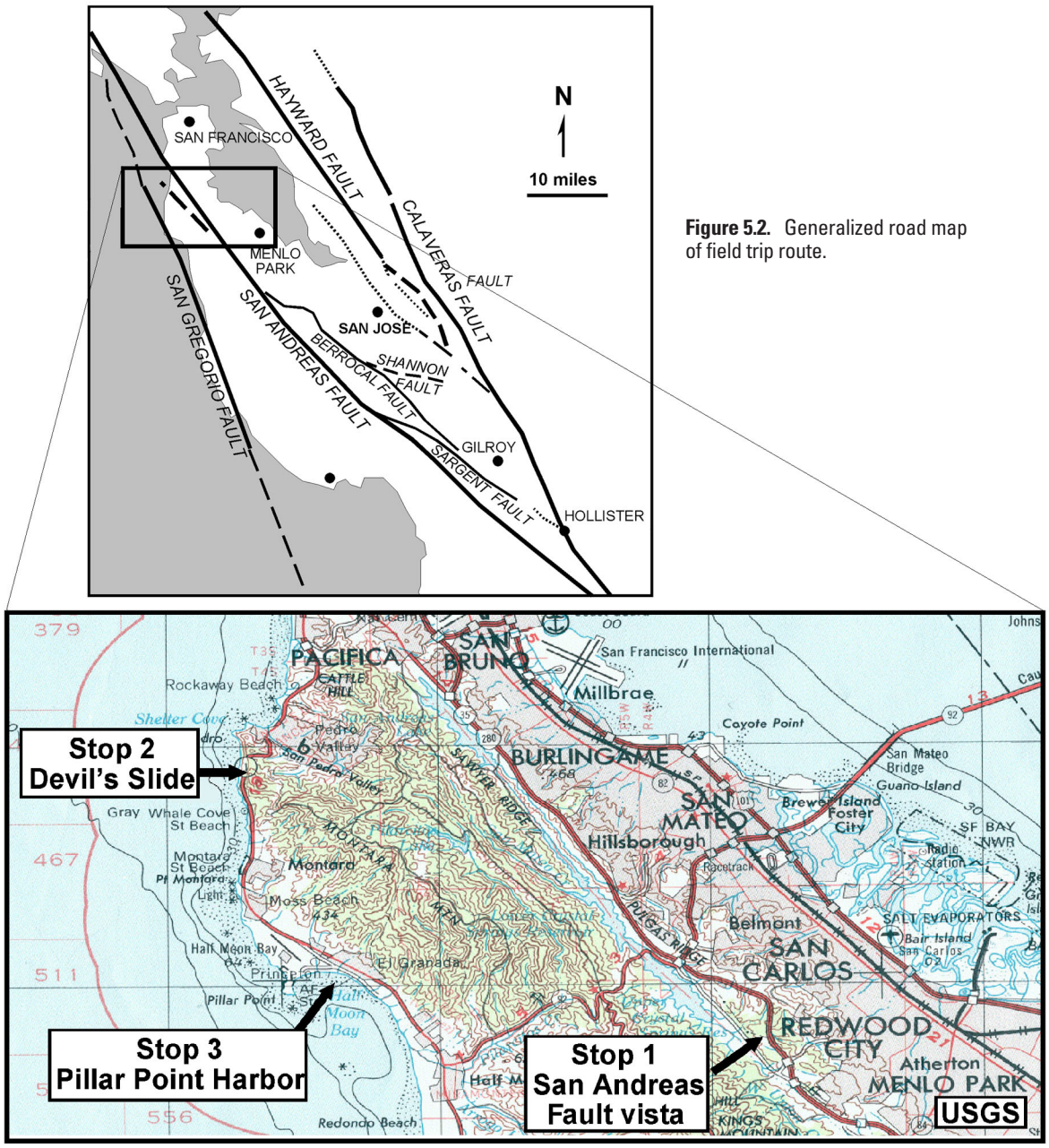

Figure 5.2. Generalized road map of field trip route.

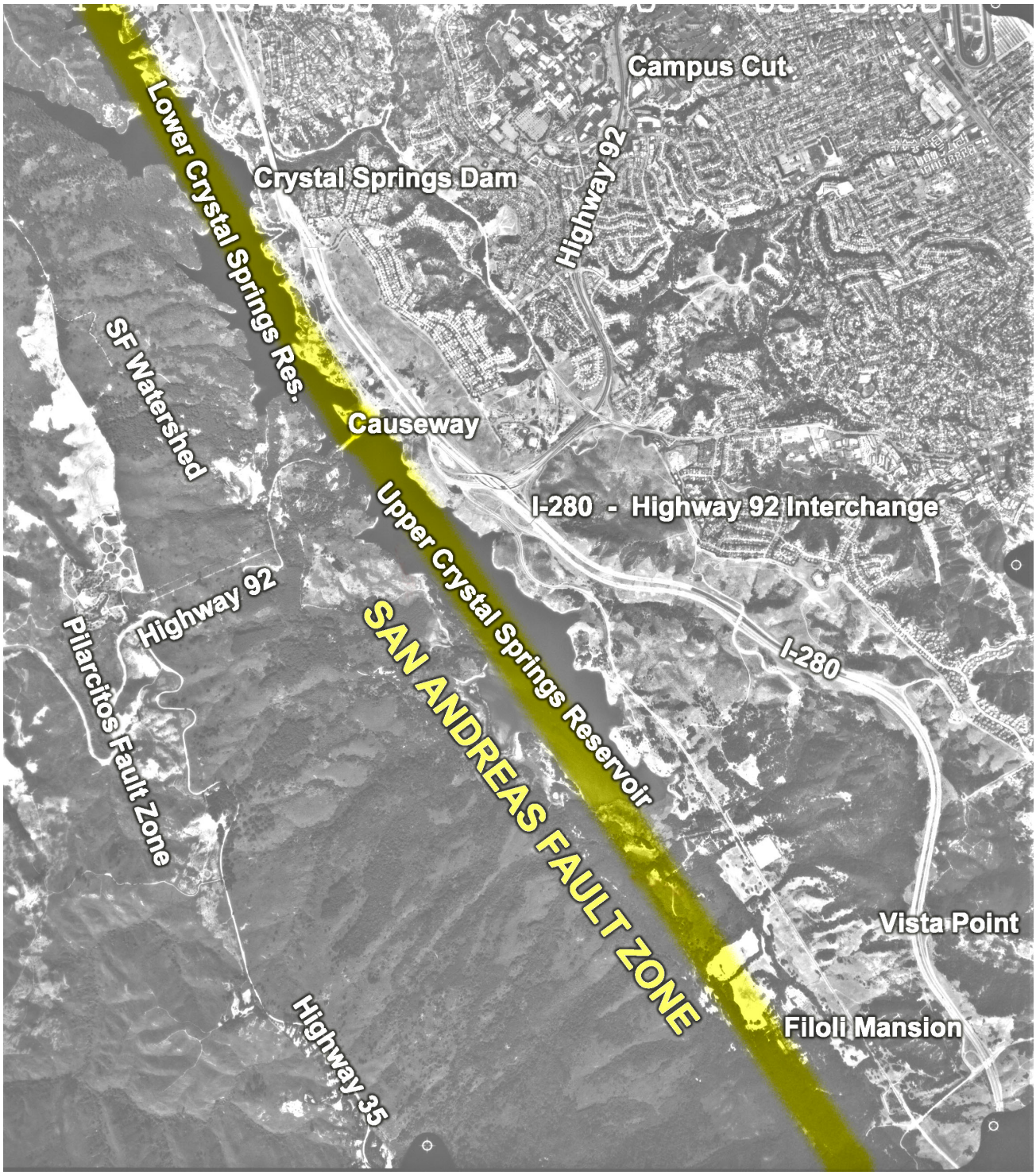

Figure 5.3. Aerial photograph taken in 1998 of Crystal Springs Reservoir, Interstate 280, Highway 92, and Vista Point (Stop 1).

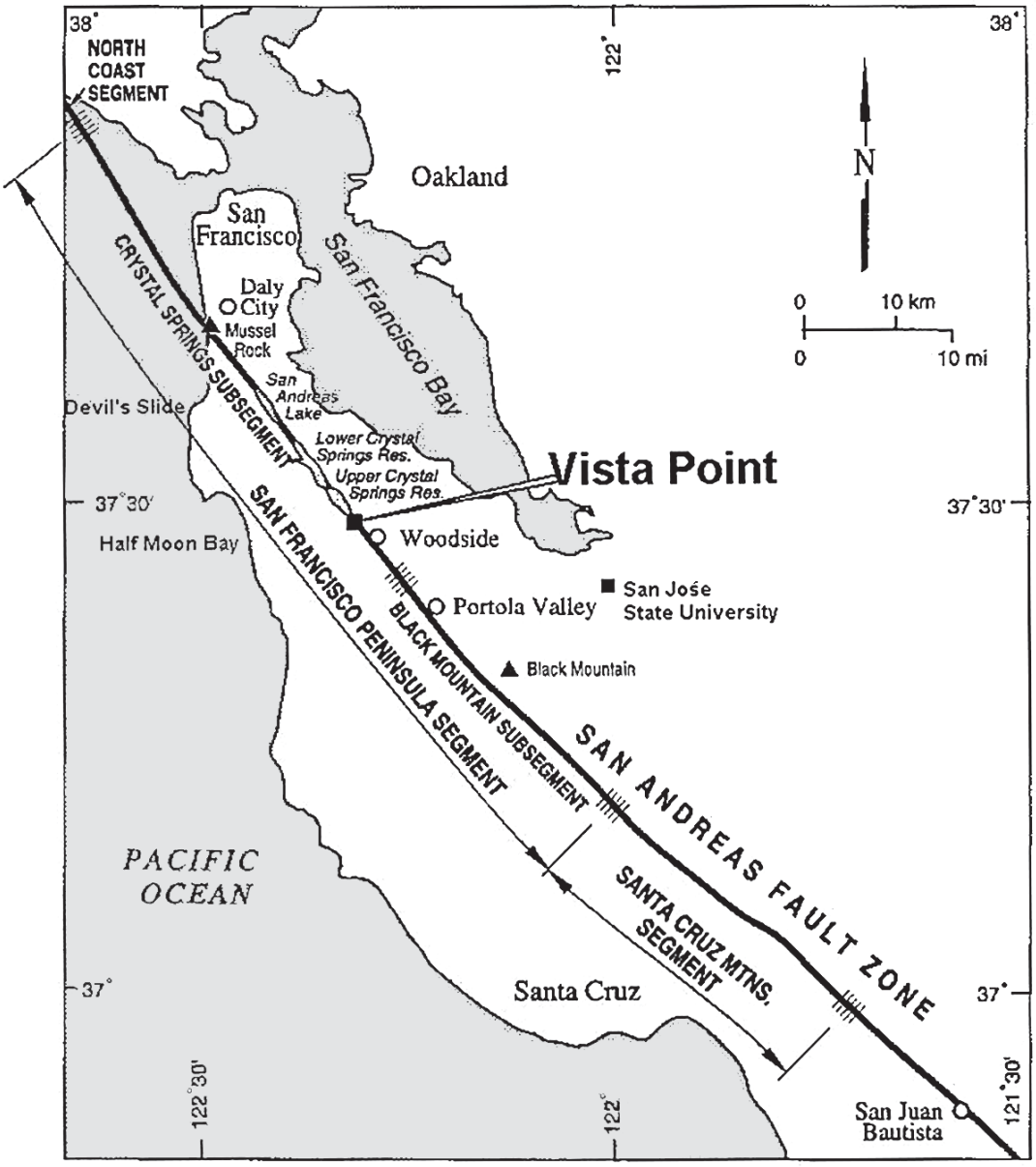

Figure 5.4. Map delineating segmentation of the San Francisco Bay area portion of the San Andreas Fault (after Wright and Hall, 2001).

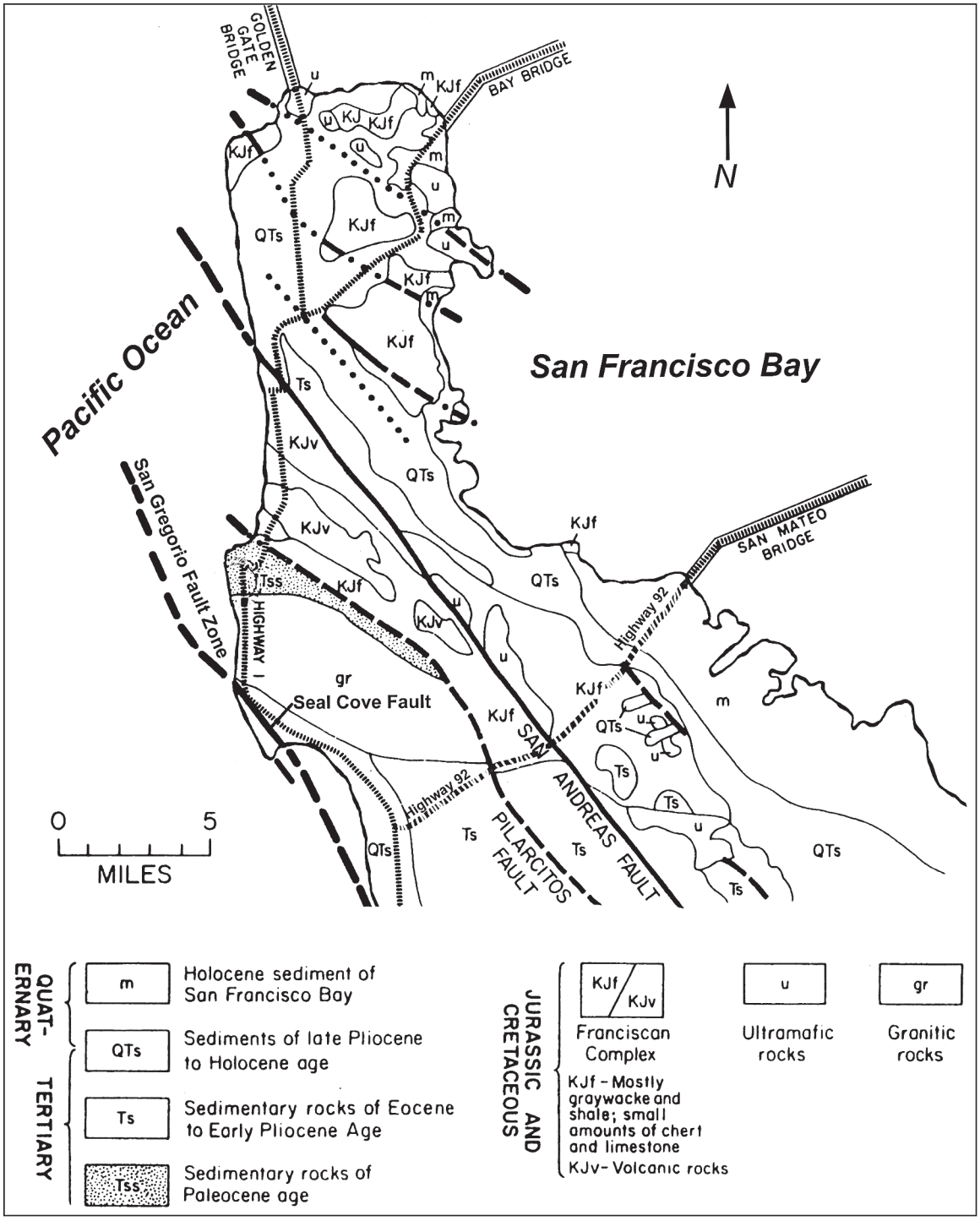

Figure 5.5. Simplified geologic map of the San Francisco Peninsula (modified from Heyes, 1984).

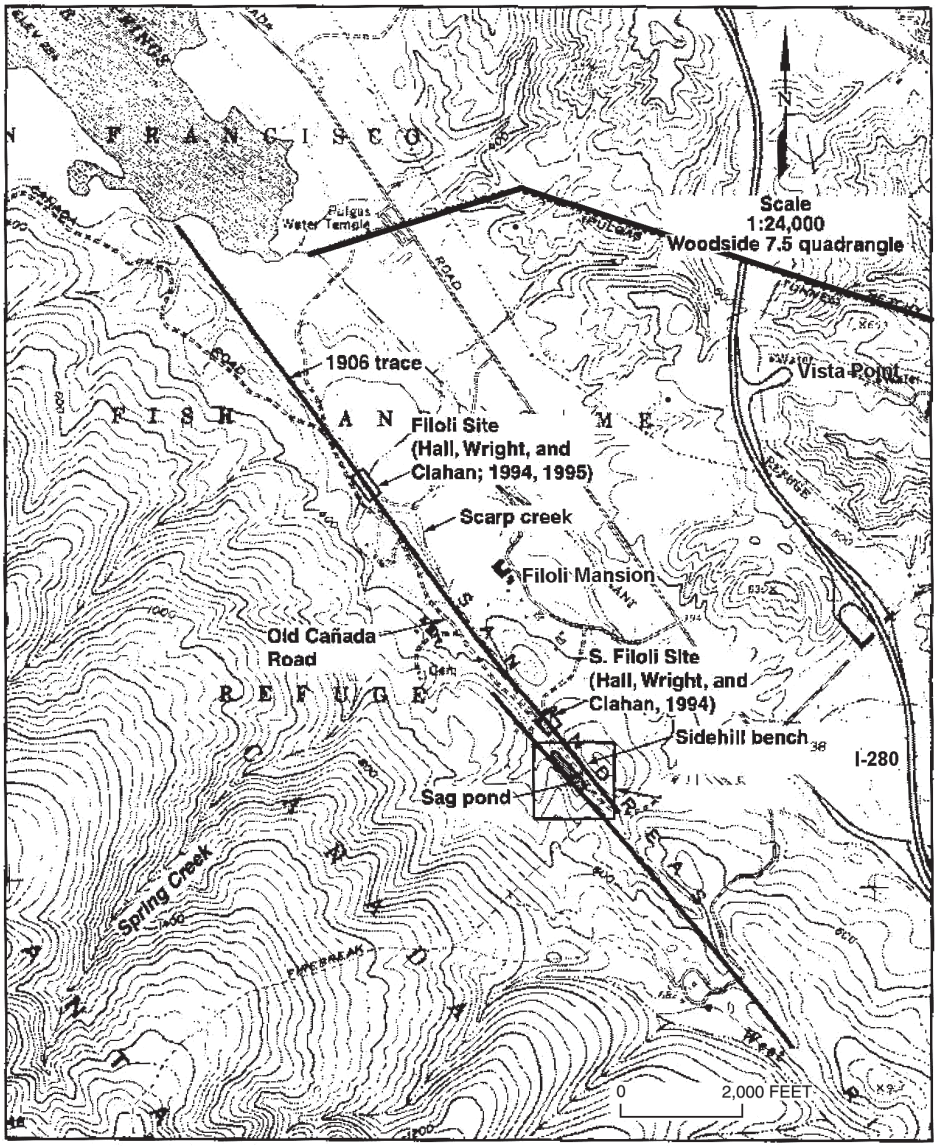

Figure 5.6. Map of the San Andreas Fault 1906 rupture trace with existing and proposed trenching sites in vicinity of the Filoli Mansion (after Wright and Hall, 2001).

Figure 5.7. Photograph of 1906 San Andreas Fault offset of fence on San Francisco Peninsula (Bancroft Collection, University of California, Berkeley).

Figure 5.8. Photograph of 1906 San Andreas Fault rupture trace on San Francisco Peninsula (Bancroft Collection, University of California, Berkeley).

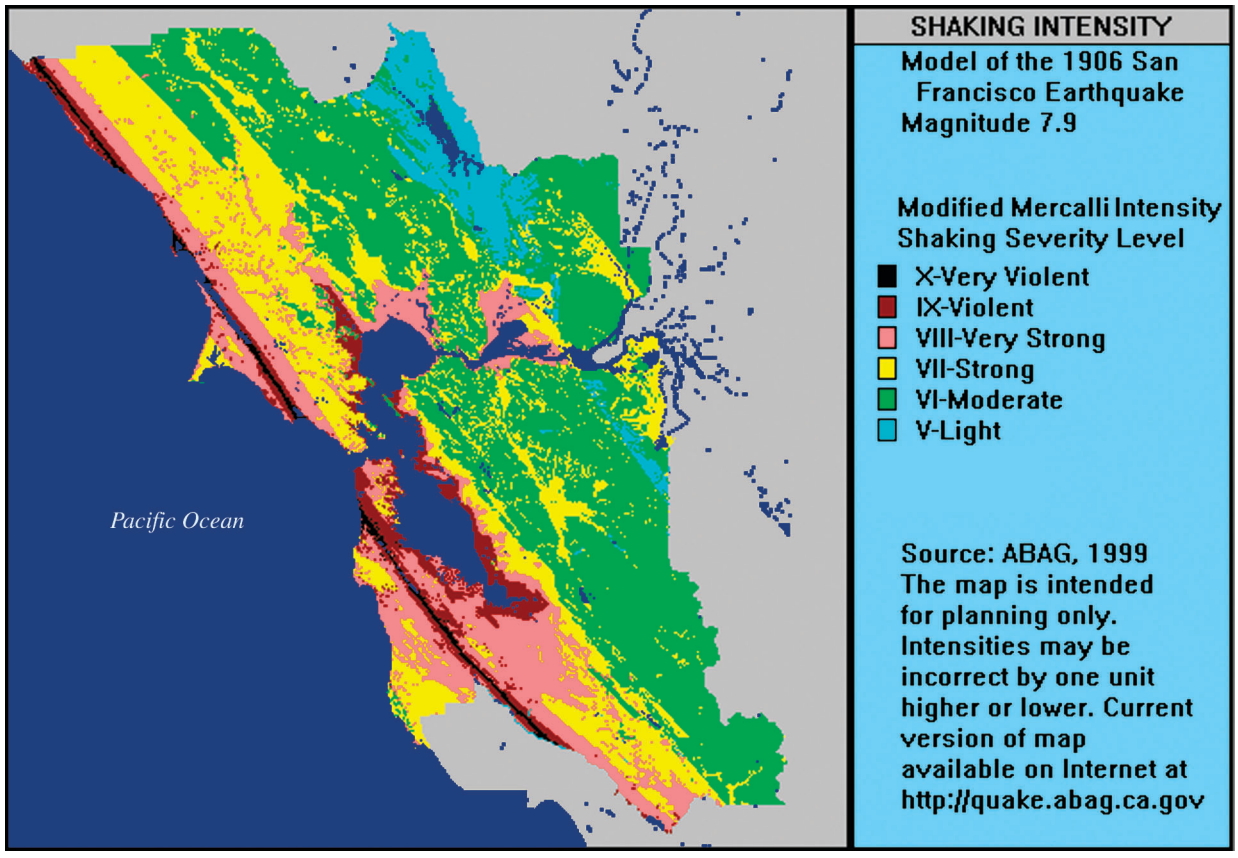

Figure 5.9. Map delineating ground shaking intensities for the San Franciso Bay area from the 1906 San Francisco Earthquake (Association of Bay Area Governments, 1999).

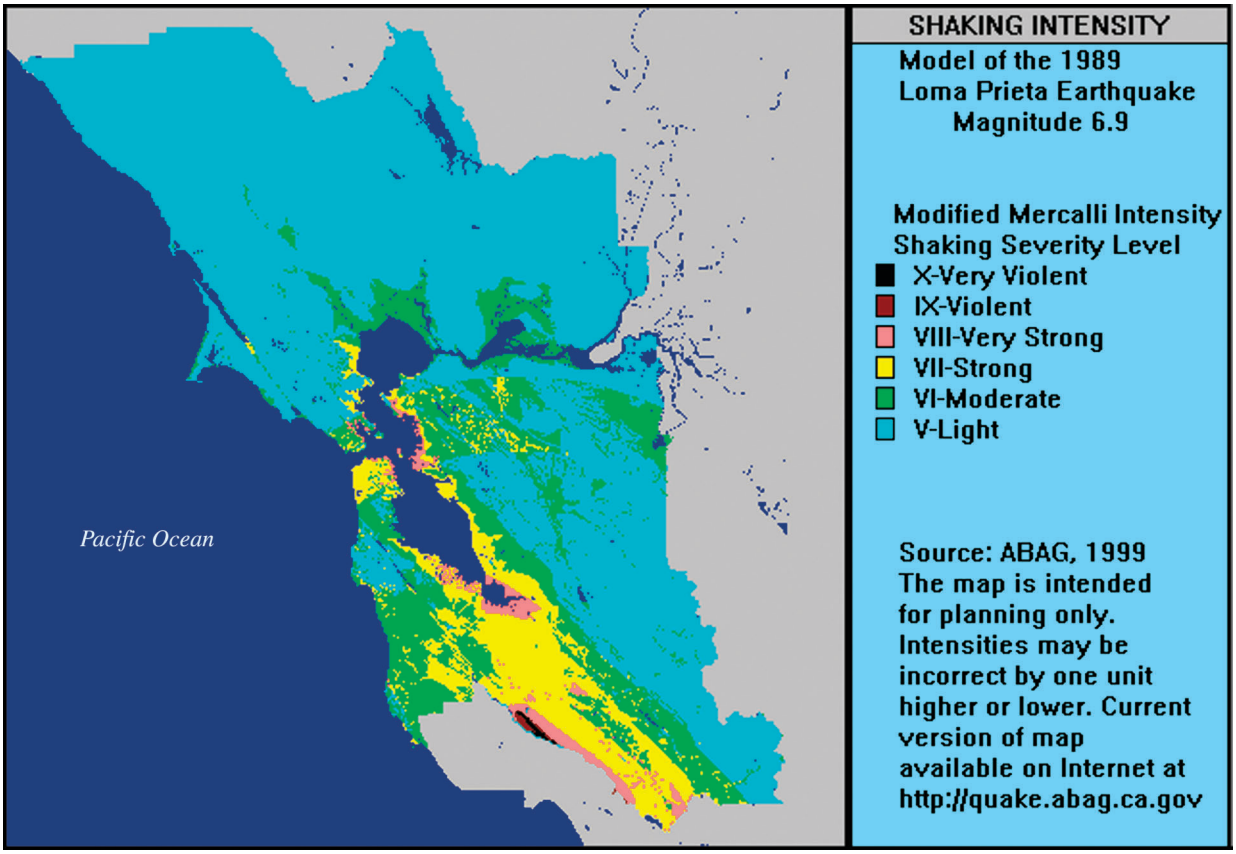

Figure 5.10. Map delineating ground shaking intensities for the San Francisco Bay area from the 1989 Loma Prieta Earthquake (Association of Bay Area Governments, 1999).

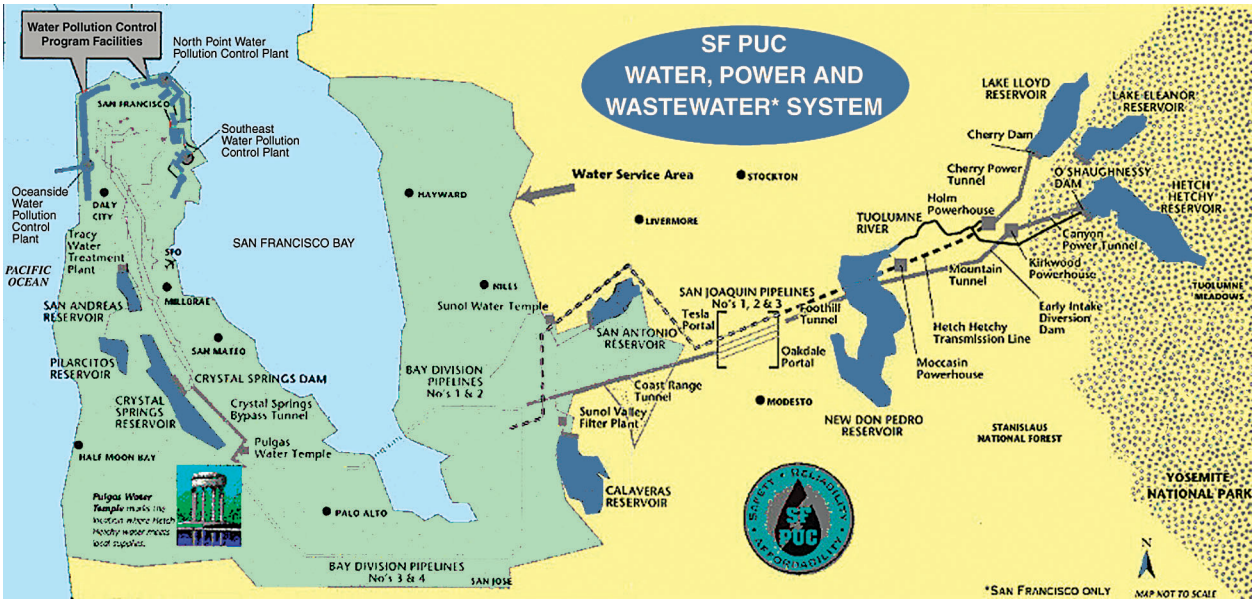

Figure 5.11. Map of Hetch Hetchy water distribution system (San Francisco Public Utilities Commission, 2001).

Figure 5.12. Photograph of soil-nailed retaining wall being constructed along Highway 92 east of Half Moon Bay. On right, slope has been nailed. On left, slope has been stabilized with shotcrete (Con-Tech Systems, Ltd. [CTS], 2001).

Figure 5.13. Photograph of completed soil-nailed retaining wall along Highway 92 east of Half Moon Bay (Con-Tech Systems, Ltd. [CTS], 2001).

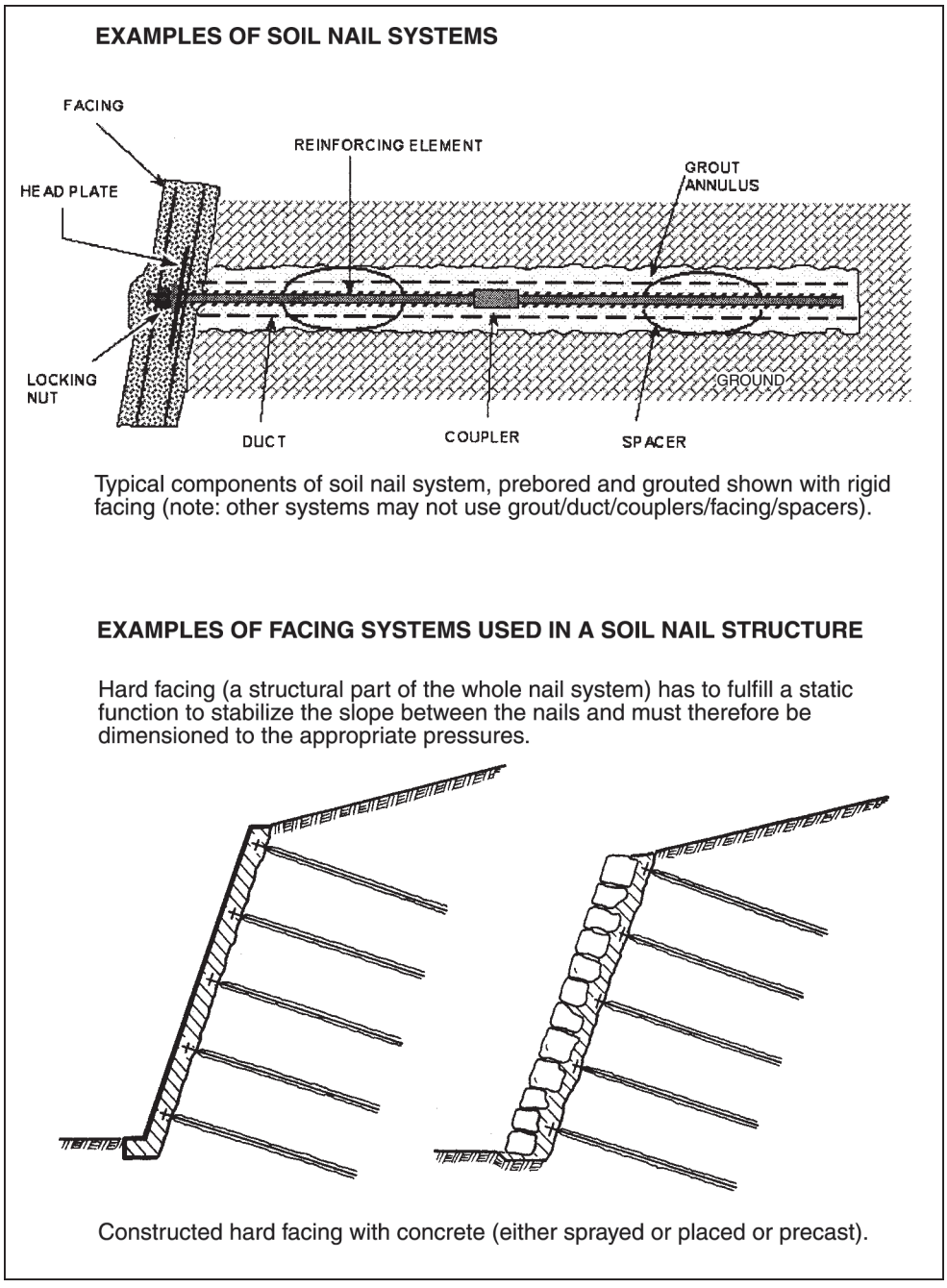

Figure 5.14. Diagrams of the basics of soil-nailing slope stabilization technique (CEN Technical Committee 288, 2000).

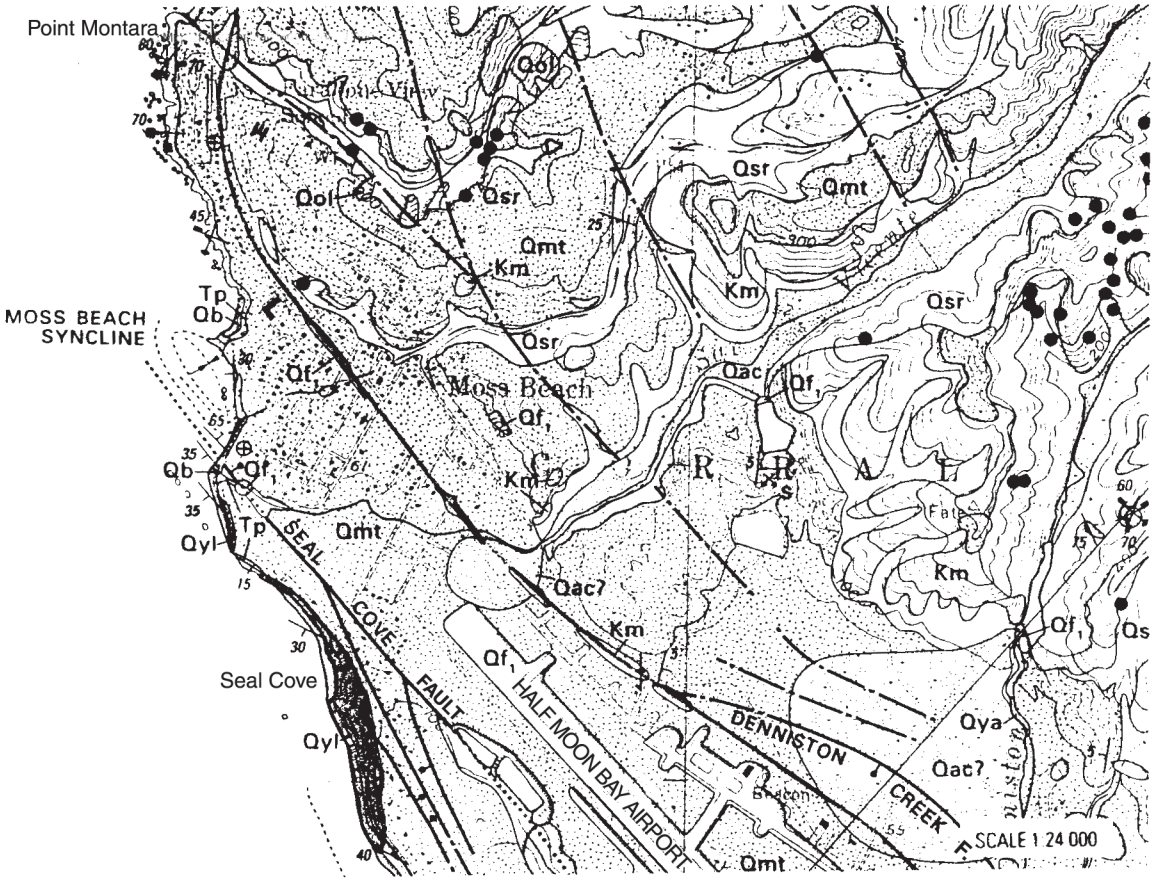

Qf_1	Artificial Fill	Qol	Holocene and Pleistocene (?) older landslide deposits
Qsr	Holocene slope wash ravine fill, and colluvium	Qmt	Upper Pleistocene marine terrace deposits
Qb	Holocene beach deposits	Tp	Pliocene Purisima Formation
Qyl	Holocene younger landslide deposits	Km	Cretaceous granitic rock of the Montara Mountain Pluton

Geologic Map of Area of Half Moon Bay Airport

Figure 5.15. Geologic map Half Moon Bay Airport area (McLaughlin and Sarna-Wojcicki, 1997).

Figure 5.16. Photograph of Moss Beach Syncline, which involves the Miocene to Pliocene-age Purisima Formation (Barnes, 1995).

Figure 5.17. Regional perspective aerial photograph of Devil's Slide area (Montara Press, 2001).

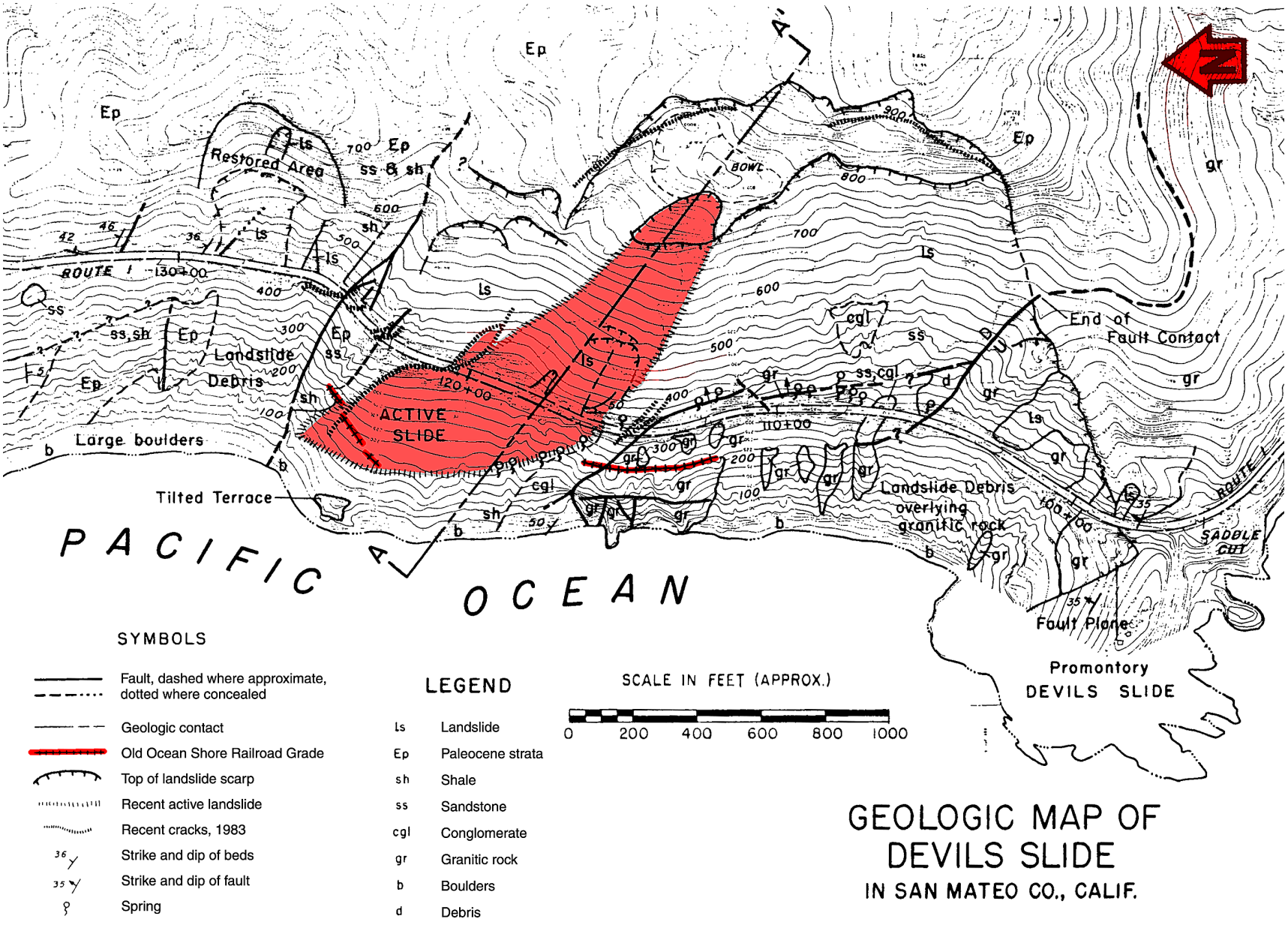

Figure 5.18. Geologic map of Devil's Slide area (Heyes, 1984).

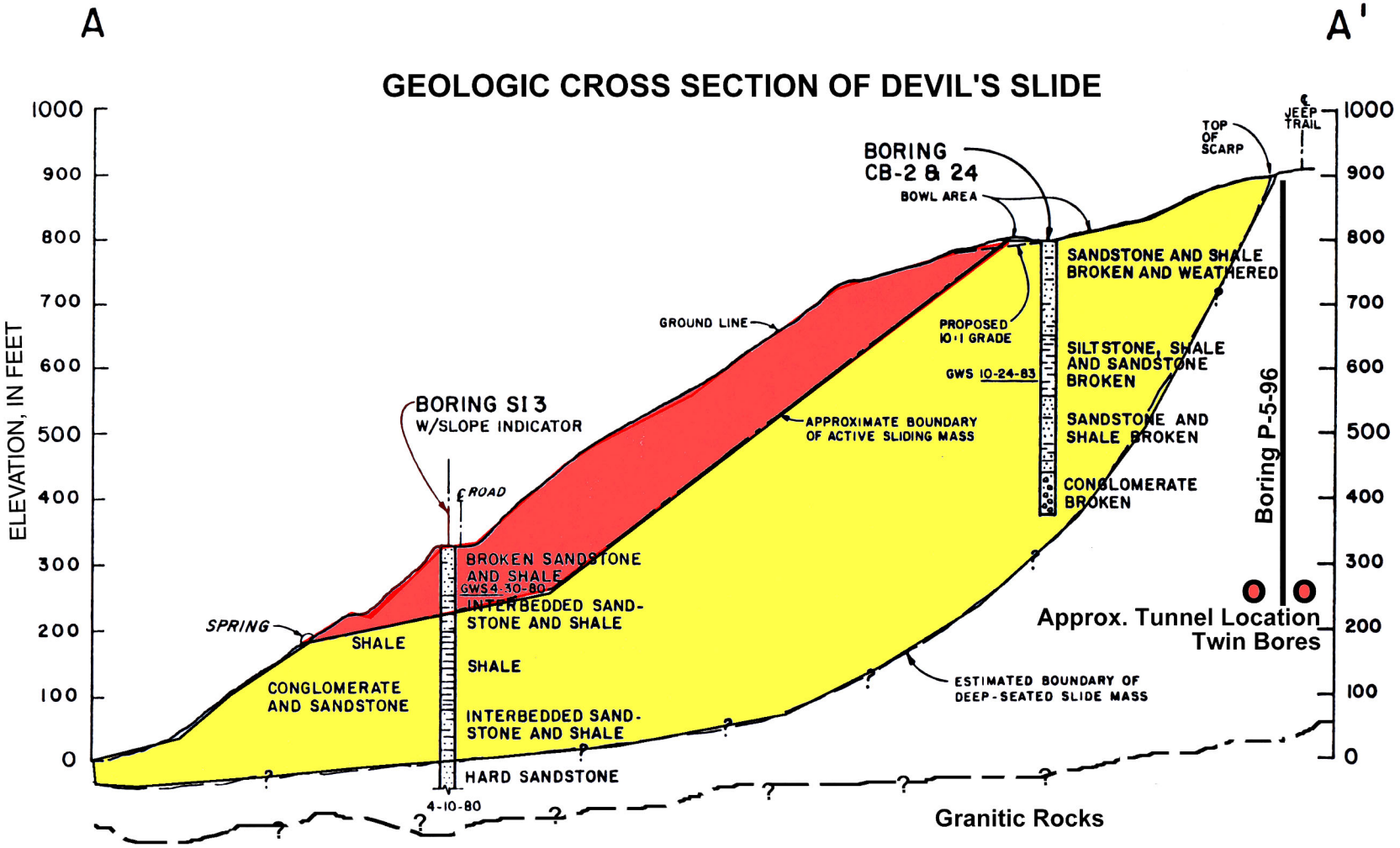

Figure 5.19. Schematic cross section of Devil's Slide (modified from Heyes, 1984).

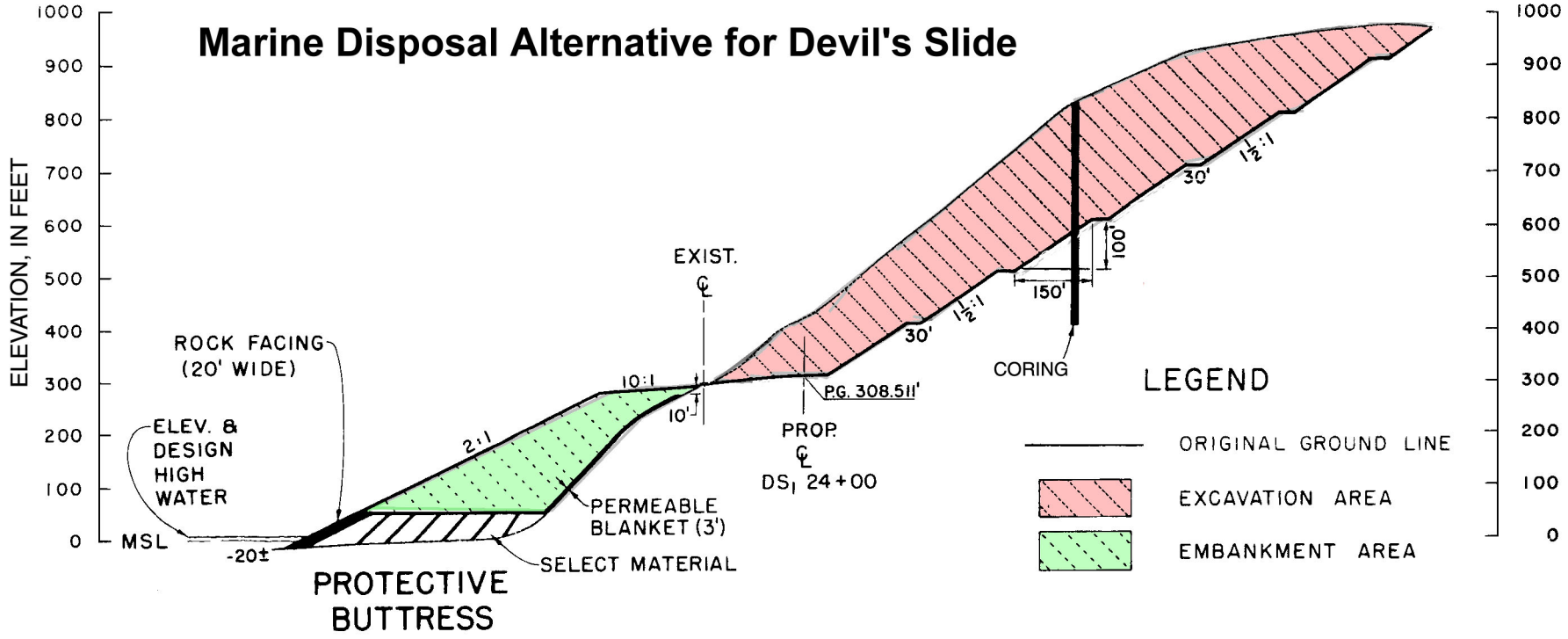

Figure 5.20. Diagrammatic cross section of marine disposal alternative for Devil's Slide. (after Heyes, 1984).

Figure 5.21. Photograph of initial 1995 failure of Highway 1 at Devil's Slide (Barnes, 1995).

Figure 5.22. Photograph of slope movement and rock falls at Devil's Slide (February 2, 1995) (Barnes, 1995).

Figure 5.23. Photograph of installation of wire mesh at Devil's Slide (Barnes, 1995).

Figure 5.24. Photograph of installation of anchors at Devil's Slide (Barnes, 1995).

Figure 5.25. Photograph of installation of grout blanket at Devil's Slide (Barnes, 1995).

Figure 5.26. Photograph of completed repairs at Devil's Slide, August 1995 (Barnes, 1995).

Figure 5.27. Artist's rendition of south portal of Devil's Slide tunnel bypass. This rendition shows a single bore, although current plans call for a dual bore (Montara Press, 2001).

Figure 5.28. Artist's rendition of north portal of Devil's Slide tunnel bypass. . This rendition shows a single bore, although current plans call for a dual bore (Montara Press, 2001).

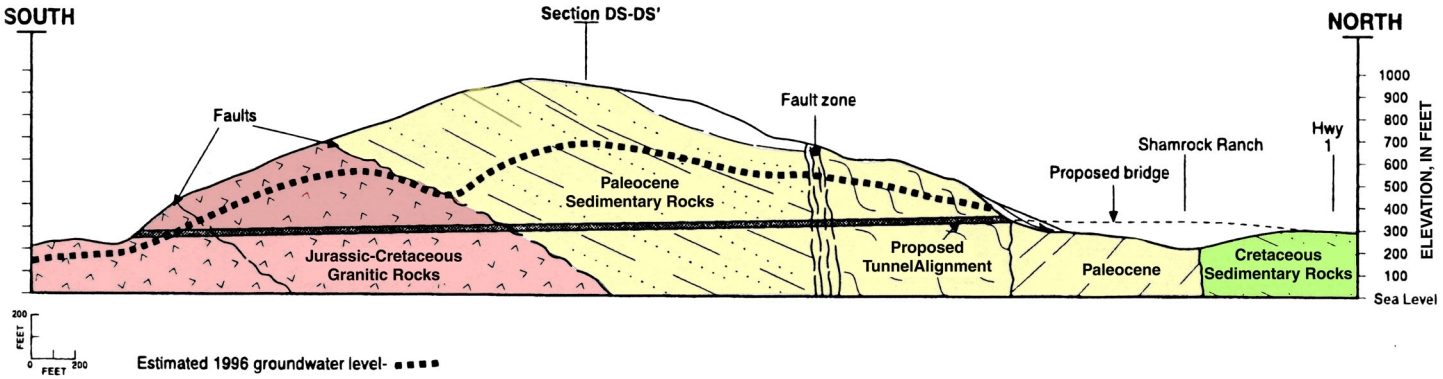

Figure 5.29. Geologic cross section along Devil's Slide bypass tunnel alignment (after Cole and others, 2000).

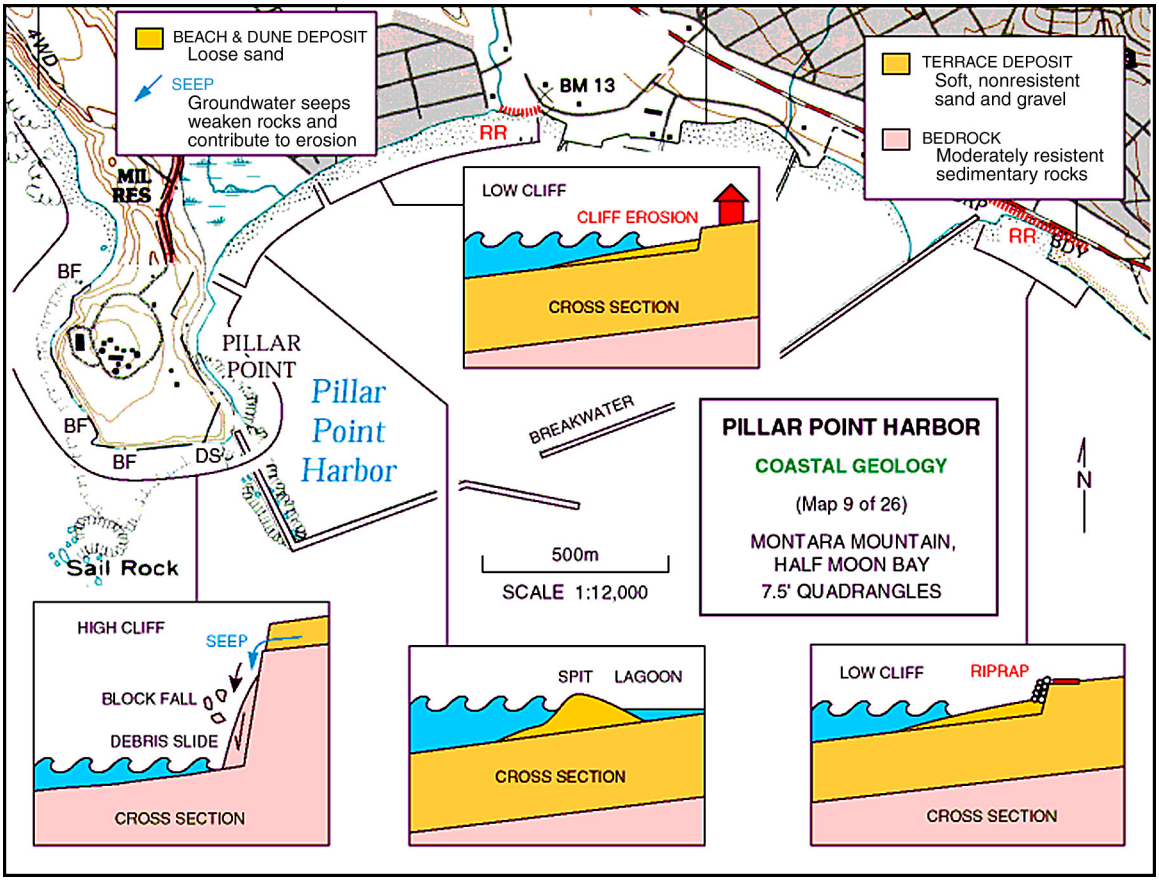

Figure 5.30. Pillar Point Harbor coastal geology map (Lajoie and Mathieson, 1998).

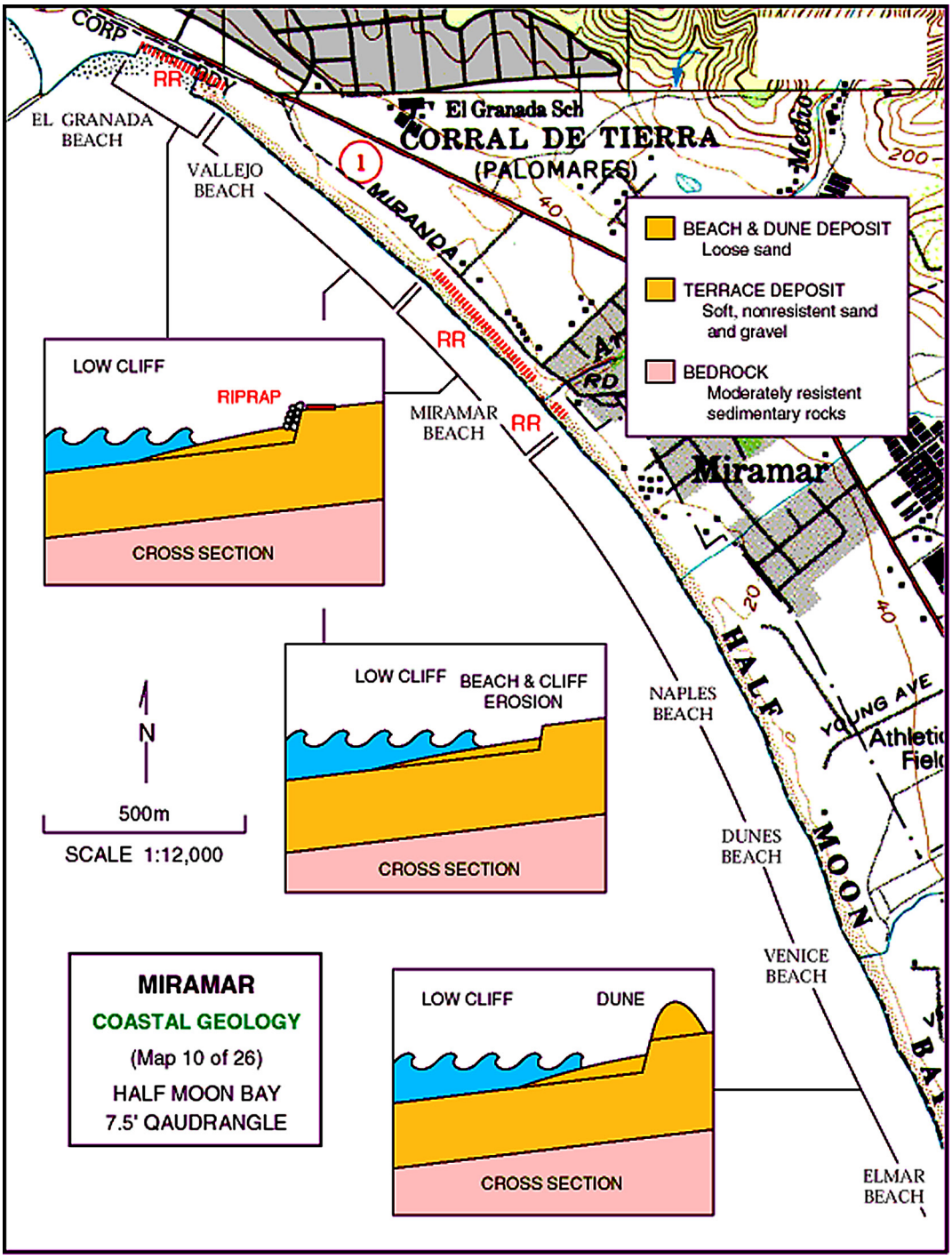

Figure 5.31. Miramar coastal geology map (Lajoie and Mathieson, 1998).

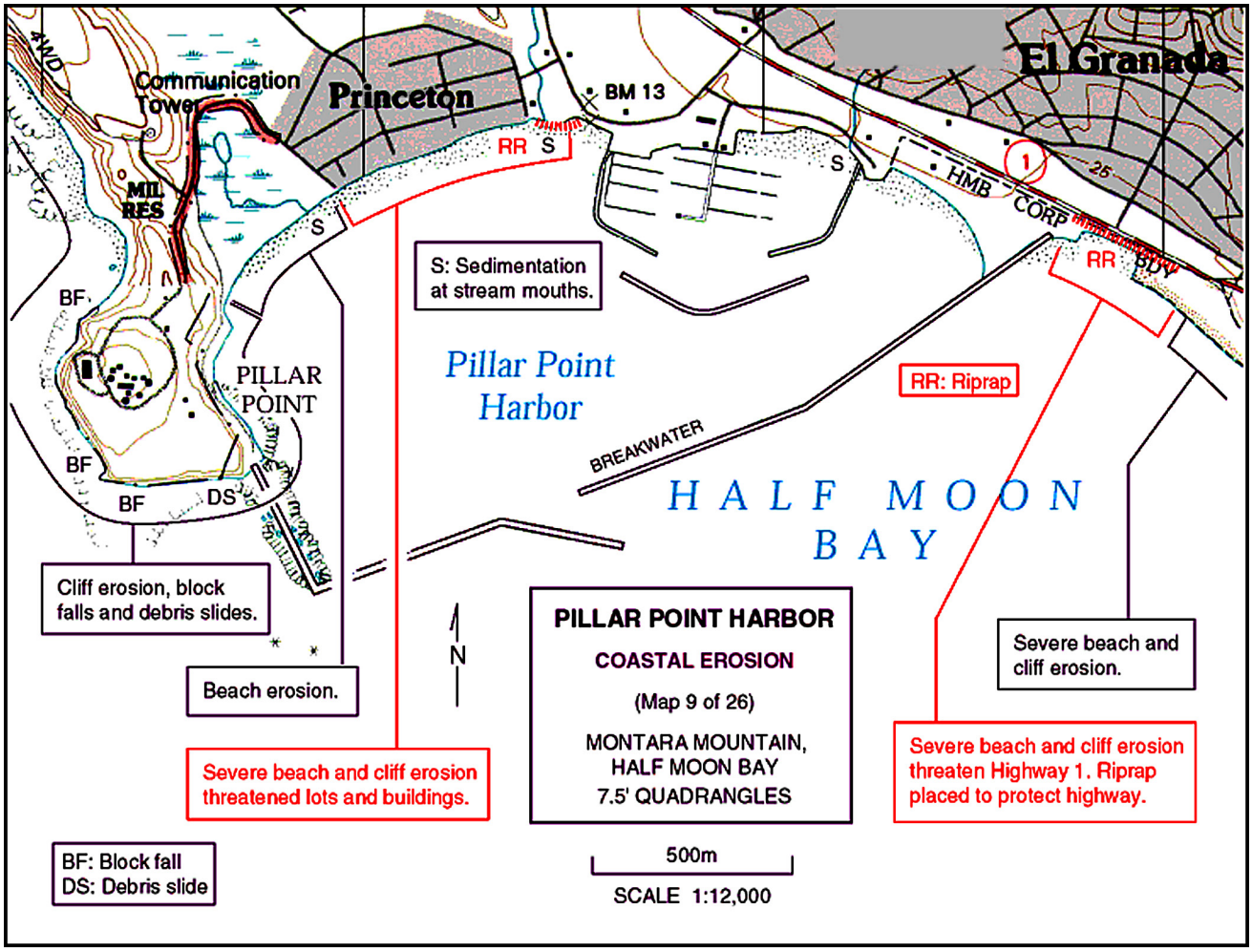

Figure 5.32. Pillar Point Harbor coastal erosion map (Lajoie and Mathieson, 1998).

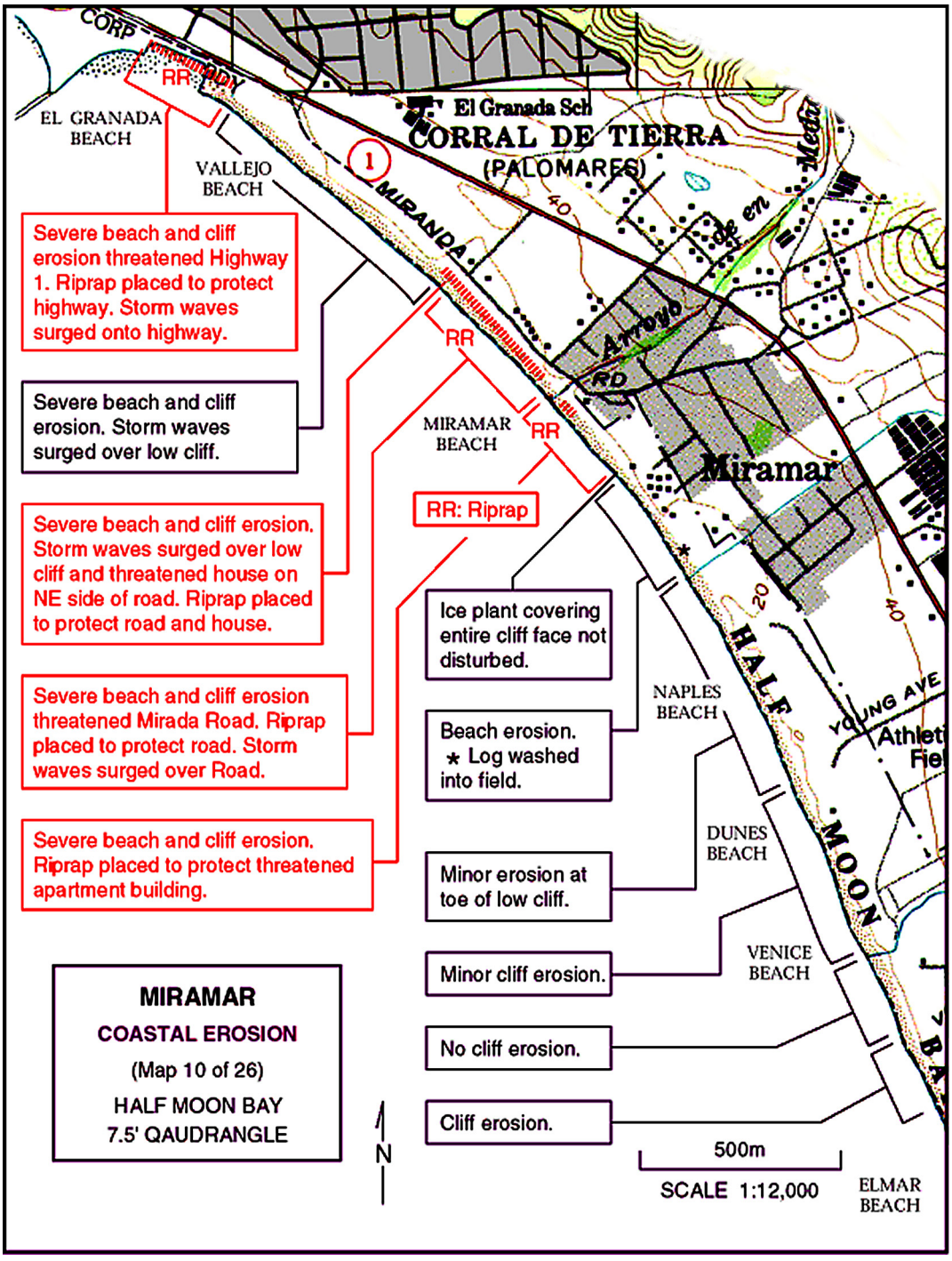

Figure 5.33. Miramar coastal erosion map (Lajoie and Mathieson, 1998).

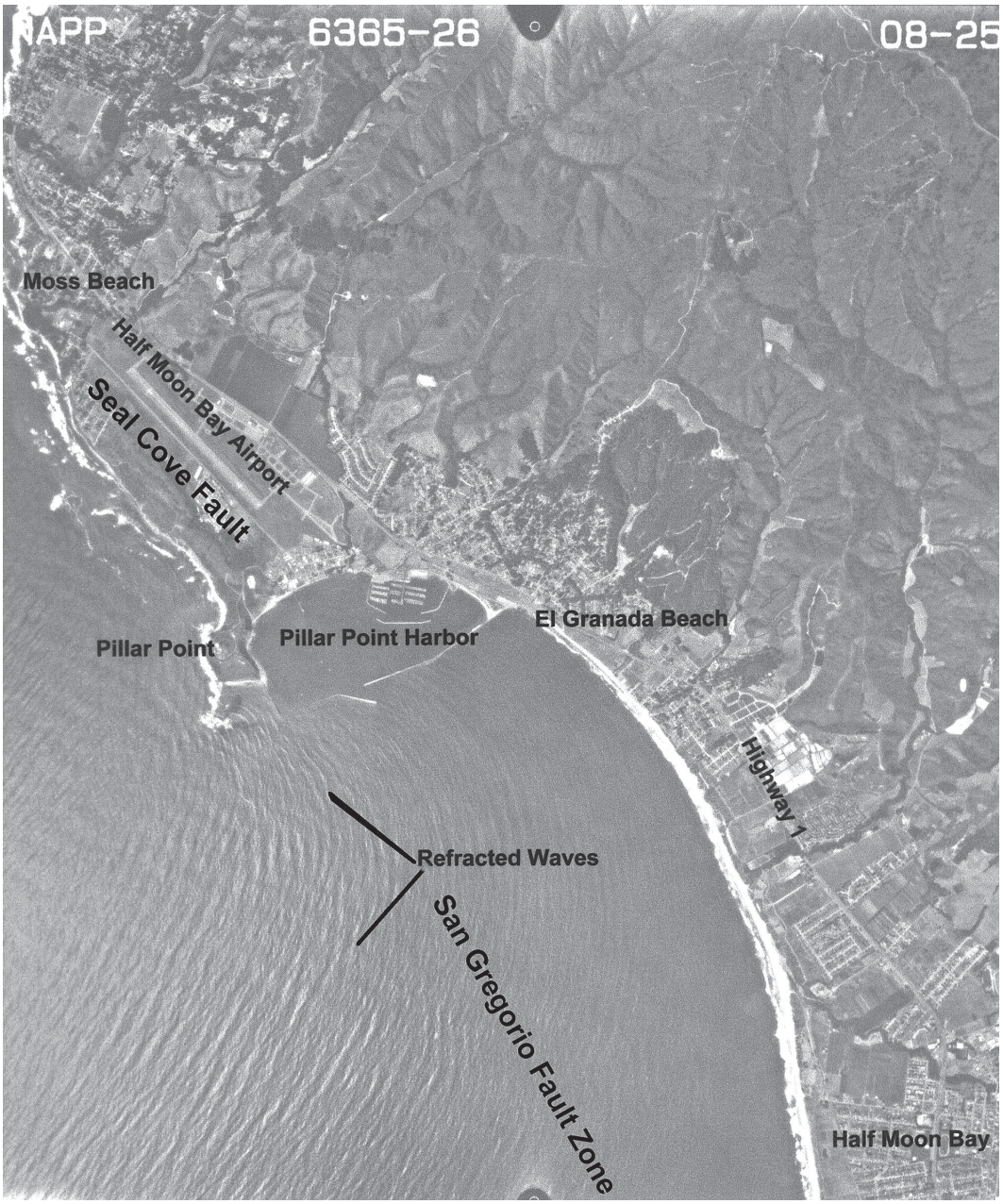

Figure 5.34. Aerial photograph taken in 1993 of wave refraction patterns at Half Moon Bay/Pillar Point Harbor.

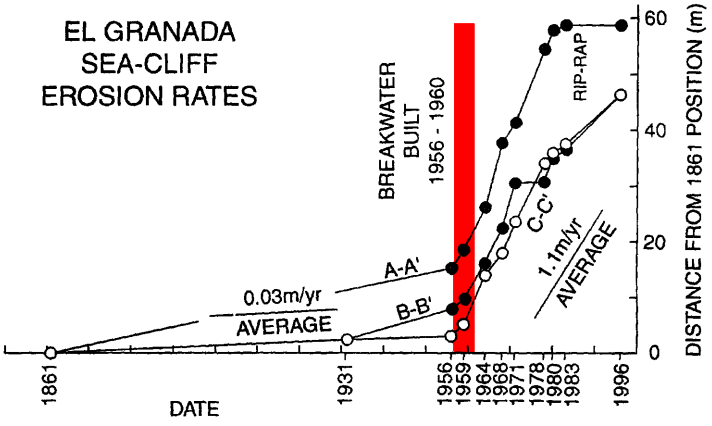

Figure 5.35. Graphical presentation of change in erosion rates at El Granada Beach before and after installation of Pillar Point Harbor breakwater (McLaughlin and Sarna-Wojcicki, 1997).

The Calaveras and San Andreas Faults In and Around Hollister

Deborah R. Harden
Department of Geology, San José State University, Calif.

Heidi Stenner,
U.S. Geological Survey, Menlo Park, Calif.

Imogene Blatz
Saratoga, Calif.

Introduction

The focus of this trip is to view the surface expression of active strike-slip faults in both manmade and natural settings. We will visit the Calaveras Fault in downtown Hollister, a small city about 90 km (55 mi) southeast of Menlo Park, and the San Andreas Fault about 15 kilometers (9 miles) southwest of Hollister. Because both faults are actively creeping in this area (Wallace, 1990), we will be able to see recently offset human structures along both fault traces. At Hollister Hills State Vehicular Recreation Area (SVRA) and along the Cienega Valley, we will also have the opportunity to see superb examples of geomorphic features created along the San Andreas Fault.

Road Log

The first portion of this excursion guide consists of a road log, with directions and mileage checked in 2001. Discussions, maps, and figures are included with the appropriate field-trip stop materials, all of which follow the road log. Figure 6.1 provides the regional setting for the route and the field-trip stops. Please note that the road log begins at the intersection of U.S.Highway 101 and Interstate 280, approximately 22 miles south of Menlo Park, and is given in miles.

Mileage/Notes

0.0 Intersection of Interstate 280 and Highway 101 (marked at the Tully Road sign on southbound 101). Our journey to Hollister takes us south through the Santa Clara Valley. South of San José, Highway 101 runs generally upstream along the alluvial valley of Coyote Creek to Morgan Hill. The Santa Teresa Hills are on the west and the Edenvale and Coyote Hills on the east.

2.0 Coyote Hills visible on left. The bedrock here is mainly serpentinized ultramafic rocks (harzburgite and dunite) of the Coast Range Ophiolite, together with melange of the central-belt Franciscan Complex (Wentworth and others, 1999).

7.2 Junction of Highway 101 and Interstate 85. Coyote Peak (1155 feet) in the Santa Teresa Hills is on the right.

11.0 Gravel and finer grained sediments crop out on the left. Pliocene to Pleistocene sediments east of the southern Santa Clara Valley can be broadly assigned to the Santa Clara Formation, which is also exposed along the San Francisco Peninsula east of the San Andreas Fault and along the western foothills of the northern Santa Clara Valley. The Santa Clara Formation is thought to be correlative in age and depositional environment with the Livermore gravels east of San Francisco Bay.

The coarse-grained fluvial gravels of Pliocene to Pleistocene age are found parallel to, but significantly elevated above, the eastern edge of the modern Santa Clara Valley. Their general distribution suggests that the valley axis has shifted westward to its modern position, probably as a result of the compression and shortening documented by recent thrust faults in the area.

In the southern Santa Clara Valley, various workers have differentiated individual gravel units, including the Packwood Gravels, mapped east of Morgan Hill by Tolman (1934). Recent mapping by Wentworth and others (1999) differentiated fault-bounded packages of Pliocene to Pleistocene sediments on the basis of distinctive source lithologies. The gravels are in thrust-fault contact with serpentinized ophiolite and melange of the Franciscan Complex.

The Silver Creek Gravels, named by Jones and others (1994) for the valley east of the Coyote Hills, are found along the foothills on the east side of the Santa Clara Valley. A tuff interbedded with the older portion of the Silver Creek gravels was mapped Wills (1995) and identified by Sarna-Wojcicki and Meyer as the Huichica Tuff. The Huichica Tuff was erupted from the Sonoma volcanic field and has been recently dated by Ar/Ar isotopic methods at 4.71 million years old (A. Sarna-Wojcicki, oral commun., 2001).

12.0 Coyote Golf Course exit. Along this portion of Highway 101, prominent white, fine-grained beds, which appear very white because of the presence of magnesite, in the median of the highway here are of probable lacustrine origin. These beds are a part of the Scheller Gravels of Wills (1995). A tephra unit identified as the Rockland Ash by Sarna-Wojcicki and others (1985) was formerly exposed along the median strip in this vicinity. The Rockland Ash, an important marker tephra throughout northern California, was erupted from the vicinity of present-day Mount Lassen. It is between 450,000 and 620,000 years old and cannot be more precisely dated at this time. It is also unknown whether the ash is interbedded with the Scheller gravels or unconformably overlying them.

14.6 Cross Coyote Creek. Anderson Dam can be seen in the hills on the left. Anderson Dam was built in 1950 and reconstructed in 1987-88. Anderson Reservoir and Coyote Reservoir, built in 1936 and located further upstream on Coyote Creek, store water imported from the Central Valley Project. Both are along the Calaveras Fault, which runs along the foothills on the eastern side of Anderson Reservoir.

16.7 El Toro Peak (1420 feet) on right overlooking Morgan Hill. While camped at "21-mile house," 21 miles south of San Jose, in August, 1861, William Brewer glowingly wrote (Brewer, 1966):

> The Santa Clara Valley (San Jose Valley of the map) is the most fertile and lovely of California. At the point where we came into it, it is about six miles wide, its bottom level, a fine belt of scattered oaks four or five miles wide covering the middle. It is here all covered with Spanish grants, so is not cultivated, but near San Jose, where it is divided into farms, it is in high cultivation; farmhouses have sprung up and rich fields of grain and growing orchards everywhere abound. But near our camp it lies in a state of nature, and only supports a few cattle. One ranch there covers twenty-two thousand acres of the best land in the valley—all valuable… We camped under some beautiful oaks, near a house, where we got hay and water. Two days were spent examining the hills to the east of the valley, from the summits of which (near two thousand feet above the valley) are to be had most magnificent views. One sharp peak rose near camp, on the west, conspicuous from every direction.

El Toro, the "sharp peak" mentioned, was in Brewer's time called "Ojo de Agua de la Coche", which on the 1:100,000-scale topographic map is the name of the land grant rancho in the area including El Toro.

18.4 East Dunne Avenue exit. In this vicinity, young terrace surfaces and gravel deposits can be seen. We are leaving the drainage basin of north-flowing Coyote Creek and entering the basin of Llagas Creek, a south-flowing tributary of the Pajaro River. East Dunne Avenue provides access to the southern end of Anderson Reservoir and Henry Coe State Park (California's largest state park). The nearby town of Gilroy is probably best known as the "garlic capital" of the world and home to the annual Garlic Festival. Garlic growing began here after World War I. However, during the 1870's, Gilroy had a brief reign as the Nation's tobacco capital and was home to our largest cigar factory. For more information see the World Wide Web at http://www.ci.gilroy.ca.us/historydoc2.html.

27.9 Junction with State Highway 152 East to Los Banos.

31.0 Exit Highway 101 onto Route 25 (Hollister-Pinnacles exit). **WARNING! This is a dangerous exit; watch for confused drivers. Route 25 is a 2-way road and has had a number of disastrous head-on collisions in recent years—be alert.**

Our route into Hollister takes us through some very productive farmland. Local crops along today's routes include garlic, strawberries, tomatoes, salad greens, and seed nurseries for flowers.

33.8 San Benito County Line (on Route 25). As happened in Santa Clara County, agriculture in San Benito County is giving way to residential development. Nevertheless, for more than 50 consecutive years, California has been the leading agricultural producer in the United States. California's agricultural output is nearly $25 billion per year, and the state grows more than half the nation's fruit, nuts, and vegetables. Agriculture still accounts for almost 1 in 10 jobs in California.

39.5 Traffic light at intersection of Route 156. Continue on Route 25 South. The low hills on either side of the road are pressure ridges along the Calaveras Fault. For further discussion of the Calaveras Fault northwest of Hollister, please see the discussion included with Stop 1 materials.

42.0 The water tank on hilltop on the right is astride a pressure ridge along the Calaveras Fault.

Hollister, with a population of 34,413, is an agricultural center undergoing a rapid transition to a suburban bedroom community. The old part of the town retains much of its Victorian architecture, and we will see many fine homes built in the late 1800's. Large tracts of new homes are concentrated south of Hollister along Route 25. The exponential growth in and around Hollister was partly fueled by the delivery of imported water from the Central Valley Project's San Felipe Project in the late 1980's; prior to that time, growth was limited by the availability of local groundwater resources. At present, imported water supplies about one third of San Benito County's need (more information at San Benito County Water District's website at http://www.sbcwd.com/).

Both the 1906 San Francisco earthquake (Rogers, 1980) and the 1989 Loma Prieta earthquake caused substantial damage in Hollister. After the 1989 quake, some buildings in the downtown area were torn down. Many chimneys were toppled, and several older wood-frame residences were either knocked from their foundations or suffered severe damage to cripple walls.

42.5 Junction of Routes 156 and 25. Continue south on Route 25 into Hollister (the road becomes San Benito Avenue). Prepare to turn right onto 6th Street. Turn west and proceed two blocks to Dunne Park at 6th Street and West Street.

43.3 **Stop 1—Dunne Park.** We will leave the vehicles here and make a walking tour along the trace of the Calaveras Fault to observe evidence of creep. The total walking distance will be about 5 blocks round-trip. Refer to Stop 1 materials for discussion. Restrooms available at this stop.

Return to vehicles and proceed back (east) on 6th to San Benito Ave. intersection.

Reset mileage at corner of 6th Street and San Benito Avenue.

0.5 Downtown Hollister.

0.7 San Benito Avenue becomes Nash Road; continue straight at the light following signs to the Hollister Hills State Vehicular Recreation Area (HHSVRA).

1.6 Turn right at stop sign (Union Road). Cross the bridge over the San Benito River. The San Benito River has a drainage area of 586 mi^2 above the bridge. It heads in the Clear Creek area and flows northwest to join the Pajaro River near San Juan Bautista. The San Benito River is reportedly a source of placer benitoite [$BaTiSi_3O_9$], our state gemstone, derived from Franciscan terranes in the headwaters. During the El Niño winter of 1997-98, the bridge was temporarily closed when scour around the pilings almost undermined the structure. The peak discharge on February 3, 1998, was 34,500 cubic feet per second, more than twice as high as any previously recorded flood peaks. For more information, see the website at http://water.usgs.gov/ca/nwis/peak.

1.7 Immediately after crossing the bridge, turn left (south) on Cienega Road. Continue following the signs to HHSVRA.

3.2 Stop sign, right turn. As we travel up the steep and winding road, we will pass road cuts on the left that expose late Tertiary sedimentary rocks to be discussed at Stop 2. On the right are some excellent views of active slump-earthflows in these sedimentary rocks. Near the summit of the Cienega Road, headward migration of one scarp has reached the road, which has been relocated at least once due to active slumping.

6.5 Cross Bird Creek.

7.0 Turn right at Hollister Hills State Vehicular Recreation Area. The San Andreas Fault runs along the valley on our left.

7.1 Pass the ranger station. Proceed on the unpaved road into the Hollister Hills SVRA. Note the erosion control structures, including sediment retention basin on right.

7.8 Turn a very sharp left and preceed uphill to the picnic tables on the south end of Radio Ridge.

7.8 **Stop 2—Radio Ridge, Hollister Hills SVRA.** Radio Ridge is a linear ridge within the San Andreas Fault Zone, and its accessible summit provides one of the best ground-level opportunities to view the geomorphic expression of the fault. The geologic and geomorphic setting of the area, as well as the SVRA itself, are discussed in the materials covering Stops 2 and 3. Pit toilet available here (multiple flush toilets available at the campground at Stop 3).

8.0 Return to intersection with main access road. Make a sharp left downhill to the campground. Park at restroom facilities.

8.2 **Stop 3—Bird Creek Campground.** This will be a brief stop to examine the strain gauge across the San Andreas Fault. Data are sent from this gauge to the U.S. Geological Survey in Menlo Park by way of the Geostationary Operational Environmental Satellite. We will also have an opportunity to view the mapped fault trace and the exposure of Bird Creek sediments along the west bank of the creek. **WARNING!**: Watch for poison oak near the creek!

Depart Bird Creek campground and continue southeast parallel to Bird Creek. We will drive by an offset weir in the Bird Creek channel. Note the dramatic change in Bird Creek as we leave the canyon and emerge onto a very flat valley at the ranger station—this is an almost-defeated stream!

9.1 Ranger Station.

9.2 Stop sign at SVRA entrance, right turn on Cienega Road. Watch for flocks of wild turkeys that frequently visit this area. The 4-wheel-drive part of the SVRA lies to the right, southwest of Cienega Road, in this area. Note the actively eroding gullies. Park housing straddles the San Andreas Fault. Park personnel frequently report maintenance nuisances due to the ongoing fault creep.

10.3 Vineyard School, built on the trace of the San Andreas Fault.

11.0 Sag pond along the San Andreas Fault. According to oral tradition passed down in the 1980's from an elderly area resident to a former ranger at the SVRA, the pond drained during the 1906 earthquake.

11.2 **Stop 4—DeRose Winery.** Park along the main winery building and watch for oncoming traffic! This historic winery, a destination of geology field trips since the 1960's, is situated directly on the San Andreas Fault. At this stop we will view the effects of creep on the winery buildings and other structures. The history of the winery and results of fault monitoring are included with the Stop 4 materials.

This is the official end of our trip. Return to Menlo Park using the route below.

Reset mileage to 0.0 at the DeRose Winery. Drive north on Cienega Road.

1.2 For the next mile, keep a forward view of the road through the breaks in the trees. There are exceptional views of the San Andreas rift valley along this stretch.

6.0 Bear left at "Y" intersection and continue on Cienega Road.

7.5 Turn left onto Union Road.

11.1 Turn left onto Route 156. Pass the turnoff to San Juan Bautista. The mission at San Juan Bautista, one of California's 21 Franciscan missions, was founded in 1797. Its location placed it a day's walk from Mission Santa Clara. The church has been in continuous use since 1803, despite damage suffered during the 1906 earthquake, when one wall collapsed. San Juan Bautista marks the boundary between the Santa Cruz Mountains segment and the central creeping segment of the San Andreas Fault (Wallace, 1990; Working Group on California Earthquake Probabilities, 1999). Today, San Juan Bautista is a popular spot for tourists seeking history, good restaurants, and shops.

18.3 Turn right onto Highway 101 North to return to Menlo Park.

Field-Trip Stop Explanatory Materials

Stop 1—The Southern Calaveras Fault In Downtown Hollister

As defined by the U.S. Geological Survey's Working Group on California Earthquake Probabilities (1996, 1999), the southern Calaveras Fault extends for approximately 26 km (16 miles) south of Coyote Reservoir and includes the portion of the fault seen at Stop 1 in Hollister. The Calaveras and San Andreas Faults merge near the town of Tres Piños (fig. 6.1; Jennings, 1994). The Working Group (1999) estimated a slip rate of 15±3 mm/yr for this segment, with approximately 60 percent accommodated by fault creep. The Working Group (1996) also considered that the 1984 Morgan Hill earthquake, M_w 6.2, is a reasonable maximum magnitude event to occur on the southern Calaveras segment.

Walking tour: At Stop 1, we will conduct a short walking tour to examine the Calaveras Fault in downtown Hollister. Because the fault is creeping at about 0.5 inch (13 mm) per year, we will be able to see its effect on human structures, including sidewalks, curbs, and buildings. Both the grid layout of the streets and lots and the historic age of many of the houses and curbs make this a particularly good place to view the surface trace of the fault (fig. 6.2). The sites visited during this trip are also described by Rogers (1969). At sites that have remained relatively unchanged since 1969, it is interesting to compare his observations of offset with those seen 32 years later.

Dunne Park, south of 6th Street, reportedly occupies the site of a former cienega, or marshy area. Two low scarps run through the park, and Rogers (1969) reported a 13-cm right-lateral offset of a fence, built in the mid-1950's, in the barbecue area. Looking west along 6th Street, note the substantial dip marking the fault trace, a particularly anomalous feature when one considers its location in the middle of an alluvial plain. The retaining curb along the north side of 6th Street is markedly offset (fig. 6.3), as are the lower and more recent curbs and sidewalks. From 6th Street, we will walk north on Powell to 4th Street. If time permits, we will also look for evidence of offset features on 5th Street.

At the intersection of Powell and 4th Street, note that Powell changes its name to Locust. **PLEASE USE CAUTION when crossing 4th Street—this is a very busy road!** After crossing the road, we will proceed east on 4th Street, examining the evidence for offset along curbs and sidewalks. The large blue house on the corner also reveals some interesting structural effects of residing on a creeping fault for more than a century.

Continue on Locust (the continuation of Powell) to the alley behind the blue house. The foundation and siding of the old garage are an excellent testimonial to the different responses of concrete and wood to fault creep. Although time does not permit us to continue our walking tour south along the fault, other dramatic evidence of fault creep can be seen near Nash Road (fig. 6.2)

Supplement to Stop 1: Paleoseismic Studies Along the Southern Calaveras Fault

Bertuccio Ranch

During 1999 and 2000, seven trenches were excavated at two sites across the southern Calaveras Fault north of Hollister (Stenner, 2000). The southern site, Bertuccio Ranch, is located 5 km northwest of Hollister (fig. 6.1), on the northern end of a 30-m-high pressure ridge. Here an east-side-up scarp delineates the fault zone and is continuous for approximately 2 km. Two creepmeters within 0.5 km of the trenches recorded creep of 14 mm per year during the period of 1971 to 1979.

Two trenches were excavated at Bertuccio Ranch. Trench 1 crosses a human-modified, ~1-m-high fault scarp at the base of a 30-m-high, fault-bounded hill. Excavated to a depth of 2 to 3 meters, this trench revealed faulting which juxtaposed colluvium from the adjacent hillslope on the east side of the fault zone against fluvial overbank deposits capped by colluvium on the west side. Evidence of faulting occurs over a 9-m-wide zone and is distributed between one main trace and numerous vertically discontinuous traces. The main trace and some of the secondary traces can be followed to the surface through fill from the early to mid 20th century, and are interpreted to be actively creeping traces.

Trench 2 (fig. 6.4) was excavated about 300 m to the north of trench 1 across a 1.8-m-high fault scarp with moderate human disturbance. Fluvial sand, overbank silt, and standing-water clay dominate the lower meter of the western half of the 2-m-deep trench. The fluvial deposits are buried by colluvium and alluvium eroded from the scarp and transported from the hill slope adjacent to Trench 1. None of the colluvial/alluvial units appear as distinct colluvial wedges, and no buried free faces were observed in the trench. Instead, the colluvium is interpreted as the result of erosion over a broad topographic scarp—either from distributed coseismic faulting across the 5-m-wide zone of deformation or from continuous creep across the zone leading to erosion of a slowly forming scarp.

Fault slip is accommodated by four major traces and numerous minor traces in trench 2. The main faults have slipped obliquely, with an approximate displacement of more than 2.5 m up-to-the-east and an unknown lateral component across the exposed zone. The fault zone has juxtaposed different facies of varying thickness, complicating measurements of vertical slip across the zone. Each fault can be traced nearly to the surface, where recognition is difficult in the massive, bioturbated, and disturbed sediments. Radiocarbon dates suggest the fluvial deposits are about 1,700 to 3,000 years old (fig. 6.4). At the current creep rate, a ~1,700-year-old fluvial sand may have experienced as much as 25 m of right-lateral slip, with perhaps one-tenth resulting in vertical slip. The upper contact of the sand is displaced ~2.4 m although the unit thins dramatically across the fault zone.

All faulting in both trenches at Bertuccio Ranch may be attributed to creep, as no fissures or consistent upward terminations were found. Coseismic rupture may have occurred at this site, but evidence for it is lacking. The absence of such features could be attributed to the likelihood that faults formed during a coseismic rupture would subsequently accommodate creep, eliminating upward terminations. The possibility that coseismic rupture was small at the surface because of attenuation caused by continuous creep may also have the effect of making event identification difficult.

Costa Ranch

Five trenches were excavated at the Costa Ranch, 9 km northwest of Hollister (fig. 6.1). During 1971-79, a creepmeter at the site recorded 15 mm of creep during one year. Another creepmeter at Shore Road, less than 2 km to the north, recorded 6.5 to 12 mm per year, depending on the averaging technique (Schulz and others, 1979; Schulz and others, 1982). The fault here makes a right step of 25 to 30 m at the southern end of the site, and north of the site the fault bends to the east, producing sag ponds in the resulting extensional zones (fig. 6.5). Trenches 1 and 2 crossed the large stepover; trenches 3, 4, and 5 crossed the fault scarp and sag pond to the north (fig. 6.5).

Trenches 1 and 2 exposed 1 to 2.5 m of overbank sediments (silt, sand, and clay), upon which a moderately to very heavily bioturbated organic horizon has developed. One dominant fault is centered approximately in the middle of the two trench exposures and strikes northward, acting as a linking fault (fig. 6.5) that transfers slip between the main faults striking northwest on either side of the stepover. Those main strands on either side of the stepover occur as secondary structures in the trench exposures. Slip is oblique here, as the fluvial units are displaced down-to-the-east approximately 50 cm across the dominant fault and ~10 cm across the secondary faults. The formation of the sag pond also suggests an extensional component of slip. The dominant fault is a 1-m-wide zone of faulting. Units on the western side have retained their original near-zero dip, but within 1.5 m of the fault zone on the eastern side, fluvial units are tilted into the fault (westward) about 15 to 30 degrees. This is probably accommodating additional extension at the main fault zone. No evidence for distinct colluvial wedge packages, fissures, or consistent upward terminations was observed. Most of the faults are traced to the surface because of continuous creep, and the other strands die out upward in the bioturbated soil horizon. These upwardly discontinuous strands may be (1) creeping, but at a rate insufficient to be detected in the youngest sediments, (2) creeping, but with most creep concentrated along the other strands near the surface, (3) currently inactive, but formerly creeping traces, or (4) formed during coseismic rupture and subsequently not creeping.

Trenches 3 and 4 exposed stratigraphy similar to that in trenches 1 and 2: fluvially deposited silt, sand, and clay overlain by an organic horizon (fig. 6.6). Three radiocarbon dates within the upper fluvial sediments yielded a range of 1,800 to 2,700 uncalibrated years BP, a comparably aged sequence to that exposed at Bertuccio Ranch. In trenches 3 and 4, an additional unit interpreted as a deposit from the sag pond is present in the fault zone. Faulting at trench 3 is localized on a 1-m-wide zone and vertically displaces a silty sand unit ~1.5 m down-to-the-east. The amount of lateral slip is unknown. On the west side of the fault zone the strata remain subhorizontal. On the east side, within 2 to 2.5 m of the fault zone, the strata are warped down into the fault as much as 10 degrees (southwest). This warping is likely accommodating extension and is the location where a silty clay (sag pond deposit) is deposited in a wedge 4 m long and more than 2 m thick against the fault scarp.

Below the sag pond deposit is a similar unit bounded on both sides by faults (labeled “fault-bounded sag pond deposits” on figure 6.6). A possible explanation for why that unit is distinct from the upper sag pond unit is that initially the continuous extension at the fault was accommodated by the down dropping of a distinct block and the subsequent filling in with fine-grained organic sediment on top of the block. As extension continued through time, an increasing percentage of it was accommodated by tilting of the sediments into the fault in addition to brittle faulting of the block, allowing broader deposition of the sag pond material across the down dropping block. The faults bounding the block continue to creep (but with only a percentage of the total slip) and have propagated into the overlying sag pond and soil deposits (see trench 4, fig. 6.6). Another possibility is that the “fault-bounded sag pond deposits” represent fill of a large fissure following coseismic rupture, but the size and shape of the unit are inconsistent with this interpretation.

Although trenches 3 and 4 are only 4 m apart, the style of deformation is different. Sediments at trench 4 are faulted over a wider zone (5m) and have been tilted more than those at trench 3, where faulting is more brittle. On the west side

of the fault, fluvial units are warped up as much as 25 degrees into the fault zone, and on the east side of the zone, the fluvial strata are tilted up to 30 degrees into the fault zone. Water saturation may play a part in the deformation of the sediment by tilting rather than by brittle faulting. In both trenches 3 and 4, some faults extend to the surface as obviously creeping faults, and many others likely are creeping but have not experienced enough creep to demarcate their location through the young, upper soil horizon. The upwardly discontinuous faults in trench 3 were difficult to trace upward through the sag pond sediments, but did not appear to terminate at a particular horizon. All deformation observed in trenches 3 and 4 can be explained solely by creep processes, but coseismic rupture cannot be excluded.

Trench 5 was excavated across the northern sag pond (fig. 6.5), revealing the structures accommodating the extension. The sag is bounded on both eastern and western sides by obliquely slipping faults (units change thickness across the structures) that let the area between them subside. The main fault zone, accommodating both normal and lateral slip, is just west of the middle of the pond. Faulting occurs throughout the area covered by the sag pond, but the main zone is ~1 m wide. As exposed in the trench, the faults either reach the surface or, as within the fairly massive sag pond clay, are difficult to trace.

Trench 5 exposed the youngest section at Costa Ranch, with approximately 2.5 m of sag pond sediment carbon dated by one sample at younger than 1,000 uncalibrated years B.P. Two dated shells suggest an even younger deposit of 300 years B.P. The sag pond strata are progressively warped down into the sag and also thicken toward the center. The uppermost unit, likely historical, also thickens into the center of the sag, and is faulted (vertical component ~1 cm each) by at least two strands that are creeping.

The deepest part of the exposure below the sag pond revealed a unit adjacent to the fault zone (and possibly crossing it) composed of both moderately organic silty clay and material comparable in appearance to the adjacent fluvial deposits. This deposit could be (1) a bioturbated mixture of scarp colluvium derived from a continuously forming scarp developed in the fluvial sediments before sag pond deposition began, (2) scarp colluvium derived from a coseismic rupture before sag pond deposition began, or (3) bioturbated pond sediment mixed with fluvial material after deposition. No fissure fills or consistent upward terminations were observed.

To date, no evidence for coseismic rupture of significant size has been found in late Holocene sediment in the 14 exposures of the southern Calaveras Fault. Creep and seismicity of micro-to-moderate magnitude may accommodate all of the fault slip, resulting in a low probability of future large earthquakes rupturing the southern part of the fault. The lack of evidence cannot preclude the possibility, however, that the fault has ruptured in a large earthquake. Coseismic rupture may have occurred at depth and did not reach the surface, or the rupture may have been severely attenuated toward the surface, with subsequent creep obscuring evidence of minor surface rupture. Future work is planned to add insight into this issue.

Stop 2 and 3—Hollister Hills State Vehicular Recreation Area

Hollister Hills

The Hollister Hills State Vehicular Recreation Area (HHSVRA) is a 6,627-acre facility operated by the California Department of Parks and Recreation. It is one of seven state-operated off-road vehicle facilities within the Department's Off-Highway Division. Approximately 4 million Californians participate in some form of off-road vehicular recreation each year (see the Division's web site at http://ohv.parks.ca.gov/html/ohvhome.htm), and the SVRAs were designed to provide safe, legal, and managed facilities to help meet this demand. Funding for staffing and maintaining the State's SVRAs comes partly from gas taxes and registration fees for off-road vehicles.

The Hollister Hills SVRA consists of two separate facilities. The portion including Radio Ridge (Stop 2) and the campground (Stop 3) is for use by off-road motorcycles, and another holding to the south (off Cienega Road en route to Stop 4) is for 4-wheel-drive vehicles (fig. 6.7). The motorcycle area includes 64 miles of trail, some of which can be seen from Radio Ridge. From Radio Ridge and while traveling through the SVRA, one can observe sediment-catchment basins, gabion baskets, and trail revegetation projects, all of which are designed to reduce and (or) mitigate erosion and sediment production.

Geologic Setting

On the southwestern side of the ridge, the linear valley of Bird Creek contains the mapped traces of the San Andreas Fault. From Radio Ridge, tall, wide-canopied sycamore trees mark the valley floor. The very steep, chaparral-covered slopes southwest of the Bird Creek valley are underlain by crystalline rocks of the Salinian block. In the area of the field trip, these rocks include substantial blocks of dolomitic marble as well as Mesozoic granitoids. Aggregate quarried from

the marble blocks has been used as road base at Radio Ridge, and large blocks have been used as decoration near the park entrance. Graniterock Company excavates marble from the hills above Stop 4.

Northeast of Radio Ridge, grass-covered and lower lying hills are underlain by Pliocene sedimentary rocks. These consist of mudstone and sandstone of both marine and nonmarine origin. Beds of lignite which today lie within the SVRA were prospected in the early 1900's, and shell fossils occur within some sandstone units. Taliaferro (1949) and Rogers (1980) mapped this unit as Purisima Formation, but other workers have assigned it to the Etchegoin Formation (Perkins, 1987). Because most workers restrict the use of Purisima Formation for units on the Pacific Plate, this unit may be more properly correlated with the lower part of the Etchegoin Formation, but Jennings and Strand (1958) have mapped it as Purisima Formation. Sandstone beds within the unit are typically vegetated with brushy chemise, whereas mudstone units are vegetated by grasses.

Soils developed on the sedimentary units northeast of the fault are fine grained and impermeable. Because they are impassable to vehicles when water saturated, this portion of the SVRA is closed during stormy weather. Hillslopes underlain by the Purisima Formation are very susceptible to failure by deep-seated slump/earthflows such as those viewed from Cienega Road en route to this stop. In contrast, soils developed on the granitic rocks southwest of the fault are coarse textured and permeable. They are highly susceptible to gullying, and several enormous gullies have formed during major storms on steep trails in the SVRA.

San Andreas Fault

Radio Ridge provides public access to one of the best places to view the geomorphic expression of the San Andreas Fault system in northern California. From the summit of the ridge, we can see examples of almost every geomorphic indicator of active strike-slip faults (fig. 6.8). The ridge itself is a topographically distinct uplift within the fault zone and may be either a compressional ridge or a laterally displaced hill. It is underlain by fossiliferous sandstone of the Purisima Formation. Northwest of Radio Ridge, a water tank marks the crest of a similarly anomalous ridge. Radio Ridge serves as a shutter ridge, deflecting Bird Creek as discussed below.

Northwest-trending linear valleys are present on both sides of Radio Ridge; the valley on the northeast side of the ridge may be a former trace of the Bird Creek channel. Sarna-Wojcicki and others (1975) mapped two traces of the fault in this area: one along the northeastern edge of the Bird Creek valley and a second along Radio Ridge. As we will see at Stop 3, the major San Andreas Fault trace, instrumented by the U.S. Geological Survey (USGS), runs along the flood-plain of Bird Creek in the approximate position of the sycamore trees. Looking southwest of Radio Ridge, one can follow the fault trace along Cienega Valley to a prominent notch in the divide seen on the skyline (fig. 6.9).

Bird Creek

Bird Creek is an excellent example of an offset stream, showing about the same amount of right lateral displacement as the length of Radio Ridge (fig. 6.7). From its headwaters, fed by perennial springs in the crystalline rocks of the Salinian block, the stream flows generally northeast to the San Andreas Fault Zone. This upper portion of the channel can be seen northwest of Stop 2—it is the valley separating the densely vegetated hillslopes from those marked by motorcycle trails and less mature chaparral, the result of a fire approximately 10 years ago. (Note: Because the park's holdings do not include the slope directly southwest of Radio Ridge, the motorcycle park itself appears to be offset along the San Andreas Fault!).

When it reaches the southeast-trending fault zone, Bird Creek, joined by its major tributary, follows the fault zone on the southwest side of Radio Ridge (fig. 6.7) for about 2000 feet (613 m) until it again turns northeast and crosses to the other side of the fault, where it has deeply incised the sedimentary rocks northeast of the fault zone. Bird Creek's gradient is dramatically flattened within the fault zone. The gradient is significantly higher in its headwater reaches, which is expected, but it is also higher downstream of the fault zone. We will have an opportunity to view low terraces and the channel of Bird Creek at Stop 3 and on our return to the ranger station.

The low terrace along the eastern bank of Bird Creek at Stop 3 contains the active trace of the San Andreas Fault. The fault is continuously creeping at this site, showing approximately 0.5 inch (12 mm) of right-lateral motion per year. A group of very large riparian sycamores and small scarp in the surface mark the fault within the campground area. An excavation along the right bank of Bird Creek, made in 1994 by Imogene Blatz, exposes a section of recent deposits of Bird Creek, including some distinctive flood deposits and calcic soil horizons. Downstream of this site, similar deposits and terraces of Bird Creek can be seen at lower elevations above the modern channel. Unfortunately, all of the low surfaces adjacent to Bird Creek have been extensively modified by motorcycles, road-building, and grazing animals. These activities have greatly hampered any definitive correlation of terraces and deposits or determination of offset across the fault.

Stop 3 also provides an opportunity to view the USGS creep-monitoring instrumentation across the main San Andreas Fault trace. The creepmeter at this site, USGS station xhr2, provides a continuous record of direct fault movement. A creepmeter is a length of wire stretched across the fault and anchored by piers on either end of the fault. When the fault moves, the wire is pulled through a measuring device, which then sends an electronic signal to the GOES satellite. The satellite antenna can be seen at Stop 3. At this particular site, vertical culverts mark the creepmeter anchors; the USGS technician services the creepmeter by descending a ladder in the culvert. Data from this station and from two instruments at Stop 4 can be accessed on the internet at http://quake.usgs.gov/research/deformation/measurements/index.html. This station showed an interesting creep event, with 5.18 mm of right-lateral slip, immediately after the 1989 Loma Prieta earthquake (fig. 6.10).

Stop 4—DeRose Winery

In the early 1850's, a Frenchman named Theophile Vache planted the first grapevines in the Cienega Valley from cuttings brought over from Europe (Williams, 1965). Vache made wine and hauled it by oxcart to San Juan Bautista, which was then a stage stop along El Camino Real, the road from Los Angeles to San Francisco. You will have the opportunity to imagine this trip when we return at the field trip's end.

The Vache vineyard was bought in 1883 by William Palmtag, who produced prize-winning wines under the labels of Palmtag Vineyard and San Benito Vineyard. In 1906, the property was sold to a group who changed its name to San Benito Vineyards Company. Vineyards in the region expanded until Prohibition, when all San Benito County wineries closed. In 1935, the vineyards reopened, and in 1943 they were acquired by W.A. Taylor and Company. (In many geological field reports, the winery is referred to as the Taylor Winery.) In 1948, San Benito County had 1,765 acres planted in grapes.

In 1953, Almaden Vineyards purchased the Cienega property and greatly expanded the capacity of the facility. At the time of Williams' (1965) report, Almaden owned 3,500 acres planted in grapes. Operations at the winery then dwindled, and the property was sold to Hueblein, Inc., in 1987, at which time it lay dormant. Pat DeRose, the current owner, began operations at the Cienega property in 1988. The vineyard currently has 100 acres in grapes, 40 of which are vines planted before 1900 (see the website at www.derosewine.com).

The San Andreas Fault Zone

As originally mapped by Taliaferro (1949), the trace of the Calaveras Fault runs through the winery buildings (fig. 6.11). On the northwestern side of the buildings, a driveway running across the fault accentuates a prominent scarp. During the 1906 earthquake, the winery buildings in the Cienega Valley were substantially damaged. The Lawson report (Lawson and others, 1908) states that "At Palmtag's winery, in the hills southwest of Tres Piños, the shock seems to have been more severe than elsewhere in the vicinity of that village. Furniture was moved, water was thrown from troughs, and an adobe building was badly cracked. One low brick winery was unharmed."

The DeRose winery is the location where fault creep was first recognized (Steinbrugge and Zacher, 1960). The main winery building was constructed by then-owners W.A. Taylor Winery in 1948. In 1956, Zacher noticed displaced concrete slabs and fractures in concrete walls during a building inspection. Using the distorted buildings, Steinbrugge and Zacher (1960) began systematic creep measurements in 1956, and reported an average rate of about 0.5 inch (12mm) of right-lateral displacement per year for the period 1948-60. They also noted a coseismic slip of 3 mm at the time of a local M 5.0 earthquake in 1960. In 1957, creepmeters were installed within and around the winery buildings (Tocher, 1960), and monitoring continues at the site today (see the website at http://quake.usgs.gov/research/deformation/measurements/index.html). Damage within the winery buildings necessitated substantial reconstruction in the mid-1990's, but continued creep already has created new cracks in the walls and floors of the main building.

On the southern side of the winery, the fault has displaced a concrete-lined drainage ditch, which in 2001 had apparently not been repaired since its construction. It is interesting to compare the amount of right-lateral offset documented in 1961 (fig. 6.12) with conditions seen on the field trip today.

References

Brewer, W. H., 1966, Up and down California in 1860-1864, Francis P. Farquhar, ed.: Berkeley, Univ. of California Press, 583 p.

California Department of Parks and Recreation, 1989, Riding the fault line on the earthquake tour: a self-guided vehicle trail, Hollister Hills State Vehicular Recreation Area: California Department of Parks and Recreation Publication 5-89,15 p.

Jennings, C.W., 1994, Fault activity map of California and adjacent areas: California Division of Mines and Geology, scale 1:750,000.

Jennings, C.A., and Strand, R.G., 1958, Geologic map of California, Santa Cruz sheet: California Division of Mines and Geology, scale 1:250,000.

Jones, D.L., Graymer, R., Wang, C., McEvilly, T.V., and Lomax, A., 1994, Neogene transpressive evolution of the California Coast Ranges: Tectonics, v. 13, no. 2, p. 561-574.

Lawson, A.C., 1908, The California earthquake of April 18, 1906, Report of the State Earthquake Investigation Commission: Washington, D.C., Carnegie Institution of Washington, Pub. 87, 2 volumes and atlas, reprinted 1969.

Perkins, J.A., 1987, Provenance of the Upper Miocene and Pliocene Etchegoin Formation: implications for paleogeography of the late Miocene of central California: U.S. Geological Survey Open-File Report 87-167, 65 p.

Rogers, T.H., 1969, A trip to an active fault in the city of Hollister: Mineral Information Service (California Division of Mines and Geology) v. 22, no. 10, p. 159-164.

Rogers, T.H., 1980, Geology and seismicity at the convergence of the San Andreas and Calaveras Fault Zones near Hollister, San Benito County, California, *in* Streitz, R., and Sherburne, R., eds., Studies of the San Andreas Fault Zone in northern California: California Division of Mines and Geology, Special Report 140, p. 19-28.

Sarna-Wojcicki, A.M., Pampeyan, E.H., and Hall, N.T., 1975, Recently active breaks, San Andreas Fault, Santa Cruz Mountains to Gabilan Range, central California: U.S. Geological Survey Miscellaneous Field Studies MF-650, scale 1:24,000, reprinted 1978.

Sarna-Wojcicki, A.M., and others, 1985, Correlation of the Rockland ash bed, a 400,000-year old stratigraphic marker in northern California and western Nevada, and implications for middle Pleistocene paleogeography of central California: Quaternary Research, v. 23, p. 236-257.

Schulz, S.S., and Burford, R.O., 1979, Catalog of creepmeter measurements in central California for 1976 and 1977: U.S. Geological Survey Open-File Report 79-1609, 375 p.

Schulz, S. S., Mavko, G.M., Burford, R.O., and Stuart, W.D., 1982, Long-term fault creep observations in central California, Journal of Geophysical Research, v. 87, no. B8, p. 6977-6982.

Steinbrugge, K.V., and Zacher, E.G., 1960, Creep on the San Andreas Fault: fault creep and property damage: Seismological Society of America Bulletin, v. 50, p. 396-404.

Stenner, H., 2000, Paleoseismic studies along the southern Calaveras Fault: Seismological Society of America, Field Trip Guide, 7 p.

Taliaferro, N.L., 1949, Geologic map of the Hollister quadrangle, California: California Division of Mines and Geology Bulletin 143 (text not published), scale 1:62500.

Tocher, D., 1960, Creep on the San Andreas Fault: related measurements at Vineyard, California: Seismological Society of America Bulletin, v. 50, p. 396-404.

Tolman, C.F., 1934, A geological report on the Coyote dam site: an unpublished report to the Santa Clara Valley Water Conservation District, 58 p.

Wallace, R.E., ed., 1990, the San Andreas Fault system, California: U.S. Geological Survey Professional Paper 1515, 283 p.

Wentworth, C., Blake, M.C., Jr., McLaughlin, R.J., and Graymer, R.W., 1999, Geologic map of the San Jose 30x60 minute Quadrangle, California: U.S. Geological Survey Open-File Report 98-795, scale 1:100,000.

Williams, Alta, 1965, Wine industry's importance to county told historians: Hollister, California, Evening FreeLance, August 10, 1965.

Wills, M.A., 1995, The Pliocene alluvial gravels in the southeastern Santa Clara Valley, California: San José State Univ., unpub. M.S. thesis, 91 p.

Working Group on Northern California Earthquake Potential, 1996, Database of potential sources for earthquakes larger than magnitude 6 in Northern California: U.S. Geological Survey Open-File Report 96-705 (see the World Wide Web at: http://quake.wr.usgs.gov/prepare/ncep/index.html).

Working Group on California Earthquake Probabilities, 1999, Earthquake probabilities in the San Francisco Bay Region: 2000 to 2030—a summary of findings: U.S. Geological Survey, Open-file report 99-517, Online Version 1.0 (see the World Wide Web at: http://geopubs.wr.usgs.gov/open-file/of99-517/).

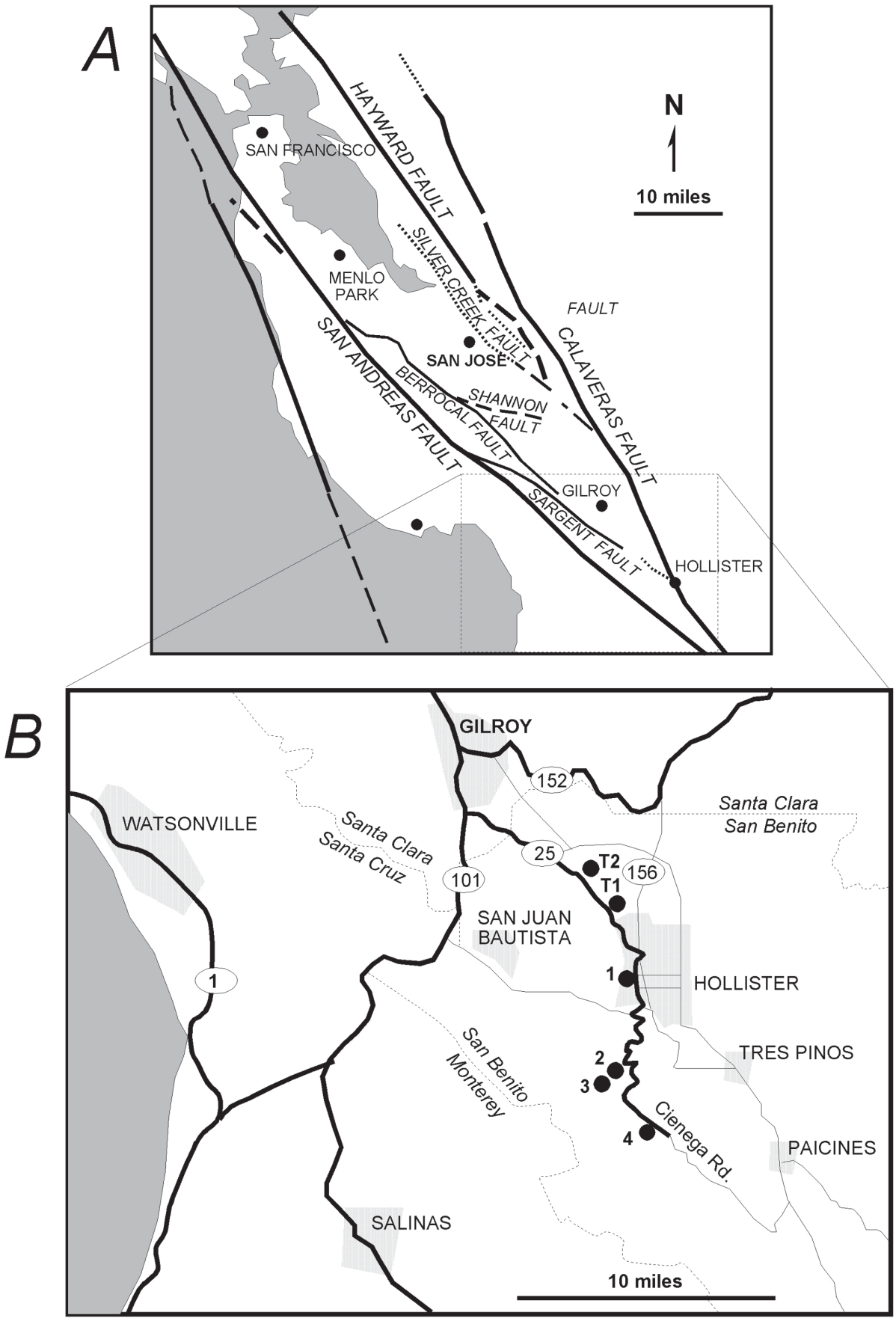

Figure 6.1. Location maps for field trip: ***A***, Major earthquake faults in the Bay area. ***B***, Field trip stops (1-4) and trench localities (T1, T2) discussed in text.

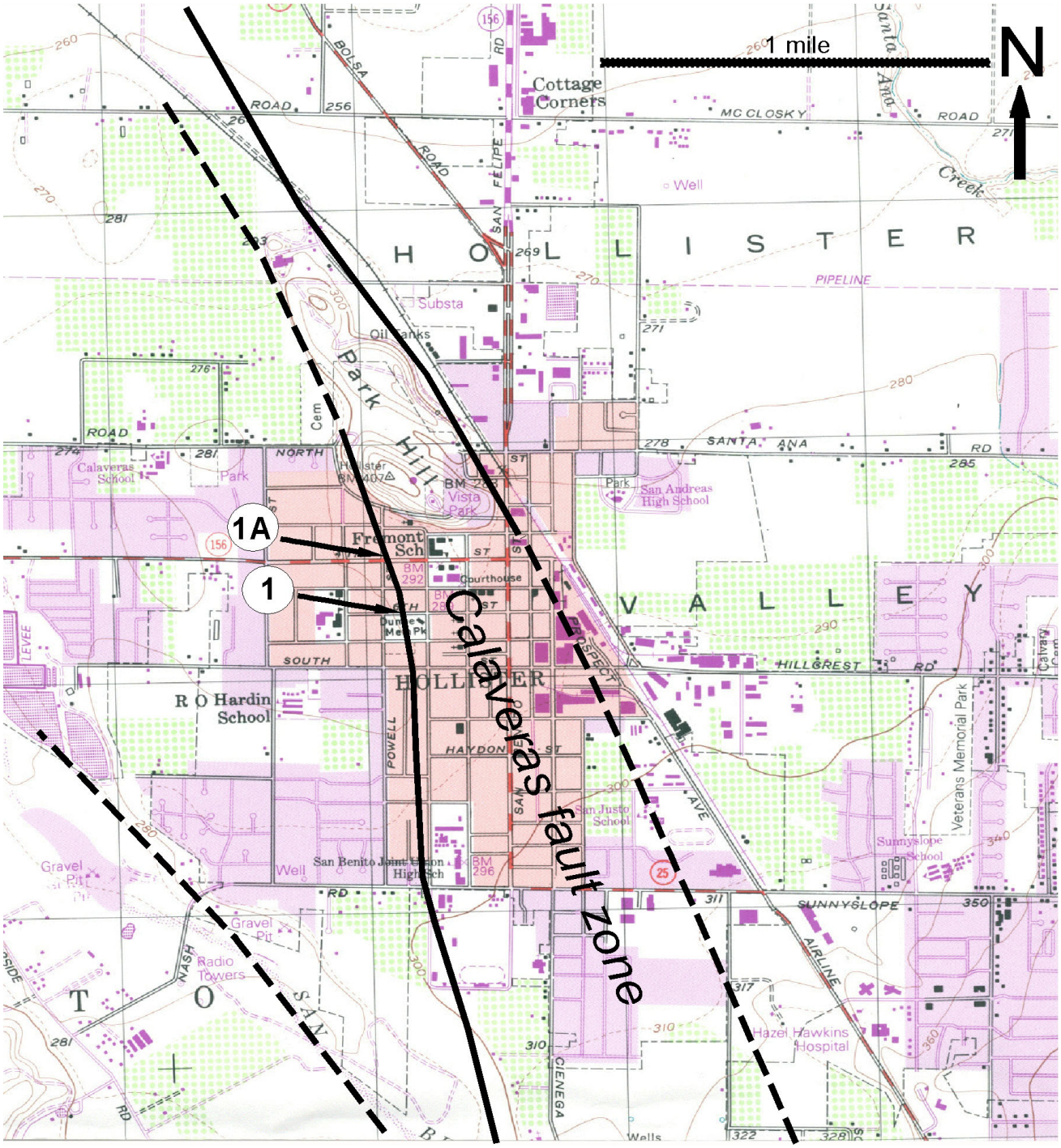

Figure 6.2. The Calaveras Fault in downtown Hollister (modified from Rogers, 1969); base map is the Hollister U.S. Geological Survey quadrangle map, scale 1:24,000.

Figure 6.3. Warped retaining wall with right lateral offset across the Calaveras Fault. View is west of 6th Street. Note rise in elevation across the fault. (Photo by Phil Stoffer, U.S. Geological Survey, 2001).

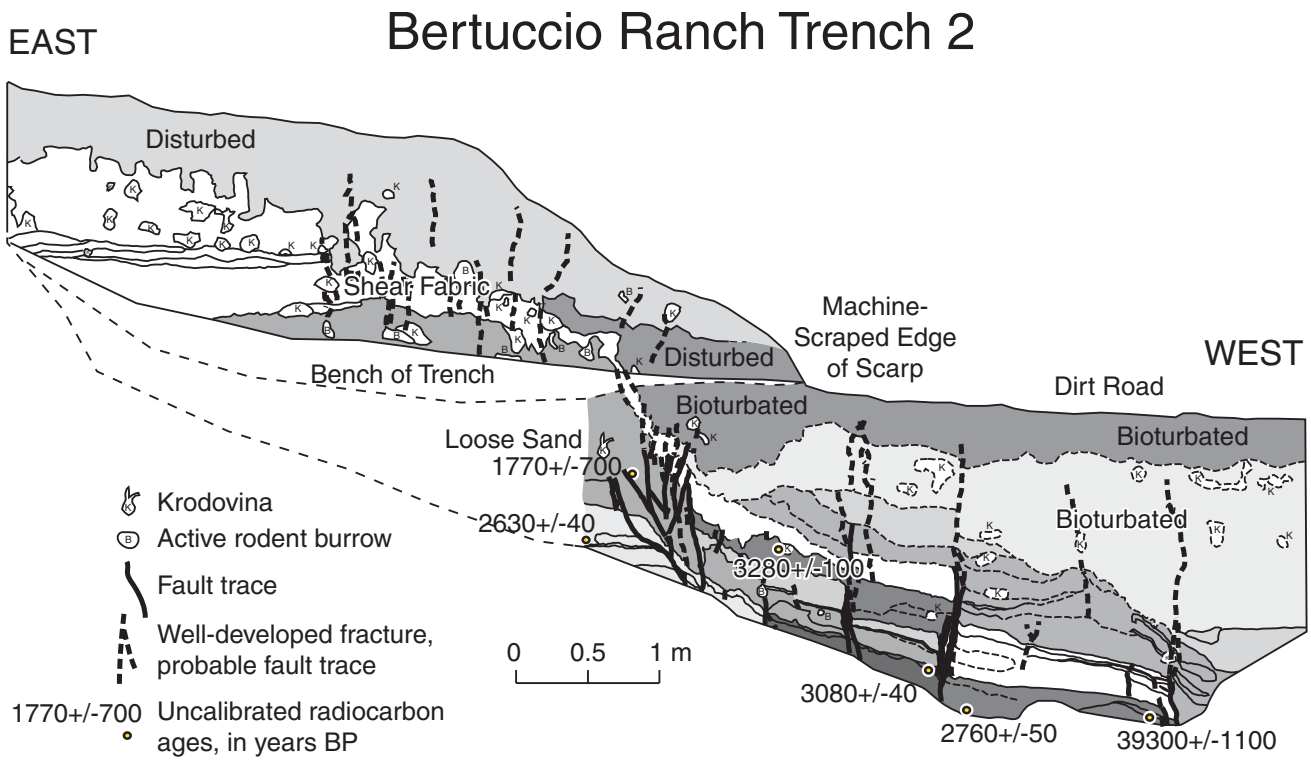

Figure 6.4. Trench log of Bertuccio Ranch trench 2. Fluvial and overbank sediments are overlain by colluvial and alluvial deposits (uppermost 3 units). Faults offset all units, and all appear to be creeping.

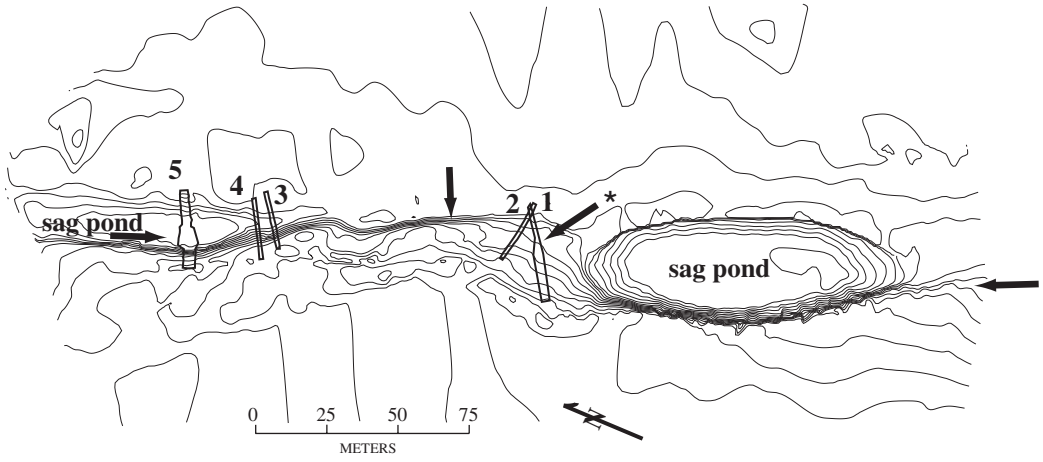

Figure 6.5. Topographic map of the Costa Ranch site. Trenches are numbered 1 through 5, arrows point at main fault, where a down-to-the-east scarp is commonly formed. Arrow labeled with asterisk marks position of linking fault. Contour interval is 15 cm.

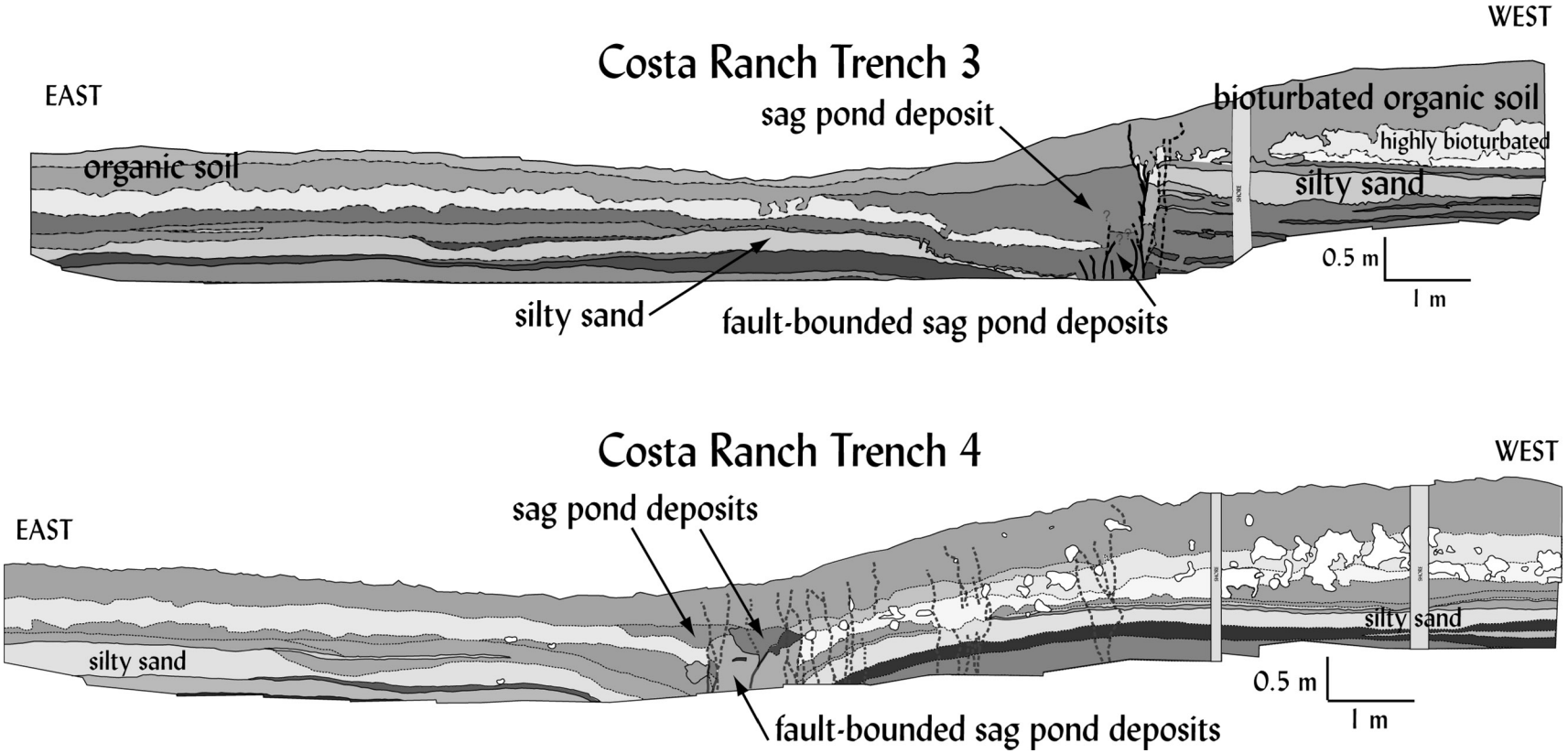

Figure 6.6. Trench logs of Costa Ranch trenches 3 and 4. Fluvial sediments, sag pond sediments, and the organic soil horizon are faulted and tilted into the fault zone to accommodate the right lateral and extensional component of slip. Although the two trenches are only 4 m apart, the styles of deformation are different.

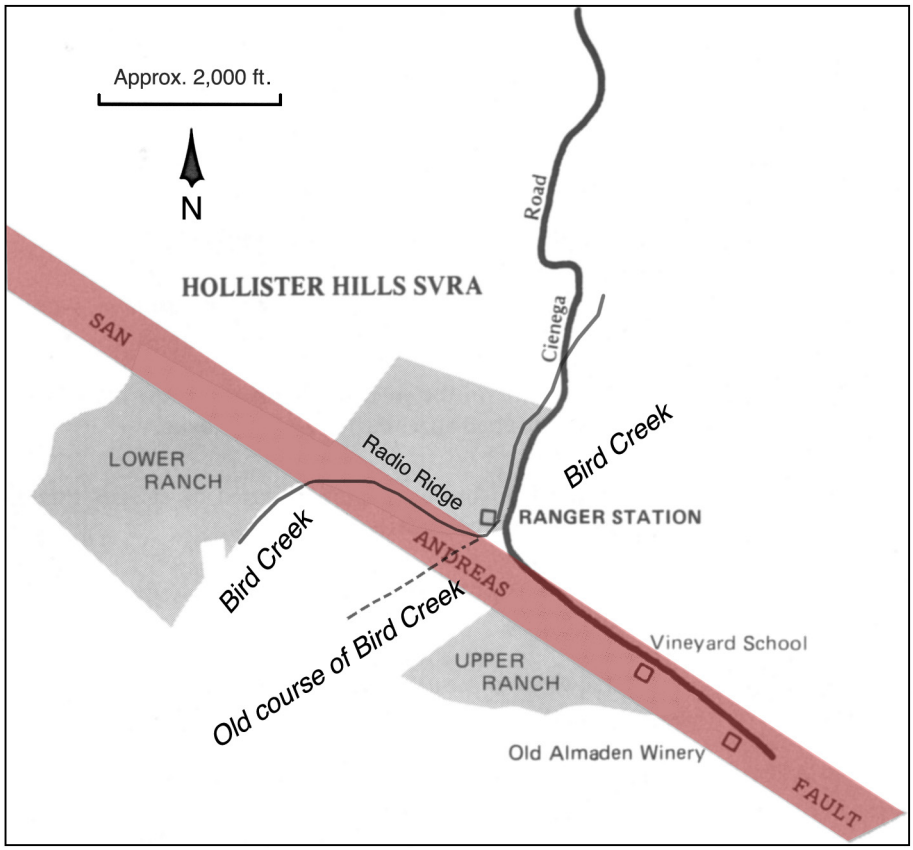

Figure 6.7. Map of Hollister Hills State Vehicular Recreation Area, showing offset of Bird Creek (modified from California Department of Parks and Recreation, 1989).

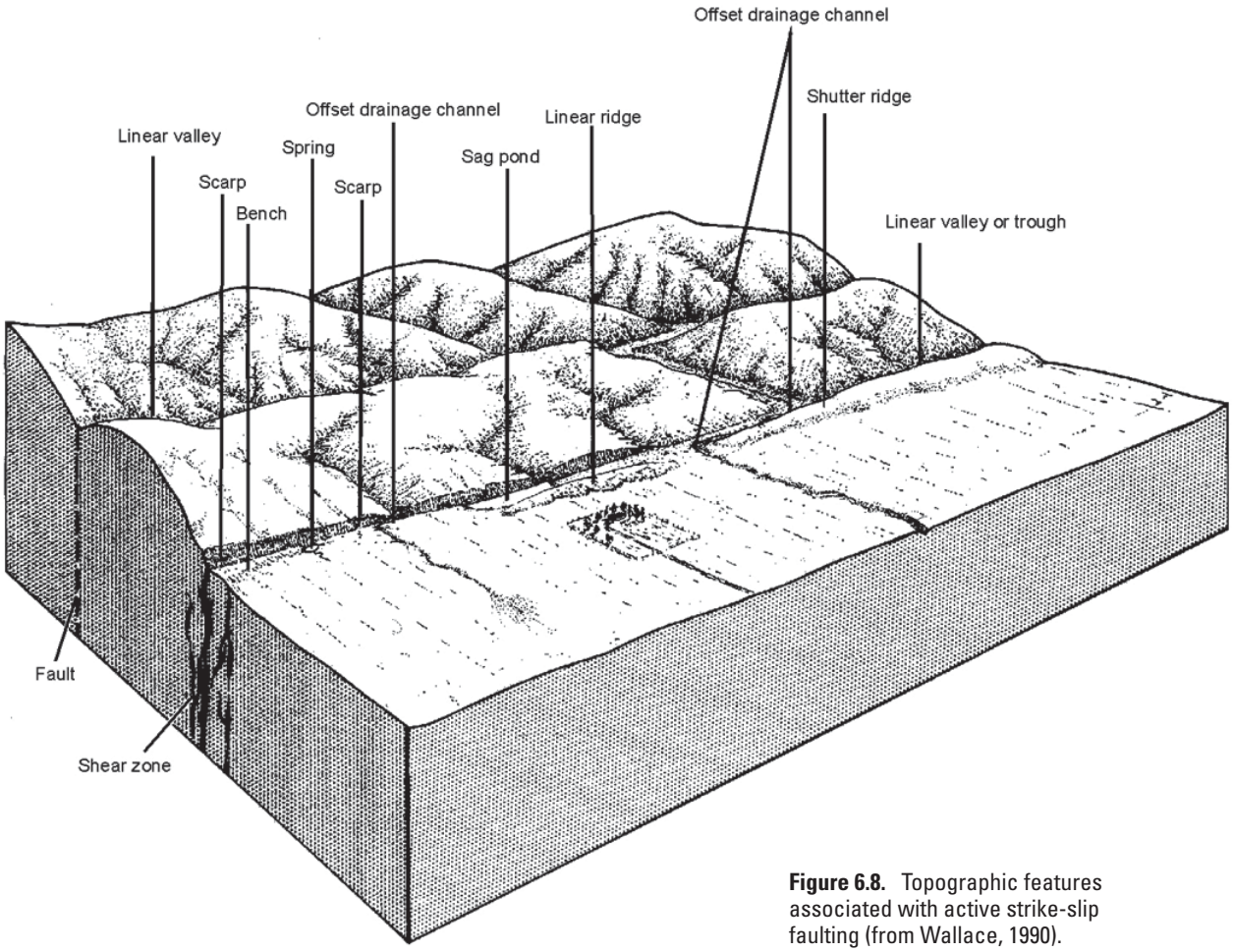

Figure 6.8. Topographic features associated with active strike-slip faulting (from Wallace, 1990).

Figure 6.9. View of the San Andreas Fault from Radio Ridge looking southwest (modified from California Department of Parks and Recreation, 1989).

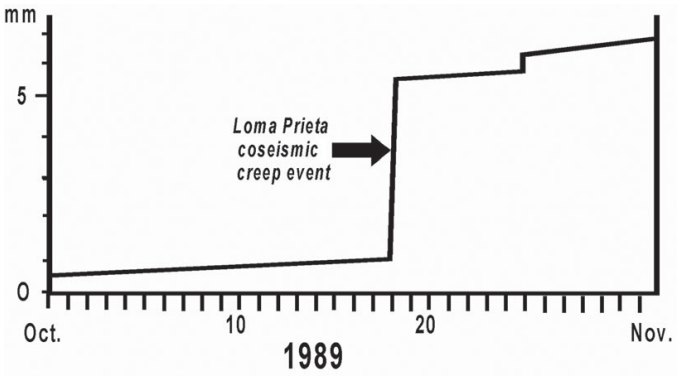

Figure 6.10. Creepmeter data for October 1989 from Hollister Hills State Vehicular Recreation Area campground (modified after a U.S. Geological Survey, 1990, unpub. manuscript).

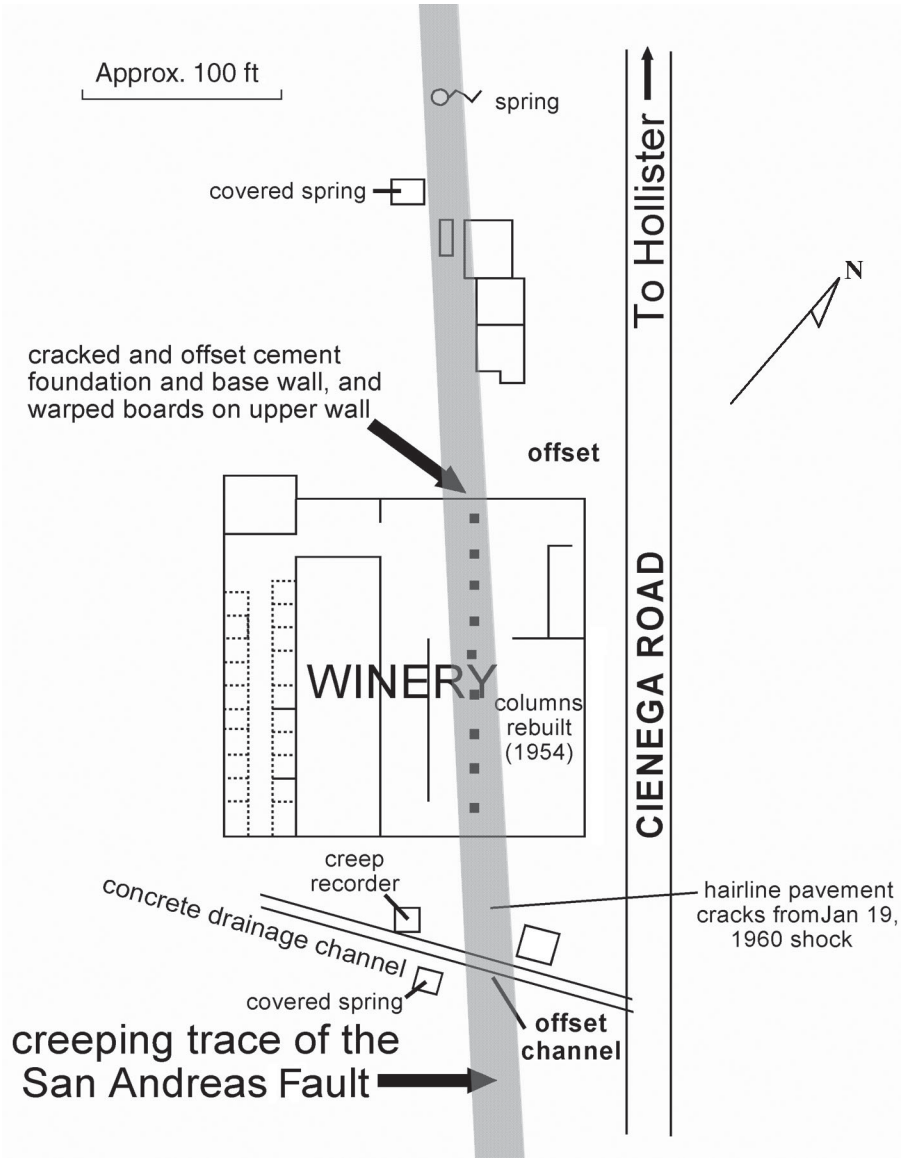

Figure 6.11. San Andreas Fault at DeRose Winery (modified from Tocher, 1960).

Figure 6.12. View northwest across San Andreas Fault trace at southern edge of DeRose Winery. Photo taken in April, 1961, by Stanley Skapinski, San José State University.

. . . And the Fog Will Burn Off By Noon—A Brief Introduction to the Weather of the San Francisco Bay Area

Scott W. Starratt
U.S. Geological Survey, Menlo Park, Calif., and
Department of Geography, University of California, Berkeley, Calif.

"*Climate is what we expect, weather is what we get.*"—Mark Twain

On the "other" coast, they often say, "If you don't like the weather, wait a few minutes." In the San Francisco Bay area, the phrase that should be spoken might be "If you don't like the weather, take a short walk." In a few hundred yards, the weather can change from gray clouds and drizzle to blue sky. Travel a little farther, and the weather requiring a sweater and parka now requires only shorts and a T-shirt. Changes in annual precipitation over short distances are just as drastic. In the mountains above Santa Cruz, rainfall averages more than 120 cm (47 inches) a year, while in the Santa Clara Valley a few miles to the east, the average precipitation is on the order of 33 cm (13 inches). These drastic variations result from a unique combination of oceanography, meteorology, and physiography.

The "typical" California climate is similar to that of the Mediterranean—a near-desert in summer, a dripping landscape in winter, and filled with glorious wildflowers in the spring. During the summer, the migrating Pacific high-pressure cell (commonly referred to as the Pacific High) deflects storms northward to Oregon and Washington, nearly preventing any measurable precipitation. In the winter, the strength of this high-pressure cell decreases and it shifts to the south, allowing moisture-laden storms to move in from the west. Often, a series of low-pressure cells can deliver heavy rains and gale-force winds. Each cell typically yields two to five days of storms, followed by a week or two of calm, clear weather.

Although dominated by the effects of high- and low-pressure cells, the climate of coastal California is moderated by the temperature of the northeastern Pacific Ocean. Ocean-related modulation reduces the intensity of cold winter temperatures, provides the source of the enormous summer fog banks, and moderates the overall annual range in temperatures (fig. 7.1; tables 7.1 to 7.3). The climate of the region surrounding the waters of San Francisco Bay lies somewhere between the extreme seasonal variations of the Central Valley and the more subdued climate of the coast because of the local topography and the constant interaction of continental and maritime air masses (Elford, 1970).

Although the moderating effect of the southward flowing California Current is apparent even during the winter (mean January temperature in Santa Cruz is 59.9°F while in Sacramento it is 53.2°F), both the magnitude and timing of the highest summer temperature changes drastically with proximity to the coast (fig. 7.1; tables 7.1 and 7.2). July temperatures in Vacaville and Sacramento in the Central Valley reach into the 90's. Two months later, as the strength of the current decreases, Half Moon Bay reaches its thermal zenith, a somewhat more moderate 66.9°F.

The dominant summer winds are from the northwest and west, and they are reinforced by the inland movement of air caused by solar heating of the air in the Central Valley (the primary reason for wind farms at Altamont Pass at the north end of the Diablo Range, east of Livermore). This effect is greatest during the day, creating both a diurnal and seasonal pattern in wind velocity. During the winter, with storm centers to the south of the San Francisco Bay area, winds may come from the east or southeast, though the prevalent wind direction is still from the west.

"*The coldest winter I ever spent was a summer in San Francisco.*"—Attributed to Mark Twain

Throughout the spring, the Pacific High increases in strength and moves closer to the coast. The combination of increased northwest wind stress and Coriolis force causes the southeastward-flowing California Current to turn to the right, away from shore. The water that moves offshore is replaced by cold, nutrient-rich water that is upwelled near the coast from intermediate water depths. The upwelled water makes the surface water temperature colder in June and July than it is during the winter.

This cold water is part of the "natural air conditioning" for which San Francisco is famous. As summer winds travel over the North Pacific, the air absorbs great quantities of moisture through evaporation. As it approaches the coast, the air is cooled by the sea, and condensation occurs. Whether the fog is thin and wispy or is so thick and heavy that anywhere else it would pass for rain depends on the temperature of the California Current and how much moisture is in the air. How far inland the fog travels depends on the temperature in the Central Valley—several days of temperatures over 100° F can draw the fog through the Carquinez Strait to the western edge of the valley. As the strength of the California Current wanes in August, the fog disappears and "summer" comes to San Francisco from August to October, the three hottest months of the year.

"*Let it rain for 40 days and 40 nights . . . and wait for the sewers to back up*"—Bill Cosby

In 1983, a new weather-related term entered the vocabulary of San Franciscans—El Niño. During an El Niño event, the temperature of the eastern tropical Pacific Ocean increases, and part of that warmer water mass migrates northward along the western coast of North America. Over the past century, most of the El Niño events have resulted in an increase in precipitation on the California coast. The 1997-98 El Niño resulted in abnormally high sea levels that contributed to millions of dollars in flood and storm damage in the San Francisco Bay area (Ryan and others, 1999). When compared to the 50-year record (fig. 7.2), the 1997-1998 El Niño showed increases in air and sea-surface temperatures (figs. 7.2*A*, *B*). Sea-surface temperatures off San Francisco and the Oregon-Washington coast were warm enough to support fish normally found in the waters off Baja California. On land, rainfall rates increased drastically, particularly in areas subject to orographic uplift of moisture-laden air masses, such as the coast range in Santa Cruz and Marin counties (figs. 7.2*C*, *D*). As a result of this enhanced precipitation, streamflow rates in northern and central California increased. At numerous sites in the Central Valley, levees in need of repairs broke, flooding many acres of farmland.

References

Elford, C.R., 1970, The climate of California: *in* National Oceanic and Atmospheric Administration, U.S. Department of Commerce, Climates of the States, v. 2, p. 538-546.

Ryan, Holly, Gibbons, Helen, Hendley, J.W., and Stauffer, P.H., 1999, El Niño sea-level rise wreaks havoc in California's San Francisco Bay region: U.S. Geological Survey Fact Sheet 175-99, 4 p.

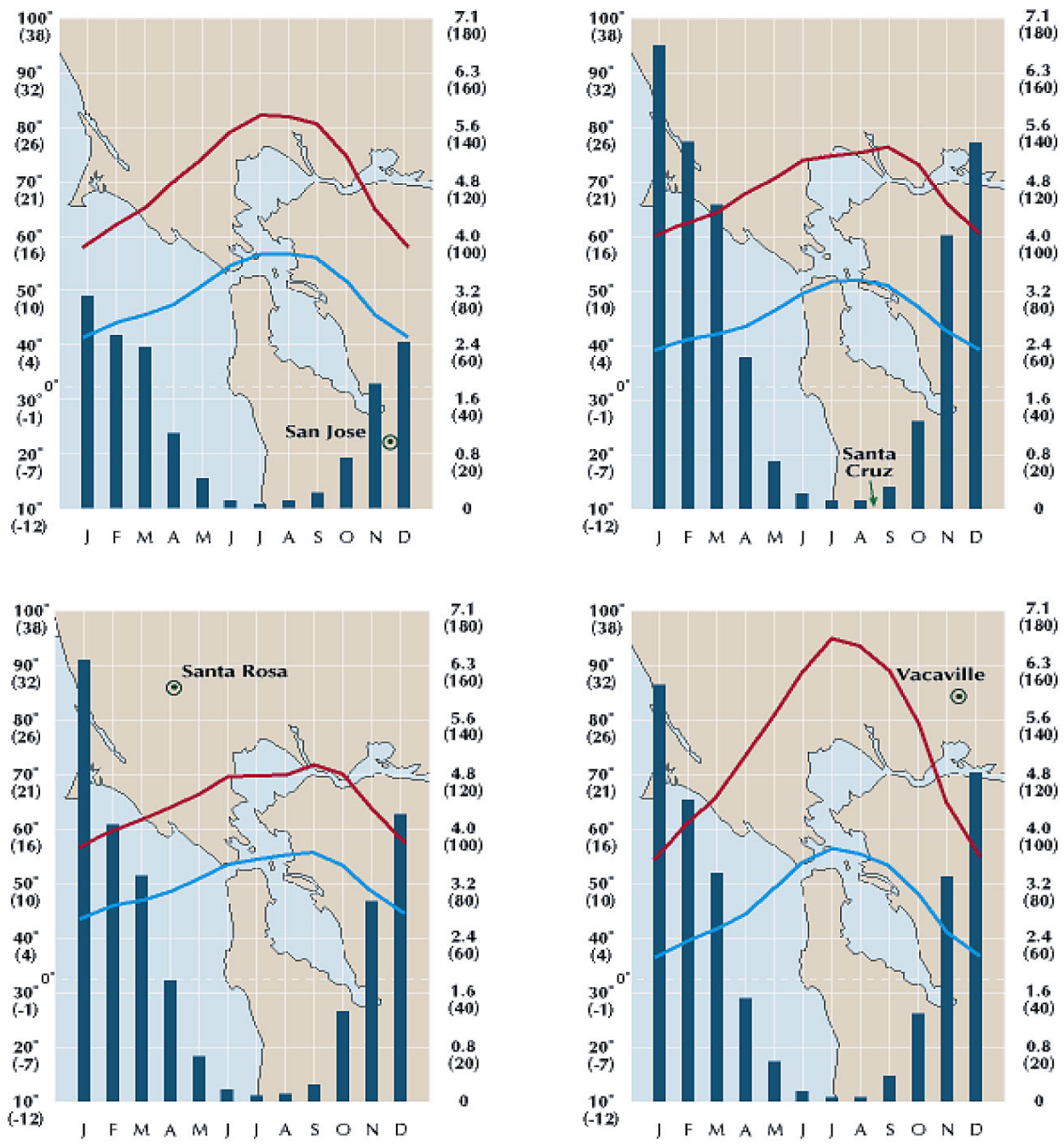

Figure 7.1. Climagraphs for thirteen sites in the San Francisco Bay area. Mean high monthly temperature (°F [°C])—red line; mean low monthly temperature (°F [°C])—blue line; precipitation (in. [mm])– blue histogram. Plotted from data in tables 7.1 to 7.3. (Data derived from the University of California, Berkeley website at http://geography.berkeley.edu/Collections/Weather/Climagraphs/Climagraph.html).

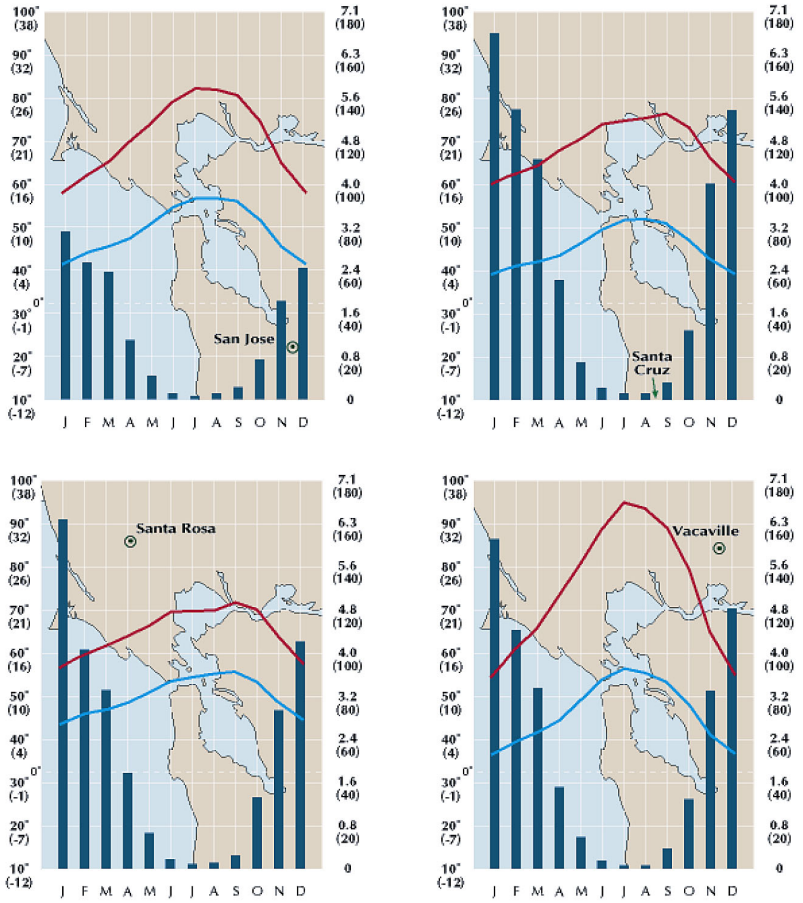

Figure 7.1.—Continued. Climagraphs for thirteen sites in the San Francisco Bay area. Mean high monthly temperature (°F [°C])—red line; mean low monthly temperature (°F [°C])—blue line; precipitation (in. [mm])– blue histogram. Plotted from data in tables 7.1 to 7.3. (Data derived from the University of California, Berkeley website at http://geography.berkeley.edu/Collections/Weather/Climagraphs/Climagraph.html).

Table 7.1. Mean monthly high temperature (°C) for thirteen sites in the San Francisco Bay region. Highest month—red; lowest month—blue (data derived from the University of California, Berkeley website at http://geography.berkeley.edu/Collections/Weather/Climagraphs/Climagraph.html).

Location	Latitude	Longitude	Jan	Feb	Mar	Apr	May	Jun	Jul	Aug	Sep	Oct	Nov	Dec
Berkeley	37.87	122.27	56.2	59.3	61.4	63.5	66.1	69.1	69.3	69.5	71.4	69.6	63.5	57.0
Fairfield	38.27	122.07	55.5	61.8	65.9	71.3	77.9	84.3	88.9	88.7	86.4	78.6	65.5	55.8
Half Moon Bay	37.47	122.45	58.1	59.3	59.6	60.5	61.4	63.0	63.8	65.1	66.9	65.9	62.8	58.7
Livermore	37.67	121.77	56.5	60.9	64.8	70.6	76.6	83.1	89.5	88.9	86.4	78.2	66.2	57.3
Los Gatos	37.23	121.97	57.9	62.0	65.4	70.7	75.9	81.6	85.9	85.3	83.1	76.0	65.4	58.2
Mt. Diablo	37.87	121.93	55.0	57.2	59.0	64.5	70.8	78.8	86.8	86.2	82.8	74.3	62.3	56.1
Petaluma	38.27	122.65	56.6	61.7	64.2	68.4	72.2	78.3	82.4	82.7	82.0	76.2	65.7	57.0
Sacramento	38.58	121.50	53.2	59.5	64.6	71.0	77.9	85.5	91.4	90.3	86.0	76.6	64.0	53.8
San Francisco	37.77	122.43	56.7	60.2	61.2	62.9	63.9	66.0	66.0	67.0	70.0	69.4	63.7	57.3
San Jose	37.35	121.90	57.9	62.1	65.3	70.0	74.3	79.2	82.2	81.8	80.6	74.7	65.1	58.0
Santa Cruz	36.98	121.98	59.9	62.5	64.3	67.7	70.6	73.8	74.6	75.3	76.3	73.2	66.2	60.5
Santa Rosa	38.45	122.72	57.4	62.1	65.4	70.0	74.4	80.0	83.2	83.4	83.1	77.3	66.5	58.0
Vacaville	38.40	121.97	54.5	61.5	66.2	73.3	81.0	88.8	95.0	93.7	89.5	79.6	65.2	55.0

Highest Month

Lowest Month

Table 7.2. Mean monthly low temperature (°C). Highest month—red; lowest month—blue (data derived from the University of California, Berkeley website at http://geography.berkeley.edu/Collections/Weather/Climagraphs/Climagraph.html).

Location	Latitude	Longitude	Jan	Feb	Mar	Apr	May	Jun	Jul	Aug	Sep	Oct	Nov	Dec
Berkeley	37.87	122.27	43.0	45.5	46.5	48.0	50.5	53.0	54.0	54.7	55.2	52.9	48.4	44.2
Fairfield	38.27	122.07	37.4	40.9	43.2	45.9	50.1	53.7	55.7	55.9	54.3	49.5	42.3	37.5
Half Moon Bay	37.47	122.45	43.0	43.8	44.1	44.7	47.4	49.9	51.6	52.7	51.6	48.6	45.9	43.4
Livermore	37.67	121.77	36.0	38.8	40.8	43.2	47.5	51.5	54.0	53.8	52.2	47.4	40.6	36.6
Los Gatos	37.23	121.97	38.2	40.5	41.9	43.6	47.4	51.5	53.9	53.6	52.6	48.3	42.6	38.4
Mt. Diablo	37.87	121.93	39.0	40.8	40.6	43.3	46.9	52.7	60.2	59.8	57.2	51.9	44.6	40.4
Petaluma	38.27	122.65	37.8	40.3	41.4	43.0	46.5	50.2	51.6	51.8	51.2	47.2	41.8	38.1
Sacramento	38.58	121.50	39.5	43.1	45.6	48.4	52.4	56.7	59.0	58.5	56.9	51.6	44.4	39.8
San Francisco	37.77	122.43	46.0	48.3	48.9	49.7	51.1	53.0	53.7	54.8	55.8	54.7	51.2	46.9
San Jose	37.35	121.90	41.3	44.2	45.6	47.5	51.1	54.6	56.7	56.7	56.0	51.8	45.8	41.5
Santa Cruz	36.98	121.98	39.0	41.0	42.0	43.3	46.4	49.4	51.6	51.8	50.8	47.2	42.7	39.1
Santa Rosa	38.45	122.72	36.8	39.4	40.5	42.5	46.1	49.8	50.9	50.8	49.9	46.1	40.6	37.4
Vacaville	38.40	121.97	36.6	39.7	42.0	44.6	49.4	54.2	56.7	55.5	53.5	48.3	41.5	36.9

Highest Month

Lowest Month

Table 7.3. Monthly precipitation (inches) (data derived from the University of California, Berkeley website at http://geography.berkeley.edu/Collections/Weather/Climagraphs/Climagraph.html).

Location	Latitude	Longitude	Jan	Feb	Mar	Apr	May	Jun	Jul	Aug	Sep	Oct	Nov	Dec
Berkeley	37.87	122.27	4.80	4.02	3.23	1.73	0.63	0.18	0.04	0.07	0.27	1.27	2.88	4.14
Fairfield	38.27	122.07	5.16	3.74	3.13	1.33	0.51	0.19	0.02	0.07	0.29	1.27	2.85	3.91
Half Moon Bay	37.47	122.45	5.49	4.20	3.95	1.84	0.73	0.27	0.11	0.21	0.41	1.60	3.31	4.64
Livermore	37.67	121.77	2.98	2.55	2.15	1.09	0.43	0.10	0.02	0.05	0.16	0.72	1.74	2.56
Los Gatos	37.23	121.97	5.64	4.69	3.85	1.63	0.49	0.08	0.03	0.06	0.26	1.09	2.93	4.40
Mt. Diablo	37.87	121.93	5.00	4.06	3.45	1.72	0.77	0.19	0.04	0.07	0.32	1.33	3.18	3.98
Petaluma	38.27	122.65	5.75	4.38	3.40	1.56	0.51	0.19	0.03	0.09	0.26	1.36	3.38	4.39
Sacramento	38.58	121.50	3.72	3.16	2.67	1.40	0.61	0.16	0.01	0.03	0.31	0.92	2.01	3.14
San Francisco	37.77	122.43	4.63	3.28	3.03	1.32	0.50	0.16	0.03	0.08	0.24	1.08	2.92	3.65
San Jose	37.35	121.90	3.05	2.48	2.31	1.06	0.41	0.09	0.04	0.09	0.21	0.71	1.78	2.38
Santa Cruz	36.98	121.98	6.67	5.28	4.36	2.16	0.66	0.20	0.09	0.10	0.29	1.24	3.92	5.27
Santa Rosa	38.45	122.72	6.35	5.04	4.21	2.07	0.83	0.28	0.03	0.11	0.35	1.75	3.75	5.44
Vacaville	38.40	121.97	5.99	4.32	3.27	1.46	0.55	0.12	0.03	0.03	0.34	1.24	3.22	4.73

Highest Month

Lowest Month

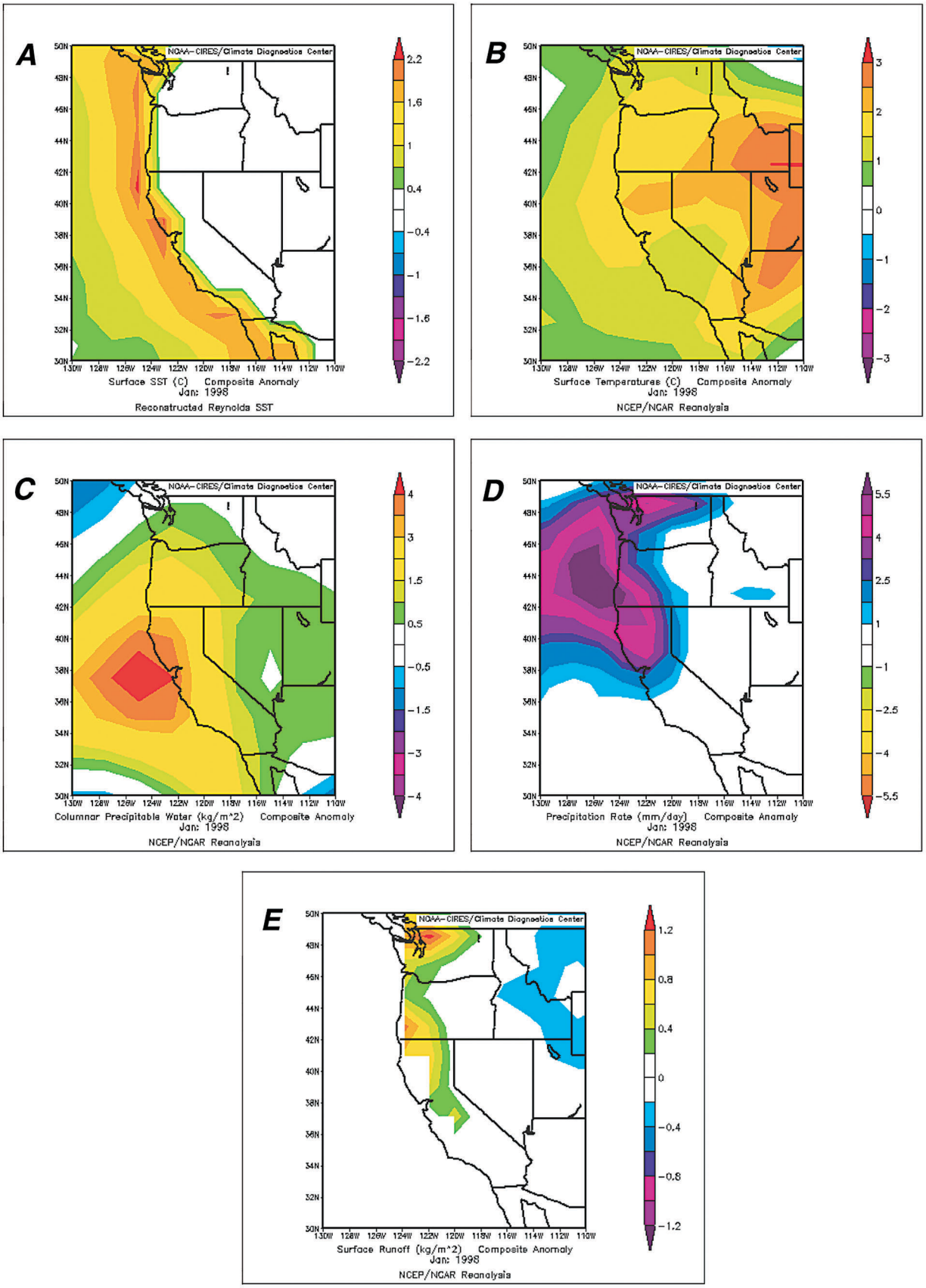

Figure 7.2. January 1998 (El Niño) variations from the mean the for period 1950-99. ***A***, sea surface temperature (°C), ***B***, air temperature (°C), ***C***, available moisture (kg/m2). ***D***, precipitation rate (mm/day), ***E***, surface runoff (kg/m^2) (data derived from the National Oceanic and Atmospheric Administration website at http://www.cdc.noaa.gov/Composites).

Consumer Uses of Industrial Minerals in the San Francisco Bay Area—Houses to Interstates

John P. Galloway
U.S. Geological Survey, Menlo Park, Calif., and
Department of Science and Math, Cañada College, Redwood City, Calif.

Judy Weathers
U.S. Geological Survey, Menlo Park, Calif.

Dave Frank
U.S. Geological Survey, Spokane, Wash.

Few people realize the importance of industrial minerals in their everyday lives. The average American uses about one million pounds of industrial minerals during a lifetime. The term "industrial minerals" includes nonmetallic minerals such as limestone, clays, cement (portland and masonry), dimension stone, and aggregates. Although aggregate is not a mineralogical definition, it is a commercial designation for a group of mineral products that include industrial sand and gravel, construction sand and gravel, and crushed stone.

California—Value of Nonfuel Mineral Production

In 1997 California was the third leading state in the Nation in total nonfuel mineral production value. The term "nonfuel mineral production" and related "values" encompass variations in meaning, depending on the minerals or mineral products. Production may be measured by mine shipments, mineral commodity sales, or marketable production (including consumption by producers) as applicable to the individual mineral commodity, (U.S. Geological Survey, 1997, p. 53). The estimated value for 1998 was $2.97 billion, with industrial minerals accounting for more than 90 percent of the total value (fig. 8.1).

California was the only state in 1998 to produce boron, rare-earth concentrates, and asbestos. Approximately 60 percent of the boron produced is used in the manufacture of glass, glass fibers, and insulation. The largest use of rare earth metals is in the manufacture of catalysts for chemical processes. Rare earths are also used as a glass additive, as phosphors in laser crystals, and in nickel-hydrate rechargeable batteries. In 1999, Americans used more than 15,000 tons of asbestos. Asbestos is used in roofing products, gaskets (which are resistant to heat and corrosion), and friction products such as in automotive brakes and clutches (Virta, 2001).

The state remained first in 1998 in the production of diatomite, portland cement, and construction sand and gravel. Diatomite is used as an absorbent for industrial spills, as pet litter, a filler in paints, insulation, mild abrasive, or as an additive in cement and other compounds. Cement is produced from a silty limestone consisting of calcite, clay minerals, and a small amount of iron oxide. Cement can be used alone but is used more commonly as a component of concrete, which is a mixture of cement, sand, gravel, and/or other industrial minerals. The most common type of cement, which hardens when water is added, is portland (or hydraulic) cement. For additional information on aggregates see Goonan (1999) and Tepordei (1997).

California continued to be second in the production of feldspar and magnesium compounds. Feldspar is used in glass and ceramics and is added to aluminum for improving hardness and durability. Magnesium compounds are used in aluminum alloys and as structural components of automobiles and machinery. California was one of only two states that reported production in 1998 for soda ash, titanium, and mercury. Soda ash is essential as a raw material in glass and detergents and in other important industrial applications, such as paper manufacturing and water treatment. Titanium is used in high-temperature applications, such as combustion engines and parts of aircraft and spacecraft. Thirty percent of the weight of a modern aircraft may consist of titanium. Mercury is used for the manufacture of industrial chemicals and for electrical applications. California was the first of two states to produce natural sodium sulfate, used in soaps, detergents, pulp and paper, and textiles.

California was also a leading producer of clays, gypsum, talc, masonry cement, industrial sand and gravel, and salt. Clays are used in sanitary ware, ceramic tiles, as an absorbent, as a sand-bonding agent added to portland cement, as a refractory product (heat-resistant bricks and blocks), and in the paper industry. Gypsum is one of the most widely used minerals in the world. It is estimated that the typical new American home contains more than 7 metric tonnes of gypsum. Talc is used in the paint, paper, and plastics industries. Salt is added to food as a flavor enhancer, used in the paper, pulp and textile, and water purification industries, and used to make many consumer-related end-use products such as neoprene rubber and polyvinyl chloride (PVC).

Industrial minerals are produced at several dozen sites in the San Francisco Bay area. Figure 8.2 shows those locations active in seven Bay area counties in 1997-1998.

A Typical House—Construction and Manufacturing Minerals

Construction and manufacturing minerals are the least recognized of the world's minerals. An average house contains 60 tons of concrete products, 7 tons of gypsum (wallboard), 5 tons of sand, gravel, and stone, and 0.1 ton of glass (Kesler, 1994). A wide variety of industrial minerals are used to build a typical house (fig. 8.3).

- Roof and attic: asphaltic roof shingles or rolled roofing, imitation red clay tile, roof sealant around vent flanges, insulation.
- Ceiling and walls: gypsum wall board, joint cement, paper joint tape, caulking compounds, paint, adhesive for pipes, decorative tile, fireplaces made of brick or stone.
- Floor and foundation: portland cement concrete slab, clays for floor tile, a sand foundation for pipes, adhesive for floor tile, and grout for ceramic tile, clay or PVC pipes.
- Appliances: porcelain kitchen sink, particle board for kitchen cabinets, ceramic tiles, adhesive and caulking, glass shelves, insulation.
- **Clays**, of various types, are used in bricks, concrete, books, cosmetics, and dishware/ceramics.
- **Limeston**e is used in concrete, books, carpets/rugs, and cosmetics.
- **Industrial sands** are used in computers, telephones (a telephone contains items made from over 40 different types of minerals), cameras, televisions, drinking glasses, windows, and microwaves. Quartz, which comes from industrial sands and gravels, is the basic constituent of glass. Glass is analogous to steel and cement in that it consists largely of a processed mineral raw material (industrial sand) with mineral additives.
- **Construction sand and gravel** are used to make our driveways (concrete pavement) and the roads we drive on. The average six-room house requires 39 tons of aggregates
- **Salt** is used not only for cooking but also in detergents and in the manufacturing of plastics and rubber products.

For a list of construction minerals used in a house see the Nevada Commission on Mineral Resources, Division of Minerals Web site on construction materials used for a kitchen (http://minerals.state.nv.us/prog_education/construct.htm) and Weathers and others (2000).

Aggregates—Buildings to Highways

Aggregates are composed of rock fragments that may be used in their natural state or after mechanical processing such as crushing, washing, or sizing. Natural aggregates include sand, gravel, and crushed stone. Recycled aggregates consist mainly of crushed concrete and crushed asphalt pavement (Goonan, 1999). Construction aggregates are used for road base, riprap, cement concrete, plaster, and asphalt. As American society grows, the demand for new infrastructures such as industrial buildings and highways grows. Natural aggregate is very inexpensive, but it cannot be transported more than a few miles from its source without becoming prohibitively expensive; transportation more than six miles from the aggregate source adds $1 per ton in transportation cost (Kesler, 1994). Mining of aggregates near urban centers can increase atmospheric pollution (particulate matter—dust) and create other environmental problems related to groundwater resources. The price of aggregates constitutes as much as half of the cost of cement in some cities in the northeastern United States. In many areas of the United States conveniently located aggregate reserves are becoming scare. As our infrastructures, especially roads, need replacement or become obsolete, they are demolished, creating large quantities of demolition waste that yields 200 million metric tons of recycled aggregates annually. Asphalt paving material is recovered from demolished roads and is recycled as aggregate for road base or as asphalt binder. It is estimated that more than 100 million tons of concrete and worn-out asphalt pavement are recycled annually into usable aggregates. "Aggregates produced from recycled concrete supply roughly 5 percent of the total aggregate market (more that 2 billion tons per year), the rest being supplied by aggregates from natural sources such as crushed stone, sand, and gravel" (Goonan, 1999). The bulk of the aggregates recycled from concrete are used as road base, the remainder for new concrete mixes, riprap, and general fill. Figure 8.4 shows the materials flow cycle for aggregates. The future of the aggregate industry will be determined by the availability of raw material (natural or recycled aggregates), demand for new infrastructure, and favorable transportation distances.

References

Goonan, T.G., 1999, Recycled aggregates - profitable resource conservation: U.S. Geological Survey, Fact Sheet FS-181-99. [http://greenwood.cr.usgs.gov/pub/fact-sheets/fs-0181-99/].

Kesler, S.E., 1994, Mineral resources, economics and the environment: New York, Macmillan College Publishing Company, 391 p.

Larose, Kim, Youngs, Les, Kohler-Antablin, Susan, and Garden, Karen, 1999, Mines and mineral producers active in California (1997-1998): California Division of Mines and Geology Special Publication 103 (revised 1999), 169 p., 1 sheet.

State of Nevada, Commission on Mineral Resources, Division of Minerals, 2001, Construction materials used for - kitchen [http://minerals.state.nv.us/prog_education/construct.htm].

Sznopek, J.L. and Brown, W.M., 1998, Materials flow and sustainability: U.S. Geological Survey Fact Sheet FS-068-98 [http://greenwood.cr.usgs.gov/pub/fact-sheets/fs-0068-98/].

Tepordei, V.V., 1997, Natural aggregates—foundation of America's future: U.S. Geological Survey Fact Sheet, FS-144-97 [http://minerals.usgs.gov/minerals/pub/commodity/aggregates/].

U.S. Geological Survey, 1997, Mineral yearbook, area report, domestic 1997, v. 2, p. 53-59.

Virta, R.L., 2001, Some facts about asbestos: U.S. Geological Survey Fact Sheet FS 012-01. [http://pubs.usgs.gov/factsheet/fs012-01/].

Weathers, Judy, Galloway, John, and Frank, Dave, 2000, Minerals in our environment: U.S. Geological Survey Open-File Report 00-144, 1 sheet [http://geopubs.wr.usgs.gov/open-file/of00-144/].

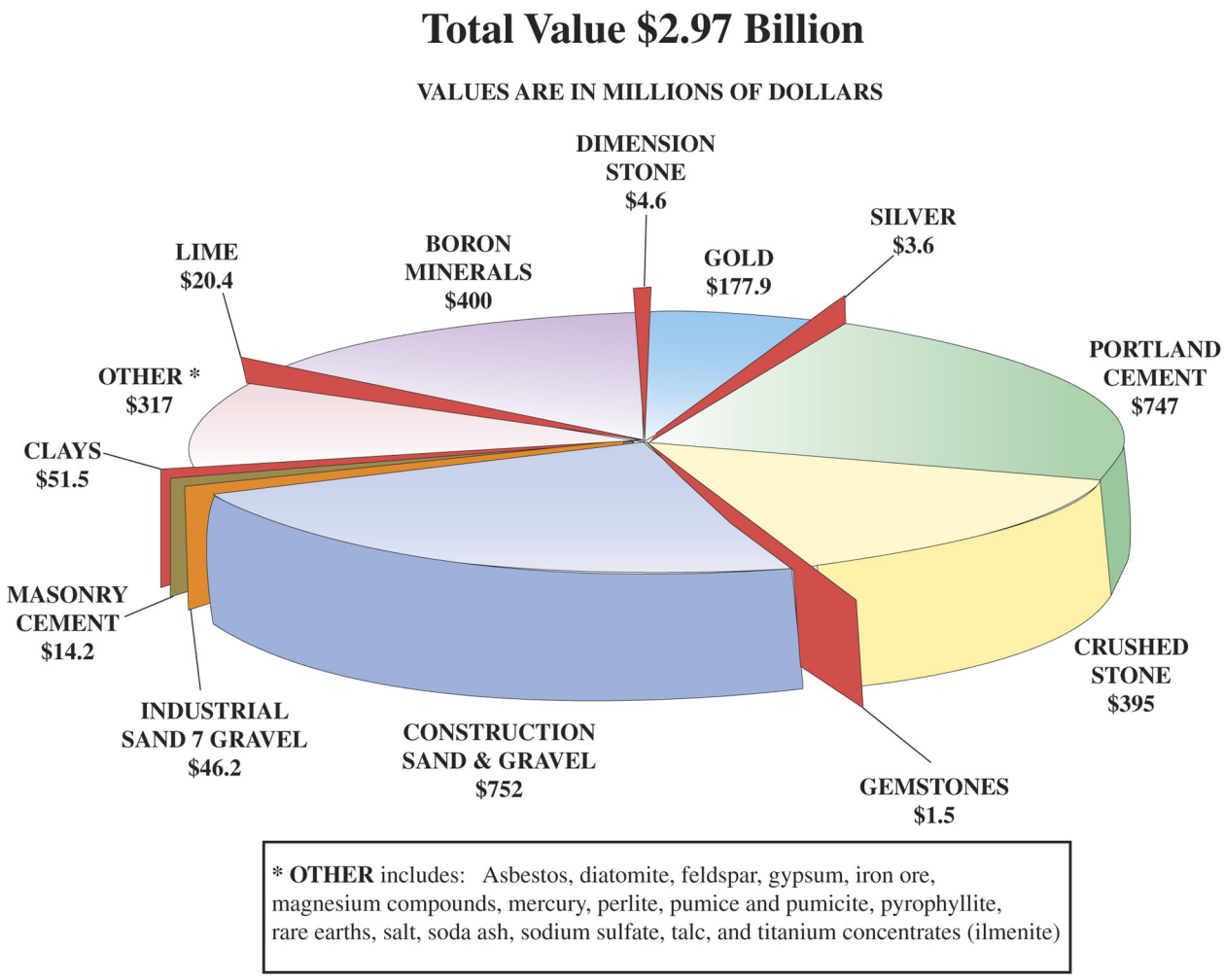

Figure 8.1. Value of production of California non-fuel minerals, 1998 (modified from Larose and others, 1999, fig. 2).

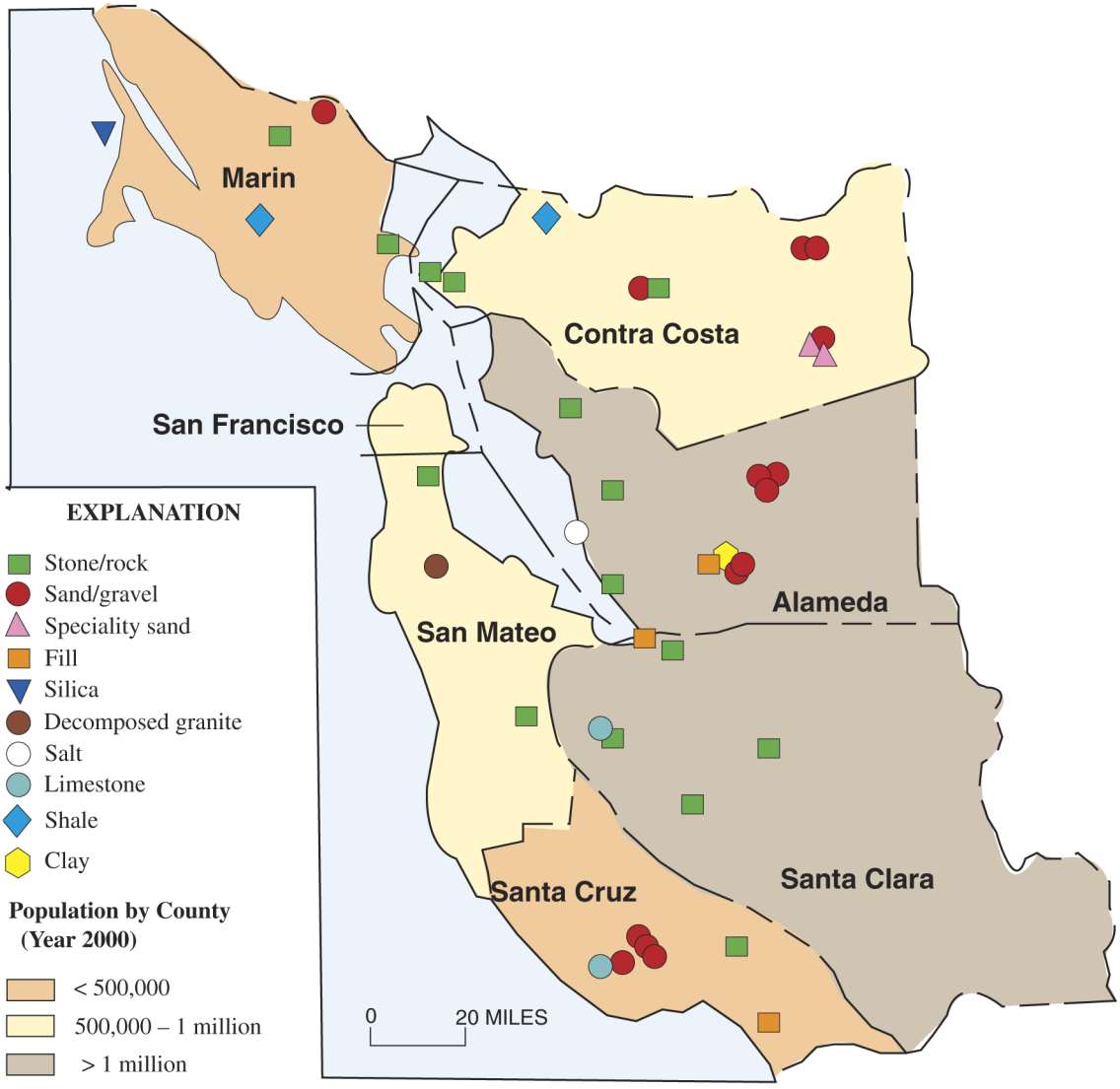

Figure 8.2. The mines and (or) mineral resource producers active in seven Bay area counties (1997-1998) and the commodities they produced (modified from Larose and others, 1999, fig. 2).

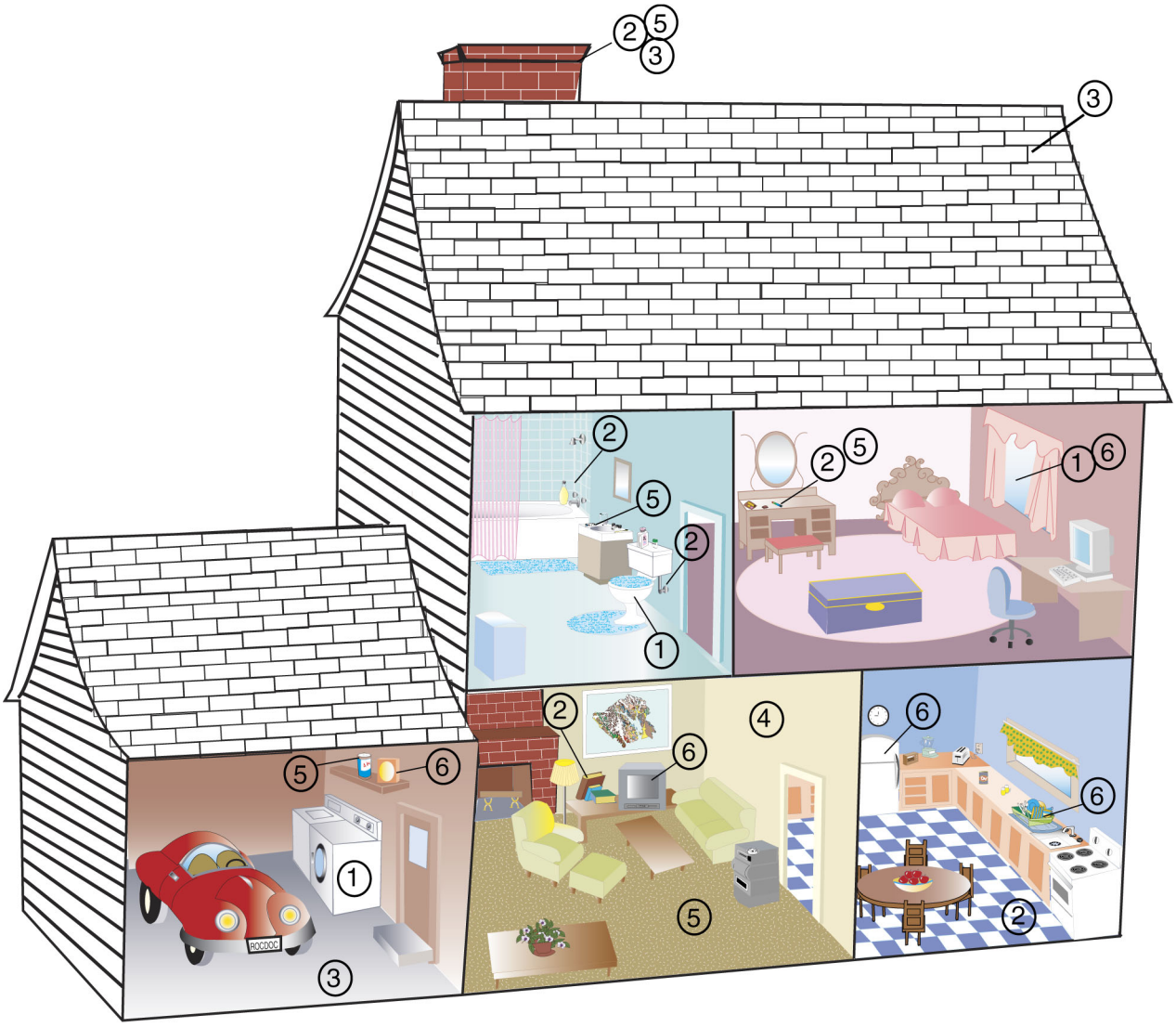

① BORON minerals - windows, toilet, appliances, insulation

② CLAYS - bricks, added to concrete, books/paper, cosmetics, plumbing, ceramics, floor tiles, dandruff shampoo.

③ CONSTRUCTION SAND/GRAVEL - combined with concrete, asphalt or plaster, crushed stone (decorative), sand bedding for sewer pipes, bricks

④ GYPSUM - plaster, wallboard, added to cement

⑤ LIMESTONE/CALCITE - portland cement, toothpaste, abrasive cleanser, books/paper, carpet, cosmetics

⑥ INDUSTRIAL SAND/GRAVEL - basic constituent of glass - windows, television, refrigerator shelves, fiberglass, dishware, mild abrasive

Figure 8.3. Some industrial mineral uses in a typical house.

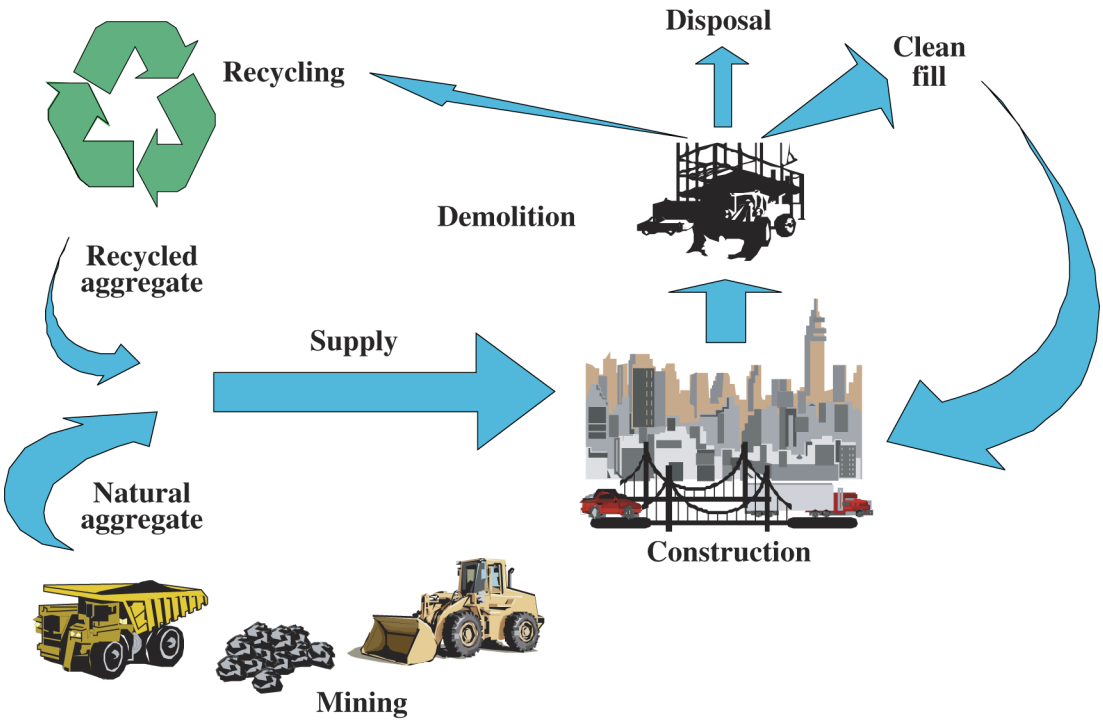

Figure 8.4. Material flow cycle for aggregates (from Sznopek and Brown, 1998).

A Brief History of Population Growth in the Greater San Francisco Bay Region

Page Mosier
U.S. Geological Survey, Menlo Park, Calif.

The population of the San Francisco Bay area is both growing and becoming increasingly diverse. The term "Greater San Francisco Bay Region" is applied to counties which are adjacent to the San Francisco Bay, including San Francisco, Napa, Sonoma, Solano, Alameda, Contra Costa, Marin, San Mateo, and Santa Clara. (Although other counties are often included in the Bay area or region, they are not included in this report.)

The first people in California were the Native Americans. Although it is hard to say exactly how many lived in California, their numbers are estimated to have been between 200,000 and 500,000 at the time of the first Spanish explorations. The native population in the Bay area was mainly of the Coastanoan, Coast Miwok, Yokut, and Wintun tribes. There were an estimated 7,000 Native Americans in the Bay area during the time that the Spanish missions were being established, including some that had been brought in by the Spanish from other areas.

Although many ethnic groups have come to the Bay area, the first group to make a major impact on the population were the Spaniards, who erected their northernmost outposts in the San Francisco Bay region and attempted to convert the Native Americans in the area to their religion. Approximately 90 percent of these Native Americans died of hardship and disease resulting from their contact with these new immigrants. Spanish contributions were both political and economic. They erected presidios, or forts, and missions, which provided the economic basis for later California settlement.

As a result of the War of Independence in 1821, Mexico attained independence from Spain, and California became part of the Republic of Mexico. San Francisco did not appear in the 1840 United States census, because it was then still part of Mexico. The majority of the immigrant population lived south of San Francisco. Land ownership consisted of large Mexican land grants covering most of the Bay area, which were given by the Mexican government to be settled by Rancheros or "Californios," as they were called. The Mexican period was one of turmoil and transition, ending with a war between Mexico and the United States. With the Treaty of Guadalupe Hidalgo in 1848, California became part of the United States territory. Eventually the major ranchos were divided into smaller properties and both land speculation and squatting were widespread.

The opening up of the West in general, and the 1849 gold rush specifically, saw the beginning of a great flow of people to California from all over the United States and the world. It was this flow of people that made it possible for California to attain statehood in 1850. Since then, this influx of people has persisted, making California the most populous state in the Union.

Because of the gold rush, the population grew and the demographics changed. By 1860, San Francisco had more than 50,000 people, and the population more than doubled in the following decade. From 1870 until the turn of the century, the rate of population growth became slower with each decade. Between 1900 and 1960 there was no consistent pattern. Slow growth occurred in the 1930's, followed by fast growth between 1940 and 1960. The influx of people during World War II and the postwar baby boom produced the highest rate of population growth since the 1870's.

In the mid and late 1800's, most of the growth occurred within the city of San Francisco. People crowded into the San Francisco metropolitan area in the 1880's, and the population grew to 274,000. The outlying areas remained mainly agricultural. The flight to, and growth in, the suburbs mainly came in the 1940's and 1950's, when the agricultural land and surrounding hills began to gain in population. The people in the San Francisco Bay area of the 1960's numbered about 3.5 million, and they were spread out over a land area more than twice the size of Rhode Island (fig. 9.1).

Since the first major mode of transportation in the Bay area was by water, it was around the ports or embarcaderos that cities first developed. Steamboat travel led to the growth of East Bay towns such as Oakland, Berkeley, Encinal, and Alameda. Local railroads reached the area in 1864, but it was not until 1869 that the transcontinental railroad began bringing tens of thousands of people to the Bay area. Railroads brought in more people and created new towns South of San Francisco, such as Burlingame, San Mateo, San Carlos, Belmont, and Atherton.

In 1863, there was also an active local ferry system between Oakland and San Francisco, as well as trolley car systems in both of these cities. These were to fade and mostly disappear as major modes of transportation after the advent of the automobile. The increasing popularity of the automobile at the end of World War I provided a major impact on California and the Bay area. Ownership of cars in California was far ahead of other states, and because of this the urban population spread rapidly between 1910 through 1940. In the 1920's and 1930's, California's population was only slightly outnumbered by New York's. Between 1920 and 1939 the population in California more than doubled.

During World War II, the population in the Bay area grew through an influx of people from other parts of the United States, such as those who came to work in the Bay area shipyards.

Areas which had largely remained agricultural, such as the Santa Clara Valley, became highly urbanized after the World War II, largely owing to the automobile (tables 9.1, 9.2). From the 1950's until the present, the Santa Clara Valley has continued to show remarkable growth because of major industries, such as missile development and the electronics and computer industries, earning it the name "Silicon Valley" and making San Jose now the largest city in the Bay area (table 9.3). The Livermore Valley at this time also changed from a purely agricultural region, growing cattle and wine, to an industrial area with the growth of what was to become the Lawrence Livermore National Laboratory and Sandia National Laboratory.

The population of the Bay area is not only growing but is becoming more and more diverse, (table 9.4), although individual communities vary dramatically. A Gallup study done in 1996-97 showed that 9.9 percent of adults in the area were African-American, 15.5 percent were Asian or Pacific Islander, 15.6 percent were Latino, 74.8 percent were white, and 0.8 percent were other ethnicities. Marin County, however is more than 95 percent white, while San Francisco is 25 percent Asian. Throughout California, groups that were once the minority are now becoming the "emerging majority." The largest growth in the State in the 1990's has involved the Asian population, many of whom have immigrated to California to find work in the technology industry. Asians, including those that are part Asian, have shown an increase of 61 percent from 1990 to the 2000 census. California gained 731,000 Asians or Pacific Islanders through immigration and 528,000 through births during the 1990's. Asians are now a majority in some cities, including the Bay area cities of Milpitas and Daly City.

Despite attempts to develop public transportation systems such as bus lines, Bay Area Rapid Transit (BART), Caltrain, and light rail, ever-increasing numbers of automobiles continue to clog major traffic arteries throughout the Bay area. The increase in traffic, and continued population growth present additional housing and transportation problems for the future. However, some forward-looking California and Bay area leaders have set aside tens of thousands of acres of open-space land for watersheds and recreation in the Peninsula, East Bay, and Marin County. These areas, which include the Golden Gate Headlands, Angel Island, East Bay Regional Parks, Point Reyes, Mount Tamalpais, and Mount Diablo, provide some refuge for the ever-expanding Bay area population, which now numbers close to seven million.

References

Association of Bay Area Governments (ABAG), 2001, 1997 Demographic charts from the internet: ABAG website, http://www.abag.ca.gov.

Bean, Walton, 1973. California an interpretive history: New York: McGraw-Hill Book Company, Second Edition, 576 p.

Calhoun, Merilyn, 1978. Early days in the Livermore-Amador Valley: Hayward, California: Alameda County School Department. 62 p.

Davis, Kingsley, and Langlois, Eleanor, 1963, Future demographic growth of the San Francisco Bay Area: Berkeley, California, Institute of Governmental Studies, University of California, Berkeley, 27 p.

Kroeber, A.L., 1925, Handbook of the Indians of California: Washington D.C., Government Printing Office, p.462-473 (reprinted by The Livermore Heritage Guild with permission by the Smithsonian Institution in 1978).

Heizer, R.F., and Whipple, M.A., 1971, The California Indians: a source book: Berkeley, University of California Press, 487 p.

Pittman, Ruth, 1995, Roadside history of California: Missoula, Montana, Mountain Press Publishing Company, 415 p.

Press Democrat, Inc. 2001, Asian population continues to grow, changing California communities (accessed April 3, 2001): http://www.pressdemo.com/census/state/03cenweb.html.

San Francisco Examiner, 1997, Bay Life '97—Who we are, where we work, how we live: San Francisco Examiner, February 9, 1997, p.W-17.

U.S. Geological Survey, 2001, Access USGS – San Francisco Bay and Delta,(accessed April 3, 2001): http://sfbay.wr.usgs.gov/access/Integrated Science/IntSci.html.

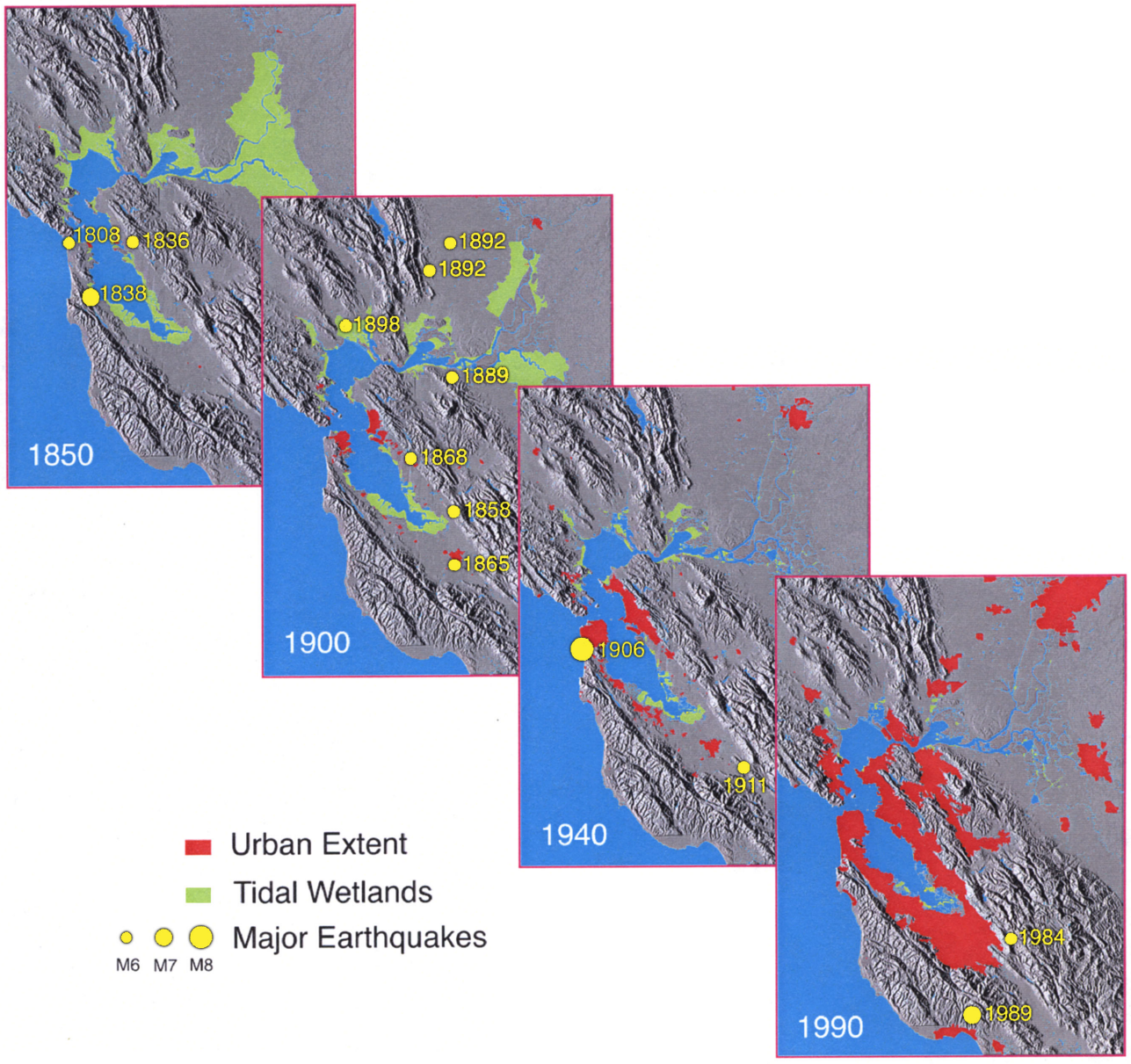

Figure 9.1. The growth of urban areas, the decline of tidal wetlands, and the epicenters of major earthquake in the Bay region since 1850 (from Leonard J. Gaydos and William Acervedo, http://sfbay.wr.usgs.gov/access/IntegratedScience/IntSci.html).

Table 9.1. Total population of San Francisco Bay area counties, 1930-90 (from Association of Bay Area Governments http://www.abag.ca.gov).

	1930	1940	1950	1960	1970	1980	1990
San Francisco	634,394	634,536	775,357	740,316	715,674	678,974	723,959
San Mateo	77,405	111,782	235,659	444,387	557,361	587,329	649,623
Santa Clara	145,118	174,949	290,547	642,315	1,065,313	1,295,071	1,497,577
Alameda	474,883	513,011	740,315	908,209	1,071,446	1,105,379	1,279,182
Contra Costa	78,608	100,450	298,984	409,030	556,116	656,380	803,732
Solano	40,834	49,118	104,833	134,597	171,989	235,203	340,421
Napa	22,897	28,503	46,603	65,890	79,140	99,199	110,765
Sonoma	62,222	69,052	103,405	147,375	204,885	299,681	388,222
Marin	41,648	52,907	85,619	146,820	208,652	222,568	230,096
Region	1,578,009	1,734,308	2,681,322	3,636,939	4,630,576	5,179,784	6,023,577

Table 9.2. Percent change in total population, San Francisco Bay area Counties, 1930-2010 (from Association of Bay Area Governments http://www.abag.ca.gov).

	1930/40	1940/50	1950/60	1960/70	1970/80	1980/90	1990/00	2000/10
San Francisco	0.0	22.2	-4.5	-3.3	-5.1	6.6	7.8	2.6
San Mateo	44.4	110.8	88.6	25.4	5.4	10.6	12.0	2.7
Santa Clara	20.6	66.1	121.1	65.9	21.6	15.6	14.8	7.3
Alameda	8.0	44.3	22.7	18.0	3.2	15.7	13.6	7.1
Contra Costa	27.8	197.6	36.8	36.0	18.0	22.4	19.8	16.3
Solano	20.3	113.4	28.4	27.8	36.8	44.7	24.3	21.3
Napa	24.5	63.5	41.4	20.1	25.3	11.7	19.8	9.0
Sonoma	11.0	49.7	42.5	39.0	46.3	29.5	22.8	13.5
Marin	27.0	61.8	71.5	42.1	6.7	3.4	11.1	6.4
Region	9.9	54.6	35.7	27.3	11.9	16.3	15.1	8.8

Table 9.3. January 1, 1997, population rankings of San Francisco Bay area cities (from Association of Bay Area Governments http://www.abag.ca.gov).

City	Population	City	Population
1. SAN JOSE	873,300	51. SAN CARLOS	28,050
2. SAN FRANCISCO	778,100	52. LOS ALTOS	28,000
3. OAKLAND	388,100	53. BENICIA	27,350
4. FREMONT	192,200	54. DUBLIN	26,750
5. SUNNYVALE	129,300	55. SAN PABLO	25,900
6. SANTA ROSA	127,700	56. SUISUN CITY	25,800
7. HAYWARD	123,900	57. BELMONT	25,200
8. CONCORD	111,800	58. EAST PALO ALTO	25,050
9. VALLEJO	110,500	59. LAFAYETTE	23,600
10. BERKELEY	105,900	60. EL CERRITO	23,300
11. DALY CITY	101,300	61. MILLBRAE	21,450
12. SANTA CLARA	100,000	62. WINDSOR	19,200
13. SAN MATEO	92,000	63. HERCULES	18,800
14. RICHMOND	91,300	64. PINOLE	18,150
15. FAIRFIELD	89,000	65. ALBANY	17,300
16. VACAVILLE	85,100	66. ORINDA	16,900
17. ANTIOCH	76,500	67. MORAGA	16,350
18. ALAMEDA	76,300	68. BRENTWOOD	14,500
19. REDWOOD CITY	73,200	69. MILL VALLEY	13,900
20. MOUNTAIN VIEW	73,000	70. DIXON	13,650
21. SAN LEANDRO	72,600	71. SAN ANSELMO	12,300
22. NAPA	68,000	72. LARKSPUR	11,750
23. LIVERMORE	67,800	73. HILLSBOROUGH	11,350
24. WALNUT CREEK	62,200	74. PIEDMONT	11,300
25. MILPITAS	61,200	75. HALF MOON BAY	10,850
26. PALO ALTO	59,900	76. CLAYTON	10,050
27. PLEASANTON	59,800	77. HEALDSBURG	9,625
28. UNION CITY	59,700	78. AMERICAN CANYON	9,025
29. SOUTH SAN FRANCISCO	57,600	79. SONOMA	8,925
30. SAN RAFAEL	53,400	80. CORTE MADERA	8,750
31. PITTSBURG	50,800	81. TIBURON	8,550
32. PETALUMA	49,000	82. LOS ALTOS HILLS	7,975
33. NOVATO	46,100	83. SAUSALITO	7,725
34. CUPERTINO	44,800	84. SEBASTOPOL	7,575
35. SAN RAMON	41,950	85. ATHERTON	7,375
36. SAN BRUNO	40,800	86. FAIRFAX	7,100
37. NEWARK	40,450	87. COTATI	6,550
38. PACIFICA	39,650	88. EMERYVILLE	6,525
39. CAMPBELL	39,300	89. ST HELENA	5,725
40. ROHNERT PARK	38,700	90. CLOVERDALE	5,525
41. DANVILLE	38,100	91. WOODSIDE	5,475
42. MARTINEZ	35,350	92. CALISTOGA	4,790
43. GILROY	35,250	93. PORTOLA VALLEY	4,470
44. PLEASANT HILL	31,450	94. RIO VISTA	3,710
45. SARATOGA	30,600	95. YOUNTVILLE	3,490
46. MENLO PARK	30,550	96. MONTE SERENO	3,360
47. FOSTER CITY	29,750	97. BRISBANE	3,210
48. LOS GATOS	29,700	98. BELVEDERE	2,280
49. MORGAN HILL	29,250	99. ROSS	2,260
50. BURLINGAME	28,550	100. COLMA	1,240

Table 9.4. San Francisco Bay area Census 2000 (from Association of Bay Area Governments http://www.abag.ca.gov).

TOTAL POPULATION	6,783,760	100.0%
RACE		
White	3,941,687	58.1%
Black or African American	511,084	7.5%
American Indian and Alaska Native	43,529	0.6%
Asian	1,289,849	19.0%
Native Hawaiian and Other Pacific Islander	36,317	0.5%
Some other ethnicity	627,004	9.2%
Two or more ethnicities	334,290	4.9%
HISPANIC OR LATINO AND RACE		
Hispanic or Latino (of any race)	1,315,175	19.4%
Not Hispanic or Latino	5,468,585	80.6%
White	3,392,204	50.0%
Black or African American	497,205	7.3%
American Indian and Alaska Native	24,733	0.4%
Asian	1,278,515	18.8%
Native Hawaiian and Other Pacific Islander	33,640	0.5%
Some other ethnicity	18,451	0.3%
Two or more ethnicities	223,837	3.3%

Resource Directory for Discovering Native Americans and Archeology in the San Francisco Bay Area

John P. Galloway
U.S. Geological Survey, Menlo Park, Calif., and
Department of Science and Math, Cañada College, Redwood City, Calif.

Web Sites

Society for California Archaeology – SCAnet – Resource directory for teaching archaeology
http://www.scanet.org/resources.html#region

Society for American Archaeology – Educational material available from SAA
http://www.saa.org/education/edumat.html

Bibliography of Northern and Central California Indians
http://www.mip.berkeley.edu/cilc/bibs/toc.html

Reference Material

Chartkoff, J.L., 1991, The archaeology of California: Stanford, California, Stanford University Press, 480 p.

Harrington, J.P., 1942, Culture element distribution XIX: Central California Coast: University of California Anthropological Records, v. 7, no. 1, p. 1-46.

Heizer, R.F., ed., 1978, California Indians: Washington, D.C., Smithsonian Press, Handbook of North American Indians, v. 8, 800 p.

Kroeber, A.L., 1977, Handbook of the Indians of California, Dover Publications, 989 p.

Margolin, Malcon, 1978, The Ohlone way—Indian life in the San Francisco Bay–Monterey Bay Area: Berkeley, California, Heyday Books, 182 p.

Moratto, M.J., 1984, California archaeology: Orlando, Florida, Academic Press, 757 p.

Artifactual and Archival Collections

Alameda County

C.E. Smith Museum of Anthropology
California State University 25800 Carlos Bee Blvd.
Hayward, CA, 94542
Phone: 510-885-3104
Hours: Mon.–Fri. 10 a.m. to 4 p.m.

Oakland Museum of California
1000 Oak St.
Oakland, CA 94607
Phone: 510-238-2200
Hours: Wed.–Sat. 10 a.m. to 5 p.m.; Sun. Noon to 5 p.m.; closed Mon. and Tue.

Phoebe A. Hearst Museum of Anthropology
103 Kroeber Hall
Berkeley, CA 94720-3172
Phone: 510-643-7648
Hours: 10 a.m. to 4:30 p.m. Wed–Sun.

San Francisco County

California Academy of Sciences
Department of Anthropology
55 Concourse Dr. - Golden Gate Park
San Francisco, CA 94418
Phone: 415-750-7163
Hours: Winter 10 a.m. to 5 p.m. (summer 9 a.m. to 6 p.m.).

Treganza Museum/Hohenthal Gallery
San Francisco State University
1600 Holloway Ave.
San Francisco, CA 94132-4155
Phone: 415-338-2046

San Mateo County

Sanchez Adobe Historic Site
1001 Lind Mar Blvd.
Pacifica, CA 94044
Phone: 650-299-0104
Hours: Tue.–Thu. 10 a.m. to 4 p.m.; Sat.–Sun. 1 p.m. to 5 p.m.

State Of California

California State Indian Museum
2618 K Street
Sacramento, CA 95816-4921
Phone: 916-324-0971
Hours: Daily 10 a.m. to 5 p.m.

Archaeological Sites

Chitactac Adams Heritage County Park.—South Santa Clara County, on Watsonville Road between Morgan Hill and Gilroy.

Chitactac Adams Heritage County Park offers a unique view into the Native American culture of Santa Clara before and after the arrival of the Spanish. A self-guided interpretive walk around the site, including eight stations with interpretive panels, is supplemented by an interpretive shelter with seven additional panels and displays. The trail panels include photographs and original art covering the Adams School, Ohlone village life, Ohlone buildings, petroglyphs (rock art), Ohlone food processing, natural history of Uvas Creek, Spanish, California and Ohlone culture and petroglyphs and their preservation." (On the web at http://claraweb.co.santa-clara.ca.us/parks/prkpages/chitacch.htm)

Coyote Hills Regional Park—8000 Patterson Ranch Rd. Fremont, CA 04555, Phone: 510-795-9385. Shellmound tour —(call for dates).

The Patterson Mound is a site located within the boundaries of Coyote Hills Regional Park and is protected by the East Bay Regional Park District. "The Patterson Mound has had a long history of excavation since its initial discovery and subsequent recordation by Nels Nelson in 1909. The University of California, Berkeley, excavated the site first in 1935. The Berkeley excavation was then followed by students from San Francisco State University who excavated the site intermittently between the years 1949 and 1968. Students from the California State University, Hayward, under the direction of Dr. C.E. Smith, excavated the site during the summers of 1966, 1967, and 1968." (On the web at http://www.isis.csuhayward.edu/cesmith/archives/328/328index.htm).

Filoli—Woodside, CA. (a property of the National Trust for Historic Preservation).

The Filoli Estate docents conduct a program called Native Plants/Native Ways, which is designed to coincide with the 4th grade curriculum by investigating the traditional use of plants and animals used by Native California Indians. On the web at http://www.filoli.org/education.html.

Selected Information Resources About the Geology and Natural History of the San Francisco Bay Area

Susan Toussaint
U.S. Geological Survey Library, Menlo Park

The following selected information resources can be useful for further exploration of the geology and natural history of the San Francisco Bay area. These resources are arranged by subject categories covering general resources, biology, geographic information, geology, natural hazards, and water. Both electronic and paper publications are included. Paper copies may be available at large academic and public libraries, or from the U.S. Geological Survey libraries.

The abundance of literature about Bay area geology and natural resources is illustrated by a search on the GeoRef database. Produced by the American Geological Institute, this database covers the period 1795 to the present and indexes primarily geoscience journal articles. Searching GeoRef by the names of the counties that make up the greater San Francisco Bay area retrieves more than 5,600 citations.

General Resources

Alt, D., and Hyndman, D.W., 2000, Roadside geology of Northern and Central California: Missoula, Montana, Mountain Press Publishing Company, 369 p.

This book gives a general picture of the geology of California. The chapters on the coastal mountains and the coastline describe some of the prominent geologic features that can be seen from major roadways.

California Department of Conservation, Division of Mines and Geology, 1971. California Geology [serial]. Sacramento, California.

The bimonthly publication, California Geology, is intended for anyone interested in the geologic landscape of the State. Articles are well illustrated with photographs and maps. It also acts as a bulletin about Division of Mines and Geology projects and products. Of special note is the "Teacher Feature" in each issue.

Geoscience Information Society, Guidebooks Committee, Richard Spohn, chair, 1996, Union list of field trip guidebooks of North America Online (6th ed.): American Geological Institute. Retrieved May 30, 2001, from the World Wide Web at http://www.agiweb.org/pubs/unionlist.

Field trip guidebooks are very valuable for in-depth geologic interpretation for a geographic area. This publication indexes fieldtrips conducted through 1988 by geographic location. The State of California has an extensive list. Many of these guidebooks are available at large academic libraries or at the U.S. Geological Survey Libraries.

Harden, D.R., 1998, California geology: Upper Saddle River, New Jersey, Prentice Hall, 479 p.

Harden has written this textbook as an introduction to the diversity and scope of California geology. Of particular interest is the emphasis on planning for and mitigation of future natural hazards.

Norris, R.M., and Webb, R.W., 1990, Geology of California (2nd ed.): New York, John Wiley & Sons, Inc., 541 p.

The geology of California as divided into geomorphic provinces, giving detailed explanations of the special features that are unique to each of them.

Biology—animals, plants

California Resources Agency, 2001, CERES California Environmental Resources Evaluation System. Retrieved May 24, 2001, from the World Wide Web at http://ceres.ca.gov.

As the primary environmental Web site for California resources, CERES has information arranged by geographic area or theme. It has direct links to educational resources pertaining to watershed and wetlands issues. Under a geographic area, searches can be by bioregion, county, or watershed.

Thompson, J., Parchaso, F., Alpine, A., Cloern, J., Cole, B., Mace, O., Edmunds, J., Baylosis, J., Luoma, S., and Nichols, F., 1999, History and effects of exotic species in San Francisco Bay: San Francisco Bay Project, Water Resources Division. Retrieved June 11, 2001, from the World Wide Web at http://sfbay.wr.usgs.gov/access/exotic-species/index.html.

This is a poster that lists exotic species in San Francisco Bay, how they got there, what impact they have had on the ecosystem, and what is being done about them.

University of California, Berkeley, 2001, Digital library project About the collections. Retrieved May 24, 2001 from the World Wide Web at http://elib.cs.Berkeley.edu/arch/about_collection.html.

The University of California at Berkeley has been instrumental in gathering and mounting datasets for the California digital library project. One of the collections contains botanical data with taxonomical information for more than 8,000 native California plants and is linked to photos and maps. The zoological data comprise similar datasets for amphibians, birds, mammals, and reptiles. There are also geographical data derived from the Bureau of the Census Tiger records for the San Francisco Bay area.

Geographic Information/Maps—geology, topography, bathymetry

Brown, C., Acevedo, W. and Buchanan, J.T., (n.d.), Dynamic mapping of urban regions, growth of the San Francisco/Sacramento Region. Retrieved June 25, 2001, from the World Wide Web at http://edcwww2.cr.usgs.gov/umap/pubs/urisa_cb.html.

An animation of the historical urban growth patterns of the San Francisco-Sacramento area using 1850 to 1990 census data.

National Weather Service, 2001, National Weather Service—San Francisco Bay Area, serving the San Francisco and Monterey Bay area. Retrieved June 5, 2001, from the World Wide Web at http://www.nws.mbay.net/home.html.

An agency of the National Oceanic and Atmospheric Administration (NOAA), the National Weather Service provides climatic data, real time forecasting, and warnings or advisories on a regional basis. It also has links to tide tables with correction information for specific points along the coast and estuary, and astronomical information for sunrise/sunset and moonrise/moonset.

U.S. Geological Survey, 2001, San Francisco Bay Area Regional Database (BARD). Retrieved July 6, 2001, from the World Wide Web at http://bard.wr.usgs.gov.

This site has digital data in the form of spatial elevation models and orthophoto quadrangles. It includes free software to view the images.

U.S. Geological Survey, 2001, National Geologic Map Database Homepage. Retrieved May 30, 2001, from the World Wide Web at http://ngmdb.usgs.gov/ngmdb/ngmdb_home.html.

The National Geologic Map Database gives citations to maps and related data on geology, geochemistry, hazards, geophysics, paleontology, and marine geology. There are links to both paper and digital maps, to a geologic names database, and to a geographic names index database.

U.S. Geological Survey, (n.d.), SFPORTS San Francisco Bay navigational aids. Retrieved June 11, 2001, from the World Wide Web at http://sfports.wr.usgs.gov.

This page is a creation of the U.S. Geological Survey, National Ocean Service, California Office of Oil Spill Prevention and Response, and the Marine Exchange of San Francisco Bay. It shows real-time data for tides, currents, winds, water temperature, air temperature, and air pressure and short-term forecasts of water level and currents.

U.S. Geological Survey, Western Region Coastal and Marine Geology, 2001, Pacific seafloor mapping project. Retrieved June 13, 2001, from the World Wide Web at http://walrus.wr.usgs.gov/pacmaps.

Images from this home page give the viewer the choice to see shaded relief or a perspective image of San Francisco Bay's bathymetry.

U.S. Geological Survey, 1997, USGS TerraWeb Central California DEM and bathymetry images. Retrieved June 7, 2001, from the World Wide Web at http://terraweb.wr.usgs.gov/projects/SFBay/ccdembth.html.

Digital elevation models of various areas of central California, including the San Francisco Bay area, are available. They can be used to map and study surficial features of the region.

Geology- general geology, subduction, tectonics

Atwater, B. F., Hedel, C.W., and Helley, E.J.,1977, Late Quaternary depositional history, Holocene sea-level changes, and vertical crustal movement, southern San Francisco Bay, California: U.S. Geological Survey Professional Paper 1014, 15 p.

An explanation of estuarine deposits of southern San Francisco Bay from Pleistocene through the Holocene in relation to sea-level changes and subsidence. Includes maps and illustrations.

Blake, M.C., McLaughlin, R.J., and Jones, D.L., 1989, Terranes of the northern coast ranges in Blake, M.D., Jr., Harwood, D.S., McLaughlin, R.J., Jayko, A.S., Irwin, W.P., Dodge, F. C.W., Jones, D.L., Miller, M.M. and Bullen, T., Tectonic evolution of Northern California, Sausalito to Yosemite National Park, California: International Geological Congress, 28th, 1989, Washington, D.C., Field trip guidebook T108, International Geological Congress, 28th, 1989, Washington, D.C., p. 3-18.

This chapter and accompanying field guide give a detailed description of the terranes of the California Coast Range ophiolite in relation to belts of the Franciscan Complex from slightly south of San Francisco Bay northward.

California Division of Mines and Geology, 2001, California Division of Mines and Geology home page. Retrieved May 30, 2001, from the World Wide Web at http://www.consrv.ca.gov/dmg/index.htm.

As California's state geological survey, the Division of Mines and Geology collects geologic data and distributes information regarding earthquakes and landslides, minerals, mining, oil, gas, and geothermal resources. The division also maps watershed regions. The home page lists Notes about single subjects such as the state gem, mineral, rock and fossil, how earthquakes are measured, information about debris flows, and how to look for fossils. Some reports can be downloaded from their Web site.

Magoon, L., 2001, Natural oil and gas seeps in California. Retrieved June 19, 2001, from the World Wide Web at http://seeps.wr.usgs.gov/seeps/index.html.

This site describes the importance of natural oil and gas seeps in California, what they are, where they are, including locations in Central California, their use by the native peoples, and a link to the most famous one of all—the La Brea Tar Pits.

Rogers, T.H., 1993, Geology of the Hollister and San Felipe quadrangles, San Benito, Santa Clara, and Monterey counties, California: California Division of Mines and Geology, Open-File Report 93-01, 26 p., 3 maps.

This report covers the geologic, seismic and economic geology of the Hollister and San Felipe quadrangles. It describes the seismic setting and history of Hollister, including pictures of the destruction from the 1906 San Francisco Earthquake. It has an inventory of existing and potential landslides and paleontological data for the area.

Sloan, D., and Wagner, D.L., eds., 1991, Geologic excursions in northern California San Francisco to the Sierra Nevada: California Division of Mines and Geology Special Publication 109, 130 p.

This field trip guidebook for the joint meeting of Geological Society of America, Cordilleran Section, and the Seismological Society of America in San Francisco covers the geological setting of the San Francisco Bay Area, the Merced Formation south of San Francisco, the Franciscan Complex and Coast Range ophiolite, and the Great Valley sequence.

U.S. Geological Survey, 2001, Geologic information about California. Retrieved May 30, 2001, from the World Wide Web at http://geology.wr.usgs.gov/docs/stateinfo/CA.html.

This site gives useful links to the more general categories of research being conducted in California by the U.S. Geological Survey. Real-time earthquake activity, coastal studies, geologic mapping projects, oil and gas seeps, geophysical mapping, mineral resources, and landslide research are among the topics, with many concentrating on the San Francisco Bay area.

U.S. Geological Survey, 2000, San Francisco Bay Region Project Western Earth Surface Processes Team. Retrieved June 5, 2001, from the World Wide Web at http://sfgeo.wr.usg.gov.

This is the primary site for geologic maps, landslide studies, and geologic information about the San Francisco Bay area. Two projects currently being developed are 3-D modeling of the region and a scenario-based hazard map of the Oakland-Berkeley hills.

Wahrhaftig, C., and Sloan, D., eds., 1989, Geology of San Francisco and vicinity: International Geological Congress, 28th, 1989, Washington, D.C., Field trip guidebook T105, 69 p.

This field trip guidebook provides a good overview of the diversity of geologic features and tectonic activity in the San Francisco Bay region. Tectonostratigraphic terranes are defined and the possible origin of the Salinian block is discussed, as is the development of the San Andreas Fault system. Areas of volcanic rocks ranging in age from 24 Ma to less than 0.01 Ma are also delineated.

Wahrhaftig, C.,1984, A streetcar to subduction and other plate tectonic trips by public transport in San Francisco (rev. ed.): Washington, D.C., American Geophysical Union, 76 p.

Wahrhafting uses public transportation to explore plate tectonic evidence in rock formations exposed in San Francisco, the Marin Headlands, Angel Island, and along the Hayward Fault. Includes a geologic time scale, glossary, and selected bibliography. There are many maps and drawings of geologic features.

Hazards earthquakes, landslides, liquefaction, tsunamis

Association of Bay Area Governments, 2001, Bay area shaking hazard maps. Retrieved June 13, 2001, from the World Wide Web at http://www.abag.ca.gov/bayarea/eqmaps/mapsba.html.

In association with the U.S. Geological Survey, ABAG has made available on the Internet earthquake ground-shaking intensity maps for all cities of the greater San Francisco Bay area. Maps show the degree of expected shaking according to different fault scenarios. There are also maps showing how areas shook in the 1906 and 1989 earthquakes in the region.

Association of Bay Area Governments, 2001, The REAL dirt on liquefaction. Retrieved June 13, 2001, from the World Wide Web at http://www.abag.ca.gov/bayarea/eqmaps/liquefac/liquefac.html.

Similar to the earthquake hazard maps, the liquefaction susceptibility maps and liquefaction hazard maps give information regarding probable damage by liquefaction in the San Francisco Bay area. There are tips on living with liquefaction and how it might impact the community.

Brown, W.M. III, ed., 1989, Landslides in Central California: American Geophysical Union, International Geological Congress, 28th, 1989, Washington, D.C.Field Trip Guidebook T381, 98 p.

A series of workshops about landslides induced by water or earthquakes and how the geology of the San Francisco Bay region requires comprehensive landslide mapping and related mitigation studies.

Collier, M., 1999, A land in motion California's San Andreas Fault: Berkeley, California, University of California Press, 128 p.

Accompanied by aerial photography of some of the San Andreas Fault's features, this is a good explanation of the San Andreas Fault and how scientists study it.

Highland, L.M., Godt, J., Howell, D., and Savage, W.Z., 1998, El Niño 1997 98: Damaging landslides in the San Francisco Bay Area: U.S. Geological Survey Fact Sheet 089-98, 2 p.

This is a brief report on the effects of El Niño during the winter of 1997-98 and the resulting economic impacts for the ten-county San Francisco Bay area.

Hirschfeld, S.E., and Klein, F., 1996, The Hayward Fault we can't ignore it [videorecording]: U.S. Geological Survey Open-File Report 95-814 A, B.

This videorecording gives the destructive history and potential future hazards along the Hayward Fault. Includes a tour of the Hayward Fault and discussion of the possibility of widespread damage for East Bay communities.

Lajoie, K.R., and Mathieson, S.A.,1998, 1982-83 El Niño coastal erosion San Mateo County, California: U.S. Geological Survey. Retrieved May 30, 2001, from the World Wide Web at http://walrus.wr.usgs.gov/elnino/SMCO-coast-erosion.

This report includes maps of erosion or stability for the approximately fifty miles of San Mateo County coastline. Lajoie and Mathieson discuss the primary causes of coastal erosion as a natural process rather than as a natural hazard with the purpose of alerting planners and residents to help minimize damage in El Niño years.

Ryan, H., Gibbons, H., Hendley, J.W., II, and Stauffer, P.H., 1999, El Niño sea-level rise wreaks havoc in California's San Francisco Bay region: U.S. Geological Survey Fact Sheet 175-99, 4 p.

El Niño storms of 1997-98 produced high sea levels that in turn caused millions of dollars in damage by coastal flooding and erosion. Sea level records for the past 100 years are presented and the variations in water temperature and sea level are graphically displayed.

Sylvester, A.G., and Crowell, J.C., 1989, The San Andreas Transform Belt—Long Beach to San Francisco, California: International Geological Congress, 28th, 1989, Washington, D.C., Field Trip Guidebook T309, 119 p.

The history and tectonic setting of the San Andreas transform belt is given, along with its seismic creep rate. Of particular interest are the descriptions of activity in and around Hollister.

Tyler, M.B., 1995, Look before you build Geologic studies for safer land development in the San Francisco Bay Area: U.S. Geological Survey Circular 1130, 54 p.

The importance of geologic studies for hazards mitigation is emphasized to avoid loss of life and property. The value of site specific maps for individual parcels vs. general hazardous zone maps is discussed. Tyler also relates the effects of the Loma Prieta earthquake on rebuilding efforts by communities and what lessons can be learned and reflected in building standards.

U.S. Geological Survey, 1995 [rev. and abridged 1997], Debris-flow hazards in the San Francisco Bay region: U.S. Geological Survey Fact Sheet 112-95, 4 p. Retrieved May 30, 2001, from the World Wide Web at http://landslides.usgs.gov/html_files/nlic/sfbayfs97.pdf.

This fact sheet describes the debris flow hazards that exist in the San Francisco Bay area, what they are, where they are located, and how to avoid becoming a victim of one.

U.S. Geological Survey, 1997, San Francisco Bay region landslide folio home page. Retrieved June 13, 2001, from the World Wide Web at http://wrgis.wr.usgs.gov/open-file/of97-745.

This folio is composed of six related reports and maps on past landslides, earth flows, and debris flows and on the importance of tracking rainfall thresholds on them for the San Francisco Bay region.

U.S. Geological Survey, 2000, USGS California Hazards-Landslides. Retrieved May 30, 2001, from the World Wide Web at http://ca.water.usgs.gov/land.

This site has reports and links to landslide facts and images and landslide hazard maps for the San Francisco Bay area and San Mateo coastal erosion. There is information on landslide recognition and safety. In addition, there is a link to the National Landslide Hazards Program located in Denver, Colorado.

U.S. Geological Survey, 2001, USGS Earthquakes Hazards program—Northern California. Retrieved May 30, 2001, from the World Wide Web at http://quake.wr.usgs.gov.

This site has everything about earthquakes and links to other sites that provide earthquake information around the world. It has real-time earthquake maps of California-Nevada, the United States and the world. For the San Francisco area, there is a special regional map, an earthquake probability report, and information on how to prepare for earthquakes at home and at the workplace. A special section addresses topics of particular interest, and there are links to additional resources.

U.S. Geological Survey, 2001, Western Region Coastal and Marine Geology Table of Contents. Retrieved May 30, 2001, from the World Wide Web at http://walrus.wr.usgs.gov/sitetoc.html.

This is a portal to research and information from the Western Region Coastal and Marine Geology Team. Topics include environmental quality and pollution, wetlands, coastal erosion with respect to El Niño weather, and salinity of estuarine waters. Of particular interest may be the online publication titled “Tsunami record from the Great 1906 San Francisco Earthquake” (http://walrus.wr.usgs.gov/tsunami/1906.html).

Wallace, R.E., ed., 1990, The San Andreas Fault system, California: U.S. Geological Survey Professional Paper 1515, 283 p.

The history, geology, geophysics, and seismology are covered in this comprehensive study of the San Andreas Fault system. It explains the processes occurring along the plate boundaries. There are many photographs and illustrations and an extensive bibliography.

Water—groundwater, surface water, tide tables, wetlands

Alpers, C.N., and Hunerlach, M.P., 2000, Mercury contamination from historic gold mining in California: U.S. Geological Survey Fact Sheet 061-00, 6 p. Retrieved May 21, 2001, from the World Wide Web at http://ca.water.usgs.gov/mercury.

Use of mercury was an important element of gold mining in California, and much of it came from the Coast Ranges in and near the San Francisco Bay area. The effects of mercury contamination to human health, the sites of mercury contamination, and location of fish consumption advisories are discussed in this fact sheet.

Association of Bay Area Governments, 2001, San Francisco Estuary Project. Retrieved May 30, 2001 from the World Wide Web at http://www.abag.ca.gov/bayarea/sfep/sfep.html.

The San Francisco Estuary Project is part of the National Estuary Program to protect and improve water quality and natural resources of estuaries nationwide. The project has information on wetlands, wildlife, aquatic, and land use resources that pertain to the San Francisco Bay-Sacramento Delta ecosystem.

California Department of Water Resources, 2001, DWR California water page. Retrieved May 30, 2001, from the World Wide Web at http://wwwdwr.water.ca.gov.

The home page of the California Department of Water Resources has information about the state water project, the CALFED Bay-Delta Program, river and reservoir information, and legislation relevant to California water projects. One of the DWR Web sites includes educational resources and more than 17,000 nature images.

Galloway, D.L., Jones, D.R., and Ingebritsen, S.E., 2000, Measuring land subsidence from space: U.S. Geological Survey Fact Sheet 051-00, 4 p.

Using Interferometric Synthetic Aperture Radar (InSAR), the subsidence of ground caused by compaction of aquifer systems can be detected and measured by satellite. Of particular interest is the section on the subsidence in Santa Clara Valley, where subsidence of 14 feet occurred between 1910 and 1995.

Ingebritsen, S.E., Ikehara, M.E., Galloway, D.L., and Jones, D.R., 2000, Delta subsidence in California The sinking heart of the state: U.S. Geological Survey Fact Sheet 005-00, 4 p.

The delta and the San Francisco estuary are the subject of this fact sheet on the danger of subsidence and the possibility of degradation of water quality if large amounts of fresh water are diverted to other areas.

National Ocean Service, 2001, Marine Sanctuaries. Retrieved May 30, 2001, from the World Wide Web at http://www.sanctuaries.nos.noaa.gov/oms/oms.html.

The home page for the Nation's marine sanctuaries links to individual sanctuary Web sites with information about biological, physical, archaeological, and cultural resources. Education activities are also included. The San Francisco Bay area is home to the Cordell Bank, Gulf of the Farallones, and Monterey Bay Marine Sanctuaries.

Oakland Museum of California, 2001, Guide to San Francisco Bay area creeks The Oakland Museum of California Creek and Watershed Information Source. Retrieved May 23, 2001, from the World Wide Web at http://www.museumca.org/creeks.

This site has a historical creek map of San Francisco, outlines the current progress of a creek-mapping project in the East Bay and includes images of topographic maps from the late 1800s of watershed areas around San Francisco Bay and links to regional and local information. There is also an animation of the stages of the evolution of San Antonio Creek into the Oakland Estuary.

U.S. Geological Survey, 2001, Access USGS—SF Bay and Delta. Retrieved May 24, 2001, from the World Wide Web at http://sfbay.wr.usgs.gov.

This site pulls together biological, geological, mapping, and water resources research studies conducted by the USGS. Some of the topics include the introduction of exotic species into the waterways, restoration of wetlands, and hazards in and around San Francisco Bay.

U.S. Geological Survey, 2001, USGS water resources of California table of contents. Retrieved May 30, 2001, from the World Wide Web at http://water.wr.usgs.gov/toc.html.

The table of contents page leads to an incredible number of information resources, available primarily from the USGS. Topics are arranged by the themes of natural resources, environmental concerns, and hazards. Real-time water data, historical data, the hydrodynamics of San Francisco Bay, land subsidence information, San Mateo coastal erosion, and potential San Francisco Bay landslides and seawater intrusion are a few of the subjects covered. Specific reports address issues from around California. There are links to comparable State agencies and to other Federal entities that give weather, tides, and water quality information. There is a category for water education with links to other interesting science resources that include museums and universities.